



PROCEEDINGS OF THE 2^D SEMINAR

Asian Workshop on Aircraft Design Education

October 17-20
2017



Nanjing, China

**Proceedings
of the 2nd Seminar AWADE**



Nanjing, China, October 17-20 2017

Nanjing University of Aeronautics and Astronautics



Proceedings of the 2nd Seminar AWADE

A form of cooperation between those involved in training aircraft design for the aviation industry – Asian Workshop on Aircraft Design Education (AWADE) successfully continued in 2017. This activity form in the field of aircraft design in education involves diverse activities of AWADE (seminars and student Olympiads, executing joint projects, preparation of educational and methodical literature, etc.) and it has the main goal – to improve the process of training students in the aircraft design field. The 2nd workshop like the 1st one took place at the Nanjing University of Aeronautics and Astronautics. The important feature of the seminar was joint sessions with the European Workshop on Aircraft Design Education (EWADE), as well as a Skype conference with participants from Russia, Germany, Ukraine, who were unable to come. The Proceedings of the 2nd Seminar AWADE include reports of all the seminar participants and also the information about EWADE seminar content which was held in Bucharest in frame of CEAS.

Edited by Prof. Anatolii Kretov

Technical editor Asst. Prof. Oleksiy Chernykh

Art design by Prof. Anatolii Kretov

Printed in Nanjing University of Aeronautics and Astronautics

© Nanjing University of Aeronautics and Astronautics

© The authors of the AWADE-2017 papers

TABLE OF CONTENTS

TABLE OF CONTENTS

Prolusion. AWADE expands its borders	6
<i>Organizing Committee of AWADE</i>	
Nanjing University of Aeronautics and Astronautics (China)	
Welcome to Asian AWADE and European EWADE	8
<i>Jizhou Lai</i>	
Director of International Cooperation Office	
Nanjing University of Aeronautics and Astronautics (China)	
Aircraft Design Education at Nanjing University of Aeronautics and Astronautics	21
<i>Pinqi Xia</i>	
Dean and Professor, College of Aerospace Engineering	
Nanjing University of Aeronautics and Astronautics (China)	
Future Trends in Aircraft Design	28
<i>Anthony P. Hays</i>	
California State University Long Beach, California (USA)	
Nature as the Best Creative Designer	37
<i>Stanislav Gorb, Anatoly Kretov</i>	
Kiel University (Germany), Nanjing University of Aeronautics and Astronautics,	
College of Aerospace Engineering (China)	
Approaches to the Choice of Constructional Materials of Airplanes	47
<i>Oleksandr Moliar, Shasha Zhang, Pingze Zhang, Zili Liu, Qiang Miao, Zhengjun Yao</i>	
Nanjing University of Aeronautics and Astronautics, College of Material Science and Technology (China)	
Economic Efficiency of Aircraft with Air Cushion Chassis Landing Gear	53
<i>Victor Morozov, Zhang Cong</i>	
Novgorod State Technical University named after R.E. Alekseev, Institute of Transport Problems, Nizhny Novgorod (Russia), Nanjing University of Aeronautics and Astronautics, College of Aerospace Engineering (China)	
Milli-Sized Piezoelectric Motors for Micro Helicopters	64
<i>Dalius Mazeika, Piotr Vasiljev, Sergejus Borodinas</i>	
Nanjing University of Aeronautics and Astronautics (China), Vilnius Gediminas Technical University, Vilnius, Lithuanian University of Educational Sciences, Vilnius (Lithuania)	
Design and Manufacturing of Polymer Composite Tail Rotor Hub	76
<i>Darya M. Bezzametnova, Venera R. Sakhubudinova</i>	
Kazan National Research Technical University named after A. N. Tupolev – KAI	
Institute for Aviation, Land Transportation and Power Engineering (Russia)	

TABLE OF CONTENTS

Practical Approach to Airworthiness Study Education – Taking a Case of an Uncontained Rotor Failure	81
<i>Zhengqiang Cheng, Oleksiy Chernykh, Zhong Lu and Junjiang Xiong</i>	
Beijing University of Aeronautics and Astronautics, School of Transportation Science and Engineering, Nanjing University of Aeronautics and Astronautics, College of Civil Aviation (China)	
A Numerical Method of Sensitivity Analysis in the Identification Problems of Heat-Loaded Structures.....	90
<i>Sheng Huang, Vladimir A. Kostin</i>	
Shenyang aerospace university, College of Aerospace Engineering, Kazan National Research Technical University named after A. N. Tupolev – KAI, Institute for Aviation, Land Transportation and Power Engineering (Russia)	
Biomimetics: Why It Is Worth of Doing It for Astronautics and Aeronautics Engineers?.....	98
<i>Stanislav Gorb, Elena Gorb</i>	
Department of Functional Morphology and Biomechanics, Zoological Institute of the Kiel University (Germany)	
Experience in Using of Electromechanical Simulation Stand of the UAV's Aeroelastic Behavior in Research Work of Students and Graduate Students of Aerospace Faculty.....	103
<i>Igor K. Turkin and Sergey G. Parafes'</i>	
Moscow Aviation Institute (National Research University), Moscow (Russia)	
The Career Guide Measures for Future Aeronautical Engineers at National Aerospace University KhAI.....	110
<i>Olena Litvinova, Alina Matskevich, Natalya Sytnyk, Dmytro Toporets</i>	
National Aerospace University KhAI, Kharkiv (Ukraine)	
Experience of the National Aerospace University "Kharkiv Aviation Institute" in the Development of Students' Creative Activity	114
<i>V.T. Sikulskiy, V. Yu. Kashcheyeva, O. O. Shatravka, D.S. Toporets</i>	
National Aerospace University KhAI, Kharkiv (Ukraine)	
Rational Designing on the Basis of Real-Life Examples	120
<i>Clifton Read, Dmytro V. Tiniakov</i>	
Executive Wisdom Consulting Group, Brisbane (Australia), Nanjing University of Aeronautics and Astronautics, College of Civil Aviation, Nanjing (China)	
Transport System for the Initial Development of the Moon	131
<i>Liu Jun, Zhang Cong</i>	
Nanjing University of Aeronautics and Astronautics, College of Aerospace Engineering (China)	
Analysis of Adaptive Landing Gear Used for Near Space Lander.....	139
<i>Mingyang Huang, Xiaohui Wei, Hong Nie</i>	
Nanjing University of Aeronautics and Astronautics, College of Aerospace Engineering (China)	
Basic UAV Development in Undergraduate Level.....	147
<i>Allan A. Dias</i>	
Nanjing University of Aeronautics and Astronautics, College of Aerospace Engineering (China)	

TABLE OF CONTENTS

Focus on Interdisciplinary Education in Airworthiness Skills Cultivation	160
<i>Piao Li, Oleksiy Chernykh and Weixing Yao</i>	
Nanjing University of Aeronautics and Astronautics, College of Aerospace Engineering, College of Civil Aviation, Nanjing (China)	
Joint Airworthiness Education for Heat Transfer Characteristic Researches on Aero-Engine Inlet Strut with Film-Slot Cover	166
<i>Lu Yi, Oleksiy Chernykh and Ke Peng</i>	
Beijing University of Aeronautics and Astronautics, School of Transportation Science and Engineering, Nanjing University of Aeronautics and Astronautics, College of Civil Aviation, Nanjing (China)	
To the 60th Anniversary of the Launch of the First Satellites: Historical and Technical Analysis.....	178
<i>ZhiJin Wang, Anatolii Kretov</i>	
Nanjing University of Aeronautics and Astronautics, College of Aerospace Engineering (China)	
Generation of the Drag Map and Derivative Plots for Commercial Aircraft.....	188
<i>Anthony P. Hays</i>	
California State University Long Beach, California (USA)	
Aircraft Noise Sources and Analysis of Ways for Noise Limitation	198
<i>Dmytro V. Tiniakov, Yuliya V. Babenko</i>	
Nanjing University of Aeronautics and Astronautics, College of Civil Aviation, Nanjing (China) National Aerospace University “KhAI” Airplanes and Helicopters Designing Department, Kharkov (Ukraine)	
Book of Abstracts of 13th European Workshop on Aircraft Design Education (EWADE 2017).....	205
<i>Edited by Dieter Scholz</i>	
Hamburg University of Applied Sciences (HAW Hamburg), DE Aircraft Design and Systems Group (AERO)	
Conclusion	218
Photo Gallery of the 2^d AWADE Seminar.....	219

PROLUSION

AWADE EXPANDS ITS BORDERS

All these components are close interconnectedness but at the 1st place stays education, which provides the preparing of employees for the needs of the aviation industry in all three mentioned components. It means that the education must be remained the most important an urgent component and it should set the strategy of training. All who is connected with this process of preparing specialists that meet modern needs for aerospace industry well knows that this type of education is very specific, it requires maximum investment and it, in turn in high level should be supported as from the side of science, so and from production. How to make all disciplines more effective for studying, how to provide a better understanding it of students, how to direct its ability to implement student fresh ideas and dreams. These questions have always existed and always remain relevant.

In November 2015 for the solutions of such problem the college of Aerospace Engineering of Nanjing University of Aeronautics and Astronautics initiated the creation of Asian Workshop on Aircraft Design Education (AWADE). This workshop should be with the assistance of experts in the field of the Aircraft Design. As a role model has been selected the European Workshop on Aircraft Design Education (EWADE), which has existed since 1994. But unlike the EWADE the Asian Workshop is considered as a wide field of activity. The forms of AWADE activity in the field of aircraft design in education involves diverse activities of AWADE: seminars and student Olympiads, executing a joint projects, the preparation of educational and methodical literature, etc. AWADE has the main goal – to improve the process of training students in the field of aircraft design.

In October 2016, the AWADE opened its official working in the first seminar format. The 2nd workshop and like the 1st took place at the Nanjing University of Aeronautics and Astronautics from the 17th till the 20th of October 2017. An important feature of this seminar was a joint sessions with the European Workshop on Aircraft Design Education (EWADE), as well as a Skype conference with participants from Russia, Germany, Ukraine, who were unable to come.

The Proceedings of the 2nd Seminar AWADE includes reports of the all participants of the seminar and also the information about content EWADE seminar which held in Bucharest in frame of CEAS.

Presented by the authors of the reports are associated with many of the issues discussed in disciplines related to aircraft design. These are questions scientific, methodological, historical and problematic nature. In contrast to the first seminar in the work of the second one were students reports. In the opinion of the organizing Committee it allows you to better understand the level of students, their strengths and weaknesses. Students - the participants made many suggestions which surely will be considered in future activities AWADE.



***AWADE has been continuing its work and we believe
that its activity forms would be giving positive results in future***

*Organizing Committee of the 2nd Seminar AWADE
October 2017*

WELCOME TO ASIAN AWADE AND EUROPEAN EWADE

Jizhou Lai

Director of International Cooperation Office
Nanjing University of Astronautics and Aeronautics
29 Yudao St., Nanjing 210016, P.R.China
e-mail: Ljz-ico@nuaa.edu.cn

Key words: Presentation, AWADE, EWADE, history, NUAA.

Abstract. *The work was prepared based on the presentations at the joint meeting of Asian and European seminars and includes basic information on these two areas: Asian Workshop on Aircraft Design Education (AWADE) and European Workshop on Aircraft Design Education (EWADE).*

PRESENTATION



Welcome Speech on
AWADE 2017 With joint participation of **EWADE 2017**
by
Professor Lai Jizhou
Executive Director of International Cooperation Office
October 19th
Nanjing University of Aeronautics and Astronautics



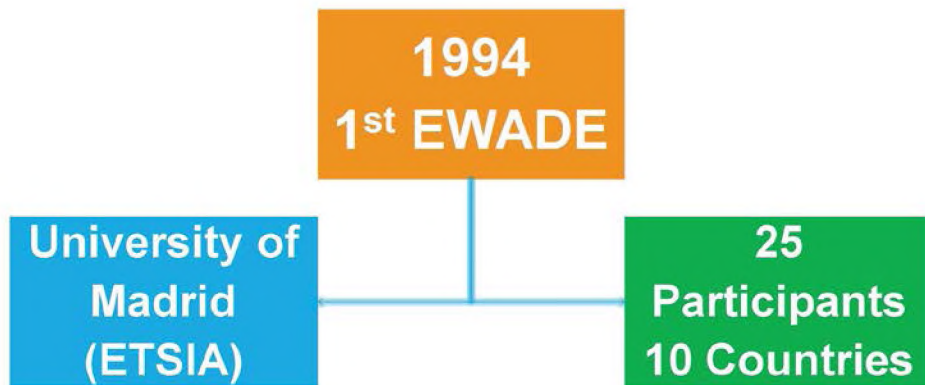
Contents

- 1 General Introduction to EWADE and AWADE
- 2 About NUAA
- 3 Future Expectation & Conclusion

南京航空航天大学
Nanjing University of Aeronautics and Astronautics



1. History of EWADE



3



20 Years of Development 1994-2017



Objective of EWADE

- To allow European lecturers concerned with Aircraft Design to continue their active collaboration.
- To discuss Aircraft Design problems as regards research and education.
- To enhance close cooperation with the aerospace industry for the two aspects mentioned above.



4

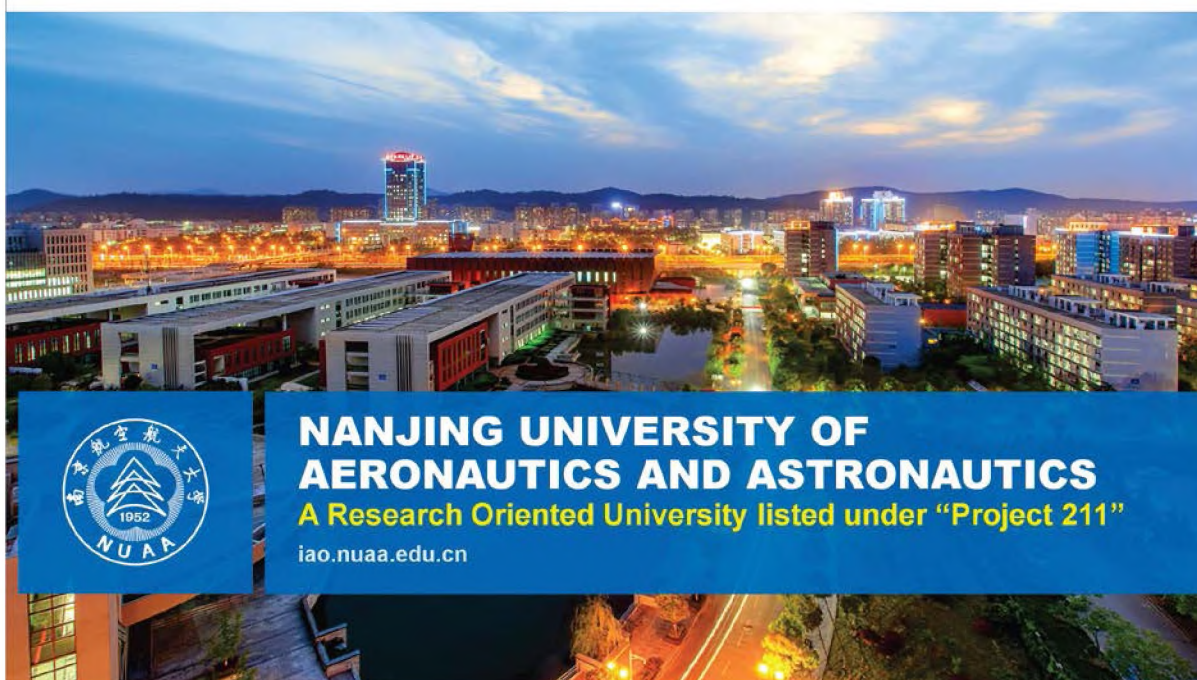


1st
**Asian Workshop on
Aircraft Design Education
(AWADE)**
NUAA, Nanjing
October 8th -16th 2016





2017 (EWADE + AWADE) WADE





2. NUAA Timeline



Location





Aeronautics



Astronautics

Aviation





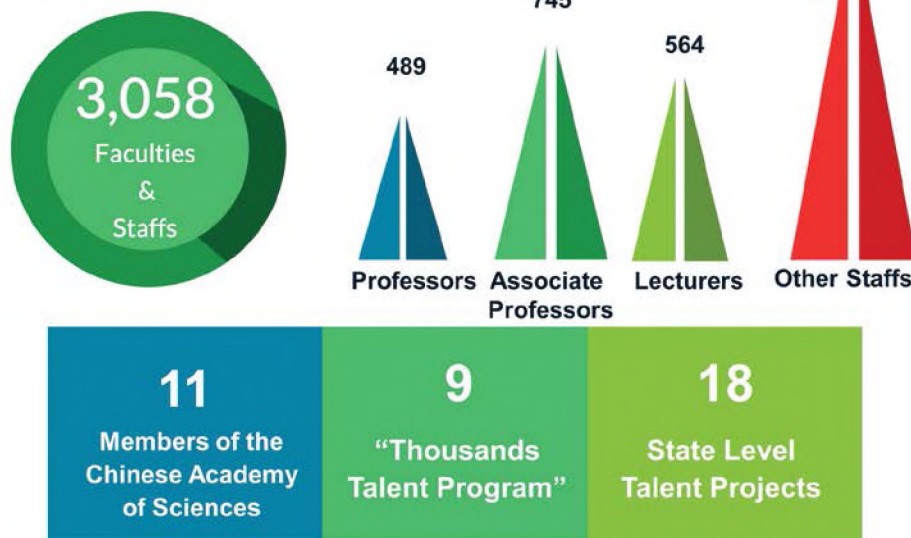
Programs and Students



14



Faculties and Staffs



15



National Key Laboratories



National Key Laboratory

Mechanics and Control of Mechanical Structures



National Key Laboratory

Helicopter Rotor Dynamics



National Key Laboratory

Air Traffic Flow Management



National Key Laboratory

Structural Strength

16



National Key Laboratories



National Engineering Research Centre
Processing of Difficult-to-Machine Materials



Ministry of Education Key Laboratory
Intelligent Materials and Devices

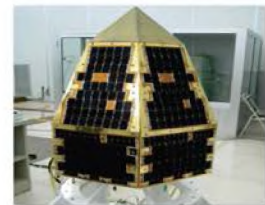
17



Leading Researches

1. Aircraft Design

- Advanced Design Technology of Flight Vehicle,
- New-Concept research,
- Engineering Model Development,
- Helicopter and Unmanned Aerial Vehicle.

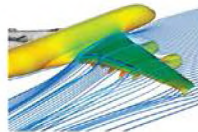
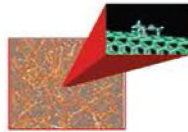
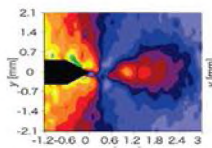




Leading Researches

2. Structural Mechanics and Control

- Nonlinear Dynamics and Control
- Analysis of Aircraft Structure Dynamics and Control
- Ultrasonic Motor Technology
- Intelligent Structures Applied in Aircraft
- Unsteady Aerodynamics and etc.



Leading Researches

3. Advanced Manufacturing

Leading domestic position in

- Premise micro-fabrication,
- Curved Surface Modeling,
- Modeling and Fabrication of Titanium Structure,
- Technology of Digital Assembly,
- Automated Placement Technology of Composite



20



Leading Researches

4. Navigation, Guidance and Control

- Airborne Precise Autonomous Navigation
- Advanced Flight control and simulation
- Smart self-repairing and Control and etc.



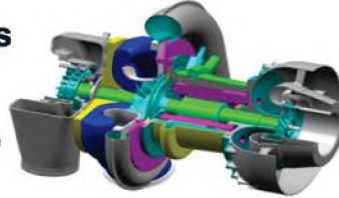
21



Leading Researches

5. Power Electronics and Power Drives

- Air Power
- Power Conversion
- Special Motor Technologies have exerted great domestic influence



22



Teaching & Experimental Facilities



Satellite Center



National Center for Mechanics Teaching



Human Factors Engineering Laboratory



Integrated Avionics Laboratory



Engineering Training Center



Mass Data Analysis Laboratory



Helicopter Research Laboratory



Compressor Test Bench

23



Colleges at NUAA

16
Colleges

College of Aerospace Engineering

College of Energy and Power Engineering

College of Automation Engineering

College of Electronic & Information Engineering

College of Mechanical and Electrical Eng.

College of Material Science & Technology

College of Civil Aviation (College of Flight)

College of Science

College of Economics & Management

College of Humanities

College of Arts

College of Foreign Languages

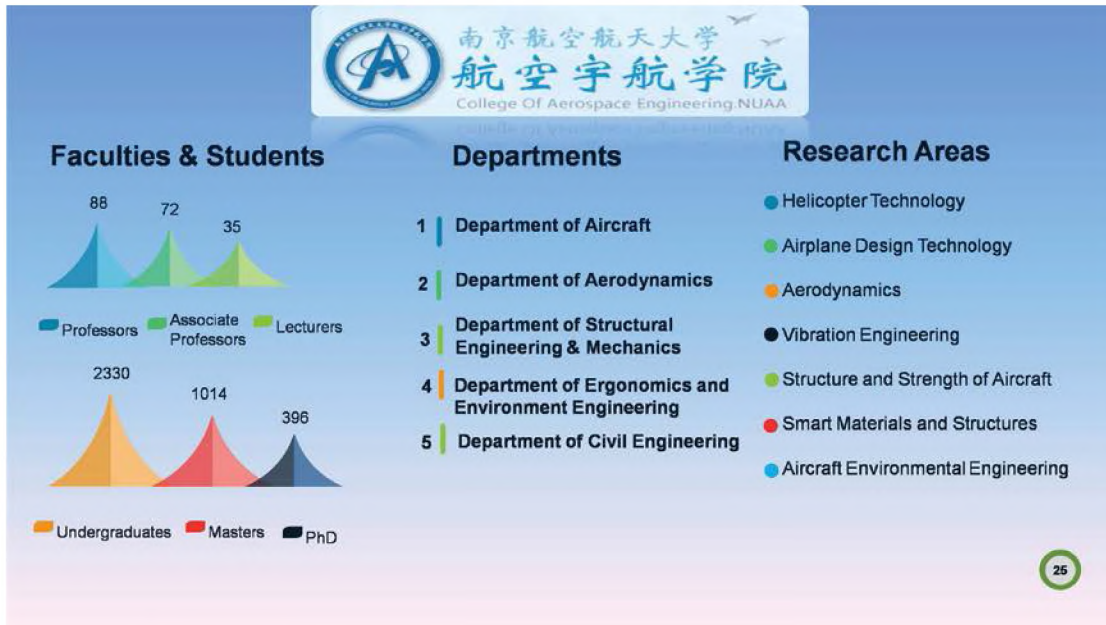
College of Space Engineering (Astronautics)

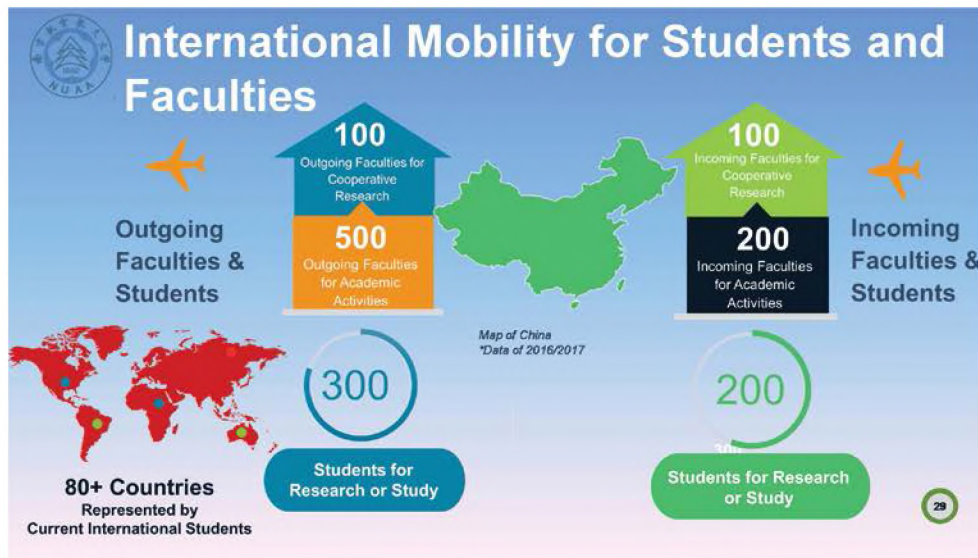
College of Computer Science & Technology

College of Marxism

College of International Education

24





3. Future Expectation & Conclusion

- Aircraft design is one of the most vibrant sectors in our times.
- Its rapid development has brought profound changes to our life as well as new opportunities and challenges to human society.
- The development of the aircraft design education knows no national or sectoral boundaries.



Thus, its sound use, development and governance calls for closer international cooperation and joint efforts to build a community of common future.

Jizhou Lai

I appreciate all the participants, especially those from the other side of the video, for joining us and sharing your valuable experience and inspirations.

I believe that your academic exchanges and discussions about the achievements will further promote the development of the field of aircraft design.

I am sure this workshop will create a new era for strengthening the academic collaboration between China, Asian countries and European countries, and also between you all and NUA.

32

I wish the conference a full success and all participants every success and good health.



33

Author



Jizhou Lai

AIRCRAFT DESIGN EDUCATION AT NANJING UNIVERSITY OF AERONAUTICS AND ASTRONAUTICS


Pinqi Xia

Dean and Professor, College of Aerospace Engineering
Nanjing University of Aeronautics and Astronautics, College of Aerospace Engineering,
29 Yudao St., Nanjing 210016, P.R.China
e-mail: xiapq@nuaa.edu.cn

Key words: Aircraft Design, Education, Practice, Engineering, Innovation, NUAA. AWADE, EWADE

Abstract. *The presentation includes the basic information and aircraft design education in College of Aerospace Engineering, Nanjing University of Aeronautics and Astronautics. The aircraft design education emphasizes practice, engineering and innovation while strengthening theoretical education. In recent 8 years, the students of aircraft design in the college have won lots of national and international students science and technology competition awards including the first-place in the Airbus Fly Your Ideas Challenge in 2011, the first-place in American Helicopter Society International's 33rd Annual Student Design Competition in 2016 and so on.*

PRESENTATION



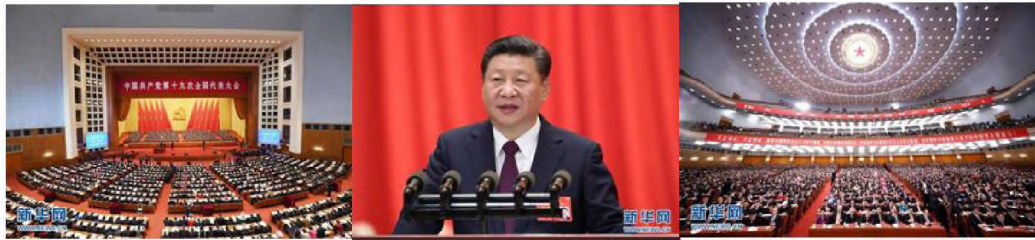
The presentation slide features a vertical decorative bar on the left with a grid pattern and a small image of a mechanical part. The main content area includes the NUAA logo (a circular emblem with a tree and the year 1952), the university's name in Chinese (南京航空航天大学) and English (Nanjing University of Aeronautics and Astronautics), and the workshop title (The 2nd Asian Workshop on Aircraft Design Education). A central graphic shows a stylized aircraft fuselage between two globes. The title 'Aircraft Design Education at College of Aerospace Engineering NUAA' is prominently displayed in red text. The presenter's name, 'Prof. Pinqi Xia', is at the bottom.

南京航空航天大学
Nanjing University of Aeronautics and Astronautics
The 2nd Asian Workshop on Aircraft Design Education

**Aircraft Design Education
at College of Aerospace Engineering
NUAA**

Prof. Pinqi Xia

Celebrating the 19th Congress of the Communist Party of China



1. Brief Introduction to the College

(1) Departments

1. **Department of Helicopter Engineering (only one in China)**
2. **Department of Aircraft Engineering (fixed wing aircraft)**
3. **Department of Structural Engineering and Mechanics (aerospace background)**
 - ① **Research Institute of Vibration Engineering**
 - ② **Research Institute of Structural Strength**
 - ③ **Research Institute of Smart Materials and Structures**
 - ④ **Research Institute of Precision Driving**
 - ⑤ **Research Institute of Micro-Nano Devices and Systems**
4. **Department of Fundamental Mechanics and Testing**
5. **Department of Aircraft Environmental Engineering**
6. **Department of Aerodynamics**
7. **Department of Civil Engineering**

(2) Faculty Members

- **Total 314 faculty members**
 - 105 full professors
 - 100 associate professors
 - 44 assistant professors
- ✓ **2 Academicians of Chinese Academy of Sciences**
- ✓ **6 Distinguished Professors of National "Thousand Talents Program"**
- ✓ **6 National Chang-Jiang Chair Professors**
- ✓ **5 Distinguished Scholars awarded by National Science Foundation**
- ✓ **3 Distinguished Young Scholars awarded by National Science Foundation**

(3) Number of Students

Total 3895 students

1. Undergraduate students: 1943 (50.0%)
2. Master students: 1069 (27.5%)
3. Doctoral students: 700 (18.0%)
4. International undergraduate students: 145 (3.7%)
5. International graduate students: 38 (1.0%)

(4) National Key Disciplines

1. Aerospace Science and Technology

- Aircraft Design
- Aircraft Environmental Engineering
- Aerospace Propulsion Engineering
- Aircraft Manufacturing Engineering



The 2nd Asian Workshop on Aircraft Design Education

(2) National Key Disciplines

2. Mechanics

- Dynamics and Control
- Solid Mechanics
- Fluid Mechanics
- Engineering Mechanics



Design Education

(5) National Key Labs

1. Laboratory of Rotorcraft Aeromechanics, founded in 1995

Research Areas:

- ① Rotor Aerodynamics
- ② Aeroelastic Dynamics of Rotorcraft
- ③ Flight Dynamics and Flight Control of Rotorcraft
- ④ Conceptual and Structural Design of Rotorcraft



The 2nd Asian Workshop on Aircraft Design Education

(5) National Key Labs

2. Mechanics and Control of Mechanical Structures, founded in 2011

Research Areas:

- ① Structural Dynamics and Control
- ② Structural Strength
- ③ Vibration Utilization and Precision Driving
- ④ Mechanics of Micro-Nano Systems
- ⑤ Smart Materials and Structures



The 2nd Asian Workshop on Aircraft Design Education

2. Aircraft Design Education




Practice in Aviation Industry Company






Innovation Center for Student Practice

The 2nd Asian Workshop on Aircraft Design Education

2. Aircraft Design Education










Final year

The 2nd Asian Workshop on Aircraft Design Education


2. Aircraft Design Education

Strengthen Practice and Pay Attention to Engineering


1. Teaching experiments in curriculum including all professional courses and some experimental courses
2. Curriculum Design for courses of mechanical design, aircraft concept design and aircraft structural design
3. Practice in Aviation Industry Company for half a month
4. Final year project for one semester (team work and chief designer model)
5. Innovation education including innovation courses and practice for four years which is required with 1 credit

The 2nd Asian Workshop on Aircraft Design Education


2. Aircraft Design Education



National Experimental Teaching Demonstration Center for Aeronautical Engineering



Aerospace Museum at the College



National Engineering Practice Education Center for Aeronautical Aerodynamics

The 2nd Asian Workshop on Aircraft Design Education


2. Aircraft Design Education

Winning Prizes of Student Design Competitions by Aircraft Design Students at the College, NUAU

year	Int'l Level	National Level				Provincial Level		
		First	Second	Third	Other	First	Second	Third
2009	1	10	6	16	18	6	10	17
2010	4	6	4	4	6	2	5	2
2011	1	7	5	18	14	16	13	9
2012	3	2	7	2	2	10	8	8
2013	4	3	6	24	5	15	6	4
2014	1	17	21	18	4	14	21	29
2015	3	7	17	18	15	28	14	5
2016	1	7	7	7	18	8	12	13
Total	18	59	73	107	82	99	89	87

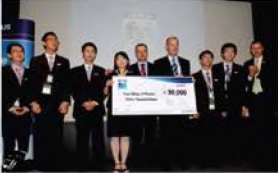
The 2nd Asian Workshop on Aircraft Design Education

2. Aircraft Design Education



NUAA undergraduate student team won first-place in the Airbus Fly Your Ideas Challenge in 2011. More than 120 thousands students from 75 countries in the world participated in the creative competition.

The 2nd Asian Workshop on Aircraft Design Education



The 2nd Asian Workshop on Aircraft Design Education

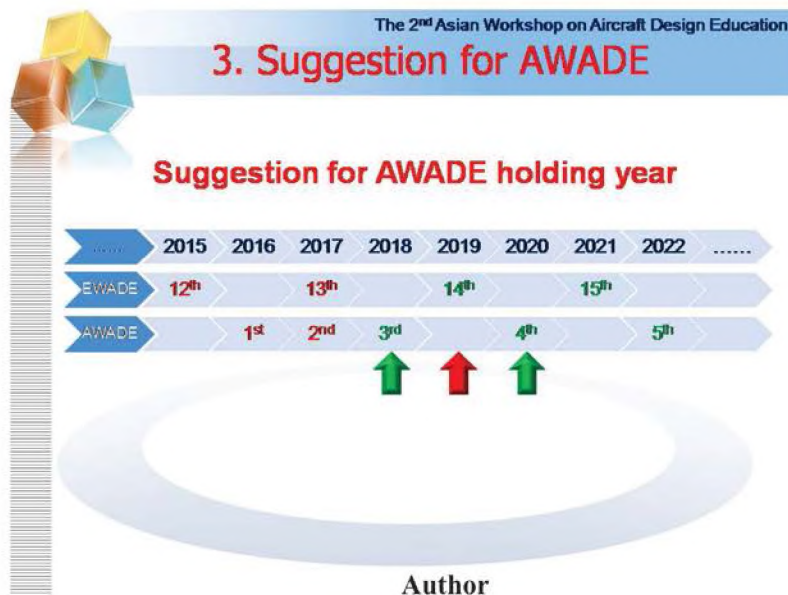
2. Aircraft Design Education



The 2nd and 3rd place teams in this year are from Georgia Tech and PENN State, respectively.

NUAA undergraduate student team won **first-place in American Helicopter Society International's 33rd Annual Student Design Competition in 2016. This is the first time that a non-US team won first place in the undergraduate category.**





Pinqi Xia

FUTURE TRENDS IN AIRCRAFT DESIGN

Anthony P Hays

Aircraft Design and Consulting

San Clemente, California, USA

Email: ahays@alum.mit.edu Web: www.adac.aero

Key words: Aircraft design, aircraft design trends

Abstract. *This paper provides an overview of future trends in aircraft design with a concentration on fixed-wing transport aircraft. Examples include ideas that are not necessarily new, but have resurfaced, and may yet submerge again, and designs that are new but do not require new technology, plus a few designs that are reliant on evolving technology. The paper concentrates on designs themselves, rather than supporting technologies, such as propulsion, structures, stability and control, or aircraft systems. The author offers opinions, for what they are worth, on the probability of success.*

1. INTRODUCTION

Many new (and some not so new) aircraft design concepts have emerged in the past few years, and especially in the area of commercial aircraft design. Many of them appear, or claim, to be superior to the conventional tube and wing concept of all current commercial aircraft designs. But the tube and wing, with engines mounted on the wing, have beneficial characteristics that are not always apparent to the casual observer, such as the short load path between engine weight and wing lift, and engine inertia loads on landing and landing gear reaction loads. Center of gravity travel is short, and a long tube gives the horizontal stabilizer a large moment arm to balance flap pitching moments. The landing gear bogies usually fit snugly into the fuselage behind the wing box. Deviation from this layout often results in significant weight penalties, as experienced by rear-engine configurations such as the Vickers VC-10. Many novel concepts may look attractive at first sight, but detailed analysis often reveals significant penalties that negate the (usually aerodynamic) benefits. Very different requirements often drive military designs, and the dominant requirement is usually that of low observability in certain regions of the electromagnetic spectrum. There are still opportunities for design improvement, although much of the work is classified.

2. TRENDS

Historically NASA has taken the lead in developing new design concepts, starting with the Bell X-1, up to the ESAero/Tecnac X-57 (Fig. 1). Not all the X-planes achieved their original design goal, but all of them expanded the field of knowledge in aircraft design. For example, the Bell X-3 was designed to fly at Mach 3, but was so seriously underpowered that it failed to reach Mach 1 in level flight. However, much was learned about titanium construction and the phenomenon of roll inertia coupling, thanks to the airplane's low moment of inertia along

its longitudinal axis. Largely because of the Cold War between the Soviet Union and North Atlantic Treaty Organization (NATO) members, the earliest X-planes evaluated concepts that were of benefit to military designs, but that emphasis is now shifting somewhat towards commercial aircraft. Of particular interest in recent X-plane designs are the Boeing X-48, a subscale remotely-controlled blended wing body, and ESAero/Tecnam X-57. Both of these X-planes may provide the groundwork for radically new transport aircraft.

1946 Bell X-1 supersonic flight		1984 Grumman X-29 forward-swept wing	
1954 Bell X-2 swept wing		1997 Boeing X-36 tailless agility	
1952 Douglas X-3 trapezoidal wing		2007 Boeing X-48 blended wing body	
1948 Northrop X-4 semi-tailless		2006 Boeing X-53 active aeroelastic wing	
1951 Bell X-5 variable-geometry wing		2012 Lockheed Martin X-56 active flutter suppression	
1959 North American X-15 hypersonic flight		2018 ESAero X-57 distributed electric propulsion	

Figure 1: Key NASA X-planes



Figure 2: Boeing Strut-Braced Wing

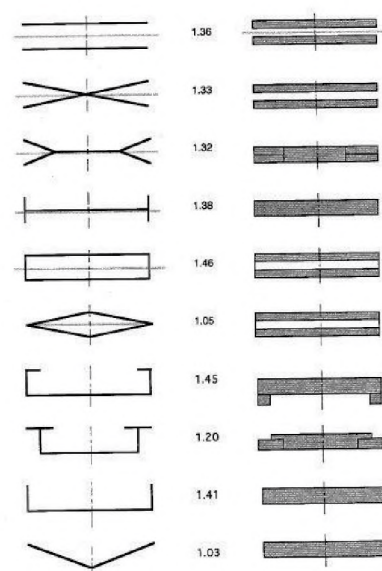


Figure 3: Span efficiency for Various Optimally Loaded Nonplanar Systems (height/span = 0.2)

One idea that has resurfaced is the strut-braced wing concept for commercial transport aircraft (Fig. 2). However, wing-strut interference drag is of serious concern, and there is no new technology to reduce it, so it's unlikely that the concept will fare any better than it did with the

Hurel-Dubois HD.31, a strut-braced wing commercial airliner introduced in 1953, of which only 11 were built. It had a cruise speed of only 146 kt (75 m/s).

In 2005 Ilan Kroo published a paper on non-planar wing concepts (Ref. 1), and one figure in the paper showed the left-hand side of Fig. 3, taken from Ref. 2. The box-wing concept, with a span efficiency 46% higher than that of a planar wing of the same planform area, solicited much interest. Unfortunately, the right-hand side of the figure was not shown, and that would have revealed how the high span efficiency was achieved. The higher span efficiency of a biplane is already well-recognized, and joining the wing-tips has an effect similar to that of winglets, adding 10% span efficiency (as indicated by comparing the span efficiency of the biplane and box wing in Fig. 3) but without any penalty in adding planform area, because the surfaces are vertical.



Figure 4: Lockheed Martin Box Wing



Figure 5: Boeing Joined Wing Sensorcraft

The box wing consists of two very high aspect ratio wings joined by winglets. Implementation of this concept is fraught with difficulty, as shown by Fig. 4, with issues such as:

- If each wing has the same thickness/chord ratio as a monoplane wing, and assuming that each wing has equal area with the same total area as a monoplane, then each wing has one-quarter of the fuel volume of the monoplane, and the aircraft therefore has one-half the wing fuel volume. It would be very difficult to find where to put fuel for a long-range configuration.
- The landing gear must go in fuselage pods, which add structural weight.
- For longitudinal static stability, the forward wing must operate at a higher lift coefficient than the aft wing. With aft-located high bypass ratio engines, it is unlikely that this configuration would balance without moving the forward wing aft, reducing the stagger benefit.
- The aft wing would have difficulty resisting the torsion moment applied by the engines.

The joined wing is a variation on this concept and offers some benefits in wing bending moment (Fig. 5), but the strut (or aft wing), is in compression and cannot take a large compressive load. It may have an application for an omnidirectional phased-array radar (as appears to be the case in this configuration).



Figure 6: MIT Double-bubble Fuselage with Aft-mounted engines

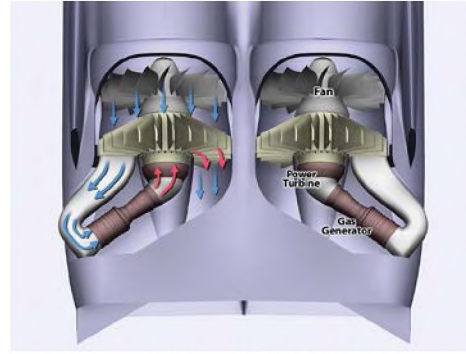


Figure 7: Propulsion System with Angled Gas Generators

Another interesting configuration is the MIT-developed double-bubble, laminar-flow wing configuration (Fig. 6). There is nothing particularly novel about this configuration, and with three adjacent engines, it is unlikely that the airplane could meet the FAR requirement for a less than 5% probability of uncontained failure of one engine causing failure of the other. One novel engine layout for a twin-engine aircraft, suggested by Pratt & Whitney, is to use an engine configuration similar to that of the PT6, with the gas generators angled such that uncontained compressor or turbine failure would not result in damage to the adjacent engine (Fig. 7).



Figure 8: Airbus Unducted Fan Airliner

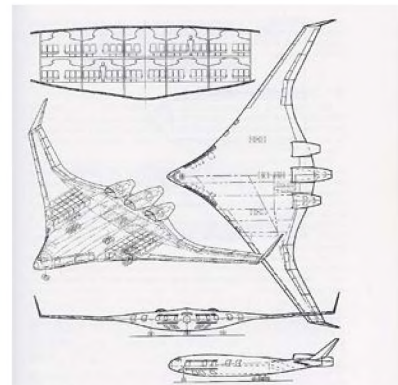


Figure 9: Boeing Blended Wing-Body

There is also the possibility of the three-surface configuration making a comeback. The best-known application is on the Piaggio Avanti, for which it was used in part to keep the wing spar aft of the cabin. Airbus is considering using it for a different purpose, this time to enable the wing, horizontal and vertical stabilizers to partially shield the noise from the counter-rotating blades of the unducted fan (Fig. 8).

Another innovative concept is the blended wing-body configuration that has been pursued by Boeing for over twenty years (Fig. 9). Advantages of this configuration include:

- Cruise at higher lift/drag ratio
- Noise shielding of jet engines
- Cruise at low lift coefficient

Offsetting these, some disadvantages are:

- Increased weight of non-cylindrical passenger cabin
- Difficult passenger ingress/egress
- More difficult engine access
- Cannot trim for high lift coefficient flaps

- Non-uniform flow into engines at high angle of incidence

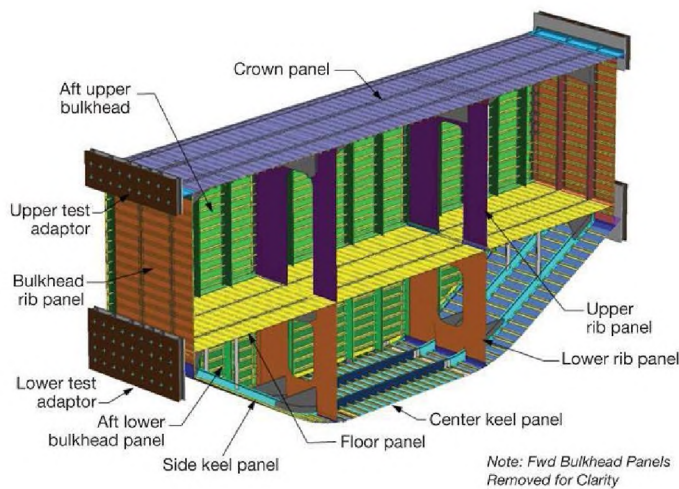


Figure 10: NASA Contract to Evaluate Non-circular Pressurized Structures



Figure 11: DZYNE Executive/Regional Jet Blended Wing-body



Figure 12: Lockheed Hybrid Blended Wing-body

Greater knowledge of this configuration is slowly being accumulated. Under contract to NASA, Boeing designed a section of the passenger and cargo structure using composite materials (Fig. 10). One of the goals was to be able to estimate the weight of this structure. Boeing also built two radio-controlled subscale models designated X-48B with a 21 ft. (6.4 m) wingspan to examine low-speed flight control characteristics. One of the models was converted to the X-48C variant, which involved moving the vertical stabilizers inboard and extending the aft fuselage to provide some jet exhaust noise shielding and increased pitch control. The blended wing-body is most likely to find an application for cargo aircraft, but a potential passenger application is for a regional or executive jet, as suggested by DZYNE Technologies (Fig. 11).

Military airlifters are usually required to operate in shorter field lengths than commercial aircraft, and this requires either a larger wing or the use of flaps. Typically, flaps are the preferred solution, and the pitching moment from flaps must be trimmed. For this a horizontal stabilizer is required, resulting in a hybrid blended wing-body as illustrated in the Lockheed concept of Fig. 12.

Putting engines on top of the wing is not new. It was successfully proven on the VFW-Fokker 614 regional jet, which was first flown in 1971. Putting engines on the rear fuselage or on top of the wing is attractive for regional or executive jets, because it permits the fuselage to be closer to the ground, and this allows easier passenger boarding or exiting without a passenger boarding bridge. Putting the engines on top of the wing rather than on the rear fuselage reduces fuselage bending moments, reduces center of gravity travel, and shortens landing load paths, although these effects are more important for an aircraft with a long fuselage. This has been implemented on the HondaJet (Fig. 13), which received a FAR 23 Type Certificate in December 2015. It has a cruise Mach number of 0.64 and maximum Mach number of 0.74. For a conventional wing/fuselage configuration, at higher Mach numbers there is a risk of interference between the upper surface shock and the engine inlet, and this limits the operational envelope for

this type of layout. A hybrid wing-body typically operates at a lower cruise lift coefficient and may be able to operate at a higher cruise Mach number with over-the-wing nacelles.



Figure 13: Honda HA-420 Honda Jet



Figure 14: Lockheed Martin Mach 1.6 Airliner

As for supersonic cruise aircraft, the future is still uncertain, although that has not stopped many design offices from trying to produce a feasible supersonic aircraft. Although the U.S. domestic market no longer dominates commercial operations, the current federal ban on supersonic operations over the United States, except for designated supersonic corridors for military aircraft, inhibits the introduction of supersonic commercial flights. NASA is in the process of developing a manned X-plane that will replicate a low sonic boom representative of an aircraft flying at about Mach 1.4, and fly the airplane to gauge public reaction in the hope of overturning the federal prohibition. In the meanwhile, Lockheed Martin has designed a low boom 81 passenger Mach 1.6 airliner with a range of 4000 nm (7408 km) (Fig. 14). There is also interest in a supersonic business jet, but unlike blended wing-body configurations, the supersonic passenger-carrying configuration cannot easily be scaled downward. Low boom aircraft requires a very high fineness ratio (length/diameter ratio), which results in a small cabin cross-sectional area for a supersonic business jet (Fig. 15). It is questionable whether a typical passenger would want to be restrained by such a small space.

There have been many attempts to develop a roadable aircraft. One of the recent efforts is the Terrafugia Transition (Fig. 16) with a cruise speed of 87 kt (45 m/s), range of 356 nm (659 km) with 30 minutes reserves, and a useful payload of 500 lb (267 kg). Although the aircraft has been in development since 2006, delivery of a production vehicle is not expected until 2019. With a price tag of over US\$300K, it is questionable if there is sufficient demand for such a vehicle. Car rental desks at general aviation airports might appear to be the preferred solution.



Figure 15: NASA/Boeing Supersonic Business Jet



Figure 16: Terrafugia Transition

There is a requirement for a low-observable replacement for the venerable Lockheed C-130, which first flew in 1954. Propellers are out, so some means must be found to provide the

same order of takeoff and landing lift augmentation that propeller slipstream provided for the C-130. One possibility is a configuration such as that designed by Lockheed Martin for the U.S. Air Force Research Laboratory's (AFRL) Speed Agile program (Fig. 17). This aircraft has a tactical radius of 500 nm (526 km) and takeoff field length of 2000 ft (610 m) with a full load. The aircraft uses a patented combined ejector lift and thrust reverser inboard, and circulation-controlled internally blown flaps outboard. Figure 18 (from Ref. 3) shows the settings for cruise (top), augmented lift (middle), and thrust reverser (bottom). In 2011, a 23% scale model was tested in the Arnold Engineering and Development Center (AEDC) wind tunnel to test the hybrid powered lift system using Williams FJ-44 engines to obtain data on lateral directional stability, ground effects, aircraft and engine performance, and engine operability.



Figure 17: Lockheed Martin Speed Agile Concept

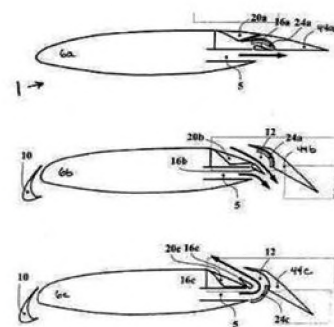


Figure 18: Lockheed Martin Speed Agile High Lift and Thrust Reverser System

The trend towards unmanned aircraft continues for the military. A considerable amount of weight is saved in not requiring a cockpit and its contents, and the airplane can be involved in combat conditions without risk to a pilot's life. The X-47B technology demonstrator (Fig. 19) successfully proved the capability of unmanned carrier operations. Although designed as an unmanned combat air system demonstrator (UCAS-D), in February 2016 the U.S. Navy changed its role to reconnaissance and aerial refuelling.



Figure 19: Northrop Grumman X-47B



Figure 20: Boeing Optionally-piloted NGAD

The follow-on to the F-22, the Next Generation Air Dominance (NGAD) fighter, will probably be unmanned, although bets are being hedged by designing the aircraft as being optionally piloted. It's quite possible that the primary combat scenario will involve attack at beyond visual range (BVR) conditions, and combat maneuverability will be subservient to low observability. The airplane may well be tailless (Fig. 20). Only one thing can be assured, and

that is that it will not look anything like any of the promotional images provided by the likely prime contractors.

The ESAero/Tecnam X-57 Maxwell is being developed by NASA to demonstrate the use of all-electric propulsion. All fourteen propellers are used during takeoff, but only the outer two at cruise. The slipstream of the twelve inboard propellers will provide lift augmentation that will permit a higher design wing loading of 50 lb/ft² (244 kg/m²) as compared with the baseline Tecnam P2600T with 17 lb/ft²(83kg/m²), as illustrated in Fig. 21. The demonstrator will use batteries with a specific energy of 200 Wh/kg, although the aircraft would 400-500 Wh/kg to be economically feasible. Range will be about 86 nm (160 km).



Figure 21: ESAero/Tecnam X-57

3. OTHER TECHNOLOGIES

Although this paper concentrates on design rather than technology, it would be remiss of the author if the enormous time and effort in contributing technologies were not given their due, especially for advances in computational fluid dynamics (CFD) enabling rapid aerodynamic evaluation of new configurations, composite materials, 3D printing of parts that could not be manufactured using conventional machine tools, innovative propulsion systems, and in particular those designed to wean aircraft propulsion off carbon-based fuels (as must eventually happen), advanced cockpit systems to reduce the probability of pilot error, ...the list is endless.

4. CONCLUSIONS

All these design innovations and technologies contribute towards a more economical transportation system, allowing more people to travel and befriend others from different cultures in distant places, and to provide a more secure defense system against those, who are not so friendly. Data from research by Küchemann et al. (Ref. 4, Fig. 1.4) show how the introduction of an improved transportation system can transform people's lives, and this is especially true of air transportation. Continued improvements in air transportation will permit an even greater percentage of the world population to travel.

ACKNOWLEDGEMENTS

Fig. 2 www.airliners.net
Figs. 4, 12, 17 Lockheed Martin
Fig. 5 Aviation Week
Fig. 6 www.nasa.gov
Fig. 7 Pratt & Whitney
Fig. 9 Boeing
Fig. 10 www.compositeworld.com

Fig. 13 www.airliners.net © Tom Parker
Fig. 14 NASA/Lockheed Martin
Fig. 15 NASA/Boeing
Fig. 16 Terrafugia
Fig. 19 Wikimedia Commons
Fig. 20 forum.keypublishing.com
Fig. 21 Wikimedia Commons

REFERENCES

- [1] Kroo, I., *Nonplanar Wing Concepts for Increased Aircraft Efficiency*, von Kármán Institute lecture series on Innovative Configurations and Advanced Concepts for Future Civil Aircraft, June 2005
- [2] McMasters, J. H., and Kroo, I., , *Advanced Configurations for Very Large Subsonic Transport Airplanes*, NASA Workshop on Potential Impacts of Advanced Aerodynamic Technology on Air Transportation System Productivity, NASA Langley Research Center, July, 1993
- [3] Zeune, C.H., *Enabling Speed Agility for the Air Force*, American Institute of Aeronautics and Astronautics, AIAA 2010-349, January 2010.
- [4] Küchemann, D., *The Aerodynamic Design of Aircraft*, American Institute of Aeronautics and Astronautics, 2012

Author



Anthony P Hays

NATURE AS THE BEST CREATIVE DESIGNER

Stanislav Gorb¹, Anatolii Kretov²

¹ Department of Functional Morphology and Biomechanics, Zoological Institute of the Kiel University
Am Botanischen Garten 9, D-24118 Kiel, Germany
e-mail: sgorb@zoologie.uni-kiel.de

² Nanjing University of Aeronautics and Astronautics, College of Aerospace Engineering,
29 Yudao St., Nanjing 210016, P.R.China
e-mail: kretov-ac@nuaa.edu.cn

Key words: Nature, design, analysis, using, flight vehicles

Abstract. *The work is examined and analyzed examples of some "designs" created by nature in the process of long evolution, which are real models for imitation and admiration. On such samples and examples, young designers can hone their knowledge and accumulate experience in designing truly optimal objects.*

1. INTRODUCTION

A designer is a specialist who creates the construction of some simplest element, mechanism, unit, apparatus, vehicle, including such a complex as a flight vehicle (FV). The designer must have a broad outlook. To learn and improve this skill a person must spend his whole life to study: at school, at university, at his workplace in a design office and even in ordinary domestic life. The objects for such studying, which is essentially the design analysis, can be found infinite set starting from what a person did at the beginning of his existence on the Earth, up to the most sophisticated technical systems.

The design process is an amazing combination of science and art. If the term science is obvious and understandable, then art is a very broad concept. In this case, we mean by art, visual art, that is, the visualization of some created object through some kind of imagination, experience and intuition.

In ancient times, the creators of unique building structures did not have computers, the finite element method, scientifically valid plate and shells theories, optimization theory and other attributes, in which the modern designer needs, like air and water to any living organism. Incredible intuition, a sense of harmony and appeal to natural examples helped the designers of antiquity create masterpieces, which still cause us all admiration. And the so-called component of art was their main. Unfortunately, the complete computerization of the design process keeps pushing the designer away from what we usually call art. But to create something unique, you often need to push aside the usual framework, including the scientific framework. And here, as such an amazing helper for the constructor, nature will act with its unique works.

Many millennia ago a man became a designer, at first to survive, and later - to satisfy his vital interests. His designed objects had been complicated, ranging from a pointed stick in the flame of a fire, to an aircraft with space velocities. In the first case he was helped by forest fires, from which he extracted his first weapon. In the latter case, he compared the aerospace aircraft he created, which is reentering from orbit, with a falling meteorite.

Any object was created (projected) by someone. However, the design philosophy is quite general. The difference in the design is only what requirements are imposed on the object being created, what is used as a role model (a kind of prototype), what level of mastery the designer, what tools can be used for design and many other features. But his majesty the designer-nature remains for the human-constructor the brightest teacher and a good example how need to design



Figure 1: From simple pointed stick to aero-space-craft

The above two examples in Fig. 1 correspond to one-time natural effects. But in this case we are interested in examples related to the evolution of the object, as a result of which some sort of optimization was carried out, and for any person involved in the construction is very useful in understanding this process from the point of view of modern scientific data and his personal experience.

It is not accidental that a new science appeared in the 20th century - bionics, whose purpose is to use in engineering the principles of the structure of biological systems and processes occurring in living organisms.

All samples designed by nature are good and often just ideal examples for the development of design thinking for beginners and for the improvement of already experienced designers.

The designer task in the analysis of natural design achievements is not just to ascertain, but to understand the design of the great designer - nature, in analyzing what was done to try to use a similar idea in FV.

2. MAIN PART

Analysis of natural objects can be performed according to the following scheme:

- the main feature of the analyzed object;
- the object form;
- load-carrying structure;
- using materials;
- kinematic structure.

About the main features

A person is very proud of one of his great inventions – it is a wheel. Nature did not go this route to ensure the movement of its objects. When Nature was creating its compositions, it might seem to her that the coefficient of friction-rolling is quite large, or the realization of this principle with the use of the transmission it turns out to be too complicated. Perhaps that's why nature came up with a very simple implementation of the reactive principle of motion, using a direct reaction. The principle of jet propulsion due to the direct reaction used by jellyfish, octopuses, squid (Fig.2, *a*) by throwing water had been noticed long time ago. The "engine" used by these inhabitants of the seas would be more correctly called a pulsating hydro-jet. One of the first who realized the principle of direct reaction was Heron of Alexandria. One hundred and

twenty years before the beginning of our era he created the first jet steam turbine (Fig.2, *b*). In 1680, Isaac Newton proposed a project of "reactive carriage" (Fig.2, *c*).

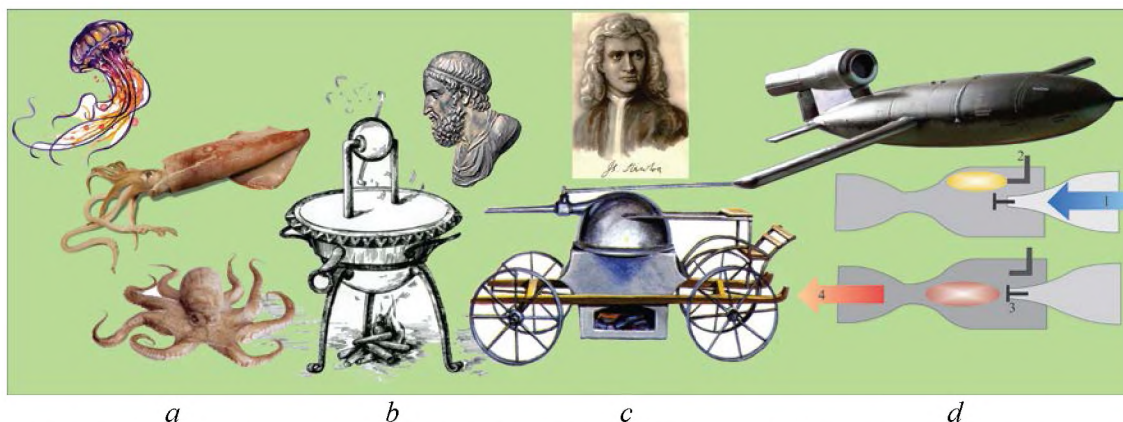


Figure 2: Realization of the principle of jet propulsion: *a* – jellyfish, squid and octopus; *b* – Heron of Alexandria and his jet turbine; *c* – Isaac Newton and his idea of a carriage with jet thrust; *d* – V-1 flare missile and a PWRM operation scheme: 1 – air intake into the combustion chamber; 2 – fuel supply; 3 – ignition of the air-fuel mixture from the spark plug and closing the inlet valve; 4 – flow of combustion products through the nozzle and the creation of a reactive traction force

They say that Swedish inventor Martin Wiberg has a claim for having invented the first pulsejet, but these details are unclear. And Russian inventor and artillery officer N. Teleshov patented a pulsejet engine in 1864.

After 80 years, this type of engine was realized - in 1944 the German cruise missile V-1 (Fig.2, *d*) was completed, equipped with a pulsating air-jet engine with a thrust of 2.9 kN. PWRM, whose operation principle corresponded to the natural analogs shown in Fig.2 *a*. He provided the FV with a starting mass of 2,160 kg, a flight range of about 300 km and a maximum speed of up to 700-800 km/h. Such type of engine is considered to be the simplest. And not for nothing there is a proverb – “All ingenious is simple”.

About an object form

Design is at the same time science and art, it is analysis and synthesis, the search for the original, the new. The study of the forms of living nature nourishes the imagination of artists-designers, gives material and helps to solve the problem of functional harmony and aesthetic principles, enriching the formal means of harmonization in search of the most expressive proportions, rhythm, symmetry, asymmetry, etc. And not for nothing that there is a regularity, which the well-known avia designer Tupolev said – “Beautiful planes fly better”.

As a rule, the form aesthetics of industrial products are closely connected with utilitarian principles, and in nature there is a close relationship between function and form, and this is perceived as a special aesthetic property of living nature. Borrowing from the nature of the design, the designer takes also natural forms that cause certain aesthetic emotions. Natural forms give the product a specific character.

A person does not always immediately understand the plan of nature. For example, it seems to us that the sharp-pointed form from the ship gives it some kind of swiftness. Japanese scientist Tako Inui theoretically and experimentally proved that the pear-shaped form of the whale head is more adapted to movement in water, rather than the knife-like shape of the bow of modern vessels. The tests confirmed that the "cetacean" ship is economical - the power of its engines is 25% less, and the speed and payload are normal. Aviation designers always preferred the drop-

shaped form of aircraft for subsonic speeds, which provides them the less aerodynamic resistance.

Very often, questions of external shape, proportions and sizes are associated with the so-called "golden ratio", which is considered a measure of harmony and beauty.

Infinite series $\varphi=1.6180339887...$. A strange, mysterious, inexplicable thing: this divine number mystically accompanies all living things.

For the first time the term "golden ratio" was described by Euclid in his 2nd book of the "Principles", written in the III century BC, where its geometric construction is given, which is equivalent to solving a quadratic equation of the form $b(a+b)=a^2$.

Nature has divided into symmetrical parts and golden proportions. We see in both the plant and animal world the formative tendency the symmetry with respect to the direction of growth and motion-persists. The golden ratio is manifested in the proportions of the parts perpendicular to the direction of growth – Fig.3.

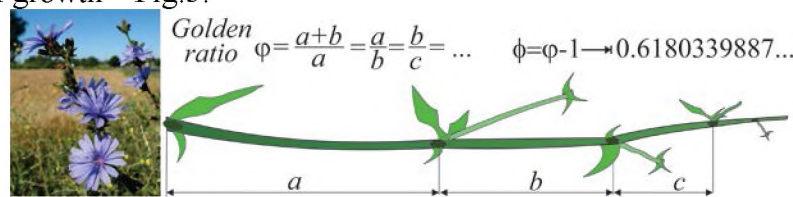


Figure3: Stalk of chicory growing according to the rule of the golden ratio

Without going into the various historical details of the this unique number use in all areas of human activity, we note that in the field of technical design this rule, providing some kind of harmony in form and size, has become firmly established in the designer's for its use. In Fig.4 the projections of fighters with the size a binding to the basic aircraft characteristics (aircraft length, wing span) are shown and the size $b=a/\varphi$ is noted, which can be used for selecting other characteristics.

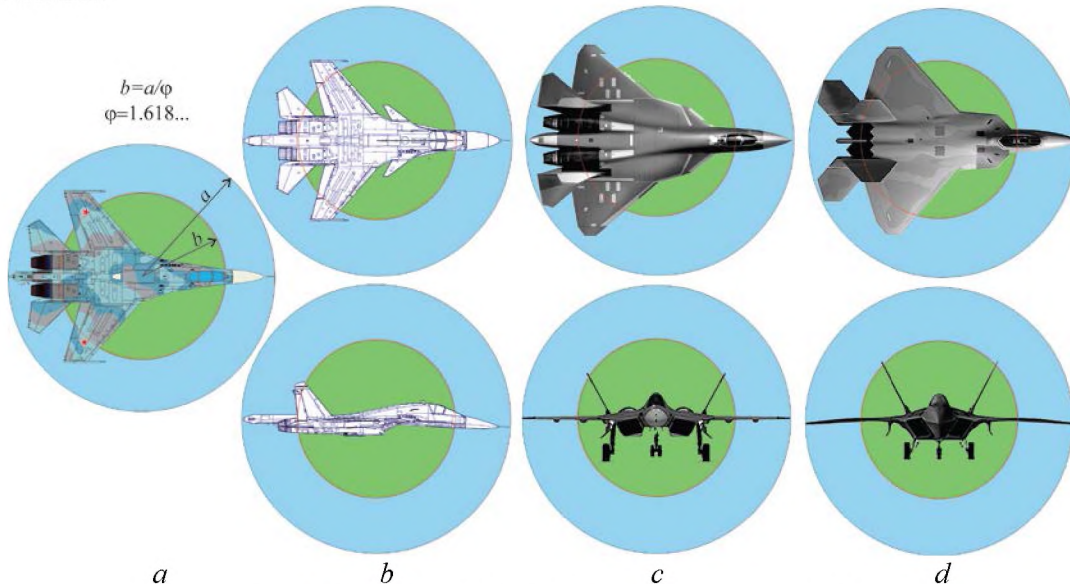


Figure 4: Analysis of aircraft shapes with using of golden ratio:

a – Su-27; b – Su-34; c – T-50; d – F-22

People have long noticed the harmony of forms. One of the first such objects was the five-pointed star. It had been already in the man-made works for about 3000 years ago. The perfect

form of this figure always attracted the attention of a person. The five-pointed star contains a number of golden ratio ratios. And it is no coincidence that the five-pointed stars are on many flags and symbols (Fig.5).

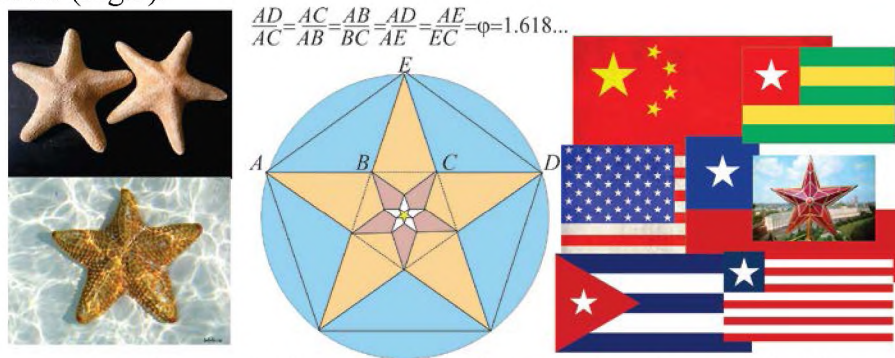


Figure 5: Five-pointed star in nature, in science and in life

If we analyze the newest fighter of the 5th generation J-20 in terms of the proportions available in the five-pointed star, we will see how its external shape fits well with this amazing geometric figure.

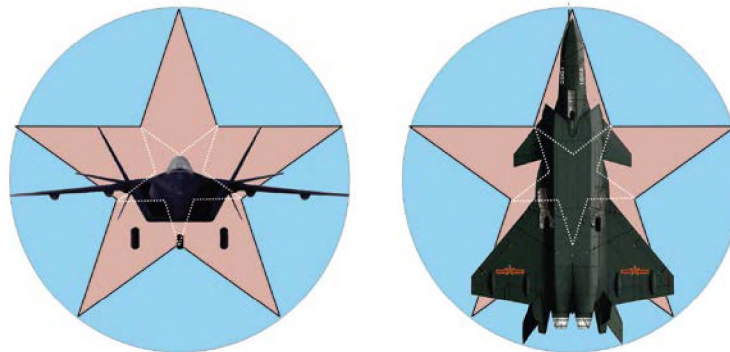


Figure 6: Geometrical analysis of fighter J-20 shape

Creating the interior designers must take into account the aesthetic side of the object, for example, when creating a crew cabin or passenger cabin. This makes not only an attractive interior, but also provides an opportunity for comfortable accommodation of the crew, passengers, provides the best conditions for work and leisure - Fig.7.

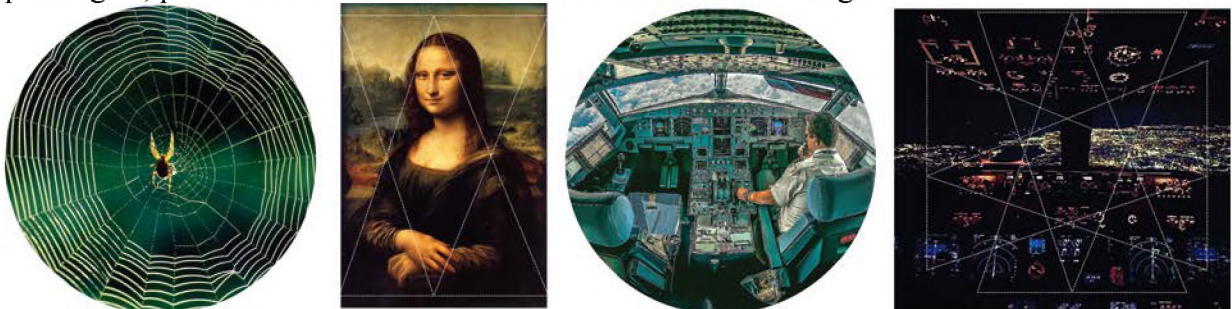


Figure 7: Geometric proportions in nature, painting and interior of the cabin of a passenger liner

And it is not by chance that good designers, as a rule, are not indifferent to nature, they can paint themselves well, they know and understand painting well. One of the most striking examples of this is Leonardo Da Vinci - a great painter and no less than a great designer.

About load-carrying structure

One of the main rules of the aircraft designer is the rule that the design must have a minimum mass and must carry the maximum load.

The most striking examples of such a rule are the structures of the bones in birds.

The human skeleton is also an example of a rational relationship between the weight and strength of a structure.

In the middle of the 19th century, the Swiss professor Hermann von Mayer investigated the bone structure of the femoral head. The head is covered with a network of miniature partitions with a strict geometric structure, so it does not break down under the weight of the body.

And then, twenty years later, being impressed by this research, Gustav Eiffel created the design of the famous tower. As a basis, he took the proportions of the human tibia, but his creation weighs 9,000 tons and rises by about 300 meters.

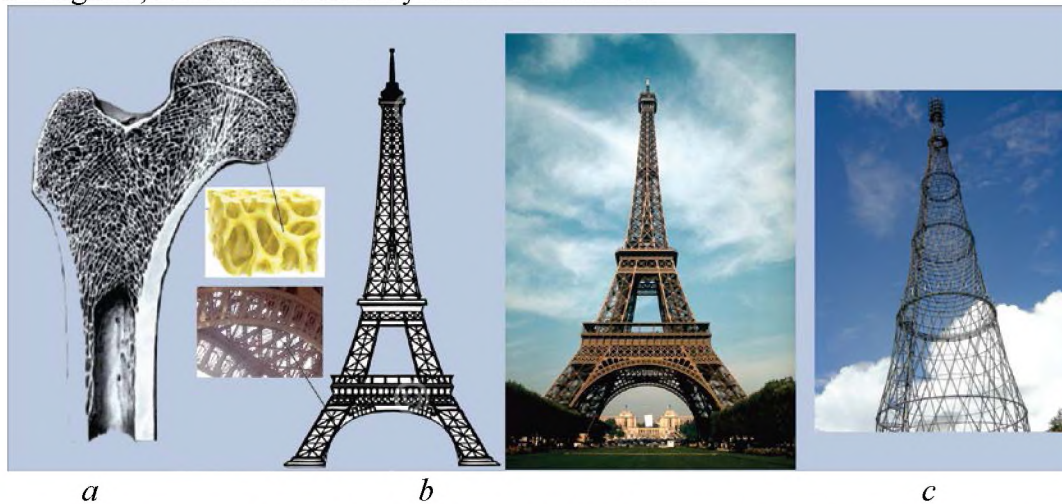


Figure 8: The rational constructions of nature and man:
a – the femur bone and the spongy structure of its head; *b* – Eiffel Tower in Paris with a fragment of the design; *c* – the tower of V. Shukhov in Moscow

The French engineer had many followers. Russian engineer Vladimir Shukhov also created the tower in Moscow on the basis of the human skeleton structure. Originally it was planned that the height of the tower would be more than 300 meters, but the quantity of metal had to be in three times less than the consumption of the tower in Paris. But due to deficit of metal, the tower was built only 150 meters high.

The designer, analyzing aircraft, first of all draws attention to the mass of the structure, which ensures the perception and transmission of the current load to the total mass

$$\mu_s = m_s / m_0$$

where m_s is the mass of load-carrying structure, m_0 is the total mass.

The human skeleton mass is about 10% of its total mass. Rare aircraft have such a unique design. One of the heaviest flying birds is considered a bustard, its mass reaches 20 kg, while the mass of its skeleton is only 110 g.

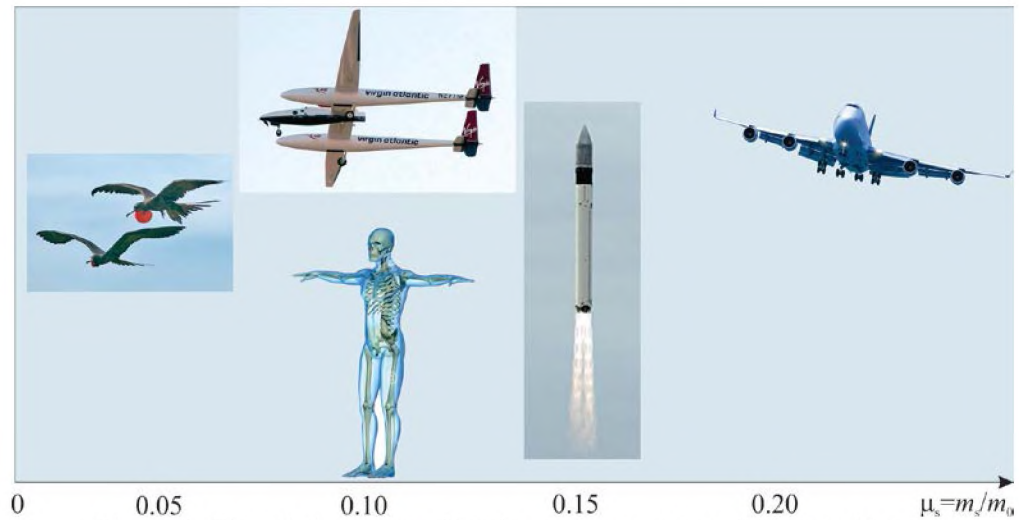


Figure 9: The relative mass of load-carrying structure different objects: birds, human, aircraft, rocket

Minimizing the mass can reduce the rigidity of the structure. In Fig. 8, we have already given an example of a beautiful solution of nature to provide the necessary strength and rigidity of human bones. In 1930 years, aircraft speeds began to grow and aircraft designers encountered the phenomenon of dynamic aeroelasticity of winged structures. There were numerous victims before the reason for the destruction of the structure became clear. This was due to self-oscillations of the flutter. The designers have learned to overcome this problem, in particular, by shifting the center of mass forward due to the installation of special anti flutter loads Fig.10

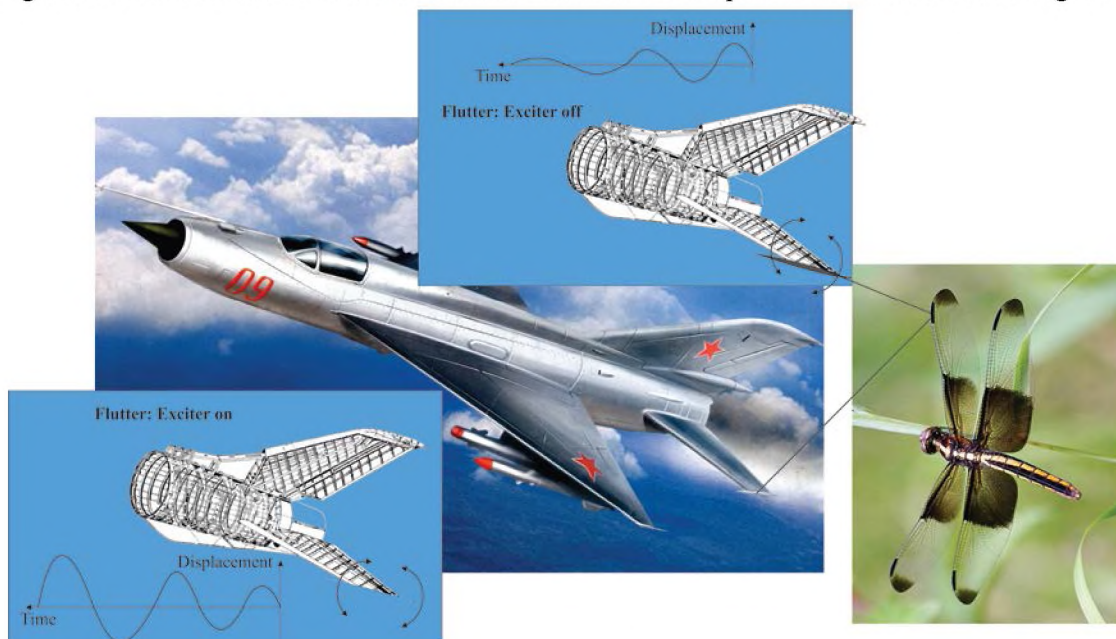


Figure 10: Means of combating with flutter on the wing of a dragonfly and on the whole-feather plumage

The brightest examples of an amazing natural construction are bee honeycombs – hexahedral prisms, arranged in parallel rows. Each row of bee cells is laid with a "dressing", as masons do, building a brick wall.

Only in 1930, the man developed this idea in a sandwich panel, which is a three-layer structure consisting of the upper and lower skins and the honeycomb layer between them. American architect Frank Lloyd Wright proposed such sandwich panels in building structures. The main idea of this invention was a combination in panels of lightness and high rigidity.

In the 1940s thin plywood hulls and fuselage with honeycomb filling were already used in the design of the English airplane De Havilland "Mosquito". In 1944, after the appearance of the phenolic glue, the first all-metal glued laminated panels with a honeycomb (honeycomb) filler were made.



Figure 11: Manufacture of honeycombs by bees, humans and their application in honeycomb panels on airplanes Mosquito and B-58

Often the elements of small thickness are completely filled with honeycombs: rudders, ailerons and all-turning tail planes of supersonic aircraft. The largest number of honeycomb panels from the total weight of the aircraft structure was used in the B-58 bomber.

Their application gives a number of advantages over solid structures: low mass and high rigidity; specific static strength is greater by 20-40%; stability at longitudinal compression is 2-4 times higher; the number of parts entering the assembly or assembly is 3-4 times less; more smooth surfaces of assemblies and units; thermal insulation properties are 3-5 times higher; acoustic characteristics are better by 3-5 times.

But the designer should also understand their shortcomings: the complexity of quality control of the glued joint of the skin and the honeycomb core; accumulation of condensate inside the panel, which can lead to acceleration of the corrosion process; relatively high manufacturing cost; labor intensity of manufacturing and design is more by 15-20%.

About using materials

The natural materials, in particular the composites, are amazing. One of the brightest representatives can be a tree, a plants. An ancient man used first the idea of composite materials when he added to clay bricks the straw. Such brick had been lighter and strengthen. The construction of a modern passenger liner consists from already 50% complete with composite materials.

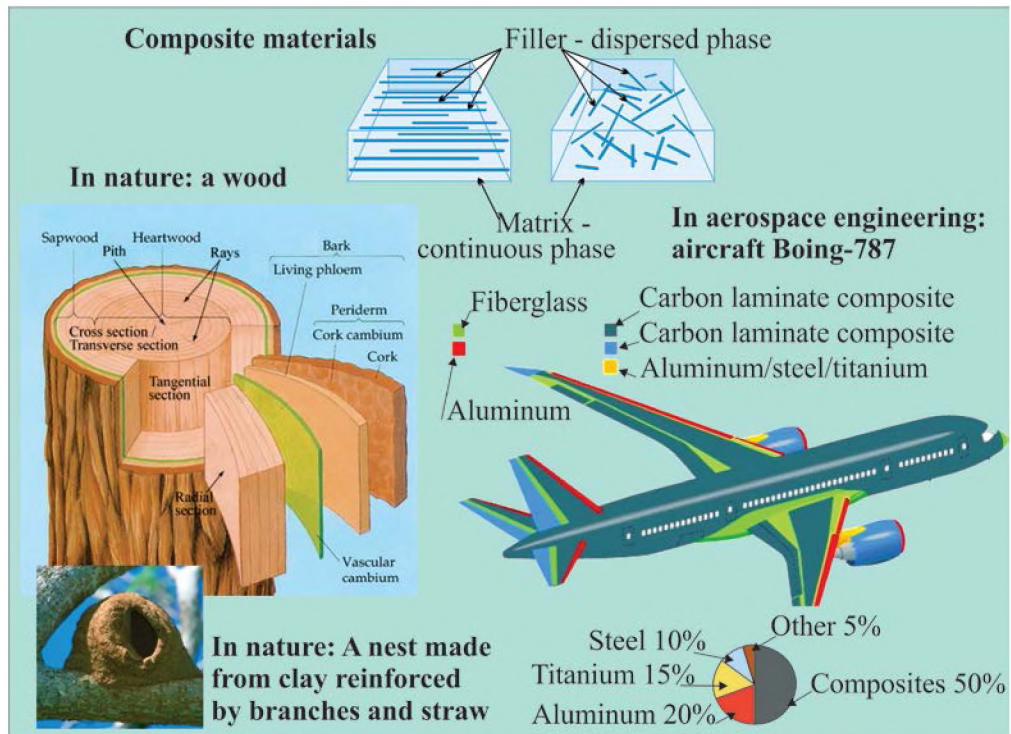


Figure 11: Composite materials in nature and in engineering

Nanotechnology, which has become one of the most innovative sciences, has good patterns in the example of materials created by nature – Fig.12.

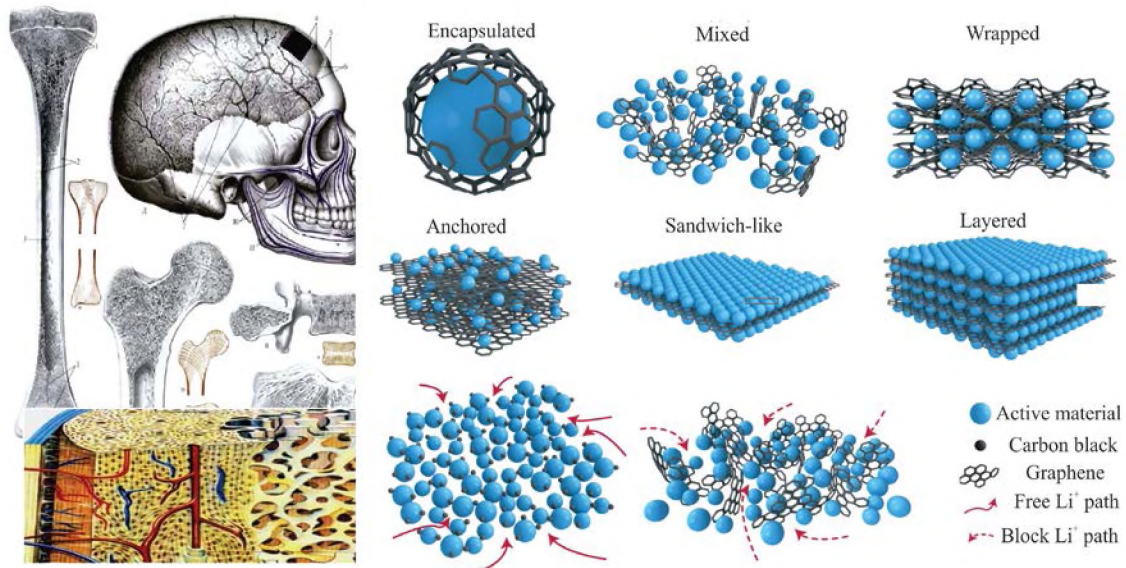


Figure 12: Create new materials from nanotechnology, using nature's experience.

About kinematic structure

The real treasure for kinematic-related developers is the natural analogies - Fig.13.

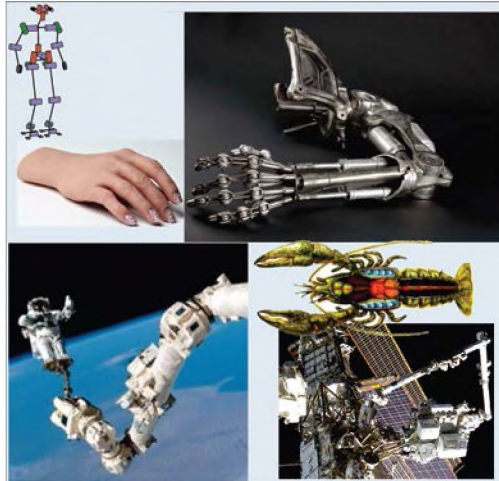


Figure 13: Kinematic samples for modeling and thinking for

3. CONCLUSIONS

Students who have made their choice of science to follow on new unopened paths often ask themselves-what can be opened when everything is almost open? The examples cited show some of the ideas and approaches that have been taken from nature. And that's just a small part of what's used. As experience in recent years has shown, the most striking discoveries occur at the crossroads of different Science. In this regard, one of the shores of such a course is nature, with its examples and millions of evolutionary experiences.



Figure 14: Design is art and science

Authors



Stanislav Gorb



Anatolii Kretov

APPROACHES TO THE CHOICE OF CONSTRUCTIONAL MATERIALS OF AIRPLANES

Oleksandr Moliar*, Shasha Zhang, Pingze Zhang, Zili Liu, Qiang Miao, Zhengjun Yao

Nanjing University of Astronautics and Aeronautics, College of Material Science and Technology

211106, Jiangsu, Nanjing, P.R.China

e-mail (*– Corresponding author): molyar.olekcandr@i.ua

Key words: Design, materials, company Antonov

Abstract. *The work focuses on the most important issue of design aircraft – selection of structural material that largely determines the success of any project. This problem is discussed on the examples of Antonov Company.*

1. INTRODUCTION

In modern aircrafts such as planes, helicopters and rockets, hundreds of categories of materials are utilized for different functional purposes. For the leading world aircraft manufacturing company Antonov during different time frames, the ratios between various materials, which are used for the manufacture of subsonic airplanes, are unequal (Fig. 1). However, the ratios don't differ obviously from An-32(1976) to An-178(2015).

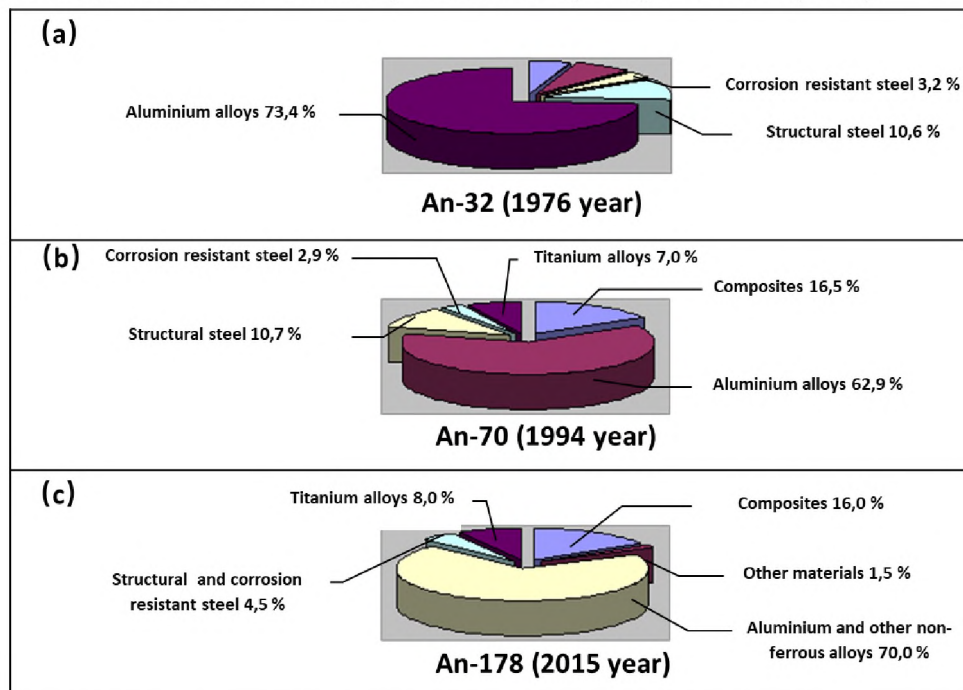


Figure 1: The main materials applied on the Antonov planes during different periods of their creation (in the brackets there is the year of the first flight)

2. MAIN PART

As shown in Fig. 1, the main constructional material (65-75%) is aluminum, more precisely its alloys for many years. Except aluminum alloys, structural (middle- and high-strength) and corrosion resistant steels (8-10%) and titanium alloys (3,5-8,0%) are take a noticeable place as the structural materials for airplanes. The fraction of magnesium alloys in the application of aviation constructions decreases in recent years due to their low corrosion resistance which fails to satisfy the increase of airplane lifetime. On the other hand, the fraction of titanium alloys in the use in aviation increases for the superior corrosion resistance. The volume fraction of composite materials increases significantly, which include nonmetallic and, to a lesser extent, metallic matrix. The composite materials make up to 20% of the airplane weight according to the estimate from most of the aircraft manufacture companies in the world. For example, the weight fraction of carbonic and epoxy composite is 50% for the Boeing 787 Dreamliner, which is the record in use of the composition materials so far.

In terms of the material choice for different components of the airplane, first of all, we need to pay attention to the mechanical strength and rigidity with the minimum mass, which gives hint on the maximum weight efficiency of the materials. The weight efficiency of material is estimated by the specific strength of σ_B/ρ , specific rigidity of E/ρ and specific crack resistance of K_{Ic}/ρ , where σ_B , E , K_{Ic} and ρ are the tensile strength, elastic modulus, fracture toughness and fracture of the materials, respectively.

From the physical point of view, the specific strength can be described as the maximum length that the material fails in the force of gravity of Earth (gravity constant, 9.8 N/kg) without other loadings, and is measured in length, as described by Eq. 1:

$$\left[\frac{\sigma_B}{\rho} \right] = \left[\frac{9.8 \cdot \text{kg} / \text{mm}^2}{\text{kg} / \text{m}^3} \right] \approx 10^7 \text{m} \quad (1)$$

When analyzing the operating conditions of the airplane in details, it is possible to draw a conclusion that most of them work in the conditions of other forces beyond gravity. To compare two different materials in the case of such loadings, the ratio of their masses will be expressed by:

- under the terms of strength

$$\frac{m_1}{m_2} = \left(\frac{\sigma_{B2}}{\sigma_{B1}} \right)^{2/3} \cdot \frac{d_1}{d_2} \quad (2)$$

- under the terms of rigidity

$$\frac{m_1}{m_2} = \left(\frac{E_1}{E_2} \right)^{1/2} \cdot \frac{d_1}{d_2} \quad (3)$$

and the ratio of sections of two components under the load will be:

$$\frac{\delta_2}{\delta_1} = \left(\frac{E_1}{E_2} \right)^{1/4} \quad (4)$$

where m_1 and m_2 are the masses; d_1 and d_2 are the diameters; E_1 and E_2 are the elastic moduli; δ_1 and δ_2 are the sections of the first and second components, respectively.

A comparison of the generalized characteristics of different materials in the application of aviation constructions is shown in table. 1. The application temperature is 20°C. It is indicated from table 1 that the specific strength and rigidity properties of the composite materials essentially exceed the traditional alloys.

Table 1. Comparative characteristics of the materials applied in aviation constructions

Material	Density ρ , kg/m ³	Strength σ_B , MPa	Elastic modulus E , GPa	Specific strength σ_B/ρ , km	Specific rigidnes E/ρ , km
Aluminums alloys	2700	400-650	72	14,8-24,0	26500
Magnesium alloys	1800	200-340	45	11,0-18,9	25000
Titanium alloys	4500	500-1300	120	11,0-29,0	26600
Middle- strength steels	7800	800-1300	210	10,3-16,7	27000
High-strength steels	7800	1300-2300	210	16,7-29,5	27000
Composites	1400-2600	500-1300	35-250	40-60	25000- 100000

In view of modern airplanes (including hyper acoustic) and also engines and rockets which work in the conditions of increased temperatures, it is often necessary to consider material properties at high temperatures. The dependence of tensile strength on temperatures for the main constructional materials is shown in Fig. 2.

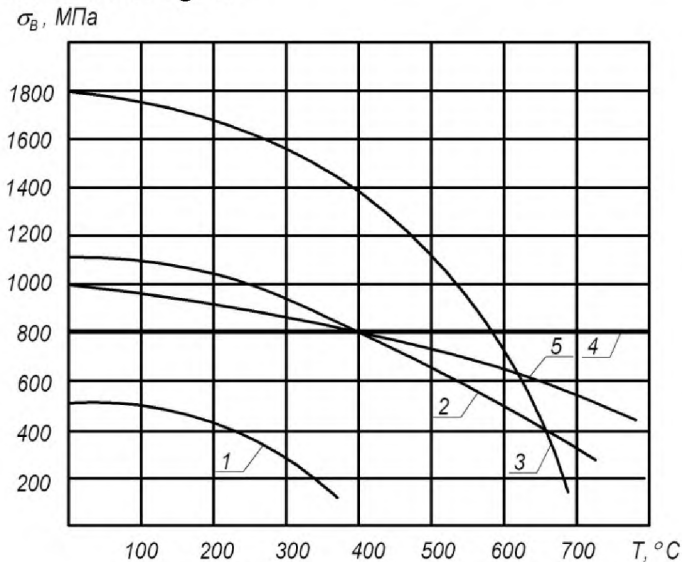


Figure 2: The dependence of the tensile strength (σ_B) of the main constructional materials on temperatures (T): 1 – aluminum alloys; 2 – middle-strength steels; 3 – high-strength steels; 4 – nickel super alloys; 5 – titanium alloys

The effect of temperature on the properties of aerospace materials can be illustrated more evidently by the "specific strength-temperature" dependence (Fig. 3). The provided characteristics demonstrate that up to the temperature of 150°C the specific strength of even dilute ($\alpha+\beta$) TC4 titanium alloy exceeds those of aluminum alloys and steels. In the temperature

interval of 300-500°C, the maximum specific strength belongs to another ($\alpha+\beta$) titanium alloy (TC18), which already exceeds that of the high-strength steels. It is indicated that titanium alloys are more effective than other constructional materials applied in aircraft constructions at high temperatures.

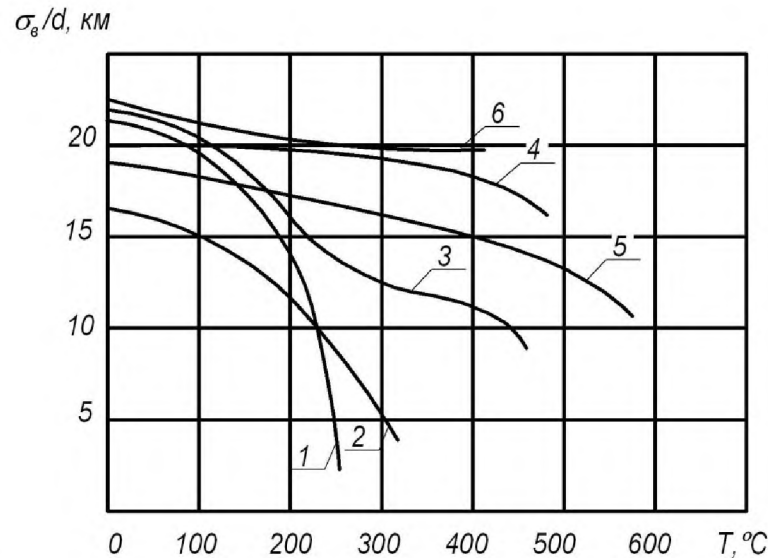


Figure 3: Dependence of the specific strength(σ_b/ρ) of structural alloys on temperature (T): 1 -7075 aluminum alloy; 2 – 2024 aluminum alloy; 3 – TC4 titanium alloy; 4 – structural steel 30Cr-Mn-Si; 5 - VNS-2 corrosion-resistant steel; 6 - TC18 titanium alloy

The "specific strength–temperature" dependence provided in Fig.3 demonstrates that material strength can decrease sharply as the increase of the temperatures. Therefore, the effect of temperature on the properties of materials needs to be considered when calculating the constructions. Besides, for the materials working at the increased temperatures it is also necessary to consider high-temperature creep property which demonstrates the change of the sizes in details under permanent loading which is sometimes much lower than the limit of material flow ability.

In order to understand approaches to the choice of materials for an airplane, it is necessary to know how its basic components work. The airplane can be conditionally divided by five basic parts: fuselage (that, in turn, divide into nasal, middle and tail parts), wing, plumage (horizontal and vertical), undercarriage and systems (management by air, hydraulic, fuel, air). Each of these parts bears loadings (always fatigue) during service. These loadings determine the choice of material for their making.

The fuselage is traditionally made from aluminum alloys: a covering and a longitudinal force set is made from 2024 aluminum alloy, whereas a cross force set is made from B93, B95 (7075), 1933 high-strength alloys. The unit loads on the fuselage (except the central part) are insignificant. Special attention is paid on the assembly technique in the underground part of the fuselage where the maintenance of the corrosion damages is most important.

The wing suffers all loadings as from airplane weight, and wind (from influence of air flows). At the same time the wing works so that its upper surface is in an oblate status, and the lower part is in expanded. Therefore, the upper part of a wing is made from high-strength 7075 aluminum alloy which has the maximum specific durability among the aluminum alloys serial, and lower surface is made from of 2024 aluminum alloy which has higher property of fatigue resistance. In

recent years the study of B96Ts3 high-strength alloy for manufacture of the upper part of a wing is carried out (generally on increase in plasticity and fatigue resistance of the alloy).

The front edges of a wing and plumage, which are warmed for frosting warning, are made from AK4-1 aluminum alloy which is less strong than 2024 aluminum alloy but can be stable at more high temperatures. The 6013 alloy used by the last planes demonstrates high processing performance comparing with AK4-1 alloy.

Wheels of control of airplane (on a wing and plumage), proceeding from conditions of the maximum rigidness (the minimum elastic deformations under deflection), are made from high-modular carbonic composites.

Plumage can be assembled by aluminum alloys, following the same approach to the choice of materials for a wing. On some planes (An-70) plumage represents integral construction from carbonic composite that provides considerable weight effect. The composites with polymeric matrix are also utilized to form fairings of wing and plumage, chassis and so on.

As it was told above, the main criteria for the choice of constructional materials, for example aluminum alloys, are their specific values of strength, rigidness and fatigue. Nevertheless, corrosion which is, as a rule, shown in constructions after 10-20 years of maintenance of the airplane also makes the demands to designing. At the design moment, the corrosion damage to be removed has been considered. Therefore, there exists the conflict between the anticorrosive requirements and the aspects of strength, maintenance (simplicity of service) and cost. A compromise is necessary at the design stage in case of the choice of materials. It is possible to confirm this consciousness with a classical example of the evolution of the anticorrosive properties and strength of aluminum alloys as the increase of the aging hardening temperature (Fig.4).

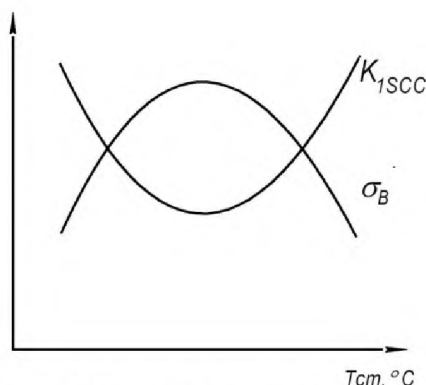


Figure 4: Dependence of the corrosion cracking (K_{1SCC}) and strength (σ_B) depending on the aging temperature (T_{cm}) of aluminum alloys

As shown in Fig. 4, the maximum strength of the alloy corresponds to the minimum corrosion resistance. The alloy requires before aging or after aging temperature for the aging hardening treatment in order to obtain a compromised corrosion resistance and strength properties. In case of a construction material choice from the point view of anti-corrosion properties, it is also necessary to consider an electrochemical potential of the contacting materials, types and coating possibility of protecting covers, operating conditions and so on.

Chassis bears considerable dynamic loads in case of take-off and, especially, plane landing. In case of the necessary minimum sizes of a unit (stands of the chassis need to be removed from outside circuits of the airplane to reduce the aerodynamic resistance) aluminum alloys fail to satisfy the requirement of the mechanical properties. Therefore, the units of the chassis are made from high-strength titanium alloys (TC18) or high-strength structural steels (30Cr-Mn-Si-Ni,

VKS170, VKS210). And titanium alloys as new construction material have superior corrosion resistance properties as well, which was mentioned earlier.

The systems of the airplane perform different functions which superimpose the requirements to the material choice for their manufacture. For example, the airplane steering wheel, the wheel column and pedals can't be miniature as the pilot shall feel control. Loads of these components are insignificant so that they are traditionally made from cast magnesium alloys having the minimum specific weight and the specific strength is sufficient for these components. The corrosion resistance for such components isn't critical. In the latest models of the airplanes, the steering wheel is made from polymers by Rapid Prototyping method. Now this method is used also for manufacture of the airplane metal components.

Pipelines of the airplane air system through which hot air is transferred (temperature up to 350°C) from the engine to front edges of the wing and plumage, it is possible to process thin-walled pipes from corrosion resistant steels or titanium alloys. As titanium has the smallest coefficient of linear thermal expansion among metals ($\alpha = 9 \cdot 10^{-6} \text{ } ^\circ\text{C}^{-1}$), low density of $\rho = 4500 \text{ kg/m}^3$ and quite high strength of $\sigma_b = 600 \text{ MPa}$ (for PT-7M alloy, Ti-2,5Al-2Zr), it is the optimum material for manufacture of the lengthy units working in the conditions of thermocycles (from -60°C to +350°C) and the titanium alloys are attached to a "cold" frame. In this case the minimum quantity of compensators which remove thermal loadings from "frame" are required. The minimum thickness of the wall of a pipe is restricted to the technological capabilities. The weight of titanium pipelines is less comparing with steels.

3. CONCLUSIONS

From the given examples it is possible to draw a conclusion that the choice of materials for parts and units of the airplane is determined by their design feature, working conditions, external factors, including corrosion and thermal, and is a creative process which requires, to the same extent, knowledge of both properties of materials and construction of the airplanes.

Presenters



Oleksandr Moliar



Shasha Zhang

ECONOMIC EFFICIENCY OF AIRCRAFT WITH AIR CUSHION LANDING GEAR

Morozov Victor¹, Cong Zhang²

1 – Novgorod State Technical University named after R.E. Alekseev, Institute of Transport Problems, Nizhny Novgorod, 603035, Russia

2 – Nanjing University of Aeronautics and Astronautics, 211106, Jiangsu, Nanjing, P.R.China

e-mail: 1 – vpmorozovnn@mail.ru; 2 – unwto@126.com

Key words: Transport efficiency, ACLG, Economic feasibility

Abstract: *The economic feasibility seems a major disadvantage to the ACLG aircraft, this paper compare ACLG aircraft with traditional general fix wing aircraft and helicopter in terms of mission flexibility, operation and field requirement to show the economic feature and impact item of those aircraft. Result shows ACLG aircraft have more economic advantage than other aircrafts when there is undeveloped airdrome infrastructure.*

1. INTRODUCTION

The problem of aircraft economic analysis with air cushion landing gear (ACLG) is that it can be hardly limited to one aspect of work since takeoff mass various from light vehicles-1.5t to special heavy aircraft, such as An-225 “Mriya”. The common tendencies in aviation are known as with increase of aircraft takeoff mass, economic efficiency of passenger and cargo transportation grows. Therefore, this article concentrates attention on light aircraft. In the Soviet Union, this category of aircraft has been incorporated with the concept “application of aircraft in the national economy (AANE)”.



Figure 1: ACLG Aircraft “Dingo”

Now in Russia, the international term “general purpose aviation” (GPA) is used. It unites

approximately the same class of aircraft as AANE. Showing the economic feasibility of ACLG aircraft as GPA, it is also good to assume similar conclusions for special heavy aircraft as well. This article widely uses the “Dingo” ACLG aircraft (Fig.1) as research object, in which several researches have been conducted. Further, landplanes with wheeled landing gear will be called “classical aircraft” in this paper.

2. NUMERICAL ANALYSIS BETWEEN ACLG AIRCRAFT AND CLASSICAL AIRCRAFT

The ACLG aircrafts are not an exclusive type, their flight performance are in the range of classical aircraft. Aviation plays the leading role in mobile high speed transportation system. Comparative advantages of aviation over other ground transports are shown in Table. 1.

Table 1. Comparative characteristics of transport means

Characteristic	Car	Railway system	Regular air system	GPA
Flexibility of operation	High	Low	Low	High
Speed	Low	Low	Low	High
Profitability	Economic	Economic	Economic	Economic
Safety	Low	High	High	High

The economic efficiency of ACLG aircraft is determined on the base of the following properties:

1. Unprecedentedly low requirement to takeoff – landing field, practical independence from runway type and surface condition (unpaved, water, ice, snow, mixed including marshy areas, shallows, etc.)
2. High efficiency (readiness to perform operation in the wide range of weather conditions) and the lowest operational expenses in the regions with undeveloped aerodrome infrastructure
3. Optimum combination of takeoff/landing and in flight performance, and kilometric fuel consumption similar to consumption of landplanes
4. Possibility of maintenance using the existing infrastructure of civil aviation

The specified features of ACLG provide a steady operation performance; low expenses for preparation of aircraft increases flying hours and by using mixed ACLG aircraft fleet, result in a low operating expense.

Now considering the efficiency assessment of the “Dingo”, the aircraft applied to the regions of Yakutia, Komi and Nizhny Volga Region in the interest of the following branches:

- a. Transport (passenger and cargo transportation)

- b.* Oil-and-gas industry (maintenance of derricks, flying around oil-and-gas pipes, delivery of repair teams)
- c.* Power engineering (flying around electric power lines, delivery of repair teams)
- d.* Agriculture (service of deer-breeder and fishermen, agrochemical operations)
- e.* Forestry (flying around the forests, forest protection, calculation of total number of wild animals)
- f.* Hunting farms (service of hunters - fieldsman)
- g.* Geology (service of geological stations, geologic survey)
- h.* Hydrometeorology (service of stations, aero photography)
- i.* Sanitary aviation (health service of the remote areas, disinfecting of territory)
- j.* Veterinary service (service of deer-breeding and fur-farming farms)
- k.* Militia and Traffic Control Inspection (patrolling)
- l.* Natural life guard (patrolling of water territories and industrial zones)

In Yakutia and Komi, the majority of operations are carried out by the helicopters Mi-2 and Mi-8, in Nyzhny Volga by the helicopters Ka-26. The An-24 aircraft is used, mainly, for patrolling or communication between small settlements having unpaved runways. Application of helicopters, in most cases, is defined by necessity of delivering passengers and cargo to inaccessible and undeveloped areas such as taiga, tundra and deltas area of rivers and land on the platforms selected from air. The main disadvantage of the helicopters is high flight cost (3-5 times higher than that of An-2) which has sharply affected their use nowadays. Range and coverage of the area served are of great importance for extensive territories of Yakutia and Komi. The helicopters have much less range than aircraft. Because of insufficient operative zone of helicopters and impossibility for An-2 to landings on unprepared platforms, there are inaccessible territories for service by air vehicles.

Patrolling of gas and oil pipes and electric power lines, as a rule, is carried out by An-2 aircraft. Helicopters are used for delivery of repair teams to a site of an accident. The similar technology of "aircraft – helicopter" operation is used for protection of forest, deer pastures and water areas, for service of fishermen, hunters and deer-breeders. Thus, it is required to have two types of airborne vehicles that result in additional expenses. Under these conditions, the advantages of the ACLG aircraft "Dingo" which combines the quality of aircraft and helicopter (from the stand point of landing on unequipped platform) are represented.

The main economic parameter of aircraft is the specific cost per flight hour at delivery of cargo or passengers, or at performing any operation. The cost of ACLG aircraft flight hour (C_{FH}) is determined by calculation of operating items:

- 1. aviation combustible-lubricant materials – E_F
- 2. amortization of aircraft fleet - E_{AM}
- 3. running repair of aircraft – E_{RR}
- 4. wages for all personnel – E_W
- 5. deduction for social insurance – E_{IN}
- 6. airport charges – E_A

The specific cost of flight hour is determined as the sum of the items stated above referred to trip efficiency:

$$C_{FH} = (E_F + E_{AM} + E_{RR} + E_W + E_{IN} + E_A) / C_P M_P V_B \quad (1)$$

where, C_P – coefficient of payload, M_P – maximum payload, V_B – block speed. All components are calculated according to the procedures accepted in aviation. Results of calculation of flight hour cost for the “Dingo” ACLG aircraft and its items in comparison with other types of aircraft are given in Table.2. The analyses of calculations are listed below:

- specific expenses on combustible and lubricant materials for the “Dingo” aircraft are comparable with fuel expenses of An-2 aircraft and Ka-26 helicopter and 1.25-1.26 times less than for other types of helicopters
- specific expenses for amortization are on a level with Mi-2 helicopter but significantly higher than for An-2 and 2.4-4.6 times less than for Mi-4 and Mi-8 helicopters (it is worth noting that if An-2 was created and constructed now, his amortization expenses would be identical with the “Dingo”)
- specific expenses on running repair for the “Dingo” is on the level with An-2 aircraft and 2-3 times less than for the helicopters
- specific expenses for wages for the ACLG aircraft are accepted in view of one pilot onboard

Total expenses for flight hour (cost of flying hour) in comparison with An-2 depending on the range of non-stop flight, for the “Dingo” ACLG aircraft: in Yakutia – 129... 120 %, in Komi – 137... 127 %, in Nizhny Volga Region – 142... 154 % from the level of An-2 aircraft. While for the helicopters, these expenses amount to:

Yakutia:	Komi:
Mi-2 - 168...164 %	Mi-2 - 157...156 %
Mi-4 - 256...244 %	Mi-4 - 270...258 %
Mi-8 - 383...374 %	Mi-8 - 407...394 %
Ka-26 - 143...142 %	Ka-26 - 132...131 %

In Nizhny Volga Region: Ka-26 - 148...145 % of expenses level of An-2 per 1 flight hour.

Thus, by the results of the calculation, the cost of one flight hour for the “Dingo” compare with other vehicles operated in the given regions shows 75 % of flying hour cost for Mi-2 helicopter, 50 % for Mi-4, 38,8 % for Mi-8, 86,9 % for Ka-26 and 124 % for An-2.

Estimated calculation of economic efficiency of the ACLG aircraft operation on Yakutia and Komi regions shows that the “Dingo” will successfully compete practically with all kinds of airborne vehicles used there. It is necessary to note, that comparison was made under equal conditions without taking into account the influence of operation qualities of “Dingo”. Further, this paper will show ACLG aircraft more effective than landplanes and seaplanes used in the

specified areas thanks to its insensitivity to runway conditions and weather conditions. It is obvious, for a high level of cross-country ability it is necessary to “pay” by increased mass of aircraft structure and some deterioration of flight performance. It is more convenient to represent the result as diagram, which is shown in Fig. 2.

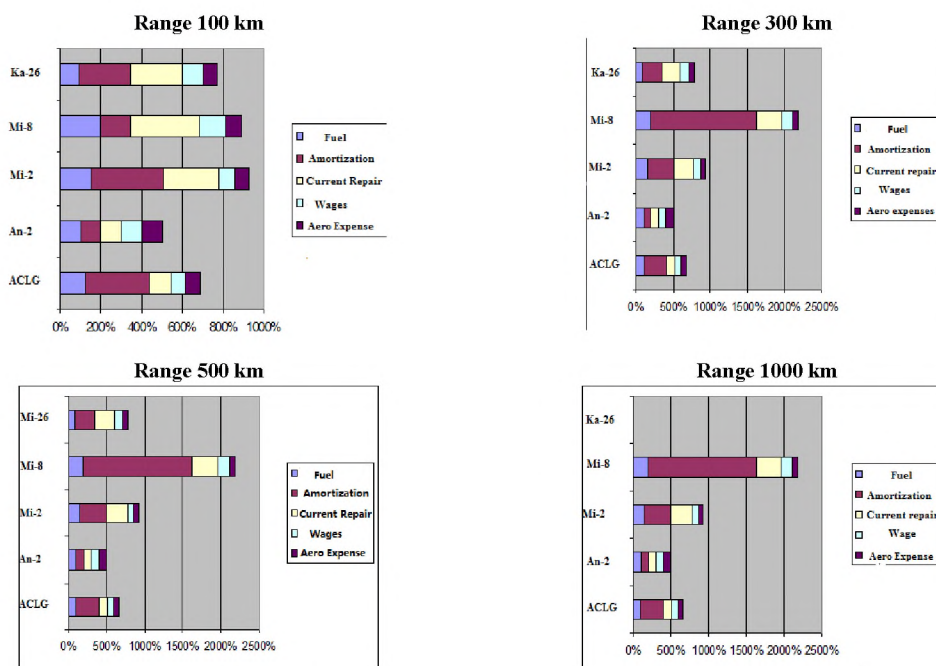


Figure 2: Comparison of items of flying hour cost for the ACLG aircraft and similar aircraft types in Yakut

Fig. 2 shows that the “Dingo” ACLG aircraft is rather closes, by level of expenses, to conventional An-2 aircraft. It is necessary to pay attention to increased amortization expenses of the ACLG aircraft and Mi-8 connected with high cost of these vehicles. Considering An-2 modification with turboprop engine (An-3 version) and the higher price would change the character of the diagrams shown as An-2 is comparable closely to the “Dingo” ACLG aircraft. The main principle of the ACLG aircraft creation is the development of such design which would provide conformity of technical, production and operational characteristics with the criterion level of modern aircraft. In other words, what exclusive cross-country ability would not the “Dingo” ACLG aircraft only have, its flight, weight, operational and technological characteristics should meet the requirements of the time. To meet the modern requirements would not be possible, if in the early stage the coordination of landing gear with airframe was not observed at the stage of aero-hydrodynamic concept design. Observance of this principle is the key moment for the “Dingo” project, distinguishing it from all early created experimental ACLG aircraft (An-14Sh, An-714, -Russia, Lake-4, Buffalo, CC-115, Canada and USA). It is allowed to create aircraft with satisfied characteristics. So, for example, the lift-drag ratio of the “Dingo” is about 11 corresponds to or even higher than that of popular aircraft such as An-2, “Yak-18T” and “Cessna-Caravan”. The load ratio is a little bit lower than at “Cessna”, however, surpasses the similar parameter of a modern amphibian “Sea Star”.

Table 2: Comparison of economic parameters of ACLG aircraft with existing types of aircraft by regions (by the cost of 1 flight hour relative to cost of that of An-2)

Region	ExpenseItem	Route Length																					
		100 km						300 km						500 km						700 km		1000 km	
		ACLG	An-2	Mi-2	Mi-8	Mi-4	Ka-26	ACLG	An-2	Mi-2	Mi-8	Mi-4	Ka-26	ACLG	An-2	Mi-2	Mi-8	Mi-4	Ka-26	ACLG	An-2	ACLG	An-2
Yakutia	Fuel	1.20	1.0	1.51	2.00	1.95	0.90	1.07	1.0	1.50	1.92	1.74	0.91	1.02	1.0	1.47	1.85	1.63	0.93	0.99	1.0	0.97	1.0
	Amortization	3.15	1.0	3.57	14.3	8.18	2.55	3.07	1.0	3.55	14.3	8.21	2.56	3.05	1.0	3.54	14.4	5.22	2.56	3.03	1.0	3.02	1.0
	Current Repair	1.08	1.0	2.74	3.37	2.17	2.54	1.08	1.0	2.74	3.37	2.17	2.54	1.08	1.0	2.74	3.37	2.17	2.54	1.08	1.0	1.08	1.0
	Wages	0.71	1.0	0.75	1.32	1.05	1.00	0.81	1.0	0.83	1.50	1.18	1.11	0.79	1.0	0.80	1.46	1.15	1.07	0.79	1.0	0.79	1.0
	Airport Expense	0.70	1.0	0.74	0.74	0.74	0.74	0.70	1.0	0.73	0.73	0.73	0.73	0.70	1.0	0.73	0.73	0.73	0.73	0.70	1.0	0.70	1.0
	Cost of Flight/h	1.29	1.0	1.68	3.85	2.56	1.43	1.24	1.0	1.65	3.79	2.48	1.43	1.22	1.0	1.64	3.74	2.44	1.42	1.21	1.0	1.20	1.0
Komi	Fuel	1.20	1.0	1.51	2.00	1.95	0.90	1.06	1.0	1.50	1.90	1.74	0.92	1.02	1.0	1.47	1.85	1.63	0.93	0.99	1.0	0.97	1.0
	Amortization	3.16	1.0	3.57	3.57	14.4	8.18	2.55	1.0	3.55	14.4	8.21	2.56	3.05	1.0	3.54	14.4	8.22	2.56	3.03	1.0	3.02	1.0
	Current Repair	1.16	1.0	1.51	1.51	1.69	1.34	1.45	1.0	1.51	1.69	1.34	1.45	1.16	1.0	1.51	1.69	1.34	1.45	1.16	1.0	1.16	1.0
	Wages	0.77	1.0	0.80	1.44	1.14	1.07	0.78	1.0	0.79	1.46	1.15	1.06	0.79	1.0	0.79	1.47	1.15	1.6	0.79	1.0	0.79	1.0
	Airport Expense	0.70	1.0	0.73	0.73	0.73	0.73	0.70	1.0	0.73	0.73	0.73	0.73	0.70	1.0	0.74	0.74	0.74	0.84	0.70	1.0	0.70	1.0
	Cost of Flight/h	1.37	1.0	1.57	4.07	2.70	1.32	1.32	1.0	1.54	3.99	2.63	1.32	1.30	1.0	1.56	3.94	2.58	1.31	1.28	1.0	1.28	1.0
Nizhny Volga Region	Fuel	1.20	1.0				0.90	1.07	1.0				0.92	1.02	1.0				0.92	0.99	1.0	0.97	1.0
	Amortization	3.14	1.0				2.54	3.08	1.0				2.56	3.05	1.0				2.56	3.03	1.0	3.02	1.0
	Current Repair	1.28	1.0				1.93	1.28	1.0				1.93	1.28	1.0				1.93	1.16	1.0	1.16	1.0
	Wages	0.77	1.0				1.07	0.78	1.0				1.06	0.78	1.0				1.05	0.79	1.0	0.79	1.0
	Airport Expense	0.70	1.0				0.74	0.70	1.0				0.73	0.70	1.0				0.73	0.70	1.0	0.70	1.0
	Cost of Flight/h	1.54	1.0				1.48	1.47	1.0				1.46	1.44	1.0				1.45	1.44	1.0	1.42	1.0

The feature of current position of aviation in Russia is weak demand for aero transport services combined with a prompt ageing of existing aircraft fleet and destruction of existing aerodrome infrastructure. For the last 15 years there was a prompt falling of annual passenger flow on air transport more than 6 times (from 125 million persons to 20 million). To a great extent, this falling took place on domestic airlines. As a consequence of falling industrial production (gross domestic product), number of aerodromes in Russia was reduced three times for the last 15 years, from 1400 in 1985 to 300 in 2014 and continues to reduce. More ever, aerodromes for local airlines have suffered, i.e. where general purpose aviation operates. On domestic lines of Russia, passenger service, mainly, has remained (employees of the Ministry of Emergency Measures, the Ministry of Foreign Affairs, Federal Frontier Service, the Ministry of Defense of Russian Federation, administrations of regions, fuel and energy complexes). In combination, all this determines significant need of off-aerodrome basing aviation in Russia. Owing to the stated above, the ACLG aircraft and helicopters in the nearest decade will be in greater demand than classical aircraft. Seaplanes – amphibian will be in less demand for a service passenger due to the seasonal prevalence of their use in Russia. But 2-4 seats amphibians, certainly, will find a place in the field of recreation, entertainment and tourism for solvent clients.

Let's consider the influence of factor of off-aerodrome on the economic efficiency of aircraft. Back to equation (1), uniting all the expenses into two groups: direct (E_D) and indirect, airport (E_{IN}). Block speed for “general purpose aviation” or “application of aircraft in the national economy” can be expressed by the formula:

$$V_B = (L_A + L_G) / (T_A + T_G + T_{MET}) = V_B C_B \quad (2)$$

where, $C_B = (1 + L^*_G) / (1 + T^*_G + T^*_{MET})$ – coefficient of block speed. L_A, T_A – length and time of airborne area of track, L_G, T_G – length and time of ground borne area of track, T_{MET} – delay of start of aircraft because of weather conditions and runway condition.

With regard to the above mentioned, Formula (1) can be expressed as:

$$C_{FH} = E_D (1 + E^*_{IN}) / C_P M_P C_B V_B \quad (3)$$

where, E^*_{IN} – relative share of indirect airport expenses ($E^*_{IN} = E_{IN} / E_D$).

In USSR, there was a procedure in which E_{IN} was taken as 20-25% of direct operating expenses. Between E_D and E_{IN} there is a deep connection, direct and reserve. It has been successfully shown by the engineers of the Experimental Design Bureau Antonov, who investigated economic parameters of the large number of effective airborne vehicles, empirical dependence of cargo transportation cost of the effective aircraft from their runway length is showed in Fig. 3.

It is obvious that the longer the runway, the lower the cost of cargo transportation. So, even the best helicopters cannot compare with the aircraft taking off from a run way in the economic sense. Vertical takeoff and landing aircraft using horizontal runway can increase the payload twice. Economically perfect classical aircraft (for example, “Cessna-Caravan”) use practically all length of the given class aerodrome. However, more length of the runway, higher cost of aerodrome, aerodrome services and E_{IN} , respectively. For example, for airports of 111 category with passenger turnover up to 25 thousand of passengers per year (turnover of a regional country town), the cost of airport construction amounts to 3310 thousand roubles in prices of 1985,

including the cost of equipment – 610 thousand roubles. The cost of construction of runways, taxiways, parking of aircraft and loading platforms amounts to 2120 thousand roubles. Operating expenses of maintenance of such airport are 600 thousand roubles of which depreciation charges make up 30 %.

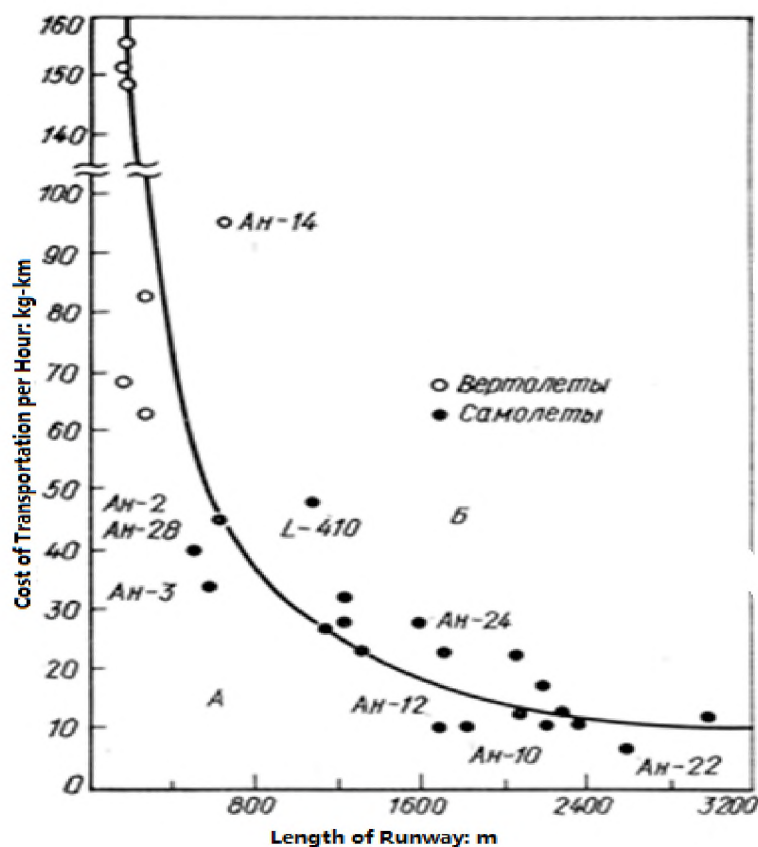


Figure 3: Dependence of Cost from length of runway

If change calculation items from flight hour cost from typical, ideal, conditions of basing (concrete runway, powerful homing radio station and instrument landing system, means of preparation and sweeping of runway from precipitation) to conditions with natural unpaved runways depending on weather conditions, the economic comparative estimations can be changed essentially. It is obvious that the more the customer's demands for the classical airplane takeoffs from natural, unpaved platform, the more additional expenses such as operation will be caused. Additional expenses are connected with a preparation and sweeping of runway from precipitations, awaiting of favorable weather conditions (reduction of annual flight hours), landing on supplementary aerodrome owing to unavailability of aerodromes of destination receiving a cargo.

In Russia there are regions where construction of aerodromes is economically very expensive and is not justified because of low intensity of passenger flow. In Yakutia, there are 64 aerodromes with capable to accept An-24, but only 8 of them have surfaced runways. According to data, the operation cost and transport system repair in central and northern areas of Siberia exceeds the expenses for the same purpose in average areas of Russia 4-6 times. With a reduction

of an aerodrome, the quantity of the ACLG aircraft grows, approximately, in geometrical progression with unequivocally predetermined ability and taking a worthy place in structure of local air traffic flows. Besides, the ACLG aircraft “Dingo” have operational flexibility and capability to fly from agricultural aerodromes and water areas independent from season. According to the researches of Krasnodar Institute about application of aircraft in the national economy, carried out by the order of SAU company, platforms suitable for operation of amphibians with runway length up to 450-540 m in Krasnodar region amounts to 240, including internal reservoirs 104, aerodromes of local airlines – 23, aerodrome for agricultural aviation – 101, bays on the Azov and Black seas coast - 12.

According to the above-mentioned, it is obviously ACLG aircraft have a possibility to serve a plenty of settlements without seasonal idle periods and consequently to reduce E_{IN} as well as E_D through the increased intensity of flight hours per year. The economic analysis of the use of the ACLG aircraft “Dingo” outside the developed aerodrome infrastructure shows that the more the number of “off-aerodrome” takeoffs and landings, the higher the economic advantages of ACLG aircraft over the classic planes. Thus, the “Dingo” ACLG aircraft substantially meets the requirements for commercial use in Russia.

The most important parameter of economic efficiency of the “Dingo” ACLG aircraft is block speed or its derivative – coefficient of block speed. General purpose aviation (GPA), in reality, is directed on minimization of time unproductive spending for operation performance. The criterion “from door to door” is widely used in GPA which takes into account not flight time but total time of cargo or passenger delivered from one addressee (“a threshold of house”) to another addressee (“a threshold of house”). It is obvious that ability of the “Dingo” ACLG aircraft to land in a city boundaries already results in reduction of block speed coefficient even if the “Dingo” is at a disadvantage in relation to the landplane by maximum cruise speed.

This opportunity is amplified by the layout features shielding noise from the propeller upwards and silent operation for the selected type of propeller for the “Dingo” ACLG aircraft. By the example of schematically transport operation which is carried out by different aircraft from Tushino – Moscow to Nizhny Novgorod (Table 3), a mechanism of influence of the “Dingo” aircraft on the reduction of operating expenses at the simultaneous increase of its efficiency is shown.

Increase of C_B has critical influence on the economic efficiency of the “Dingo” ACLG aircraft and not only due to decrease of $T^*_{G.}$ and $L^*_{G.}$ but also of all T^*_{MET} , (refer to formula 2). The latter parameter takes into account delays of flight due to weather conditions, inter-seasonal idle times, preparation of runway or platforms for temporary basing (increased humidity of soil, snowfalls, drying and shallowing of reservoirs, early freeze-up or drifting of ice, motion of ground with formation of small cracks, craters, etc.).

It is obvious that increase of C_B and significant reduction of operational restrictions result in the decrease of E_{IN} and E_D . Certainly, in each particular operation, it is necessary to take into account all external factors. The “Dingo” ACLG aircraft having high operational flexibility, particularly can operate in traditional market niches of wheeled landplane, helicopter and amphibian, however, it cannot replace them completely. So, the “Dingo” ACLG aircraft will compare unfavorably with classical aircraft in Europe and USA whose aerodrome infrastructures

are fully developed. It cannot compete with seaplanes in open sea because of seaworthiness. It is not capable to move passenger from a roof of skyscraper. However, application of the “Dingo” ACLG aircraft can be very effective in conditions of undeveloped aerodrome infrastructure with a wide range of transport operations.

Table 3: Comparative transport efficiency of the “Dingo” ACLG aircraft

No.	Operation Name	“Gzhel”	Mi-2	Lake-4	“Dingo”
	Initial Data				
	Cruise Data: km/h	350	180	200	285

Takeoff Power: hp	750	800	350	1100
Direct Operating expense: %	100 *	160	120	120
Indirect Operating expense: %	20	10	10	10
Passengers	5	4	4	7
Departure from office in Moscow, h	0	0	0	0
Arrival Tushino, h	0.5	0.5	0.5	0.5
Flight from Tushino to Gorky	1.15	2.20	2.00	1.40
2.1. to "Strigino" airport				
2.2. to boating channel (Volga)				
Way from aircraft parking to office	0.50	0.25	0.25	0.25
Meeting in Gorky	2.0	2.0 **	2.0	2.0
Way from office to aircraft parking	0.5	0.25	0.25	0.25
Flight from Gorky to Tushino	1.15	2.20	2.00	1.40
Journey from Tushino to office, Moscow	0.50	0.50	0.50	0.50
Total flying time, h	2.30	4.40	4.00	2.80
Total groundborne time, h	2.00	1.50	1.50	1.50
Total flight time, h	4.30	5.90	5.50	4.30
Total distance, km	880	860	860	860
Block speed, km/h	204.6	145.0	156.4	200.0
Coefficient C _b	0.58	0.81	0.76	0.70
Cost of flying hour ***	0.12	0.30	0.21	0.094
$CH = ED (1 + EIN) / N_{pas} * VB$				

* - direct operating expenses of "Gzhel" are taken as basic, ** - helicopter is compelled to fly at this time in Strigino for re-fuelling, *** - conditional comparative cost of transportation having dimension (% referred to passenger - kilometer)

3. CONCLUSIONS

According to the issues mentioned above, following conclusions can be drawn:

- A. The “Dingo” ACLG aircraft takes intermediate position between the helicopters and aircraft surpassing the first and comparing unfavorably with the second by the means of economic efficiency.
- B. The ACLG aircraft economic feature is at disadvantage compare to classical aircraft which operated from aerodrome with surfaced runway, but absolutely surpasses it when operate from undeveloped aerodromes with unpaved, water or mixed (water-ground) runways.
- C. The ACLG aircraft surpasses the classical aircraft by the level of operative readiness for performance of multi-purpose transport operation in the regions with undeveloped aerodrome infrastructure or in those regions, where maintenance of similar infrastructure completely or partially economically inexpedient (temporary works) or where weather conditions (torrential rains, long snowfalls) make operation of classical aircraft and helicopters inconvenient.
- D. The ACLG aircraft surpasses the classical aircraft by multi-propose, if by the transport scenario, even partially, takeoff and landing on various surfaces are guaranteed.

Authors



Victor Morozov



Zhong Cong

MILLI-SIZE PIEZOELECTRIC MOTORS FOR MICRO HELICOPTERS

Dalius Mazeika^{1,2}, Piotr Vasiljev^{1,3} Sergejus Borodinas^{1,2}

¹Nanjing University of Aeronautics and Astronautics, Nanjing, China

² Vilnius Gediminas Technical University, Vilnius, Lithuania

³ Lithuanian University of Educational Sciences, Vilnius, Lithuania

Email: Dalius.Mazeika@vgtu.lt, Piotr.Vasiljev@leu.lt, Sergejus.Borodinas@vgtu.lt

Keywords: Piezoelectric motor, micro helicopter, mechanical vibrations

Abstract.

The paper covers research and development of two small size piezoelectric motors, that operate based on two different principles: resonant standing wave and inertial principle. Both piezoelectric motors transfer high frequency mechanical vibrations of the stator into rotational motion of the rotor. Introduced piezoelectric actuators can be characterized by different design, rotation speed and torque. Both of them can be used for micro helicopters to drive rotor. Operating principle and excitation regimes of piezoelectric actuators are described and results of numerical modelling and experimental study are presented.

1. INTRODUCTION

Artificial flying micro devices, including artificial bugs, helicopters, quadcopters, drones are becoming devices of the future technologies and will be widely used for different military and civil purposes as for example reconnaissance, observing dangerous areas, hostages rescue and etc. Micro flying devices can acquire video and sound information in different environment and stay unobserved at the same time. Artificial intelligence can be added to these devices so smart flying robots can be developed. According to US DARPA and NASA [1, 2, 3], flying micro devices (helicopters, robots and etc.) will be used for different purposes as for example the colonies of micro flying robots and probes in micro, mini and macro level will become a routine requirement of reliability in space exploration [3]. Micro-size flying devices, including artificial bugs, helicopters, quadcopters will also be used for observing dangerous areas, hostages rescue and etc.

A lot of small size helicopters were developed till now that use DC motors to drive rotor as for example Pixelito [4], Nanoflyer [5] Estes Proto X nano quadcopter [6] and etc. However conventional DC motor, which is used in the micro-size flying devices, has low efficiency. Efficiency of DC motor strongly depends on size of the motor and it decreases when size of the motor is reducing. As for example small size DC motors with the weight less than 1,5 g have 20% efficiency. It means that most of electric energy obtained from the lithium ion battery is converted into the heat because of Joule losses.

There are several micro flying devices developed till now where piezoelectric motors are used. They have different names such as flying micro robot, nano copter or nano helicopters. Micro-flying robot was developed by Seiko-Epson Corporation in 2004. It uses contra-rotating propellers powered by an ultra-thin piezoelectric ultrasonic motor [7]. High-density mounting technology is used to reduce weight packaging the micro-robot's two micro controllers, including EPSON original S1C33 family 32-bit RISC. U.S. Defense Agency has funded research supporting the development of bug-size flyers to carry out reconnaissance, search-and-rescue and environmental monitoring missions without risking human lives. Prototype of bug size flying robot was developed in Microrobotics Lab at Harvard university, USA in 2012 [8]. Movement of the robot's wings were copied from the movements of the butterfly wings during his fly. Piezoelectric actuator was used to drive bug size robot.

Two small size piezoelectric motors are presented and investigated in the paper. Results of numerical and experimental study are presented and discussed. Proposed piezoelectric motors have good output characteristics and can be used for micro helicopters.

2. DESIGN AND OPERATING PRINCIPLE OF THE MOTORS

Investigated piezoelectric motors are composed type ultrasonic devices. Both motors are driven by bimorph type piezoelectric actuator. The first proposed actuator is disc type coplanar bimorph piezoelectric actuator (Fig. 1). Actuator consists of an oscillating cylinder and a bimorph piezoceramic disc with an internal beryllium copper layer.

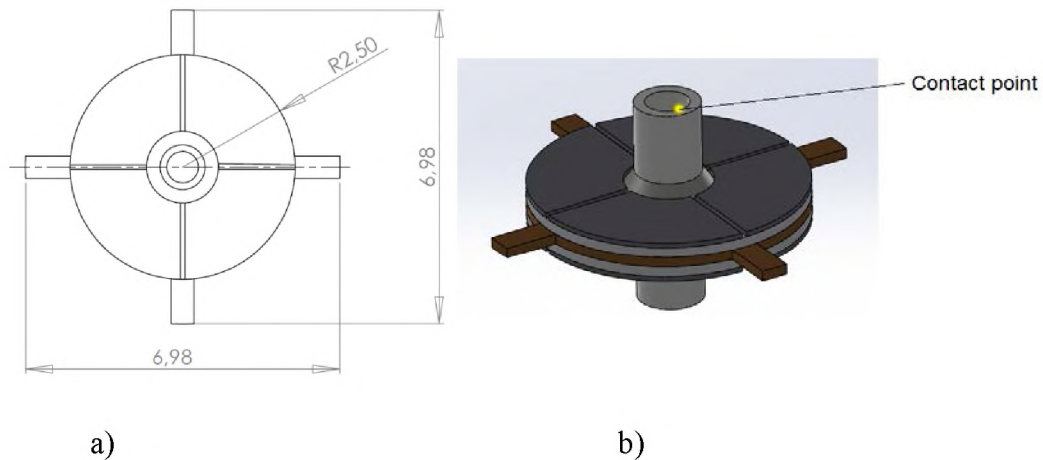


Figure 1: The principal scheme of the actuator: a) dimensions; b) 3D view

The internal plate has the four “legs” used for clamping. Two PZT-8 discs are used for the active layers. PZT-8 piezoceramics has high mechanical quality, low loss factor and high power capability. These features are mandatory to design a small size, but powerful enough actuator. PZT-8 discs are glued to the both sides of the internal beryllium copper plate. The diameter of the disc is 5.0 mm, and the total thickness is 0.8 mm (Fig. 1a). Polarization of the piezoceramic is oriented along thickness of the disc, and the d31 piezoelectric effect is used. A hollowed carbon fiber cylinder is used as a contacting element. It is glued in the center of the bimorph disc. All components are adhered using epoxy. The electrodes of the both piezoceramic discs are divided into the four equal sections. The electrode section from one side of the

piezoceramics is connected with the same part from another side in parallel. The actuator is excited using four harmonic signals with the shifted phases by $\pi/2$; i. e., \sin , \cos , $-\sin$ and $-\cos$ signals are used (Fig.2).

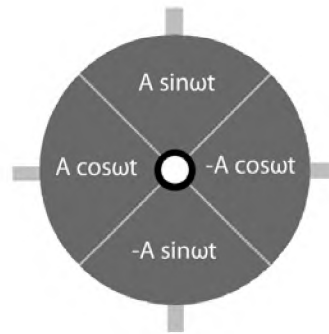


Figure 2: Excitation scheme of the actuator

The rotational motion of the carbon cylinder about the symmetry axis of the disc is achieved when the flexural traveling wave oscillations is excited. The disc type rotor with the hole in the center is designed for the motor. The carbon cylinder contacts the inner surface of the rotor hole and drives the rotor due to the frictional force. Clockwise and counterclockwise rotation of the rotor can be achieved by shifting the voltage phase of the two opposite electrode sections by π .

Principle scheme and isometric view of the second piezoelectric inertial plate type rotary motor is shown in Fig.3. Motor consists of stator, clamping frame and a rotor. Stator is located inside the clamping frame and is connected to it by four hinges. Clamping frame and stator are made from beryllium bronze and make an indissoluble system. Length and width of the stator are denoted as L_1 and H_1 , respectively. Clamping frame has four holes for clamping bolts. Diameter of the holes is 2 mm. Length, width and the thickness of the frame are denoted as H , L and T respectively. Eight piezo ceramic plates are glued on the stator from the both sides i.e. four piezo ceramic plates are glued on the top surface and four plates on the bottom surface. Dimensions of the piezo ceramic plates are $8 \times 4 \times 0.2$ mm. Polarization vector of piezo ceramics is pointed along the thickness of the plates. PZT plates located on the top and bottom surfaces have opposite directions of the polarization. Rotor of the motor has cone shape and is located in the center of the stator. Coupling of the stator and rotor is made thru a special cone type hole. Diameter of that hole is 1.5 mm.

The second in-plane bending mode of the stator is employed to drive the rotor. Node of the plate vibrations is located in the center, therefore maximum value of transverse deformations is obtained and used to rotate the rotor. In plane vibrations of the stator are excited because of d_{31} piezoelectric effect. Schemes used for stator excitation are shown in Fig. 2. Eight piezo ceramic plates are divided in two groups A and B, respectively. Piezo ceramic plates of each group are connected in series. Two saw-tooth type signals with phases shifted by π are used for stator excitation (Fig. 5). Saw – tooth signals are used to achieve inertia type interaction between stator and rotor.

Operation of the motor consists of two basic phases that are described below.

1. Stick phase. Two slowly rising and falling excitation signals are applied to the electrodes of piezo ceramics appointed to groups A and B, respectively. The second in-plane bending mode of the stator is excited. Friction force between stator and rotor is greater than inertial force of the rotor therefore rotation of the rotor is obtained.

2. Slip phase. The excitation signal suddenly changes state to opposite and inertial force of the rotor becomes greater than friction force between stator and rotor therefore rotor slips and rotation moment is not transferred to the rotor.

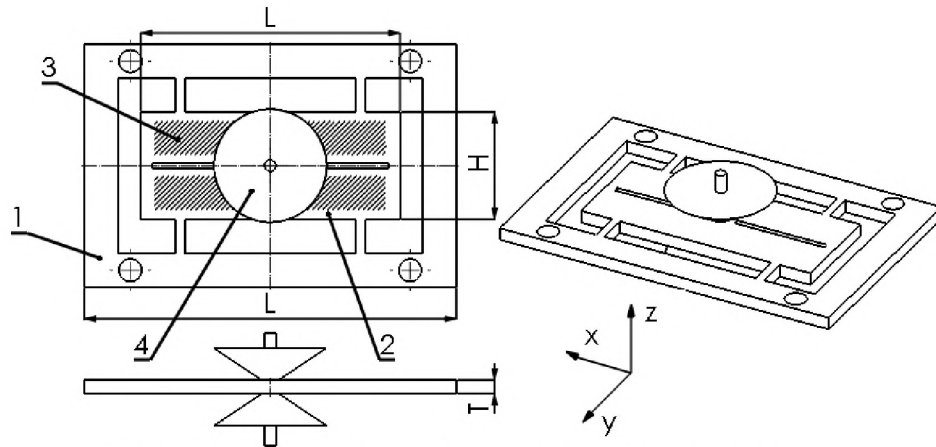


Figure 3: Sketch of the inertial piezoelectric rotary motor:

1 - clamping frame with supporting beams; 2 - stator; 3 - PZT plates; 4 – rotor

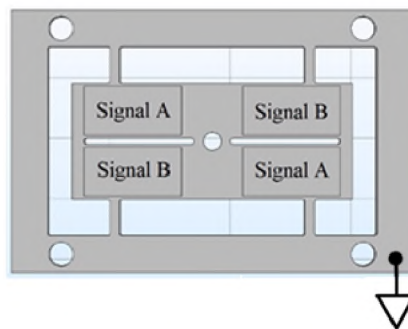


Figure 4: Excitation scheme of the stator

This type of the excitation signals with frequency close to resonant frequency of stator are supplied periodically, therefore rotor rotates continuously. Reversal rotation of the rotor can be obtained by switching phase of the excitation signals by π .

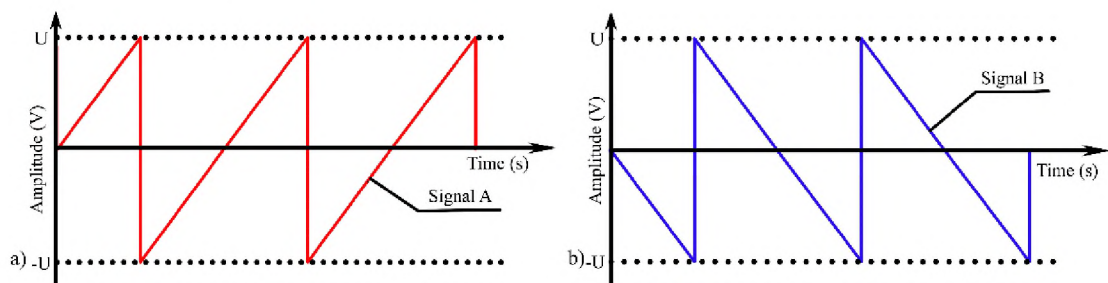


Figure 5: Excitation signals; a - Signal A; b - Signal B

3. FINITE ELEMENT MODELING AND RESULTS

The finite-element method (FEM) was used to perform modal frequency and harmonic response analysis to calculate trajectories of the contact point. Basic dynamic equations of the piezoelectric actuator are derived from the principle of minimum potential energy by means of variational functionals and can be written as follows [9, 10]:

$$\begin{cases} \mathbf{M} \ddot{\mathbf{u}} + \mathbf{C} \dot{\mathbf{u}} + \mathbf{K} \mathbf{u} + \mathbf{T} \boldsymbol{\varphi} = \mathbf{F}, \\ \mathbf{T}^T \mathbf{u} - \mathbf{S} \boldsymbol{\varphi} = \mathbf{Q}, \end{cases} \quad (1)$$

where \mathbf{M} , \mathbf{K} , \mathbf{T} , \mathbf{S} , \mathbf{C} are matrices of mass, stiffness, electroelasticity, capacity and damping, respectively; \mathbf{u} , $\boldsymbol{\varphi}$, \mathbf{F} , \mathbf{Q} are, respectively, vectors of nodes displacements, potentials, external mechanical forces and charges coupled on the electrodes.

The driving force of the actuator is obtained from the piezoceramic disc. Finite-element discretisation of the disc consists of elements with the nodes coupled with electrodes that have the known values of electric potential. The nodal electric potential of remaining elements is calculated during solution. The dynamic equation of the piezoelectric actuator in this case can be expressed as follows [7, 8]:

$$\begin{cases} \mathbf{M} \ddot{\mathbf{u}} + \mathbf{C} \dot{\mathbf{u}} + \mathbf{K} \mathbf{u} + \mathbf{T}_1 \boldsymbol{\varphi}_1 + \mathbf{T}_2 \boldsymbol{\varphi}_2 = \mathbf{F}, \\ \mathbf{T}_1^T \mathbf{u} - \mathbf{S}_{11} \boldsymbol{\varphi}_1 - \mathbf{S}_{12} \boldsymbol{\varphi}_2 = \mathbf{Q}_1, \\ \mathbf{T}_2^T \mathbf{u} - \mathbf{S}_{12}^T \boldsymbol{\varphi}_1 - \mathbf{S}_{22} \boldsymbol{\varphi}_2 = \mathbf{0}, \end{cases} \quad (2)$$

here

$$\mathbf{T} = [\mathbf{T}_1 \quad \mathbf{T}_2], \quad \mathbf{S} = \begin{bmatrix} \mathbf{S}_{11} & \mathbf{S}_{12} \\ \mathbf{S}_{12}^T & \mathbf{S}_{22} \end{bmatrix}, \quad (3)$$

where $\boldsymbol{\varphi}_1$, $\boldsymbol{\varphi}_2$ are, respectively, the vector of nodal potentials of nodes coupled with electrodes and the vector of nodal potentials calculated during numerical simulation.

Mechanical and electrical boundary conditions are determined for the piezoelectric actuator, i. e. mechanical displacements and velocities of the fixed surfaces of the actuator are equal to zero and the electric potential of the nodes that are not coupled with electrodes are equal to zero as well. Natural frequencies and modal shapes of the actuator are derived from the modal solution of the piezoelectric system:

$$\det(\mathbf{K}^* - \omega^2 \mathbf{M}) = 0, \quad (4)$$

where \mathbf{K}^* is a modified stiffness matrix. In case when $\mathbf{Q}_1 = 0$ it can be written as follows:

$$\mathbf{K}^* = \mathbf{K} + \mathbf{T} \mathbf{S}^{-1} \mathbf{T}^T. \quad (5)$$

In the case when $\boldsymbol{\varphi}_1 = 0$ the modified stiffness matrix is:

$$\mathbf{K}^* = \mathbf{K} + \mathbf{T}_2 \mathbf{S}_{22}^{-1} \mathbf{T}_2^T. \quad (6)$$

Harmonic response analysis of the piezoelectric actuator is carried out applying sinusoidal varying voltage with different phases on electrodes. Due to the inverse piezoelectric effect corresponding mechanical forces are obtained:

$$\mathbf{F}_1 = -\mathbf{T} \boldsymbol{\varphi}_1, \quad (7)$$

here a vector of nodal potentials $\boldsymbol{\varphi}_1$ can be written as:

$$\boldsymbol{\varphi}_1 = \mathbf{U} \sin(\omega_k t), \quad (8)$$

where \mathbf{U} is a vector of voltage amplitudes, applied to the nodes coupled with electrodes. Referring to Eqs. (2), (7) and (8), the vector of mechanical forces can be calculated as follows:

$$\mathbf{F}_1 = (\mathbf{T}_2 \mathbf{S}_{22}^{-1} \mathbf{S}_{12}^T - \mathbf{T}_1) \mathbf{U} \sin(\omega_k t). \quad (9)$$

Referring to Eq. (2) the vector of nodal charges \mathbf{Q}_1 can be written as follows:

$$\mathbf{Q}_1 = (\mathbf{T}_1^T - \mathbf{S}_{12} \mathbf{S}_{22}^{-1} \mathbf{T}_2^T) \mathbf{u} + (\mathbf{S}_{12} \mathbf{S}_{22}^{-1} \mathbf{S}_{12}^T - \mathbf{S}_{12}^T) \boldsymbol{\varphi}_1. \quad (10)$$

Results for structural displacements of the piezoelectric actuator obtained from harmonic response analysis are used to determine the trajectory of the contact point's movement.

A numerical simulation of both piezoelectric actuator was carried out by employing FEM software COMSOL Multiphysics. The finite element models of the actuator were built. It contains all assembling parts mentioned in the previous section. Three-dimensional free tetrahedral finite elements were used to mesh the actuator. The appropriate finite element mesh was defined after several iterations. Only mechanical boundary conditions were applied in the finite element model. The material properties used for the actuator modelling are listed in Table 1.

Table 1. The mechanical properties of the motor materials

Materials	Young's modulus x 10^{10} [N/m ²]	Poisson's ratio	Density [kg/m ³]
Beryllium copper	12.8	0.30	8250
Silver	7.60	0.37	10490
Carbon fiber	17.4	0.30	1740
Epoxy	0.12	0.22	2500
Piezoceramic PZT-8			7600
(Elasticity matrix x 10^{10} [N/m ²]) $c_{11}= 14.68$; $c_{12}= 8.108$; $c_{13}= 8.105$; $c_{33}= 13.17$; $c_{44}=3.29$; $c_{66}=3.14$			

The modal and harmonic response analysis were performed by using the Pardiso solver with the nested dissection multithreaded preordering algorithm. Modal shapes of the analyzed actuators are presented in Fig. 6.

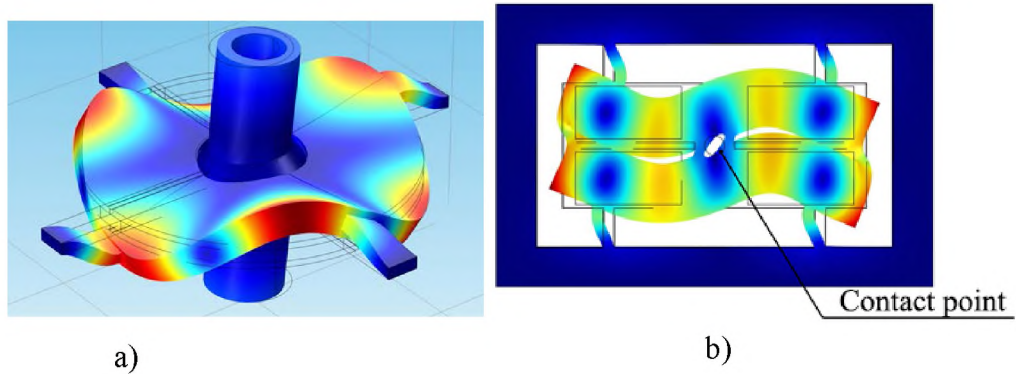
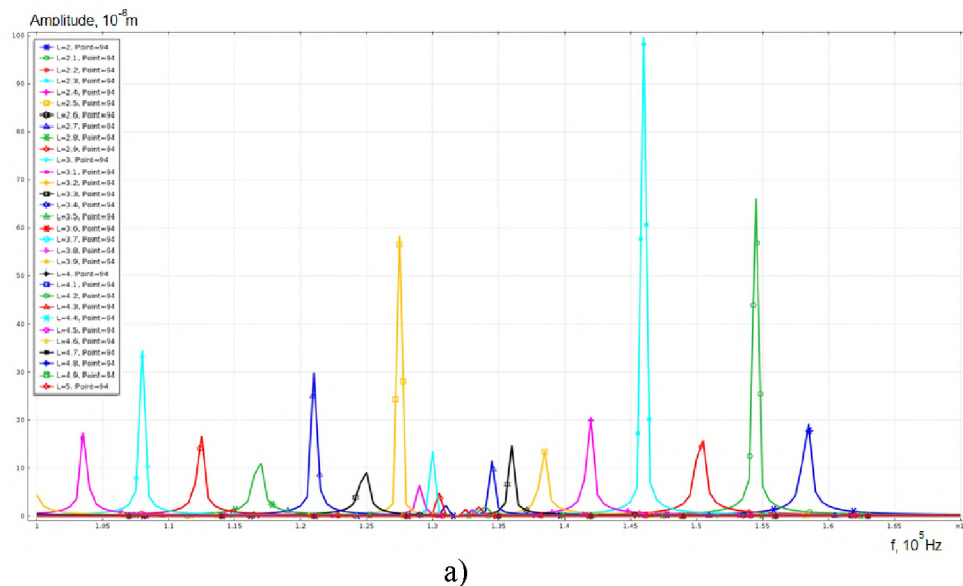


Figure 6: The modal shape of the actuators: disc type (a), plate type (b)

Optimization of the geometrical parameters of the both stators was performed in order to increase displacement of the contact point. Harmonic response analysis was carried out under different dimensions of the actuator and parameters that provide the highest amplitudes of contact point vibrations were chosen as optimal. Result of calculated amplitude-frequency characteristic when parametrical sweep was performed is presented in Fig. 7.

Calculations of the contact point's moving trajectories were performed for the disc type actuator when the length of the cylinder was set to 2.3 mm and 4.0 mm at the corresponding resonant frequencies. The trajectories of the contact point motion are illustrated in Fig. 8. It can be seen that the trajectories have elliptical shapes but they are very close to the circle shape. The ratio between the major and minor axis of the ellipses is 0.99. It can be noticed that the length of the major axis is 8.1 times larger when the length of the cylinder is 2.3 mm, and the contact point motion at this length of the cylinder is more powerful. Based on the results of the numerical simulation it can be concluded that the excitation frequency at 146 kHz should be used as the operating frequency of the current actuator with the carbon cylinder length equal to 2.3 mm.



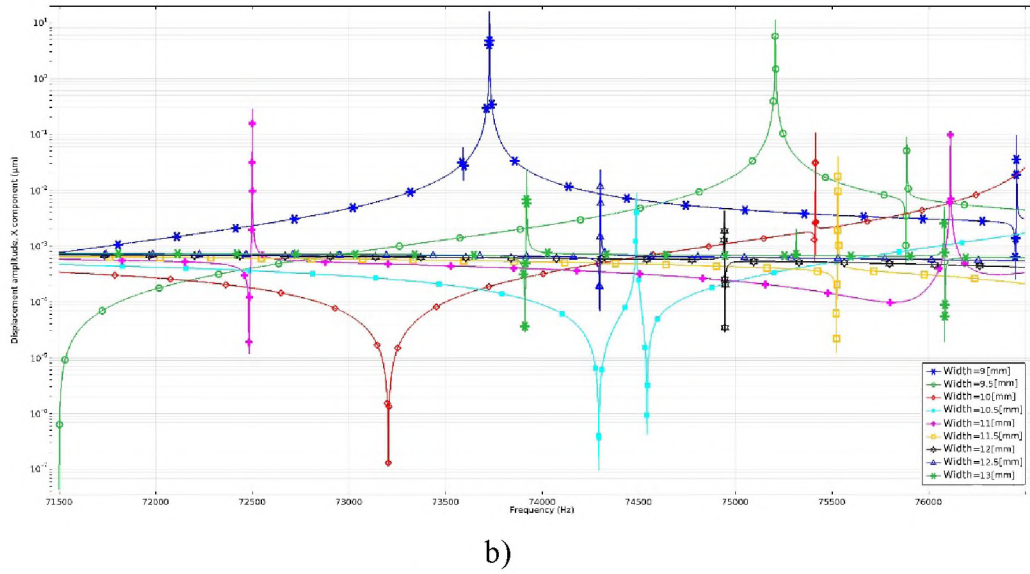


Figure 7: Amplitude - frequency characteristics of the actuators: disc type (a), plate type (b).

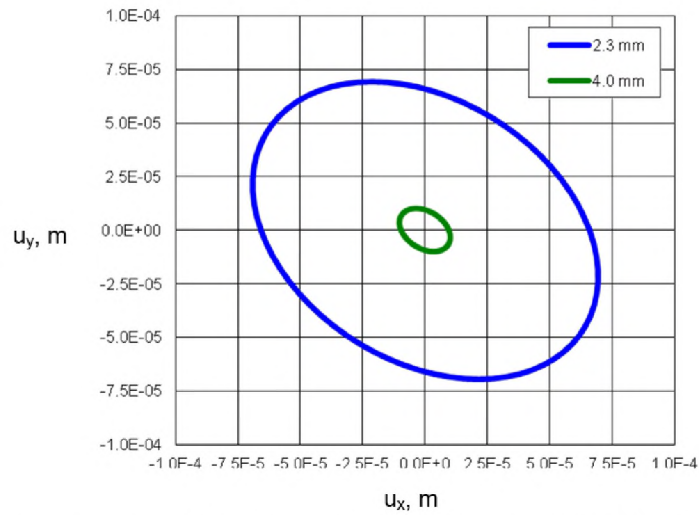


Figure 8: The trajectories of the contact point movement of the disc type actuator in the xy plane when a different length of the cylinder is used

Time domain study of the plate type actuator was performed in order to validate operating principle of the motor. Frequency of the excitation signals was set to 73.681 kHz. Analyzed time range was set to one period of excitation frequency i.e. 13.57 μ s. Moreover, time step was set to 1 μ s, i.e. approximately 1/14 of the period. Results of the study are given in Fig. 9. Left side of Fig. 9 shows stick phase between stator and rotor. It occurs during time period from 0 μ s to 6.9 μ s. Friction force between stator and rotor is higher than inertial force of the rotor and clockwise rotation of the rotor is obtained. Time interval from 6.9 μ s to 7.1 μ s represents slip phase. It occurs because electric signals suddenly change states and friction force becomes lower than inertial force of the stator therefore rotor is not rotated counter-clockwise. Time interval from 7.1 μ s to 13.57 μ s is also stick phase and generates clockwise rotation of the rotor as in first motor operation stage.

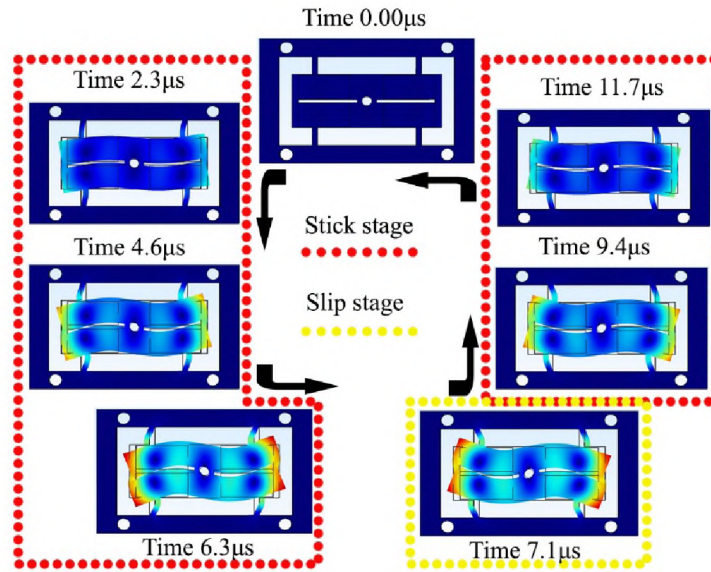
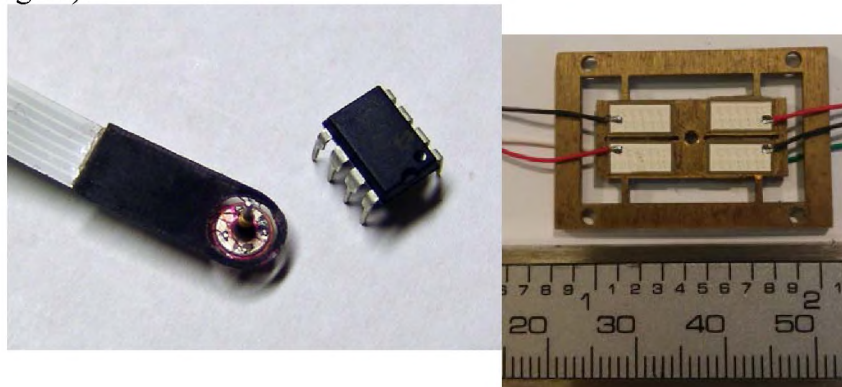


Figure 9: Phases of the plate type motor operation

4. EXPERIMENTAL INVESTIGATION

Experimental investigation was performed to validate operation principle and to assess mechanical and electrical characteristics of the proposed motor. Prototype of the motor stator was made with the strict respect to geometrical parameters obtained during numerical investigation (Fig.10).



a) b)
Figure 10: Prototype piezoelectric actuators: disc type (a) and plate type (b)

Firstly, impedance - frequency characteristic of the both actuators was measured using Hewlett Packard 4192 A LF impedance analyzer. Results of the measurements are given in Fig.11. It can be noticed that values of measured resonant frequencies of the both actuators are close to resonant frequency values obtained during numerical modelling, at 74.4 kHz. The difference between measured and calculated frequency is up to 3.9%.

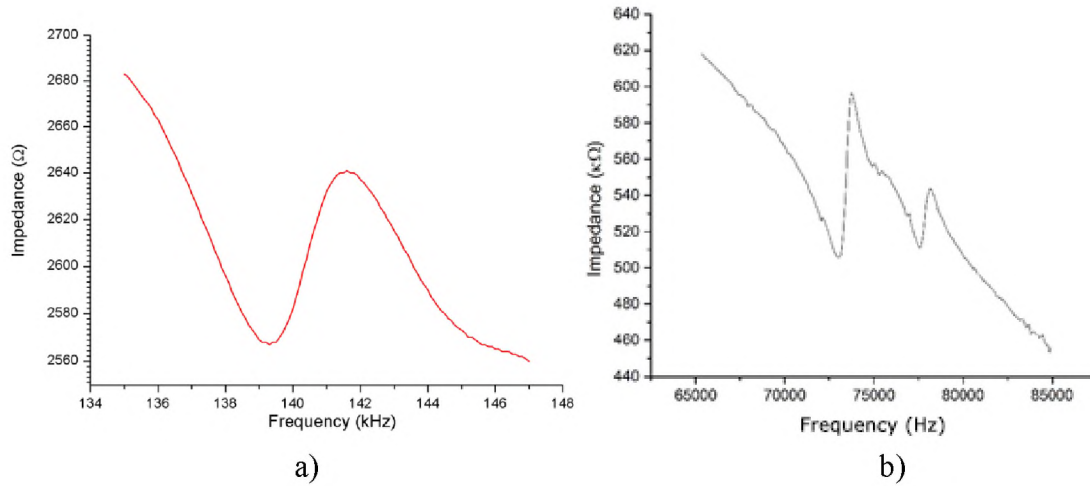


Figure 11: Measured impedance versus frequency: disc type actuator (a) and plate type actuator (b)

A special rotor from alumina was made for the investigating mechanical output characteristics of the actuators. Experimental setup was built as well. It consisted of digital signal generator with two output channels, power amplifier and oscilloscope. Also, LTH 209 - 01 photo interrupter and preprogrammed microcontroller AT mega 328P were used in order to measure angular speed of the rotor. Computer was used for data acquisition and management. Principle scheme of the experimental setup is shown in Fig.12.

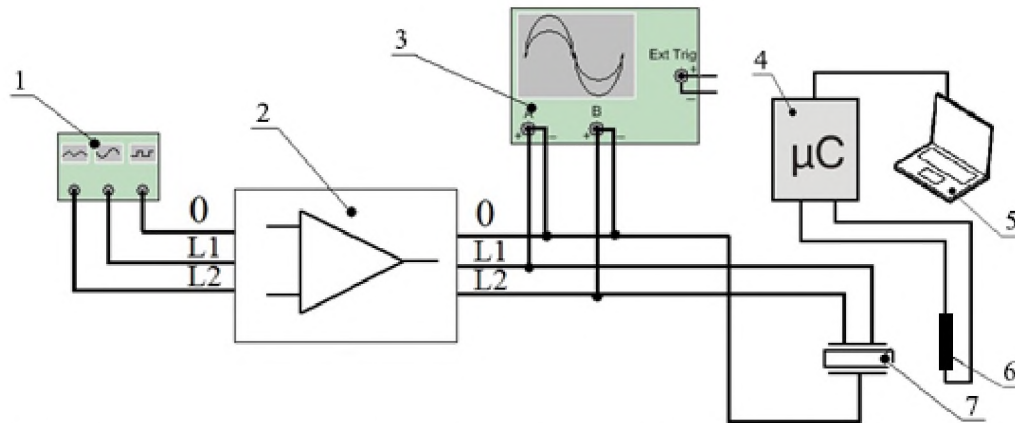


Figure 12: Principle scheme of the experimental setup: 1 - digital function generator; 2 - power amplifier; 3 - oscilloscope; 4 – microcontroller; 5 – computer; 6 - photo interrupter; piezoelectric inertial motor.

Fig. 13 presents the results of rotation speed measurements of the disc type actuator when different length of the carbon cylinder is used i. e., 2.3 mm and 4 mm. It can be seen that the rotation speed exhibits a nearly linear increases when the driving voltage increases. However, the rotation speed increases quicker when the length of the cylinder is 2.3 mm and reaches 3850 rpm at 80 V driving voltage. The difference between the measured maximum rotation speeds of the two motors is 1.4 times at 80V. Also, it can be indicated that the optimized bimorph piezoelectric actuator has the higher efficiency with the lower power consumption.

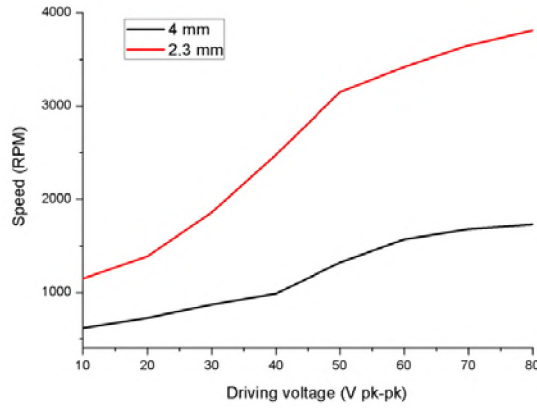


Figure 13: Rotation speed of the rotor versus driving voltage of the disc type actuator

Measurement of rotor rotation speed of the plate type motor is shown in Fig. 14 when constant preload force 24.5mN was applied. It can be noticed that maximum rotation speed was equal to 59.5 r/min. This value was obtained at 60V. Tolerance interval of the measurement is ± 3.2 r/min. It can be concluded that motor has liner characteristics and motor rotation angle could be controlled with the high precision thru the voltage amplitude.

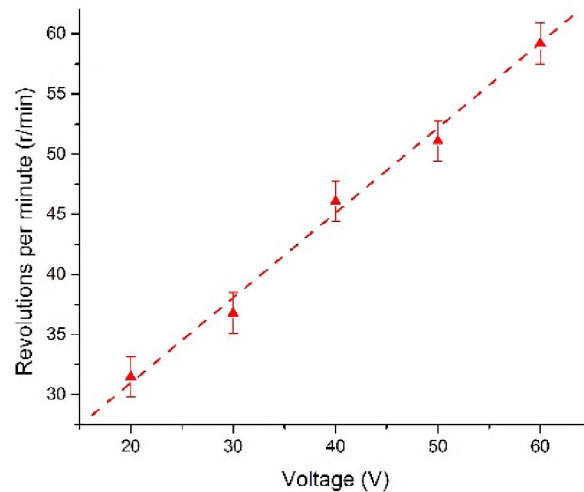


Figure 14: Rotation speed of the rotor versus driving voltage of the plate type actuator

5. CONCLUSIONS

Two piezoelectric type motors were presented and investigated. Numerical and experimental studies validated operation principle of the proposed motors. The geometrical parameters were calculated and amplitudes of contact point vibrations were increased. Prototype motors were made and measurements of electrical and mechanical output characteristics were performed. Experimental investigation confirms that the higher rotation speed and efficiency of the motor can be achieved when the optimized actuator design is used. Almost linear rotations versus preload force characteristics show a good stability of the piezoelectric motors.

REFERENCES

- [1] Tousley, B., Micro Air Vehicle (MAV) Advanced Concept Technology Demonstration, (ACTD), June 29, 2005.
- [2] McMichael, J. M., and Col. M. S. Francis, "Micro Air Vehicles - Toward a New Dimension in Flight," DARPA, USA, August 7, 1997.
- [3] J. Bardina. R. Thirumalainambi. Micro-Flying robotics in space missions. 2005. SAE International, NASA.
- [4] Proxflyer. <http://www.proxflyer.com/meny.htm>
- [5] Pixelito. http://stupidevilbastard.com/2004/08/pixelito_tiny_remote_controlled_mode_1_helicopters/
- [6] Review: Estes Proto X nano quadcopter. <http://www.gizmag.com/review-estes-proto-x-nano-quadcopter/29813/>[5]
- [7] Seiko Epson Corporation. Epson Announces Advanced Model of the World's Lightest micro-Flying Robot, August 18, 2004.
- [8] Bug-sized flying robots. Insect research assisting development. <http://www.macroevolution.net/Bug-sized-flying-robots.html#.VDj-YhZTu88>
- [9] H.S. Tzou. Piezoelectric Shells, distributed sensing and control of continua, Kluwer Academic Publishers, Dordrecht, 1993.
- [10] S. Borodinas, P. Vasiljev, D. Mazeika. The optimization of a symmetrical coplanar trimorph piezoelectric actuator. Sensors and actuators. A-Physical. Elsevier Science. ISSN 0924-4247. 2013, Vol. 200, p. 133-137.

Authors



Dalius Mazeika



Piotr Vasiljev



Sergejus Borodinas

DESIGN AND MANUFACTURING OF POLYMER COMPOSITE TAIL ROTOR HUB

Darya M. Bezzametnova, Venera R. Sakhbutdinova
Supervisors: Valentin I. Khaliulin and Dimitrii Yu. Konstantinov

Kazan National Research Technical University
named after A. N. Tupolev – KAI
Institute for Aviation, Land Transportation and Power Engineering
No.10, K.Marx St., Kazan, Tatarstan 420111, Russia
e-mail: pla@kai.ru; dashatoropcova@yandex.ru

Key words: Nature, design, analysis, using, flight vehicles

Abstract: *A possibility to develop a high-loaded integral body of tail rotor hub was studied. Materials and manufacturing processes were selected. Physical mechanical testing of structurally similar elements was performed. Based on the results of testing, tail rotor hub structure and manufacturing process were selected.*

1. INTRODUCTION

The aim of the work was to study a possibility to develop rotorcraft flight structure using polymer composites. The object of study is the body of tail rotor hub presented on Fig. 1.

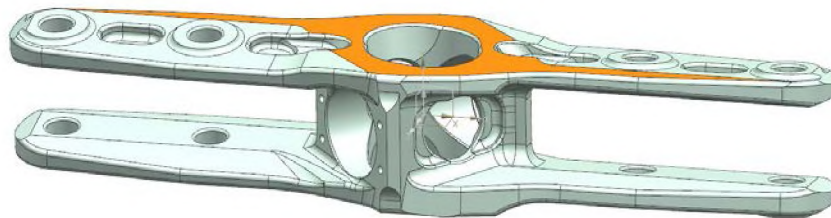


Figure 1: Body of Tail Rotor Hub

Main disadvantages of the structure are:

- Weight of the tail rotor hub (mass of metal part is 2.9 kg)
- Strength of metal part is not enough to bear operational loads (a small amount of machine hours)

At the current stage of technical development these problems are solved by replacement of metal part with composite (most often carbon) one.

2. MAIN PART

To produce tail rotor hub preforms, braiding and tailored fiber placement (TFP) were suggested. Recently these methods have been widely applied to ensure rational reinforcement of polymer composite structures. Advantages of these methods are as follows:

- Automated preform manufacturing process
- Manufacturing net-shape preforms
- High material ratio

When designing tail rotor hub, the following limitations have to be taken into account:

- Keeping mounting surfaces and openings of tail rotor hub compliant with propeller blade and control system
- Compliance with general dimensions of the tail rotor hub.

Based on the requirements, pilot variants of tail rotor hubs were designed that may be produced using suggested preform manufacturing technologies (Fig. 2 - 5).

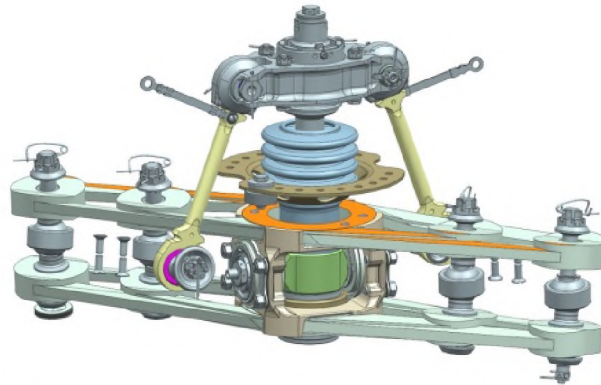


Figure 2: Aggregate variant; preforms are manufactured using TFP

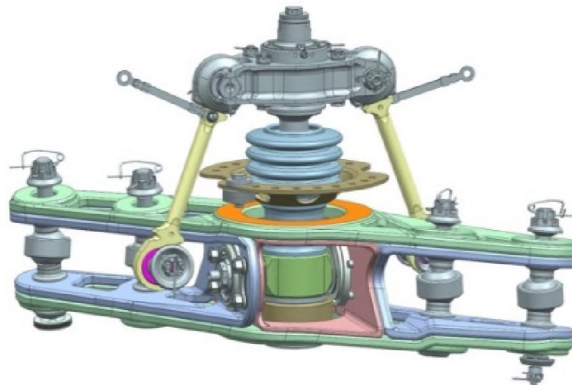


Figure 3: Integral variant; preforms are manufactured using TFP

Materials with high tensile and compressive moduli of elasticity are usually selected for high-loaded structures. Reinforcement materials and resins selected for manufacturing of the body of tail rotor hub are presented in Tables 1 and 2.

To compare testing and calculation results, computation of the samples was performed in ANSYS. After that a batch of samples was produced from aluminum D-16 and T-200 carbon fiber using TFP method. Then tensile testing was performed, and it demonstrated the following results:

- Strength of specimens that were produced using TFP is 3 times higher compared to aluminum counterparts
- Results demonstrated good agreement with computation results.

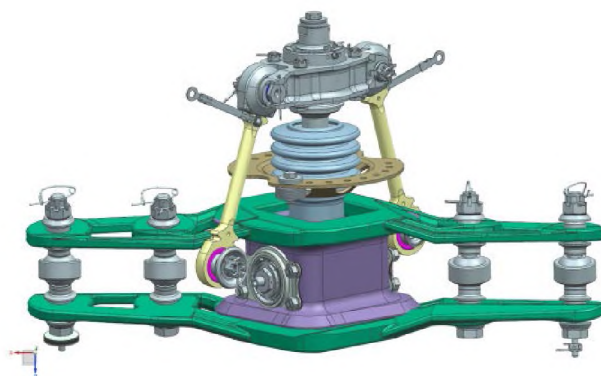


Figure 4: Integral variant; preforms are manufactured using radial braiding

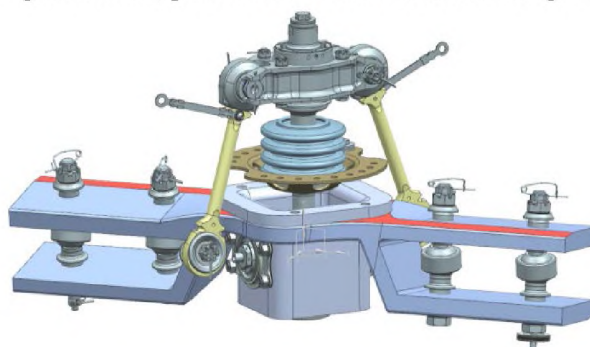


Figure 5: Integral variant; preforms are manufactured using radial braiding

Table 1 – Properties of Reinforcement Materials

Material	Ultimate Tensile Strength, MPa	Tensile Modulus, GPa	Density, kg/m ³	Country of Production	Certification	Approx. Cost, rub.
T-700 (Torayca®)	4,900	230	1.800	Japan	BKY-45Ж (VIAM) (certified prepregs)	8,000
UMT42-12K	4,200	235	1.800	Russia (Elabuga)	-	12,000

Table 2 – Properties of Resins

Material	Type	Glass Transition Temperature	Density, kg/m ³	Country of Production	Certification	Approx. Cost, rub.
T-26	epoxy	≈180	-	Russia (INUMIT)	Certified resin	5,000
BCЭ-21	epoxy	≈180	-	Russia (VIAM)	Certified resin (VIAM)	~ 10,000
RTM-6	epoxy	≈180	1.14	USA (Hexcel)	-	15,000

T-700 fiber and T-26 resin were selected considering availability and cost. Mechanical testing of samples produced by TFP and radial braiding was performed in order to select a method of preforms manufacturing. Based on the results of testing, TFP was selected.

Further, mechanical properties and processing parameters of structurally similar elements were studied. These studies are necessary to determine properties of material and optimize reinforcement pattern at the early stage of development.

The first selected element was the one presented in Fig. 6 (a bracket); however, due to a very complex shape it was divided into a plane rhomb and an eyebar.

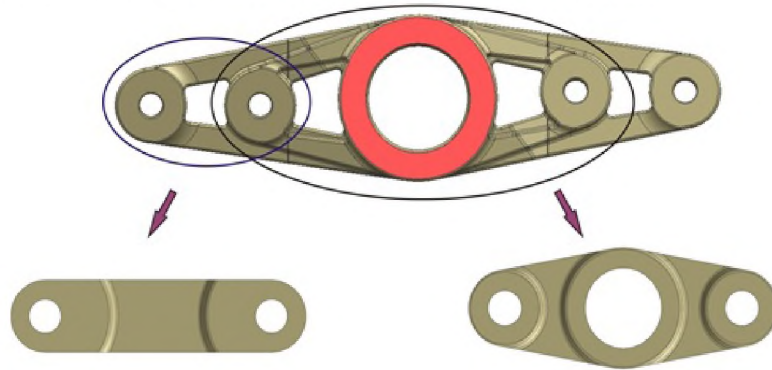


Figure 6: Structurally similar elements: a plane rhomb and an eyebar

The next step was testing of the bracket. This structurally similar element was also computed in ANSYS.

Tensile and flexural testing of the bracket were performed. Based on the results of testing one may say that specific strength of plane composite bracket is approximately 2.63 times higher compared to aluminum part.

Based on the results of analysis of structurally similar elements, it is found that integral variant of tail rotor hub is the most promising one.

Integral variant is a monolith structure that consists of 6 sub-preforms manufactured using TFP and is impregnated in one shot (Fig.7).

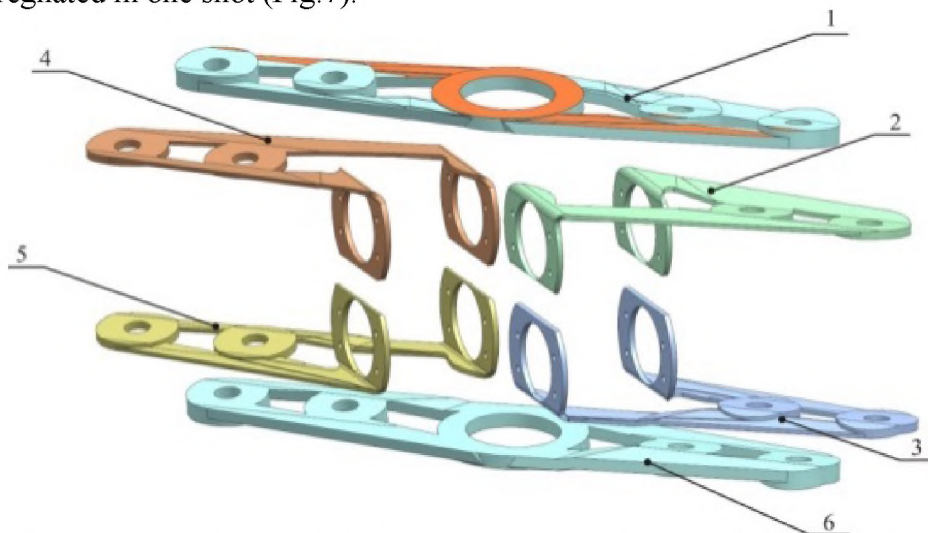


Figure 7: Sub-preforms of Integral Tail Rotor Hub; here: 1 – upper sub-preform; 2, 3, 4, 5 – L-shaped side preforms; 6 – lower sub-preform

Integral body of tail rotor hub is produced using Resin Transfer Molding (RTM). This technology ensures production of parts with given fiber volume fraction and net-shape geometry.

3. CONCLUSIONS

The following has been done in the course of the project:

1. Different variants of tail rotor hubs have been designed, and manufacturing process has been selected.
2. Processing parameters and mechanical properties of structurally similar elements have been studied.
3. A variant of tail rotor hub design has been selected.
4. Integral polymer composite tail rotor hub has been manufactured.

REFERENCES

- [1] Khaliulin, V.I., Shapaev, I.I. Technology of Composite Parts Manufacturing. Teaching Aid, Kazan: KSTU-KAI Publishing House, 2004, 234 p. (In Russian)
- [2] Endogur, A.I. Aircraft Structure. Design of Parts and Units: Teaching Aid – M.: MAI Publishing House, 2013, 556 p. (In Russian)
- [3] Endogur, A.I. Design of Aircraft Structures. Design of Parts and Units: Teaching Aid – M.: MAI-PRINT Publishing House, 2009, 540 p. (In Russian)
- [4] Richard Lee, Master of Applied Science. Tailoring the Acoustic Properties of Truss-Core Sandwich Structure. Graduate Department of Aerospace Science and Engineering University of Toronto. 2012. 05.08.2015.

Authors



Darya M. Bezzametnova,



Venera R. Sakhbutdinova

Supervisors



Valentin I. Khaliulin



Dimitrii Yu. Konstantinov

PRACTICAL APPROACH TO AIRWORTHINESS STUDY EDUCATION – TAKING A CASE OF AN UNCONTAINED ROTOR FAILURE

Zhengqiang Cheng¹, Oleksiy Chernykh², Zhong Lu³ and Junjiang Xiong⁴

^{1,4} Beijing University of Aeronautics and Astronautics
School of Transportation Science and Engineering
37 Xueyuan Road, Beijing, 100191, China

^{2,3} Nanjing University of Aeronautics and Astronautics
College of Civil Aviation

29 Jiangjun Avenue, Nanjing, 211106, Jiangsu, China

e-mail: ¹zhengqiangcheng@buaa.edu.cn, ²alex@nuaa.edu.cn, ³luzhong@nuaa.edu.cn,
⁴jjxiong@buaa.edu.cn

Key words: airworthiness technology, educational research study case, engine rotor, uncontained failure.

Abstract. *The Aircraft Airworthiness Technology as a new discipline in Chinese Aerospace-related universities involves a wide range of knowledge, but it is easy to fall into study of airworthiness regulations exceptionally. In order to professionally cultivate senior technical personnel in airworthiness works, students of the new Airworthiness major are assigned to study broader range of learning contents and research processes through deeper involvement into real practical tasks. Taking an uncontained failure event of an engine rotor as an educational practical example, this paper expounds the main steps of an airworthiness research study: an analysis of technical ideas, core outline of necessary works, suggestions for key aspects of an object airworthiness. In addition, prerequisite basic knowledge of the airworthiness field is discussed, and concrete highlights of practical research works are given in depth.*

1 INTRODUCTION

Airworthiness of aircraft refers to inherent properties of aircraft that can safely fly under the expected operating environment and defines the use of restricted conditions. It is required that an aircraft always conforms to its type design and is always in a condition for safe operation. It is thus clear that the airworthiness duty is to ensure aviation safety. The Aircraft Airworthiness Technology has been established as a new important discipline in Chinese Aerospace-related universities. Its educational goal is to develop a basement of aviation basic knowledge, engineering practical ability, to master aviation professional knowledge, airworthiness regulations, airworthiness verification technology, airworthiness certification technology and airworthiness project management theory of the senior technical personnel. Therefore, Airworthiness major students have to learn basic knowledge, such as math and physics, and master other professional knowledge: airplane, engine, aircraft systems, airborne equipment, aircraft manufacturing, airworthiness regulations, airworthiness verification technology, airworthiness certification technology, engineering management, etc.

The more in-depth stage of mastering background of the relevant airworthiness knowledge is performing a specific airworthiness project for a student research study. Similar to most research topics, there are general research backgrounds, research significance, research status, specific methods,

examples and other processes. But an airworthiness project needs to ensure safety as the ultimate goal, therefore airworthiness standards define to study and interpret the lowest level of security. Relevant issues are related to advisory circulars and other relevant documentation with regulations. In view of this, this paper will combine the engine rotor uncontained failure event as an airworthiness study case, elaborate the main content of airworthiness research study, highlight airworthiness research recommendations.

2 MAIN RESEARCH CONTENTS OF AN AIRWORTHINESS STUDY CASE

The definition of a problem is the beginning of any research. After the definition of airworthiness issues, the need is to produce the background of the current research problem. For example, an uncontained rotor failure is defined as *“After the high-speed engine rotor failed, the excess energy of the rotor fragments will be thrown from the engine case, broke down the adjacent fuel tank, fuselage, system components, etc., which will have a serious impact on the aircraft structure and system.”* The problem arises because of the catastrophic aviation accidents that have occurred in the history due to uncontained failures of rotors.

In addition, because of special nature of airworthiness, airworthiness standards, advisory circulars and other materials, research and interpretation are one of the key works. Since the catastrophic aviation accidents caused by an uncontained rotor failure have occurred many times in history, the American Federal Aviation Administration (FAA), the European Aviation Safety Agency (EASA), and the Civil Aviation Administration of China (CAAC) have issued proper airworthiness regulations to take design precautionary measures in order to minimize hazards caused by an uncontained rotor failure event that seriously endangers civil aviation safety^[1-6]. The Society of Automotive Engineers has collected 676 uncontained rotor events recorded from 1962 to 1989, that have amounted to 15 cases of catastrophic accidents^[7-9]. The FAA revised the corresponding advisory circular^[10], but the literature^[11,12] showed the definition of the spread angle in the advisory circular was too small to reflect the actual risk level. In [13], the fragment characterization of the turboprop, low-bypass ratio and high-bypass ratio engines was further statistically analyzed. The results showed that there are differences in characteristics of uncontained rotors in different types of engines. It was found that the actual fragment spread angle was greater than the recommended value.

The goal of the project is to take technical means to avoid the occurrence of the problem, or reduce probability of problem occurrence, so that it is at the level of acceptable risk, which has been one of the core works of airworthiness research. In the case of an *“uncontained rotor failure”*, in [14], the general safety analysis method is proposed for the Uncontained Turbine Engine and Auxiliary Power Unit Rotor and Fan Blade Failure. In the literature^[15,16], based on the collision detection of uncontained debris hazard identification method, the Monte Carlo simulation was conducted, finally achieving uncontained rotor failure triggered by the minimum cut set of identification and safety quantitative analysis.

3 TECHNICAL IDEAS OF THE RESEARCH – AN UNCONTAINED ROTOR EVENT ANALYSIS PROCESS

In order to further solve the problem, it is necessary to formulate technical ideas and study the technical process after carrying out literature research on the problems involved in the airworthiness project. For example, for the uncontained rotor failure, the proposed overall process is divided into (1) the risk identification stage and (2) the risk assessment stage.

The specific flow chart is shown in Figure 1.

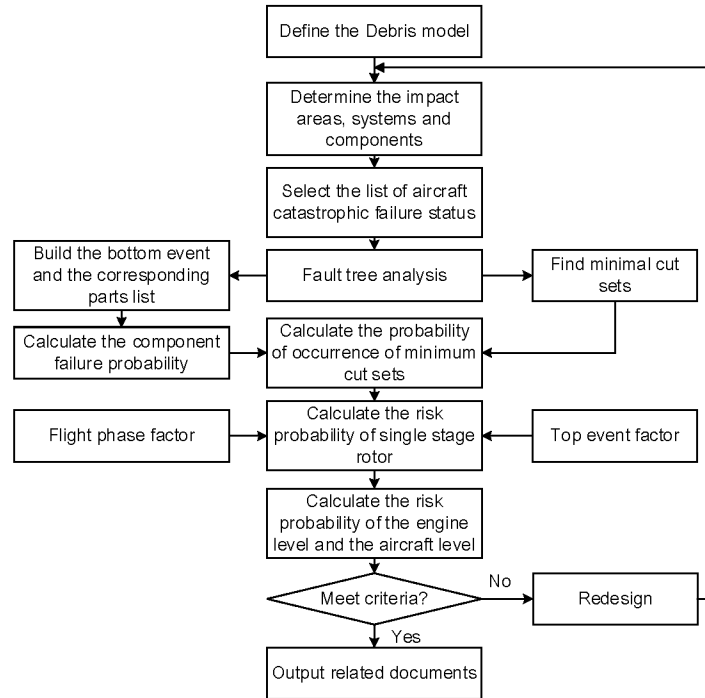


Figure 1: The overall process of the risk assessment

3.1 Risk identification stage

Based on historical data and continued increased uncontained rotor event, the failure model of the rotor debris was determined. The following conservative assumptions have been made in analyses: (1) the uncontained debris has infinite energy; (2) the spread angle of the debris is independent of the translational angle; (3) the probability of debris release within the maximum spread angle and translational angle is uniformly distributed. Some typical rotor debris failure models are shown in Table 1.

Category	Single One-Third Disk Fragment	Intermediate Fragment	Alternative Engine Failure Model	Small Fragment	Fan Blade Fragment
Maximum dimension	One-third of the disk with one-third blade height	One-third of the bladed disk radius	One-third piece of disk	Half of the blade airfoil	Blade tip with one-third the blade airfoil height
Spread angle	$\pm 3^\circ$	$\pm 5^\circ$	$\pm 5^\circ$	$\pm 15^\circ$	$\pm 15^\circ$

Table 1: Rotor debris failure models

When the risk identification of a debris model is carried out, the spread angles of the first stage rotor fragment and the last are used to determine the impact area of the debris. The aircraft structure and system components in the impact area are simplified to determine key systems and components in rotor uncontained impact areas. In addition, the aircraft's top-level function failure is analyzed selecting out the catastrophic functional failure list that is possibly caused by an uncontained rotor failure. The fault tree analysis of the catastrophic function failure event is

carried out to find the components that caused the failure of the function and to determine the trajectory, spread angle and translational angle of the rotor debris. The graphical method^[17] has been used to draw the relevant angle, as shown in Figure 2.

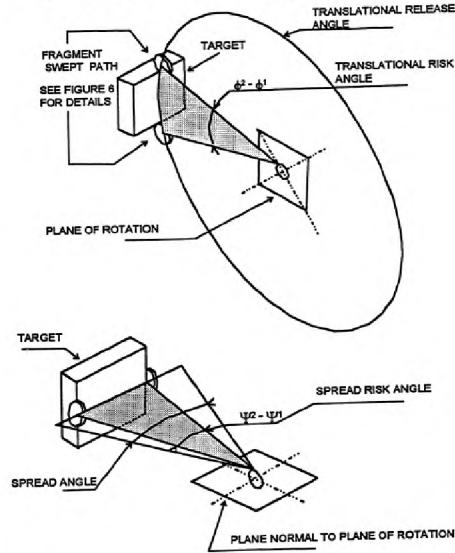


Figure 2: The translational angle and spread angle

3.2 Risk assessment stage

Based on the risk assessment method of the fault tree analysis, the failure probability of catastrophic top events has been calculated. Considering civil aircraft in actual operation, the ratio of the uncontained engine debris that can occur at different flight phases, the risk weights of different catastrophic top events, and the risk probability of single-stage rotor fragment debris failure models have been calculated. For the debris failure model, the same risk identification and assessment process for all engines and all-stage rotors have been summarized and averaged, taking the average probability of all rotor risks as the whole aircraft risk probability.

Finally, the risk probability of the aircraft was compared with the acceptable risk level for the corresponding debris failure model. If it is to meet appropriate criteria, practical design precautions have been taken to minimize damage that can be caused by uncontained engine debris, and that is in compliance with the airworthiness standards. If the risk is higher than the standard value, it is necessary to do further design correction. After several design changes being done as iterations until the aircraft risk probability value meets airworthiness standards, a complete risk assessment process ends.

4 THE CORE RESEARCH WORK – THE RISK ASSESSMENT METHOD BASED ON THE FAULT TREE

4.1 Fault tree analysis

Taking a generic twin-engine aircraft as an object, the risk value of the whole aircraft failure caused by an uncontained event was analyzed for the type of "Single One-Third Disk Fragment" of the engine rotor failure. According to the historical data, the spread angle of the debris type was defined as $\pm 3^\circ$. In addition, it was assumed that (1) each engine has a 10-stage rotor, and (2) the probability of an uncontained rotor failure is 1.0. From the spread angle of the debris, it can

be seen that the area, where the first-stage rotor is 3° forward and the last-stage rotor is 3° afterward, is the impact area affected by the uncontained event. The main systems involved are the flight control system, hydraulic system, fire systems, fuel systems, power systems, environmental control systems, power plant and auxiliary power units. According to the identified affected system, the key components in systems were identified as hydraulic pumps, hydraulic piping and other components in the hydraulic system, which will be used as one of the input materials for the fault tree analysis.

In addition, through the analysis, the aircraft level functional failures were determined to be 200 in the total number, of which there were found 62 catastrophic functional failures. Through the functional risk analysis (FHA), it was determined 5 catastrophic functional failures affected by the engine rotor uncontained events. They are, respectively, "*loss of engine thrust*", "*uncontrollable fire*", "*loss of roll control function*", "*loss of pitch control function*", "*loss of yaw control function*". This catastrophic functional failure list is used as the fault tree analysis for the top event input material.

Through the comprehensive understanding of the affected system structure, principles, failure mode, failure cause and impact, the fault tree was verified from the top event (from top to bottom) and from the key components (from bottom to top). Then the minimum cut sets of the fault tree were found.

Taking the "*uncontrollable fire*" as an example, the fault tree is constructed as shown in Figure 3.

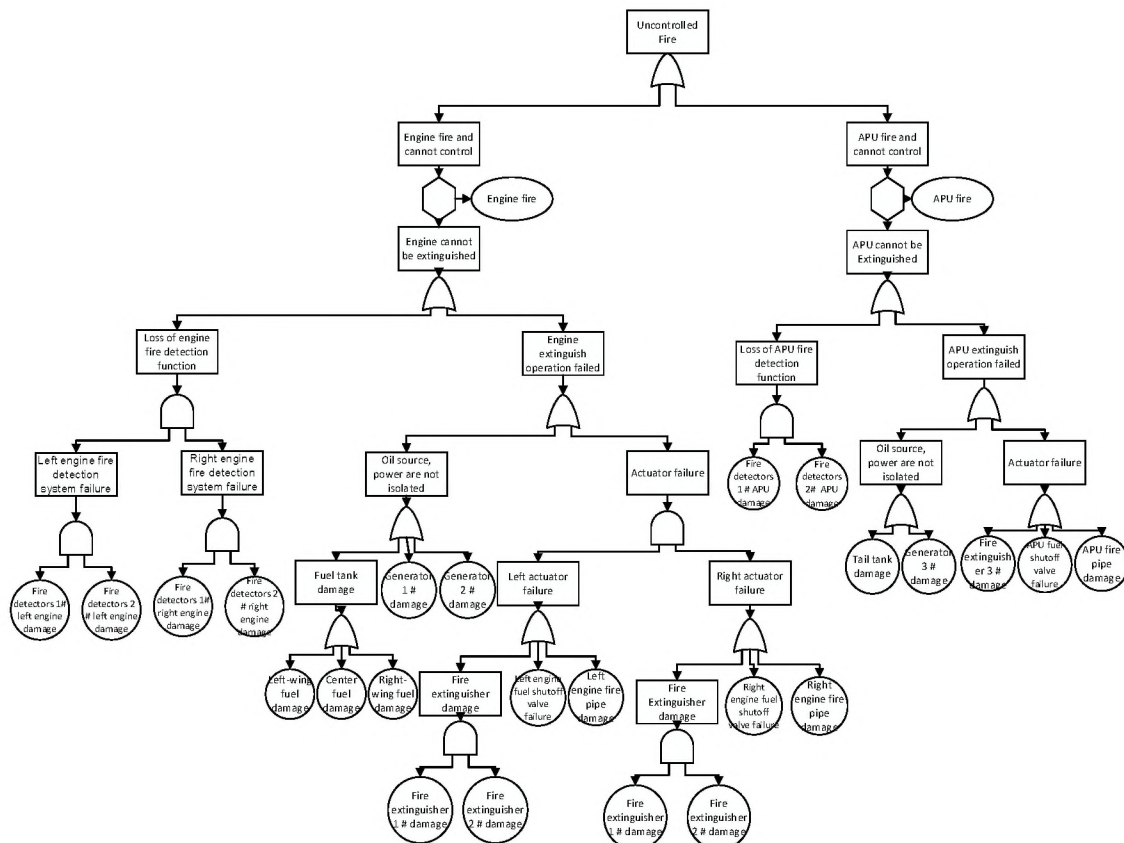


Figure 3: The "*uncontrollable fire*" fault tree

4.2 Bottom event information standardization

The normalized information of the bottom event should normally include rotor information, fragment category, component information, bottom event, spread angle, translational angle, probability of the spread angle range, probability of translational angle range, probability of component, and so on. This paper will be standardized by component information table to achieve the top event information standardization, see Table 2.

Rotor information: xx stage					Fragment category: xx fragment				
Tabulators: xxx					Date:				
Component number	Component name	Bottom event number	Translational angle α_1	Translational angle α_2	Spread angle β_1	Spread angle β_2	Probability of translational angle range p_x	Probability of spread angle range p_y	Probability of component p_c

Table 2: A normalization table of the component information

Where, after rotor debris flying at the rotational direction, the translational angle is interfered with a component in the radial 360° range; the spread angle is forward and afterward from the center of the plane of rotation initiating at the engine centerline. According to the basic assumptions that the spread angle and the translational angle of fragments are independent and uniformly distributed, it can be obtained:

$$p_x = \frac{|\alpha_1 - \alpha_2|}{360} \quad (1)$$

$$p_y = \frac{|\beta_1 - \beta_2|}{D} \quad (2)$$

$$p_c = p_x \times p_y \quad (3)$$

4.3 Quantitative risk assessment of the whole aircraft

The minimum cut sets information has been obtained by the fault tree analysis, and the component failure probability of the normalized table can be obtained as follows:

$$p(\phi_i) = \prod_{c=1}^n p_c \quad (4)$$

Where: c is the number of component corresponding to the bottom event of minimum cut set; n is the total number of components corresponding to the bottom event of minimum cut set; ϕ_i is the i -th minimum cut set.

The top event probability matrix for the minimum cut sets:

$$\mathbf{p}(\phi) = \begin{bmatrix} p(\phi_{1-1}) & \cdots & p(\phi_{1-i}) & \cdots & p(\phi_{1-n}) \\ \vdots & \vdots & \vdots & \vdots & \vdots \\ p(\phi_{j-1}) & \cdots & p(\phi_{j-i}) & \cdots & p(\phi_{j-n}) \\ \vdots & \vdots & \vdots & \vdots & \vdots \\ p(\phi_{m-1}) & \cdots & p(\phi_{m-i}) & \cdots & p(\phi_{m-n}) \end{bmatrix} \quad (5)$$

Where: $p(\phi_{j-i})$ is the probability of occurrence of the i -th minimum cut set in the j -th top event.

Since the number of the minimum cut sets and the orders in the actual situation has been large, the calculation of failure probability of the top event is very complicated. Therefore, the first order approximation can be used to reduce the workload while the calculation accuracy is still acceptable. So the top event failure probability matrix is:

$$\mathbf{P}(\mathbf{T})^T = [\sum p(\phi_{1-i}) \quad \cdots \quad \sum p(\phi_{j-i}) \quad \cdots \quad \sum p(\phi_{m-i})] \quad (6)$$

Taking different flight phases into account, the uncontained rotor event may occur with different probabilities. So it is necessary to consider the influence of the flight phase and define the flight phase influence factors μ

$$\mu = [\mu_1 \quad \mu_2 \quad \cdots \quad \mu_f] \quad (7)$$

Where: μ_f is the probability of occurrence of uncontained rotor events in the f -th flight phase.

In addition, in different flight phases, the top event does not necessarily cause catastrophic consequences. Therefore, it is necessary to consider impact of the top event and to define the top event impact factor τ

$$\mathbf{T} = \begin{bmatrix} t_{11} & t_{12} & \cdots & t_{1f} \\ \vdots & \vdots & \vdots & \vdots \\ t_{j1} & t_{j2} & \cdots & t_{jf} \\ \vdots & \vdots & \vdots & \vdots \\ t_{m1} & t_{m2} & \cdots & t_{mf} \end{bmatrix} \quad (8)$$

Where: t_{jf} is probability of catastrophic consequences after an uncontained rotor event for the j -th top event in the f -th flight phase.

The risk value for a single fragment is:

$$P_i = \sum \text{diag}(\mathbf{P}(\mathbf{T}) \mu \mathbf{T}^T) \quad (9)$$

Calculating the risk value for a single fragment of all engine rotors for the certain debris type, then taking the average value, and getting the whole aircraft risk probability for the corresponding debris type:

$$P_A = \frac{1}{EK} \sum_{e=1}^E \sum_{k=1}^K P_{ik} \quad (10)$$

Where: K is the number of engine rotors; E is the number of engines.

5 CONCLUSIONS

1) This paper highlights the main contents of airworthiness research study: definition of a problem origin; airworthiness standards, advisory circulars, and other materials; airworthiness technology as the focus of the research work of airworthiness projects.

2) Taking the uncontained rotor event analysis process as an example, the technical ideas have been explained and the technical process has been analyzed.

In the field of "*Aircraft Safety Design and Analysis*", an uncontained rotor failure is a typical type of aircraft special risk and it has to meet strict conditions of catastrophic event probability of less than 10^{-9} , which indicates that an aircraft has a high safety level.

3) Taking the risk assessment method based on the fault tree analysis as an example, this paper elaborates the core research work, including the specific method of analysis and the method of quantitative risk assessment.

In the validation phase of the aircraft Type Certificate, an aircraft design organization needs to provide appropriate evidence to indicate compliance with airworthiness regulations. Where FAR § 25.903 / § 23.903 requires "*Design precautions must be taken to minimize the hazard to the airplane in the event of an engine rotor failure or of a fire originating within the engine which burns through the engine case*".

In this work, the MoC3 (Safety Assessment) Mean of Compliance was used, and the final submission of the safety analysis document indicated its compliance with the provisions.

REFERENCES

- [1] Federal Aviation Regulations. *FAR 25, Part 25 Airworthiness Standards: Transport Category Airplanes*. U.S.A.: Federal Aviation Administration, 2008.
- [2] Federal Aviation Regulations. *FAR 23, Part 23 Airworthiness Standards: Normal, Utility, Acrobatic, and Commuter Category Airplanes*. U.S.A.: Federal Aviation Administration, 2007.
- [3] Certification Specifications. *CS 25, Large Aeroplanes*. European Aviation Safety Agency, 2016.
- [4] Certification Specifications. *CS 23, Normal, Utility, Aerobatic, and Commuter Category Aeroplanes*. European Aviation Safety Agency, 2015.
- [5] China Civil Aviation Regulations. *CCAR 25-R4, Airworthiness Standards: Transport Category Aircrafts*. Civil Aviation Administration of China, 2016.
- [6] China Civil Aviation Regulations. *CCAR 23-R3, Airworthiness Standards: Normal, Utility, Acrobatic, and Commuter Category Aircrafts*. Civil Aviation Administration of China, 2005.
- [7] Aerospace Information Report. *AIR 1537, Report on Aircraft Engine Containment*. U.S.A.: Society of Automotive Engineers, 1977.
- [8] Aerospace Information Report. *AIR 4003, Uncontained Turbine Rotor Events Data Period 1976 through 1983*. U.S.A.: Society of Automotive Engineers, 1987.
- [9] Aerospace Information Report. *AIR 4770, Uncontained Turbine Rotor Events Data Period 1984 through 1989*. U.S.A.: Society of Automotive Engineers, 1994.
- [10] Advisory Circular. *AC 20-128A, Design Considerations for Minimizing Hazards Caused by Uncontained Turbine Engine and Auxiliary Power Unit Rotor Failure*. U.S.A.: Federal Aviation Administration, 1997.
- [11] C. E. Frankenberger. Aviation Research. *AR-99/7, Small-Engine Uncontained Debris Analysis*. U.S.A.: Federal Aviation Administration, 1999.
- [12] C. E. Frankenberger. Aviation Research. *AR-99/11, Larger Engine Uncontained Debris Analysis*. U.S.A.: Federal Aviation Administration, 1999.

- [13] Silvia Seng, John Manion, Chuck Frankenberger. Aviation Research. *AR-04/16, Uncontained Engine Debris Analysis Using the Uncontained Engine Debris Damage Assessment Model*. U.S.A.: Federal Aviation Administration, 2004.
- [14] Aerospace Recommended Practice. *ARP 4761, Guidelines and Methods for Conducting the Safety Assessment Process on Civil Airborne System and Equipment*. U.S.A.: Society of Automotive Engineers, 1996.
- [15] Zhang Y., Sun Y. Hazards identification of UERF based on collision detection. *Aircraft Engineering and Aerospace Technology*, 2015, 87(4): 322-329.
- [16] Zhang Y., Sun Y., Zeng H., et al. Computer aided analysis for uncontained rotor failure safety. *Acta Aeronautica et Astronautica Sinica*, 2013, 34(2): 291-300.
- [17] Jia D., Song F. Determination of the Translational Risk Angle of Uncontained Rotor Fragments. *Journal of Aircraft*, 2014, 51(6): 2031-2035.

Reporter



Zhengqiang Cheng

Co-authors



Oleksiy Chernykh



Zhong Lu



Junjiang Xiong

A NUMERICAL METHOD OF SENSITIVITY ANALYSIS IN THE IDENTIFICATION PROBLEMS OF HEAT-LOADED STRUCTURES

Sheng Huang^{1,2}, Vladimir A. Kostin²

¹Shenyang aerospace university,
College of Aerospace Engineering

No.37 Daoyi South Avenue, Shenbei New Area, Shenyang, China

²Kazan National Research Technical University

named after A. N. Tupolev – KAI

Institute for Aviation, Land Transportation and Power Engineering

No.10, K.Marx St., Kazan, Tatarstan 420111, Russia

e-mail: hs-kai@mail.ru

Key words: mathematical modeling, identification, heat structure, sensitivity analysis

Abstract. *The problem of identifying the stiffness of ribs of a four-rib wing-box working under a complex of mechanical and temperature load is considered. An iterative approach using the objective function and the sensitivity matrix based on the Odinokov's and superelement models was proposed by the authors. Numerical results show the suitability of the proposed approach for identification purpose and almost the same accuracy of two models evaluating the sensitivity.*

1. INTRODUCTION

At present, the problem of accurate definition the thermal strength material properties of thin-walled structural components remains urgent in the aerospace field. The thermal load has a significant influence on the bearing capacity by changing the characteristics of materials. This problem belongs to the class of inverse problems, which for the most part are incorrectly posed. The use of regularization methods does not always lead to an acceptable result.

2. MATHEMATICAL DESCRIPTION OF THE ISSUE

It is assumed that the experimental values of thin-walled structures deformation made up of ribs and panels are known. It's required to determine the tension-compression stiffness of the longitudinal ribs. The issue turns to a mathematical problem of optimization with an objective function to minimize:

$$J = \sum_{i=0}^n (f'_{\text{exp}i} - f_i)^2 dz \rightarrow \min \quad (1)$$

where n is the number of ribs, of which the deformations are considered, $f'_{\text{exp}i}$ - experimental deformations, f' - calculated deformations. In the vector-matrix form we have:

$$J = (\{f'_{\text{exp}}\} - \{f'\})^T (\{f'_{\text{exp}}\} - \{f'\}) \rightarrow \min \quad (2)$$

here $\{f'_{\text{exp}}\}$, $\{f'\}$ - n dimensional column vectors. In the following on the basis of (2) an the extremal condition of the functional $J(\beta, x)$, the sensitivity matrix $[\psi]$ can be written as [1][4]:

$$[\psi]^T [\psi] \{\partial C\} = [\psi]^T (\{f'_{\text{exp}}\} - \{f'\}), \quad (3)$$

where $\{\partial C\}$ – column-vector of increment, which is used for the iteration; β – stiffness parameters, $\psi(\beta, x)$, derivative of the vector-function of the deformations with respect vector variable β :

$$[\psi] = \begin{bmatrix} \frac{\partial f'_1}{\partial \beta_1} & \dots & \frac{\partial f'_1}{\partial \beta_j} & \dots & \frac{\partial f'_1}{\partial \beta_n} \\ \vdots & \ddots & \vdots & \ddots & \vdots \\ \frac{\partial f'_i}{\partial \beta_1} & \dots & \frac{\partial f'_i}{\partial \beta_j} & \dots & \frac{\partial f'_i}{\partial \beta_n} \\ \vdots & \ddots & \vdots & \ddots & \vdots \\ \frac{\partial f'_n}{\partial \beta_1} & \dots & \frac{\partial f'_n}{\partial \beta_j} & \dots & \frac{\partial f'_n}{\partial \beta_n} \end{bmatrix}, \quad (i, j = \overline{1, n}) \quad (4)$$

A four-ribs square wing-box is considered, one end of which is rigidly fixed, and on the other - axial and moment loads are applied. At the same time, the ribs are subjected to still different temperature loads, which are constant along the length of the structure (Fig. 1).

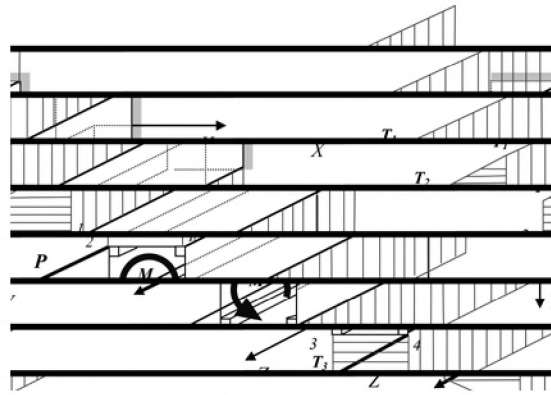


Figure 1: Wing-box with mechanical and temperature load

The elements of the matrix $[\psi]$ are found in two ways: 1) by Odínokov's equations; 2) by the model of superelements.

As the equations of state, we take the equations of Yu.G.Odínokov [2]. The mathematical model describing the behavior of a thin-walled structure under the influence of an arbitrary external load has the form:

$$-(F_i E_i f'_i)' + \sum_{k=1}^n a_{ik} f_k + d_i = 0 \quad (i = \overline{1, n}) \quad (5)$$

$$\begin{cases} F_i E_i f'_i = P_{il} + P_{iT} & \text{at } z = l \\ f_i = 0 & \text{at } z = 0 \end{cases} \quad (i = \overline{1, n}) \quad (6)$$

As can be seen from the formulas, equations (5) - (6) are the system of ordinary differential equations with boundary conditions. Here $F_i E_i$ is the tension-compression rigidity of the rib i , f_i - the axial displacement of the rib i , P_{il} - the axial load on the rib i at $z = l$, $P_{iT} = E_i F_i \alpha_{iT} T_i$; a_{ik}, d_i - the coefficients characterizing the work of the skin under shear and external load respectively: $d_i = \frac{\lambda_i}{B_1^0} Q_x + \frac{\mu_i}{B_2^0} Q_y + d'_i M_z + p_i + p_{iT}$ - value of additional axial load from temperature in rib i ; in which $\lambda, \mu, B_1^0, B_2^0$ - the coefficients characterizing the geometric character; Q and M_z , respectively, the transverse force and the moment of the wing-box section, p_i - axial force per unit length, $p_{iT} = dP_{iT}/dz$.

To apply numerical solution methods, the problem is transformed to the discrete form with the help of integrating matrixes [3]. Thus, in the vector-matrix form:

$$[C + H]\{f'\} = \{P - S\} \quad (7)$$

$[C]$ is $nk \times nk$ order diagonal stiffness matrix of the structure longitudinal ribs along the sections. $[H]$ is $nk \times nk$ order matrix of coefficients depending on the shape and rigidity in the cross sections of the wing-box, $[H_{ik}] = [I_2][A_{ik}][I_1]$ ($i, k = 1, \dots, n$, and A_{ik} is made up of elements a_{ik}). $\{P\}$ is a column vector of size nk representing axial forces applied in the ribs at the free end of the structure ($z = l$), $\{S\}$ is a column vector of size nk , determined by loading the structure, $[I_1] = \int_0^x \dots dx$, $[I_2] = \int_x^l \dots dx$.

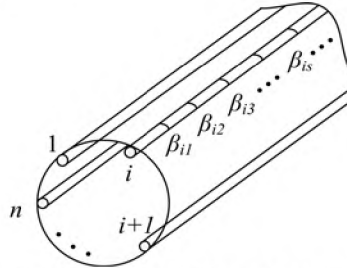


Figure 2: The distribution of β in a thin-walled structure

Variables FE are denoted by the design variables $\beta = \{\{\beta_1\}\{\beta_2\}\dots\{\beta_i\}\dots\{\beta_n\}\}^T$ ($i = \overline{1, n}$) (Fig. 2). Here $\beta_1 = \{\beta_{11}\beta_{12}\dots\beta_{1s}\dots\beta_{1k}\}^T$ ($s = \overline{1, k}$) is the column vector of the rigidity parameters of rib 1 with respect to k sections, $\beta_2 = \{\beta_{21}\beta_{22}\dots\beta_{2s}\dots\beta_{2k}\}^T$ - rib 2 with k sections, etc.

Then the coefficients $[\psi]$ in (4) have the structure:

$$\frac{\partial f'_i}{\partial \beta_j} = \begin{bmatrix} \frac{\partial f'_{i1}}{\partial \beta_{j1}} & \dots & \frac{\partial f'_{i1}}{\partial \beta_{jk}} \\ \vdots & \frac{\partial f'_{is}}{\partial \beta_{js}} & \vdots \\ \frac{\partial f'_{ik}}{\partial \beta_{j1}} & \dots & \frac{\partial f'_{ik}}{\partial \beta_{jk}} \end{bmatrix}, \quad (i, j = \overline{1, n} \quad s = \overline{1, k}) \quad (8)$$

Differentiating equation (7) with respect to β_{is} , we obtain:

$$\frac{\partial [C + H]}{\partial \beta_{is}} \{f'\} + [C + H] \frac{\partial \{f'\}}{\partial \beta_{is}} = \frac{\partial}{\partial \beta_{is}} \{P - S\}$$

here $\partial [H] / \partial \beta_{is} = 0$, since the shear rigidity of the skin does not depend on the rigidity of the ribs

$$\frac{\partial [C + H]}{\partial \beta_{is}} = \frac{\partial [C]}{\partial \beta_{is}} = \frac{\partial}{\partial \beta_{is}} \begin{bmatrix} [C_1] & & \\ & \ddots & \\ & & [C_n] \end{bmatrix} \quad (\beta_{is} = C_{is} = (EF)_{is}) \quad (9)$$

Here, almost all the derivatives of the terms of the matrix $[C]$ after differentiation will be zeros, except for one, whose indices coincide with the index β , will be 1. It follows:

$$\left\{ \frac{\partial f'}{\partial \beta_{is}} \right\} = -[C + H]^{-1} \left[\frac{\partial [C]}{\partial \beta_{is}} \right] \{f'\} \quad (\beta_{is} = C_{is} = (EF)_{is}) \quad (10)$$

Then, using (4) (9) (10), all matrixes of the sensitivity coefficients $[\psi]$ are calculated.

In the second version of the structure model, the representation in the form of superelements [5] is adopted, having the following approximation for displacements:

$$u(x, y, z) = \sum_1^M g_i(x, y) \phi_i(z) \quad (i=1, 2, 3 \dots M), \quad (11)$$

$$f(x, y, z) = \sum_j^N r_j(x, y) \xi_j(z) \quad (j=1, 2, 3 \dots N). \quad (12)$$

where u is the transverse displacement of the panels; f - longitudinal displacement of the ribs; , r - generalized coordinates; ϕ, ξ - generalized displacement, which are solved in the FEM equation:

$$K^g F^g = L^g \quad (13)$$

where K^g – the global stiffness matrix, F^g – the global matrix-column of generalized displacements: $F^g = \{F^1 \dots F^e \dots F^k\}^T$, $F^e = \{\varphi_1^e \dots \varphi_M^e \quad \xi_1^e \dots \xi_N^e\}^T$, $e = \overline{1, k}$ and k here denotes the number of superelements; $L^g = L_M^g + L_T^g$ - loads, composed of mechanical and thermal load;

Denoting $\{\xi\} = T_f \{F\}$, $\{f\} = R \{\xi\}$ and $\{f'\} = T_d \{f\}$, and carrying out the variation of (13), it is can be obtained:

$$[\psi] = -[T_d][R][T_f K^g T_f^T]^{-1} \left[\frac{\partial T_f K^g T_f^T}{\partial \beta} \right] [R][T_f] \{F^g\}. \quad (14)$$

In contrast to (8), here $[\psi]$ has a different structure:

$$[\psi] = \begin{bmatrix} \frac{\partial f'_1}{\partial \beta_1} & \dots & \frac{\partial f'_1}{\partial \beta_k} \\ \vdots & \ddots & \vdots \\ \frac{\partial f'_k}{\partial \beta_1} & \dots & \frac{\partial f'_k}{\partial \beta_k} \end{bmatrix}, \frac{\partial f'_i}{\partial \beta_j} = \begin{bmatrix} \frac{\partial f'_{i1}}{\partial \beta_{j1}} & \dots & \frac{\partial f'_{i1}}{\partial \beta_{jn}} \\ \vdots & \ddots & \vdots \\ \frac{\partial f'_{in}}{\partial \beta_{j1}} & \dots & \frac{\partial f'_{in}}{\partial \beta_{jn}} \end{bmatrix} \quad (i, j = \overline{1, k}) \quad (15)$$

Having obtained ψ in the two previous approaches, with the help of (3) our problem will be solved by an iterative method:

$$\{C^{k+1}\} = \{C^k\} + e \{\partial C\}, \quad (16)$$

4. CALCULATION RESULTS

The above method was tested with the following initial data: wing-box length $l = 100$ cm, panel width $s = 15$ cm, panel thickness $\delta = 0.1$ cm (for all panels), $E = 686500$ kg / cm², cross sectional area F of each rib change according to Table 1:

Table 1

Cross-sectional areas of design edges in numerical simulation ("Experiment")

No. of element	1	2	3	4	5	6	7	8	9	10
F, cm^2	3	3	3	3	2,5	2	2	1,5	2	3

The axial load applied to the ribs 2 and 4 is the same: $P = 10500$ kg; moment $M_z = 100,000$ kg; temperature of the ribs: $T_2 = T_3 = 150^\circ\text{C}$, $T_1 = T_4 = 200^\circ\text{C}$.

Due to the lack of data from the physical experiment, numerically, using FEM, deformation values were obtained by solving a direct problem. In order to use these results later as an approximate value of the physical experiment, artificial errors are introduced about 2%, which is typical for measurements of deformations in a structure with one end fixed. These values are presented in Table 2.

The initial stiffness EF of the ribs was constant along the length, and the graph shows how, with the increasing of iteration step, the stiffness values are specified to the experimental values (Fig. 3).

Table 2

Distribution of experimental structural deformations

No. of element	1	2	3	4	5	6	7	8	9	10
rib 1	0,0074	0,0073	0,0075	0,0074	0,0086	0,0106	0,0105	0,0139	0,0095	0,0053
rib 2	0,0062	0,0060	0,0061	0,0062	0,0074	0,0093	0,0097	0,0135	0,0108	0,0080
rib 3	0,0063	0,0060	0,0062	0,0061	0,0074	0,0091	0,0087	0,0110	0,0078	0,0042
rib 4	0,0073	0,0072	0,0075	0,0073	0,0088	0,0114	0,0115	0,0161	0,0127	0,0093

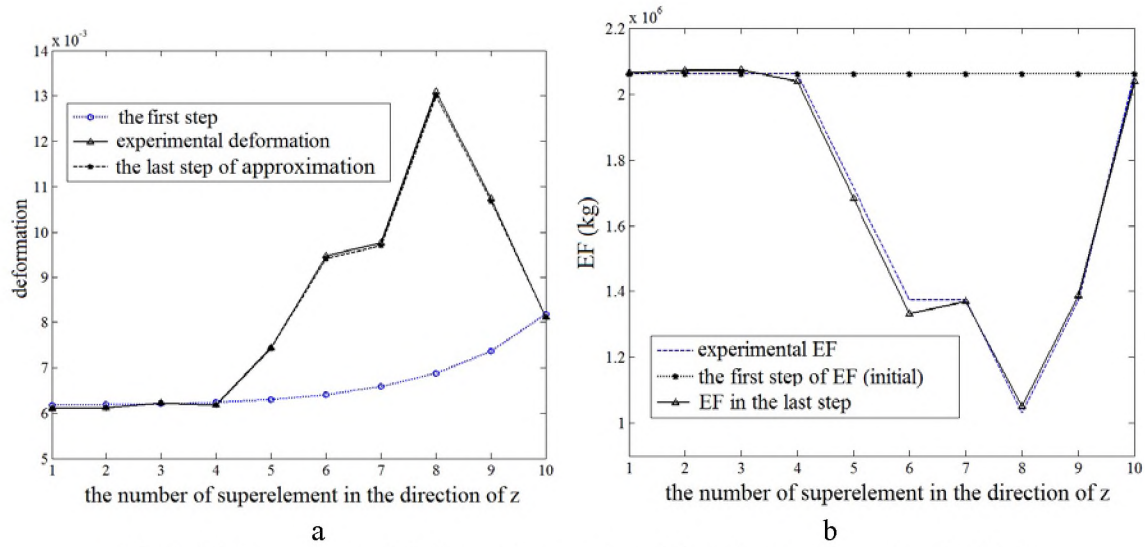


Fig.3. (a) Experimental deformations and model at first and last steps in rib 2
(b) Initial / given stiffness and stiffness of the last step of the rib 2

The sensitivity of ψ to the variables β in the first step and the last step is shown in Fig.4.

Obviously, the more distant the two variables are from each other, the less influence they have on each other. Consequently, the sensitivity of the variable to itself has the greatest absolute value from all the sensitivities to this variable. During the iteration process, i.e. from the first step to the last step, the maximum of the sensitivity values moves from the free end to the weakest section, where the greatest value of the stress appears.

To illustrate the trend of changing the sensitivity by the iteration steps, the sensitivity of the variable rib 2 by the iteration steps is shown in Fig.5. A comparison of the changes in the target function on the basis of the superelement model and the Odinokov's model can be seen in Fig.6.

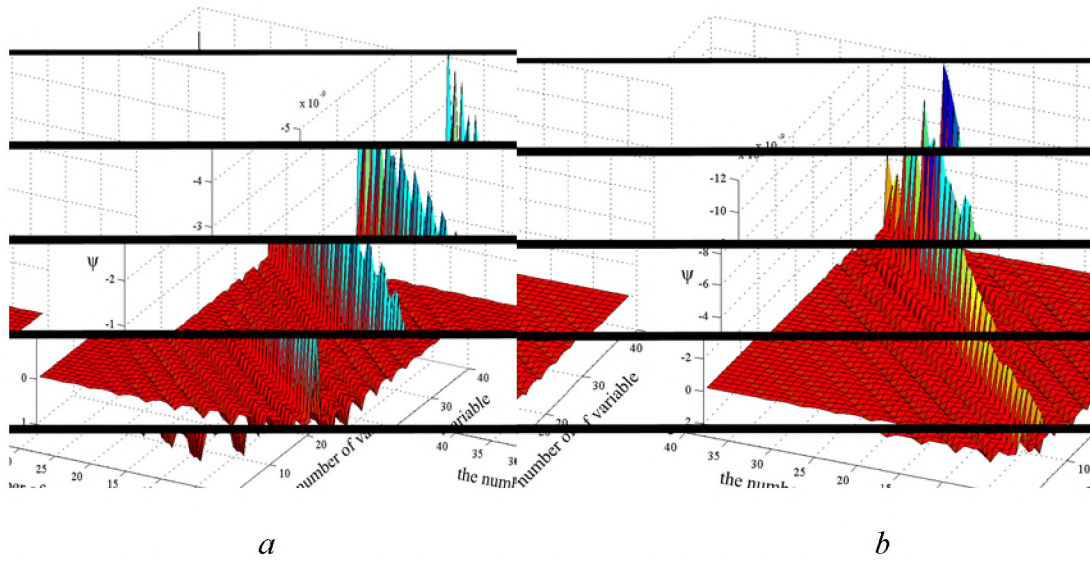


Figure 4: (a) The sensitivity of ψ from the variables β at the first step (b) The sensitivity ψ of the variables β at the last step

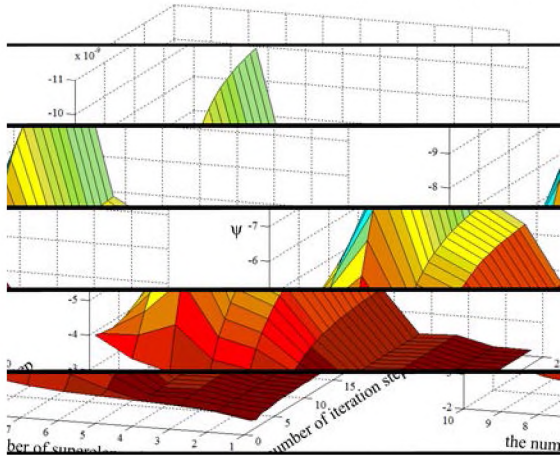


Figure 5: The sensitivity of rib 2 by step iteration

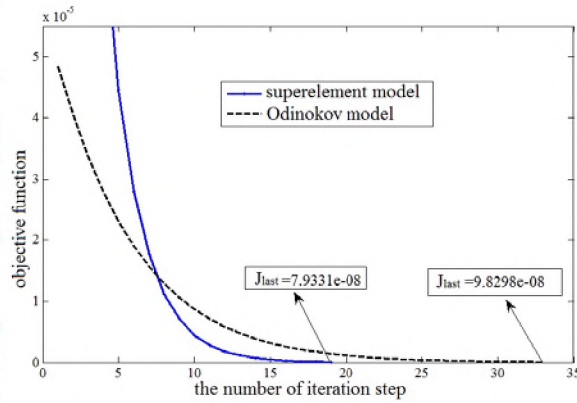


Figure 6: Objective functions based on superelement and Odinokov's models

5. CONCLUSIONS

The proposed approach makes it possible to solve the problems of identification of thin-walled structures under the temperature field and mechanical loads. The sensitivity analysis method, which is realized by the superelement model and the Odinokov's continuum model, is illustrated through the distribution and trend of the sensitivity function, respectively, in space and in the iteration steps.

The sensitivity analysis based on the two models enables us to compare the above approaches to solving the inverse strength problems with the combined action of the temperature field and mechanical loads of the structural elements. A comparison of the convergence of the objective function solved by the two models shows that the superelement model in this prob-

lem converges faster in the time of analyzing the sensitivity. The results of the study may be useful for further development of methods for identifying or optimizing designs using sensitivity analysis.

REFERENCES

- [1] Kostin V.A., Valitova N.L. Theory and Practice of Strength Testing Aircraft Structures, Kazan, Kazan State Tech. Univ. Publ., 2014, 140 p. (in Russian)
- [2] Odínokov Yu.G., Calculation of Thin-walled Structures such as Wing, Fuselage and Aircraft Feathers [Proc. of KAI], 1948, No. 20. pp. 39-106. (in Russian)
- [3] Vakhitov M.B. Integrating Matrices as the Apparatus of Numerical Solution of Differential Equations in Construction Mechanics, Russian Aeronautics, 1966, No.3. pp. 50-61. (in Russian)
- [4] Haug E.J., CHOI K.K., Kovkov V., Design Sensitivity Analysis of Structural Systems, Academic Press, 1986, 381 p.
- [5] Wang Z., Kang L., Kretov A.S., Huang Sh., Strength Design Model for Thin-Walled Structures, Russian Aeronautics, 2016 г. No. 1, pp. 116-122.

Authors



Sheng Huang



Vladimir A. Kostin

BIOMIMETICS: WHY IT IS WORTH OF DOING IT FOR ASTRONAUTICS AND AERONAUTICS ENGINEERS?

Stanislav Gorb, Elena Gorb

Department of Functional Morphology and Biomechanics, Zoological Institute of the Kiel University
Am Botanischen Garten 9, D-24118 Kiel, Germany
e-mail: sgorb@zoologie.uni-kiel.de

Key words: Biologically-inspired design, bionics, biomimetics.

Abstract. *Humans learned the majority of unusual creative ideas in technology from Nature. Natural solutions for engineering problems are usually very effective, especially their precision and resource efficiency. For example, the plane wing profiles are based on those inspired by birds and winglets of modern air jets are implemented according to the feather arrangement at the bird wing tip. Nowadays, all engineering inventions and discoveries are subdivided in 40-80 classes, belonging to various branches of technology. However, «the patent library» of the Nature is actually endless. This paper provides general rules of biomimetics (science dealing with creative transfer of ideas from biology to engineering) and several examples of such inventions taken from insects.*

1. INTRODUCTION

Insects are among the most diverse groups of animals on Earth, including more than a million described species and representing more than half of all known living organisms. The number of extant species is estimated to be between six and ten million [1] and approximately represents over 90% of animal life forms [2]. Insects can be found in nearly all environments. During their evolution, insects and related arthropods have evolved a huge variety of shapes and structures. Despite often looking miniature and fragile, they can nonetheless deal with extreme mechanical loads. Many functional systems responsible for their evolutionary success are based on a variety of ingenious materials and structural solutions. The rich sensory equipment of insects, including their compound eyes, chemoreceptors, mechanoreceptors and infra-red (IR) receptors taken together with their rather compact brain reveals self-adaptive control patterns and often supports remarkable behavioral features.

Studies revealing the functional principles of insect structures, materials, sensors, actuators, locomotion and control systems are, on the one hand, of major scientific interest, since we can learn about the mechanisms behind the structures and their biological roles. On the other hand, this knowledge is also highly relevant for various engineering applications including those in the field of astronautics and aeronautics. Two of the greatest challenges for today's engineering are energy saving and sustainability. During their evolution, insects and other arthropods have solved many problems dealing with their external lightweight skeleton. Additionally, these animals build a number of remarkable constructions based on silk, glue and surrounding non-living materials [3]. Biologists have collected a vast amount of information about the structure and function of such animal-made constructions and about the materials and structures utilized in their bodies. This information can be used to mimic them for diverse applications in modern engineering.

The main fields, in which insect-inspired solutions can be applied, are as follows: (1) new materials, (2) constructions, (3) surfaces, (4) adhesives and bonding technology, (5) optics and photonics (Fig. 1). Possible innovations might also appear on the boundary between biology and engineering [4]. Some selected examples are discussed in this paper, but with more than one million species as a source for inspiration, many more ideas might arise from the study of insects to be used for biomimetics in astronautics and aeronautics.

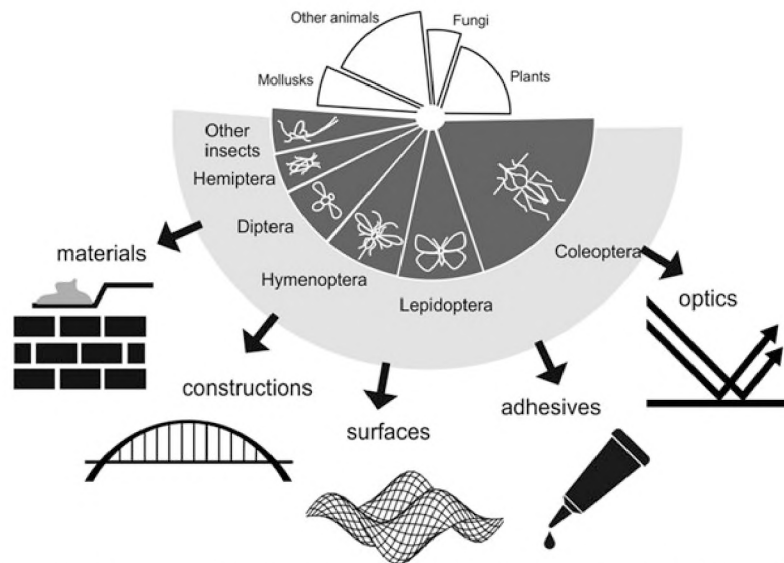


Figure 1: Diagram demonstrating insect diversity (dark grey segment of the pie) as a source of biomimetic ideas for application in engineering science [4].

2. MAIN PART

Previous studies of the bird flight contributed to the modern methodology of the wing lift force calculation, the force that holds the aircraft in the air. These results are a basis of the modern aerodynamics. However, insects have even more elaborate flight mechanism. Their speed and maneuverability are really remarkable even in comparison to other biological flying systems, but even more impressive for modern aeronautics. Insects have not only a very promising wing structure and its material composition [5], but very effective sensory equipment. One of the last exciting engineering developments is so-called oscillatory gyroscope that is based on studies of halteres (flies' clavate appendages originating from the hind wings). This kind of the gyroscope is used for the determination of angular declinations from the flight trajectory in planes and missiles.

Another example is honeycomb structures that occur often in Nature and can be actively constructed by mostly social insects, such as bees and wasps, from completely different materials, e.g. wax and paper. This geometrical pattern is well known to represent the most densely packed units in two-dimensional space, which is an interesting principle for its implementation in aerospace technology. Technical honeycomb structures can be made of a stronger variety of materials, such as plastics, ceramics and metals, and by using a diversity of processing techniques, such as the cutting of hexagonal sheets and subsequent gluing, the insertion of strips of glue between the sheets and subsequent stretching or the application of

moulding techniques, especially when polymers are used. Honeycomb-patterned lightweight materials can be used in engineering lightweight constructions in the sandwich panels and composite designs.

For example, Dr. Mirtsch GmbH has developed a broad variety of three-dimensional (3D) metal tins having various thicknesses of sheaths. These structures often originate from a highly specific method of production by using self-organization. The structures are rather impressive not just because of their beautiful optical appearance, but mainly due to their convincing technical properties (Fig. 2). Among their functional features, the most striking are (1) much stronger bending stability at much lower material use (ultra-lightweight), (2) enhanced crash-resistance properties attributable to stronger energy dissipation, (3) further enhancement of bending stiffness because of their combination into sandwich-like structures, and (4) their ability for combination with other, also dissimilar, materials.

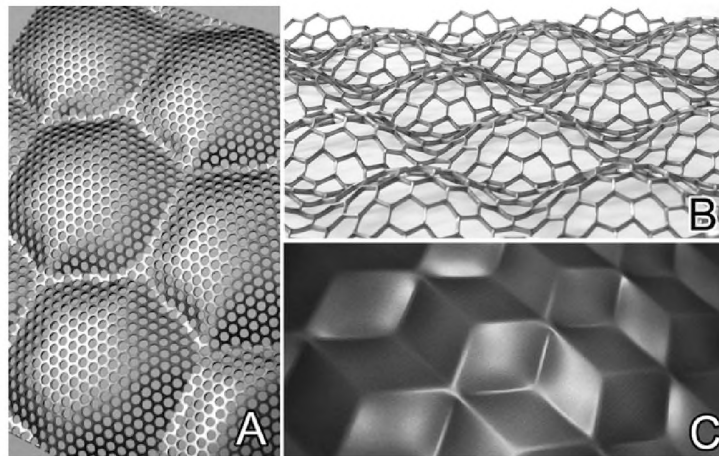


Figure 2: Technical honeycomb structures for potential use in aircraft design. Dr. Mirtsch GmbH, Courtesy of Frank Mirtsch (www.woelbstruktur.de).

Insect wings are usually thin and delicate outgrowths of the body wall. In order to prevent their damage, some groups, such as beetles, earwigs or bugs, have fore wings that serve a protective function and are therefore thickened and stiff. The hind wings must exhibit a certain area in order to be aerodynamically functional and they are indeed larger than the thickened fore wings. The only possibility for the hind wings to be completely covered by the fore wings is to be folded (Fig. 3) [6]. The folding pattern depends on the wing venation pattern and the material properties of the structures involved. Consequently, the morphology of wings in insects with an additional folding function differs from the wings without the folding capability.

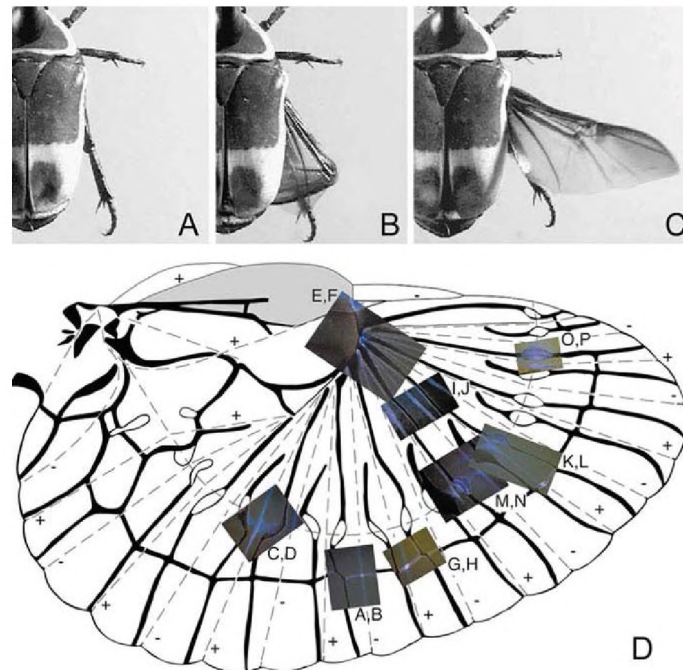


Figure 3. Insect wings folding structures. (a–c) Beetle *Pachnoda marginata*, single frames from a video sequence of the wing unfolding [7]. (d) Distribution of resilin, a rubberlike protein, in a hind wing of the earwig *Forficula auricularia*. Blue autofluorescence shows the presence of resilin, rubber-like protein material [6].

The design of foldable wings is a compromise between flight and folding. For example, the hind wings of earwigs (Dermaptera) are strongly folded and covered by the small, thickened and sclerotized fore wings. The area of the unfolded wing is ten times larger than that of the folded wing [6]. The folding pattern in earwigs is rather complicated and is made possible by the combination of muscle activity, the pleating pattern, and the specific distribution of resilin, a rubber-like protein, within the folds (Fig. 3D). The specific pleating pattern is responsible for high elasticity of the wing. Three-dimensionally pleated wings have an asymmetric torsional rigidity [8]. Another mechanism is based on a gradient-like distribution of the rigid and soft resilient materials of the thin membranous areas of wing cells [7].

3. FURTHER DEVELOPMENTS

What can be done to advance aircraft design by using biomimetics? The first and obviously, additional research on biological materials, constructions and surfaces will help in the application of biological knowledge to recent challenges in astronautics and aeronautics. The incorporation of additional biological knowledge into the design of artificial systems will potentially improve their performance. Unfortunately, biologists still do not have a complete understanding of how biological materials and structures are constructed and what their performance is. Hence, many technological areas will benefit from additional biomechanical research. Additionally, a huge variety of animals and their structures have never previously been studied. Screening for new biological systems with interesting properties therefore remains an extremely important research field in the near future.

4. CONCLUSIONS

Statistics shows that American companies generate, on average, 0.5 ideas per employee per year, whereas typical Japanese companies generate 9 ideas per employee per year; both numbers are relatively low. Our creativity is obviously limited. However, we can extend this by employing the great bank of ideas from living nature. Every organism on the Earth has evolved through adaptation and the survival of the fittest and, hence, organisms have retained only those evolutionary adaptations that make them strong. Considering the details that we have just discussed, it can be concluded that deep studies of biological structures and shapes provided numerous inventions in engineering during relatively short time. These advances in biomimetics provide an important reason for further studies of biological systems, because in doing so, we might overall harmonize relationships between biological evolution and technological development.

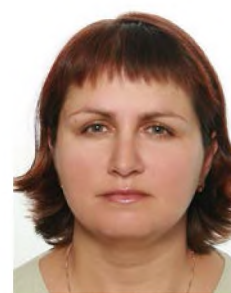
REFERENCES

- [1] Chapman A. D. (2006) Numbers of living species in Australia and the world. Australian Biological Resources Study, Canberra. ISBN 978-0-642-56850-2.
- [2] Erwin T. L. (1982) Tropical forests: their richness in Coleoptera and other arthropod species. *Coleopt Bull* 36:74–75.
- [3] Hansell M. (2007) *Built by animals: the natural history of animal architecture*. Oxford University Press, New York.
- [4] Gorb S. N. (2011) Insect-inspired technologies: Insects as a source for biomimetics. In: Vilcinskas A. (ed) *Insect biotechnology*. Springer, Dordrecht, pp 241–264.
- [5] Gorb, S. N. (1999) Serial elastic elements in the damselfly wing: mobile vein joints contain resilin. *Naturwissenschaften*. 86:552–555.
- [6] Haas F., Gorb S. N., Wootton R. J. (2000) Elastic joints in dermapteran hind wings: materials and wing folding. *Arthr Struct Dev* 29:137–146.
- [7] Haas F., Gorb S. N., Blickhan R. (2000) The function of resilin in beetle wings. *Proc Roy Soc Lond B* 267:1375–1381.
- [8] Wootton R. J. (1991) The functional morphology of the wings of Odonata. *Adv Odonatol* 5:153–169.

Authors



Stanislav Gorb



Elena Gorb

EXPERIENCE IN USING OF ELECTROMECHANICAL SIMULATION STAND OF UAV'S AEROELASTIC BEHAVIOR IN RESEARCH WORK OF STUDENTS AND POSTGRADUATES OF AEROSPACE FACULTY

Igor K. Turkin and Sergey G. Parafes'

Moscow Aviation Institute (National Research University),
125993, Volokolamskoe shosse, 4, Moscow, Russia

e-mail: kafedra_602@mail.ru Web: <http://mai.ru/education/space/>

Key words: Unmanned aerial vehicle (UAV), stand, aeroelastic stability, electromechanical simulation, test

Abstract:

The description of an electromechanical simulation stand of the aeroelastic behavior of the unmanned aerial vehicle is given; the basics of the method of electromechanical simulation of aerodynamic forces are described; the experience in the use of the stand in the research work of undergraduate and graduate students of the Aerospace faculty is analyzed.

1. INTRODUCTION

The actual designing problems of maneuverable unmanned aerial vehicles are ensuring security from flutter and aeroelastic stability with control system[1 – 3]. Design, design-experimental and experimental methods are used to solve them. One of the methods that provide reliable results about the boundaries of flutter and stability of the loop "elastic UAV – control system" is a method of the electromechanical simulation (EMS) of the aerodynamic forces [4, 5]. In the EMS method the mechanical force is applied to the structure, formed the computing device by the signals of the vibration sensors in accordance with aerodynamic theory in real time. Tests with an artificial "flow" of air allow you to control the results of the interaction of elastic UAV and control system, assessment of stability with open or closed loop.

2. ELECTROMECHANICAL SIMULATION STAND OF UAV'S AEROELASTIC BEHAVIOR

The Department 602 "Aviation and missile system" MAI (on the basis of the equipment purchased in the framework of the National Research Universities development Program in 2010) established stand of electromechanical simulation of aerodynamic forces to study the aeroelastic characteristics of the UAV (the EMS stand)[6, 7]. The stand includes:

– means of excitation and measurement of vibrations – energizers and power amplifiers (TMS, USA), accelerometers and impedance head (PCB Piezotronics);

- a managing complex consisting of a personal computer, a measuring and control real-time system Compact RIO (National Instruments, USA), and National Instruments standard software (National Instruments);

- means of implementation of boundary conditions.

Boundary conditions are implemented in two variants. The first variant simulates the conditions of UAV's free flight. For implementation of this boundary condition the stand has portals for the elastic suspension of the UAV. The second variant is to hard mount the UAV or its separate parts. For implementation of this boundary condition the stand has force plates for fastening of its parts.

Specialists of the Department 602 had developed the software for the system Compact RIO (in Lab VIEW) to control the tests. The software implements different modes of excitation of the test design, provides measurement and processing of sensor signals and calculating the aerodynamic forces in real time.

For the control of the tests is using a specially designed graphical interface. One of the typical windows "Amplitude-phase frequency characteristic (APFC)" is shown in Fig. 1.

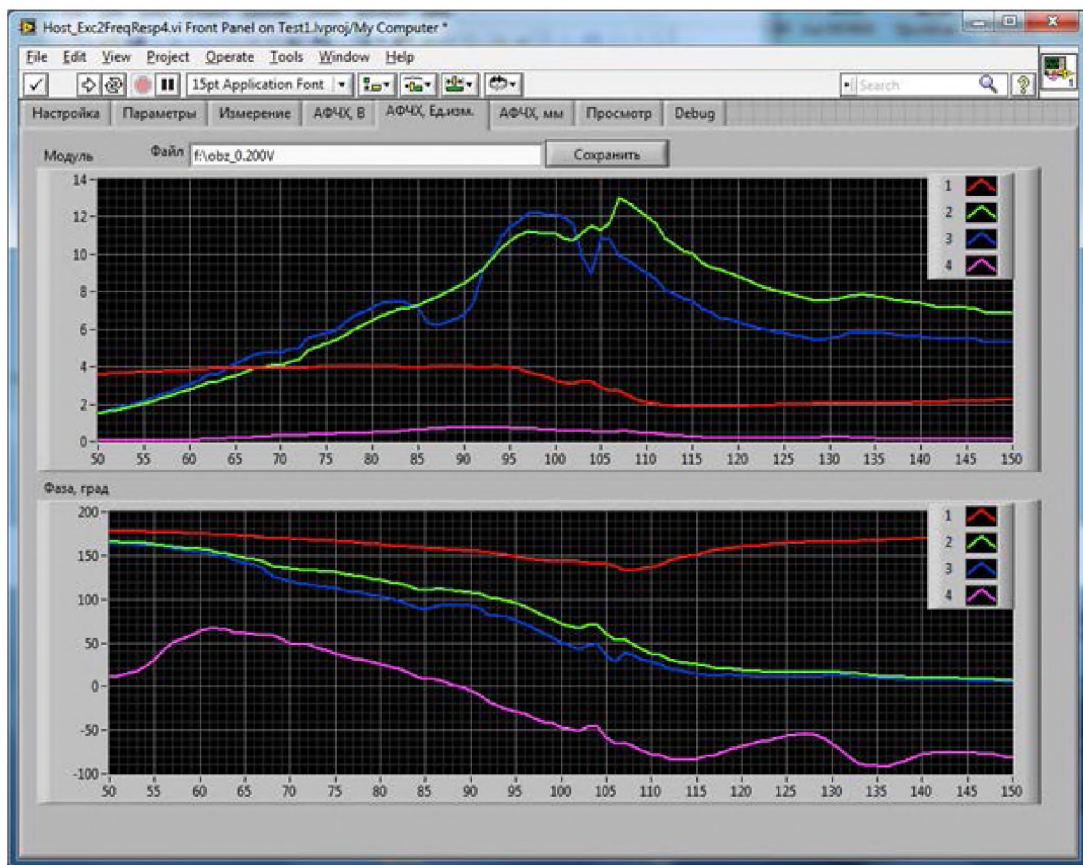


Figure 1: The graphic interface: the window "Amplitude-phase frequency characteristics"

The EMS stand allows the comprehensive experimental study of the UAV aeroelastic stability, including: determining characteristics of the UAV elastic design oscillations, the study of UAV flutter; determining characteristics of the system "surface control – actuator" (amplitude and frequency characteristics, stability, dynamic rigidity); determination of frequency

characteristics of control system; the study of the possible self-oscillation nature (frequency, limit cycles, the vibration overloads level) etc., as well as computational and experimental determination of the loop "elastic UAV – control system" stability.

From the list of submitted tasks to be solved by EMS stand, it follows that researches of the UAV's aeroelastic behavior with electromechanical simulation of aerodynamic forces is an important but not the only purpose of the stand using. The stand due to the presence of dynamic multipoint excitation allows also to perform an extensive research of the UAV's design oscillation characterizations, the frequency characteristics of the actuator, etc., which are also important for solving problems of aeroelasticity during the development process of the UAV.

Computational and experimental determination of the the loop "elastic UAV – control system" stability is also possible using the experimental characteristics.

3. METHOD OF THE ELECTROMECHANICAL SIMULATION OF THE AERODYNAMIC FORCES

In the EMS method the computing device is formed mechanical forces applied to the design by the signals of the vibration sensor in accordance with aerodynamic theory in real time (Fig. 2) [5, 8]. The method is a calculation-experimental, because the simulated aerodynamic forces applied to the UAV are determined by calculation, and are reproduced later in the experiment. Its distinctive features are [5, 8]:

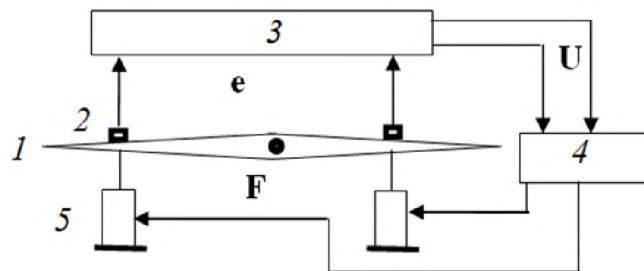


Figure 2: The scheme of the electromechanical simulation of the aerodynamic forces:

1 – wing; 2 – accelerometers; 3 – computing device;
4 – power amplifier; 5 –energizers

- the experiment preparation includes, in particular, the choice of the option of replacing the distributed forces equivalent concentrated (in the calculation part of the method), as well as the definition natural forms and frequencies (in the preliminary experiment);

- the most significant "fundamental" tones in the study of the flutter and in the study of the loop "elastic UAV – control system "are defining based on the data of the flutter preliminary calculation;

- the real design (UAV or its components) with the real distribution of mass, damping and stiffness, including possible nonlinearity and a functioning control system, is studying;

- the restrictions on aerodynamic parameters (the modes of the simulated flight) do not exist; the modeled parameters of the "flight" are not limited by the parameters of the atmosphere or a wind tunnel. This advantage is particularly important when actual inventories are measured as with closed and open loop of the control system;

- the computing device change modes (air density ρ , speed V , the number M), while the effect of elastic-mass parameters of the UAV, the control system coefficients, etc. can be studied by varying their parameters;
- the study methods, both in frequency and in time domains are available;
- the tests are non-destructive and fully observable, the conditions of the stand allow you to repeat every "start";
- the simulation of aerodynamic forces, as in the calculation is limited by the choice of aerodynamic theory, with distributed flow effects are replaced to few concentrated forces applied to UAV's design.

The basic ratios of the EMS method are based [5, 8]:

- the first, the linear mechanical-electric transform of the displacement (vector \mathbf{y}) of the UAV individual points when its vibrations on the stand through the vibration sensors into electric signals (vector \mathbf{e}), that is, the ratio of the form:

$$\mathbf{e} = \mathbf{R}\mathbf{y},$$

where \mathbf{R} is a diagonal matrix of the calibration coefficients of the sensors;

- the second, the transformation of the arbitrary, including nonlinear, the signal \mathbf{e} by the computing device in its output signal \mathbf{u} :

$$\mathbf{u} = \mathbf{K}\mathbf{e},$$

where \mathbf{K} is a matrix of transform coefficients in the computing device, depending on the simulated flight regime, numbers ρ , V , M ;

- the third, the electromechanical conversion of the instantaneous values of the signals \mathbf{u} into the mechanical forces \mathbf{f} :

$$\mathbf{f} = \mathbf{Q}\mathbf{u},$$

where \mathbf{f} is the vector of the mechanical forces, \mathbf{Q} is a calibration coefficients diagonal matrix of the energizers with power amplifiers.

In the EMS method at a known dependence of the instantaneous values of the vector of the concentrated aerodynamic forces \mathbf{f}^A from the displacements of individual points: $\mathbf{f}^A = \mathbf{L}^A\mathbf{y}$

\mathbf{L}^A – a matrix of correlations between the oscillations of the UAV and accompanying aerodynamic forces) is the equality of forces \mathbf{f} simulated at the stand (outside the flow) and the aerodynamic forces: $\mathbf{f} = \mathbf{f}^A$.

The correct modeling of external power influences at the oscillations of the UAV in flight will be implemented when the condition

$$\mathbf{U} = (\mathbf{Q}^{-1}\mathbf{L}^A\mathbf{R}^{-1})\mathbf{e}.$$

This condition requires functioning in real-time all elements of the EMS stand (Fig. 2): sensors, the computing device, power amplifiers and electrodynamic energizers with the acceptable accuracy. At the frequency language – all elements of the EMS stand should not make errors in module and phase in the investigated frequency range.

A generalized block diagram of the experiment is shown in Fig. 3, which includes the elastic suspension for the formation conditions of free flight; the excitation system, containing sources of harmonic voltages and energizers with the power amplifiers; a measurement system (sensors with matching converters); control and verification equipment of UAV systems (in particular control systems); the computing apparatus for forming of aerodynamic forces produced by the energizers. Vibrations of elastic UAV are measured by sensors, whose signals are received at the computing device, in which an aerodynamic model calculates the instantaneous forces, which are applied to the UAV by means of energizers (EMS cycle 9, Fig. 3). At that the distributed aerodynamic forces are replaced by the few concentrated forces, the number of which is determined by the capabilities of the computing device, as well as the number of energizers and requirements to accuracy of reproduction of forces.

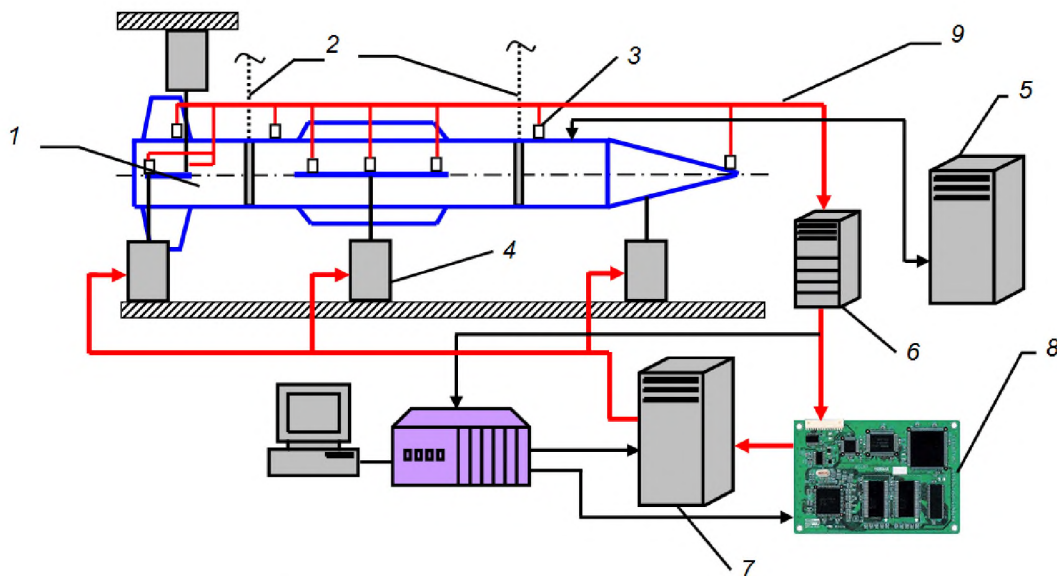


Figure 3: The scheme of the EMS stand:

- 1 – UAV; 2 – elastic suspension; 3 – accelerometers; 4 – energizers;
 5 – computing device; 6 – matching signal converters; 7 – power amplifier; 8 – computing device;
 9 – EMS-cycle

4. AN EXPERIENCE IN THE USING OF THE STAND IN THE RESEARCH WORK OF AEROSPACE FACULTY STUDENTS AND POSTGRADUATES

Using the EMS stand the experimental researches are conducted at the present time. The researches include: determining characteristics of oscillations of the elastic design of UAV, the study of flutter of UAV; the determining characteristics of the system "surface control – actuator" (amplitude and frequency characteristics, stability, dynamic rigidity); the determination of frequency characteristics of the control system; the study of the possible self-oscillation nature (frequency, limit cycles, the level of vibration overloads) etc.

Undergraduate and graduate students of the aerospace faculty of MAI are hired to work experimental researches. They are directly involved in conducting the specific experimental researches using the EMS stand and take part in further expanding the functional capabilities of the stand through the development of additional control programs and interfaces.

Students and graduate students use in their research work, present papers at scientific conferences and publish articles in scientific journals the results of these experimental researches.

5. CONCLUSIONS

The Department 602 "Aviation and missile system" of MAI established electromechanical simulation stand of aerodynamic forces to study the aeroelastic characteristics of the UAV (the EMS stand). The stand includes: the means of excitation and measurement of vibrations, managing complex, portals for the elastic suspension of the UAV and force plates for fastening of the compartments when tested.

Using the EMS stand the experimental researches are conducted at the present time. They include: determining the UAV elastic design characteristics of oscillations, the study of UAV flutter; the determining characteristics of the system "surface control – actuator"(amplitude and frequency characteristics, stability, and dynamic rigidity); the determination of the control system frequency characteristics; the study of the possible self-oscillation nature (frequency, limit cycles, the level of vibration overloads) etc.

Undergraduate and graduate students of the aerospace faculty of MAI are hired to work experimental researches. They use the results of these experimental researches in their research work, present papers at scientific conferences and publish articles in scientific journals.

REFERENCES

- [1] Unmanned aerial vehicles. Fundamentals of structure and functioning / P.P. Afanas'yev, I.S. Golubev, S.B. Levochkin, V.N. Novikov, S.G. Parafes', M.D. Pestov, I.K. Turkin. Ed. I.S. Golubev and I.K. Turkin. Moscow. 2010. 654 p. (in Russian).
- [2] Parafes' S.G., Smyslov V.I. Methods and means of aeroelastic stability of unmanned aerial vehicles. Moscow, Izd-vo MAI, 2013, 176 p. (in Russian).
- [3] Livne E. Integrated Aeroservoelastic Optimization: Status and Direction // Journal of Aircraft. 1999. Vol. 36. No. 1. pp. 122 – 145.
- [4] Karkle P.G., Smyslov V.I. [Electromechanical simulation in aeroelasticity problems]. Polet [Polyet (Flight)]. 2008. No. 10. pp. 25 – 31. (in Russian).
- [5] Karkle P.G., Smyslov V.I. Modal tests of aircraft and the playback of force effects. M.: Tekhnosfera, 2017. – 155 p. (in Russian).
- [6] Bykov A.V., Kondrashev G.V., Parafes' S.G., Turkin I.K. Electromechanical simulation stand of aerodynamic forces to study the aeroelastic behavior of unmanned aerial vehicle // Materialy XX Mezhdunarodnogo simpoziuma im. A.G. Gorshkova, T. 1. – Moscow: OOO «TR-print», 2014. pp. 38 – 40 (in Russian).
- [7] Parafes' S.G., Turkin I.K. Actual problems of aeroelasticity and dynamics of structures, highly maneuverable unmanned aerial vehicles. Moscow, Izd-vo MAI, 2016. 183 p. (in Russian).

Igor K. Turkin and Sergey G. Parafes

[8] The test of flight vehicles (unmanned aerial vehicles)] / P.P. Afanas'ev, V.V. Burkin, A.N. Gerashchenko, I.S. Golubev, V.V. Doronin, I.P. Kirillov, S.B. Lyovochkin, S.S. Lyovochkin, S.G. Parafes'. Ed..I.S. Golubevand S.B. Lyovochkin. – Kaluga: IP Strel'cov I.A. (Izdatel'stvo «EHidos»)) [published by Eidos], 2015. – 504 p. (in Russian).

Authors



Igor K. Turkin



Sergey G. Parafes'

THE CAREER GUIDE MEASURES FOR FUTURE AERONAUTICAL ENGINEERS AT NATIONAL AEROSPACE UNIVERSITY KhAI

Olena Litvinova, Alina Matskevich, Natalya Sytnyk, Dmytro Toporets

National Aerospace University KhAI,
Ukraine, 61070, Kharkiv, 17 Chkalova street
E-mail: dean10@khai.edu

Key words: labor market, career, aircraft engineers, alumni

Abstract. *The objective of this paper is to share the measures established at KhAI to help graduates find the appropriate job positions on labor market. The measures were provided with attention paid to the specific group of graduates as prospective and aspiring aerospace engineers and related experts. The career guide has been created on the basis of practical experience of previous graduates.*

Generation and implementation of effective graduate employment policy at higher educational institutions by profession are an important and highly urgent state task, which should be solved in close cooperation with employers, universities and youth themselves. The purpose of KhAI in this matter is to prepare its students to solve problems of employment, develop their activity and psychological ability to overcome failures at the stage of job search, improve self-presentation skills as one of the key factors of competitiveness on the labor market, and gain skills to use traditional and new methods of employment.

The following career guide measures have been provided at KhAI:

- 1) KhAI has formed the Committee for Student Employment affiliated to KhAI Student Association and the Department of Assisting KhAI Students and Alumni in Employment, which organize the annual Job Fair. Such events are an excellent opportunity to establish communication between employers and potential employees. It is always more efficient to talk in person, ask questions, discuss some ideas. Many students after such fairs come to businesses for practical trainings and internships. Such aerospace companies as PJSC *Motor-Sich*, *Antonov*, State Enterprise *Kharkiv Machine Engineering Plant FED* and PJSC *FED*, and *Progresstech-Ukraine* are participating at KhAI job fair. Apart from

these more than 40 companies in IT sector provide vacant positions and social and economic services.



Figure 1: Motor-Sich realizes their own regular passenger flights.

- 2) KhAI Student Association administrates the communities on the social networks where enterprises and companies publish information about vacant positions.
- 3) KhAI Departments cooperate with universities from other countries, such as Tampere University of Technology (Finland), National Polytechnic Institute and Queretaro University (Mexico), Institute of Electronics and Telecommunications of Rennes University (France) and others in implementation and realization of scientific projects KhAI students have an opportunity to take part in.
- 4) International Relations Office organizes student workshops for writing resumes and cover letters, as well as testing of English knowledge, since successful employment means a B2 level in English at least.
- 5) Inclusion to the curriculum of the subject "Key factors for successful employment", during which students study the labor market, determine their place on the market, familiarize themselves with the organization of job search process, simulate interviews for employment, learn non-verbal communication.

As the result of such extensive cooperation and collaboration with multiple organizations and establishments the students of KhAI have endless career opportunities after graduation. Our alumni can progress to become licensed aircraft engineers, which allows them to supervise and sign for completed work. They may then choose to move into a team leader or supervisory role overseeing a number of engineers, allocating work and assessing completed work.

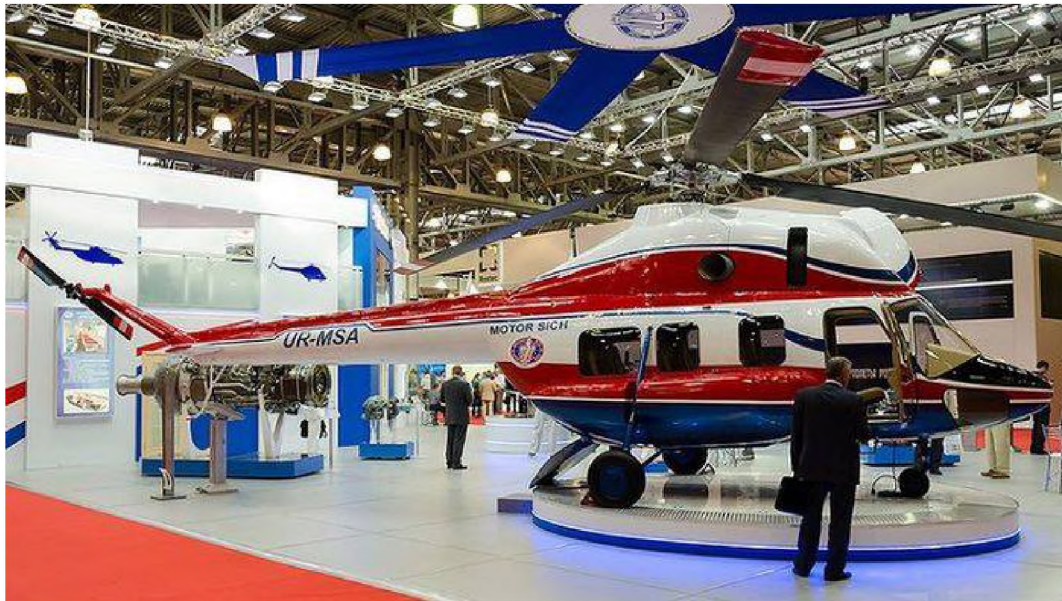


Figure 2: Motor-Sich presented a helicopter of its own production MCB-2.

Some engineers may complete further studies and move into aeronautical engineering. Avionics engineers can also move into roles in general electronics, such as electronic engineer or technician.

Having elaborated the educational system covering full engineering cycle in aviation industry our University has managed to cover all the job offers coming from various employers in aforementioned industry. Our graduates succeed in working at companies all over the world from North America to Australia making KhAI name a real brand. And as a real brand we are striving to develop even more programs, courses and internships with national and international organizations in order to help our students be competitive, successful and confident as they proudly spread the good name of our University to infinity and beyond.

Authors



Olena Litvinova



Alina Matskevich



Natalya Sytnyk



Dmytro Toporets

Biography

Olena graduated from University with honors in 2001. She is a senior professor of Language Training Department and Head of International Office. She has published 21 articles.

Alina graduated from University in 2001. She is a manager of International Office. She has published 5 articles.

Natalya graduated from University in 2003. She is an assistant professor of Language Training Department and Head of Academic Mobility Department. She has published 10 articles.

Dmytro graduated from University with honors in 2011. He is an assistant professor of Applied Linguistics Department and manager of International Office. He has published 10 articles.

EXPERIENCE OF THE NATIONAL AEROSPACE UNIVERSITY "KHARKIV AVIATION INSTITUTE" IN THE DEVELOPMENT OF STUDENTS' CREATIVE ACTIVITY

V.T. Sikulskiy, V. Yu. Kashcheyeva, O. O. Shatravka, D.S. Toporets

National Aerospace University KhAI,
Ukraine, 61070, Kharkiv, 17 Chkalova street
E-mail: vsikulskij@gmail.com

The organization of scientific activities is coordinated by the Council of Young Scientists, Postgraduates and Students (Council), which is a voluntary academic association of students, graduate students and young scientists under the age of 35 who take an active part in research work.

The purpose of the University Council is to create conditions to unleash scientific, inventive and creative potential of students training at the University, the development of their scientific thinking and research skills, promotion of various branches of science at the University; development of innovation activities, organizational assistance to the University's leadership in the optimization of scientific and educational work among youth.

The University Council performs the following functions:

- representative – it analyses and represents the interests of young scientists interested in research work and have a desire to participate in it;
- communicative – it provides a communicative field for communication, exchange of meaningful scientific ideas, presentation of the results of individual scientific developments, publication of the results of scientific work discussing them with their colleagues, i.e. young specialists;
- informational – it provides up-to-date scientific and organizational information that helps to navigate events and scientific information;
- organizational – it carries out organizational support of scientific initiatives, proposals, projects, research teams;
- educational – it carries out propaganda activities at the university in order to attract talented young scientists to research as a possible career and profession.

An important step to involve students in scientific work in our university was the inclusion of the course "Student research work" in the curriculum of specialists and masters. This course allows every student to try their abilities in a scientific topic, which each student receives from the supervisor and performs under their guidance. More active students can do scientific or design work outside of school hours. Students and masters who study under an individual program are entrusted the implementation of individual elements of research conducted at the university. The results of students' scientific papers are discussed at scientific seminars, forums, round tables, intellectual games, presentations of scientific projects, exhibitions of student works.

Thus, scientific work becomes an integral part of the educational process, contributes to the formation of a scientific outlook, the development of creative thinking, initiative, erudition and individual abilities of students.

An important factor to improve the quality of training aviation specialists is the involvement of students in scientific activities, which in the first place can be achieved through their participation in the implementation of contractual and state budget projects that are carried out by the university. The most capable students who have gained experience in junior courses can be involved in the implementation of domestic and international projects (grants) that are carried out at the university.

There are all the possibilities for this, because we have advanced airmodel sports, paragliding, hang gliding, parachuting, etc. Designing and manufacturing of hang gliders, paragliders, etc. is carried out under the guidance of teachers and research staff.

The results of scientific and technical developments and the best practices are being implemented by the university teachers in the educational process. Review presentations, containing information on the current world level of science and technology development, as well as lecture courses and laboratory works developed in the light of new experience, help to improve the process of training students at all levels of study. Individual elements of scientific research at KhAI are performed by students and masters who study according to individual program.

Students' scientific work is also carried out on the basis of structural divisions of the University, which carry out work on the design and modeling of various aircraft and their constructive elements, design technological equipment, create control programs for machines, etc.



Figure 1: Remote control complex designed with participation of students

The KhAI Student Design and Technology Bureau was organized more than 40 years ago, it has created more than 30 aircraft, and their authors became famous scientists and designers. Widely known were the production of experimental products made of composite materials, the design and manufacture of a ULF airliner, tight airplanes, air cushion vehicles, autogyros, wind power plants, and more.

An important role in the training of highly skilled aviation specialists was played by the creation of research and production complexes at existing enterprises, where senior students are trained, acquire practical skills and are engaged in the actual design of aviation engineering samples.



Figure 2: KhAI student presents his own scientific development at the All-Ukrainian exhibition

Every year, inter-faculty, general-level mass events are held at the university: competitions, contests, reviews, exhibitions of student's scientific creativity, etc. The best scientific publications are published in scientific journals, so in 2016 the number of scientific publications of students (articles, abstracts): in co-authorship – 673, independent – 609. Number of students who participated in all-Ukrainian thematic competitions, schools, tournaments is 68.

KhAI holds over 60 international projects annually with universities and enterprises, including the development of high-tech equipment and technologies with developed countries of the European Union.

Integration of young scientists and specialists of Ukraine into the European and world community is an urgent need of our time. There are various ways to accomplish this task. One of them is training students for joint programs and in close cooperation with the leading profile universities of the world. In 2008, the framework cooperation project for a double diploma was signed. According to the approved plan, students study for two years at the National Aerospace University, and then two years at the Torino Polytechnic University, where after graduation they are qualified and obtain a bachelor's degree in Aerospace engineering. At the same time as studying in Italy, students continue their studies at the KhAI,

study the relevant disciplines, pass exams, and also qualify for a bachelor's degree and a state diploma in Ukraine.

The practical implementation of the agreement is the joint training under the double diploma program of the KhAI students in the field of "Logistics", as well as the exchange of postgraduate students and scientific and pedagogical staff.



Figure 3: KhAI Students in front of modern main building of Beihang University

In 2006, a permanent agreement on scientific and technical cooperation was signed between KhAI and Aviation Research Institute at Beihang University. The purpose of the agreement is to jointly create new models of aviation-space technology, create implementation of research projects, mutual training and training of specialists, creation of new methods for designing samples of new equipment.

KhAI has been actively involved in international research projects funded by the European Union within the framework of the Aviation, Space and Information Technology Research Programs in the past six years as the main research areas of the KhAI. In addition, the scientific developments of our employees in the field of ecology, safety, advanced materials and production technologies also meet the priorities of European research.

The KhAI partners in the framework programs are organizations from such countries as France, Great Britain, Italy, Sweden, Finland, Greece, Spain, Romania, Israel and others. Of these, the most famous are AIRBUS, ONERA, Thales Alenia, EOARD, IAI, AVIC.

Participation in research projects within international consortia (with participation of more than ten organizations) enables KhAI employees to get acquainted with advanced European experience in the field of research and development, new technological processes, the process of introducing new developments in production, etc.

Within the framework of the WASIS project, the KhAI scientists together with 11 partners from 8 European countries are working on designing an innovative design of a composite wafer fuselage with a minimum number of connecting units, which will significantly reduce the weight of the future medium-range passenger aircraft.

The HPH.COM project is aimed at the development, optimization and manufacture of low-thrust plasma rocket engines using helicopter radio frequency technology and its use to control the position of the microsatellite.

The final workshop of the AERO-Ukraine Project "Ukraine's Potential in the Development of Aerospace Science and Technology" brought together leading scholars and researchers from Ukraine and Europe, who are interested in further cooperation.

In July 2011, the National Contact Point (NCP) of the Seventh EU Framework Program for Research and Technological Development on the thematic area "Transport" (including Aeronautics) was established on the basis of the KhAI.

In addition, during this period, a national contact point website (<http://ncp.khai.edu>) has been created to provide access to the most important European transport information sources, which contains up-to-date information on open competitions, new trends in European transport policy and major Ukrainian and European events devoted to FP7 and transport research.

Since September 2011 the EWENT international academic exchange program under the ERASMUS-MUNDUS program has been implemented (<http://ewent.meil.pw.edu.pl>). This project is considered by the European Commission as an element of the overall European cooperation and partnership. The project is aimed at launching a research and educational network, which includes universities from the European Union, Ukraine, Belarus and Moldova.

The project provides scholarships for mobility for students and teachers from Belarus, Moldova and Ukraine to European universities.

Thanks to this project, 12 students and university lecturers received short-term internships at European universities, and our first students from Italy, Spain, and Poland came to our university.

KhAI is a participant of the program for the creation of a micro-satellite basic model of universities in Ukraine with the expanding the structure and equipment possibility of the flight test and development of scientific ideas and hypotheses, new technical solutions, device samples, obtaining low-budget access to space images, space radio communications, satellite Internet .

The project involves cooperation with leading foreign technical universities, in particular with:

- Berlin Technical University;
- Lessius University of Belgium;
- Dutch University of Fontys.



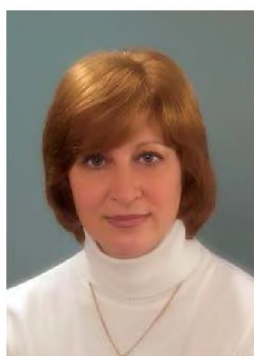
Figure 4: The design of microsatellite built by students from Ukrainian and European universities

The development and creation of a university microsatellite in the form of a microplatform, which can accommodate various targeted research equipment within the existing masses, power systems, tolerances on thermal modes and angular stabilization of the platform, is proposed.

Authors



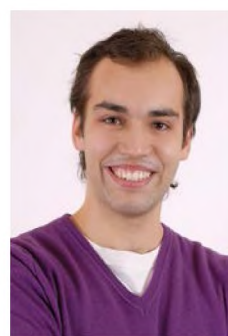
V.T. Sikulskiy



V. Yu. Kashcheyeva



O. O. Shatravka



D.S. Toporets

RATIONAL DESIGNING ON THE BASIS OF REAL-LIFE EXAMPLES

Clifton Read^{*}, Dmytro V. Tiniakov[†]

^{*}Executive Wisdom Consulting Group, Brisbane, Australia
68 Mayfield Road
Carina 4152 QLD Australia
e-mail: cliftonread@y7mail.com

[†]Nanjing, Nanjing University Aeronautics and Astronautics
Jiangjun Road, 29, Nanjing, Jiangsu, China, 211106
e-mail: Tinyakov_Dm@mail.ru, web page: <https://www.facebook.com/tinyakov.d>

Key words: Aircraft design, training methodology, analysis, interesting examples

Abstract. *This paper deals with methods of teaching aircraft design based on extensive use of interesting examples to contribute to the consolidation of teaching materials, as well as increasing the potential interest of the student audience. Using real examples of design gives many instances of how real conditions can influence aircraft structure. Many airframe design solutions may be useless or injurious if implemented without first applying deep analysis of the external conditions that the aircraft may encounter in service. Some irrational or unproven design features have led to the ultimate problem, a crash. So, to provide logical training in order to decrease the potential for this problem to arise, design teachers need to carefully analyze the experiences of previous designers. This will assist in educating new designers who can use the experiences of the past to make for more logical, reasoned and safer aircraft projects.*

INTRODUCTION

The university course Aircraft Design is for students enrolled in Aeronautics or other related majors and is one of the fundamental subjects in the field of aeronautics. It is difficult because it includes a number of related but separate disciplines which students have to learn in detail (Figure 1). So the material that students must take on board to successfully study aircraft design is not only complex in nature, requiring a strong foundation in engineering sciences, but is also taken from a range of subject areas that are specialties in their own right. It makes reasonable sense then, to integrate practical examples into the teaching regime in order to allow students the opportunity to more fully understand the application of various design solutions.

The other side of the same coin of course is, that it is not practical to show a real structure for every theoretical position. Similarly, the number of top level designers who have the time and inclination to teach their different specialties is relatively small, so the most efficient way to disseminate their knowledge is to use examples of real designs, both successful and unsuccessful. An artist trains by studying the works of famous painters, and repeating and refining those methods to develop a technique of their own, one that gives them the results that they seek. As the designers of the future need to understand not only what does work (and why), they must also

learn what has already been tried and has not worked. It is important for the student to determine what factors influenced a designer to use a particular structural solution and what the outcomes were. It is this analysis that will help the design student become one of the new high-level designers.

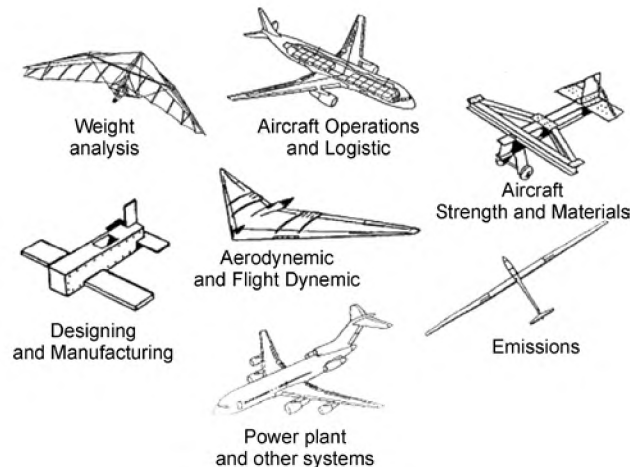


Figure 1: Components of an "Aircraft Design" course

The great Russian aircraft designer Andrey Tupolev spoke a simple, but very accurate phrase about aircraft – "Only the beautiful planes fly beautifully"[1]. This would imply that the inverse may also be true, and while Tupolev's statement may be somewhat subjective, students should be able to learn not only from the successful aircraft designs, but they also study those designs that failed - in some cases, crashed - so as to learn what not to do. The analysis of real-life examples can be applied to all phases of the design process: the development of requirements; formation of technical specifications; the technical proposal; preliminary design; technical design; production; testing and refinement; exploitation, including upgrades and changes during in-service period; and after an aircraft has completed its operational life.

EXAMPLES AND THEIR ANALYSIS

Here we would like to discuss some examples that we found may provide some student interest if they were to be used in the course of teaching Aircraft Design.

Example 1. Conceptual Selection of Flight Speed

The development of flight in the first sixty years of the 20th century is unprecedented in human history. From the Wright's first powered flight at Kitty Hawk in 1903 which covered about 36 metres in about 12 seconds, in just 50 years' people were able to fly across continents and oceans in jet-powered passenger aircraft. By the late 1950's and into the early 1960's, the question of the next major direction for aviation development had arisen. There were two very different schools of thought as to the best way to move into the future:

1. to increase flight speed; or
2. to increase passenger capacity.

All of the major countries and companies involved in aviation embarked on projects to provide answers to these questions, and the resulting research eventually provided quantum leaps in passenger air travel. Two of the players decided that the answer lay with speed, lots of speed. The Tupolev company of the Soviet Union started work on the Tupolev Tu-144 (fig. 2a), while a European consortium comprising the British Aircraft Corporation and Aerospatiale of France, along with financial backing from both British and French governments, began construction of the first prototype of the Concorde (fig. 2b) in 1965.

In the United States, several private companies had also begun research into Supersonic Transport (SST) passenger aircraft, with both the Lockheed and Boeing companies receiving congressional approval and funding to proceed with their designs. Boeing however, also began work on the B747 (fig. 2c), an aircraft designed to double passenger capacity and increase the range of the most popular jet aircraft in service at the time, the Boeing 707 and Douglas DC-8.

At the time, it was widely thought that supersonic aircraft would eventually supersede non-supersonic passenger aircraft for medium-and long-haul flights and this was to have an effect on design requirements for the B747. Developing a new aircraft is very expensive and so the design brief included that the B747 be easily adapted to carry freight and thus remain in production even if sales for passenger aircraft declined.

Both design directions provided enormous challenges for the designers. The aerodynamic demands of supersonic speed meant that new materials and new manufacturing processes had to be devised and developed. The B747's passenger capacity of 400+ required a larger fuselage diameter which also saw new materials and manufacturing processes come into being.

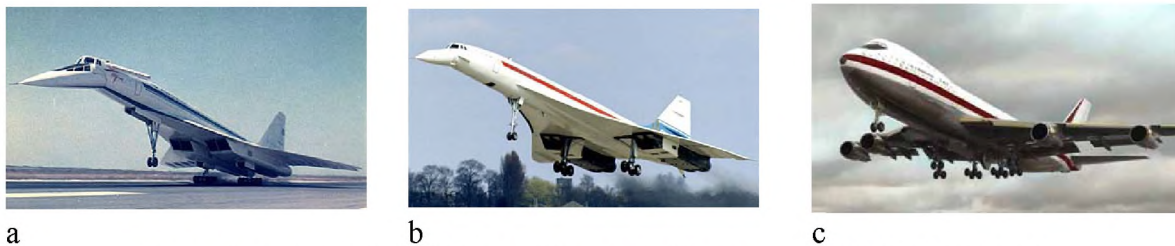


Figure 2: a – Tu-144 (USSR), b – Concorde (Europe), c – B-747 (USA) [1,2]

So what were the operational differences between supersonic airplanes and the B747, and how can we make realistic comparisons to highlight the best design solutions when considering all of the salient factors in the decision-making process?

First, passenger capacity. The aerodynamics of supersonic flight means that a large diameter fuselage is simply not possible. This is borne out by the fact that the fuselage diameter of the B747 is roughly twice that of the supersonic aircraft. The 6.1meter fuselage of the subsonic Boeing also presented designers with many challenges. For example, the problem of how to get around 400 people onto the aircraft and to their seats and then off again at their destination in a reasonable timeframe led to the development of the first twin-aisle configuration. Wide-body jets with twin passenger aisles are now the industry standard, even for the smaller-capacity medium- to long-haul models like the B787.

Table 1: Characteristics of aircraft [1]:

	<i>Tu-144</i>	<i>Concorde</i>	<i>B747</i>
<i>Fuselage Diameter (Interior)</i>	3.3m	2.62m	6.1m
<i>Passenger Capacity</i>	150	95-128	400+
<i>Cruise Speed</i>	2200 Km/h	2160 Km/h	895 Km/h
<i>PEK-SVO</i>	5600 Km	5600 Km	5600 Km
<i>Flight Time</i>	2.6 hrs	2.6 hrs	6.2 hrs
<i>Range</i>	6000	6500	9000
<i>Fuel Consumption</i>	36 t/h	20 t/h	15 t/h
<i>Total Fuel Burn(PEK-SVO)</i>	94 tons	52 tons	93 tons
<i>Passenger Capacity</i>	150	128	400
<i>Fuel per Pax</i>	0.62	0.40	0.23

At this point a student may ask, why is this such an important design consideration? It is very important as, simply put, the cost of the flight has to be distributed among the passengers. The ability of the aircraft to carry more paying passengers means either the price per ticket can be reduced, or the airline can make a higher profit. Somewhere in the between the cheapest ticket price and maximum profit lies the reality of running a profitable airline that sells tickets at affordable-enough prices to entice people to buy them, while still making a profit and returning dividends to its shareholders.

In Table 1 we see the huge advantage the supersonic aircraft have over the B747. Using a flight from Beijing to Moscow as an example, the more-than-double cruise speed advantage is translated into a comparably lower flight time.

However, speed is not the only factor to consider. For most passengers, the most important factor is the price of the ticket. If a major influencer on the ticket price is the cost of fuel, the B747 emerges with a considerable advantage, courtesy of its fuel burn per passenger value, nearly half that of Concorde and one third that of the Tupolev. From an airline's point of view, this factor alone tips the scales heavily in the B747's favor. Consider that Concorde could fly Beijing – Moscow 3 times and still not carry the same number of passengers as the Boeing's single flight. Even ignoring turn-around times, the supersonic speed advantage is nullified, and the total amount of fuel used would be more than double that of the B747.

A third factor was the total range the aircraft could fly on one non-stop leg. The supersonic aircraft were limited in size by their aerodynamic requirements, which severely limited their payload and fuel capacity. One of the designers' juggling acts is the trade-off between fuel and payload when calculating MTOW. Simply put, at an aircraft's maximums, the more fuel you carry, the less paying freight you can take (whether it walks on by itself or you have to load it), and vice versa.

So we see that high speed has only one advantage – flight time. The B747's ability to carry a much greater load (of passengers, freight and fuel) over greater distances in a single flight revolutionized air travel by putting it within reach of many more people, despite the dominant view at the time it was being designed that it would be superseded by supersonic aircraft and relegated to use as a freighter (hence the hump). Total production for the B747 was estimated to be around 400 aircraft. Actual production up to this year (all variants) is 1,536 aircraft delivered since 1970, 17 more ordered, yet to be built/delivered, for a total production of 1,553, to date. By

comparison, 16 Tu-144's were built, and 20 Concorde. The Tupolev had a short commercial career, flying from 1975 to 1978. Concorde was in service with Air France and British Airways from 1976 until 2003.

Example 2. The Flying-wing Configuration

The history of the flying-wing (Fig. 3) configuration is very long. Despite being a very complex concept, designers keep returning to it, which begs the question, why?



Figure 3: YB, The Northrop Flying Wing [1,2,3]

An aircraft is a device which uses aerodynamic principles to fly. That means the aerodynamic force of lift is required for it to fly (Fig. 4). Any device that produces lift also produces drag, and the ratio of these 2 forces helps determine the efficiency of the design.

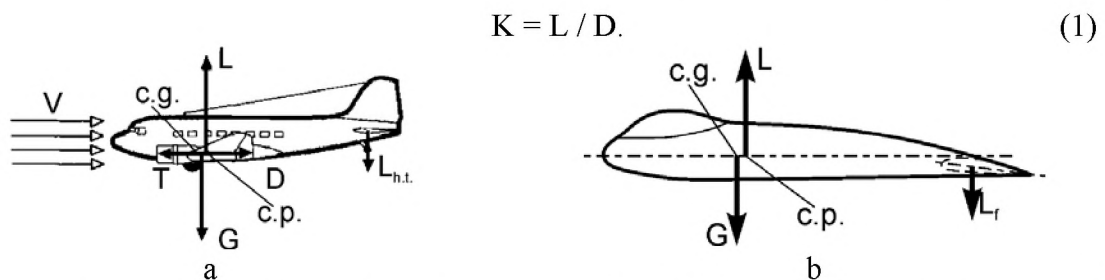


Figure 4: Aircraft balancing configuration: a – complex of balancing forces for the normal configuration, b – complex of balancing forces for the flying-wing configuration

The higher lift-to-drag ratio then the higher operational efficiency of aircraft. This ratio can be improved in 2 ways: increase lift; and/or decrease drag. Improving wing design to improve lift has been a major factor in the improvement of efficiency over the relatively short history of aviation but there are major benefits also to be found by reducing drag, so many designers look for ways to cut drag.

There are two basic types of drag: parasitic drag, so called because it in no way functions to aid flight; and induced drag, which is developed as a result of the airfoil producing lift.

Parasitic drag is comprised of all the forces that work to slow the aircraft's movement and is identified in three types: interference drag; form drag; and skin friction drag. The sum of form drag and skin friction drag is known as profile drag, and it is generated by the shape and size of the aircraft, as well as the friction of the air moving against the skin of the airplane. Therefore, the larger aircraft, the greater drag. As the whole shape of a flying wing aircraft is designed to generate lift, and there are no additional airframe structures like a fuselage and tail plane, this type of design is very effective in reducing profile drag.

Interference drag is also greatly reduced by the flying wing design. Interference drag comes from the intersection of airstreams that create turbulence or restrict airflow. For example, the intersection of the wing and fuselage at the wing root creates significant interference drag. Since the flying wing has only one unit in the airflow, interference drag is minimized.

From this, we can see that this type of design has some advantages, but what kind of problems or disadvantages might it create?

As the flying wing has no tail, it needs some kind of balancing force to control pitch. The horizontal stabilizer on a conventional aircraft serves to balance the device around its lateral axis by creating negative lift (Fig. 4a), with the elevator controlling longitudinal stability.

So, the total lift force equals:

$$L_a = L - L_{h.t.}, \quad (2)$$

where L_a – total lift force of aircraft, L – lift force on the wing, $L_{h.t.}$ – lift force on the horizontal tail.

On a flying-wing configuration, flaperons are needed to create that balancing force.

On (Fig. 4b) we can see the aerodynamic forces present to balance the flying-wing configuration. If we compare it with (Fig. 4a), we can see that the distances between the wing and horizontal tail (on the normal configuration), and between wing and flaperons (on the flying-wing configuration) are different. On the normal configuration it is longer. So, to balance the flying wing we must increase area of the flaperons, because the leverage generated by them of is less than the leverage of the tail, as well as the total aircraft lift force being smaller.

$$L_f > L_{h.t.} \quad (3)$$

As flaperons have the double function of controlling pitch (lateral movement - elevators) and roll (longitudinal movement – ailerons), the control systems become much more complex. These are some of traditional problems of this type of configuration. However, modern computer-controlled fly-by-wire systems allow for many of the aerodynamic drawbacks of the flying wing to be minimized, making for an efficient and effectively stable long-range aircraft.

Since we are considering aircraft design from a commercial perspective, in particular, carrying passengers (and their baggage, plus, perhaps, freight), considering the flying wing configuration as a more efficient option reveals another problem: how to match the carrying capacity of modern jetliners, and how to arrange the seating and cabin configurations in such a way that a potential passenger would want to buy a ticket and get on the aeroplane.

The seat maps shown in Fig. 5a are typical for a 3-class B747. The projection for Fig. 5b is a possibility for a future flying-wing airplane.

From these seat maps, you can appreciate the next issue facing designers of a flying wing passenger aircraft: the standard international airworthiness requirement that in an emergency, all passengers and crew are able to exit the aircraft within 90 seconds. Designers of conventional passenger aircraft have spent considerable time devising emergency exit systems and strategies in order to meet this strict requirement, including intensive crew training, and the placement of emergency exit doors and slides at strategic intervals along the length of fuselage. The second option would not appear to be available to the flying wing designers, particularly for the inner rows of seats and the lower deck. This is one problem for which a solution still needs to be found before the flying wing passenger concept can move beyond the concept stage.

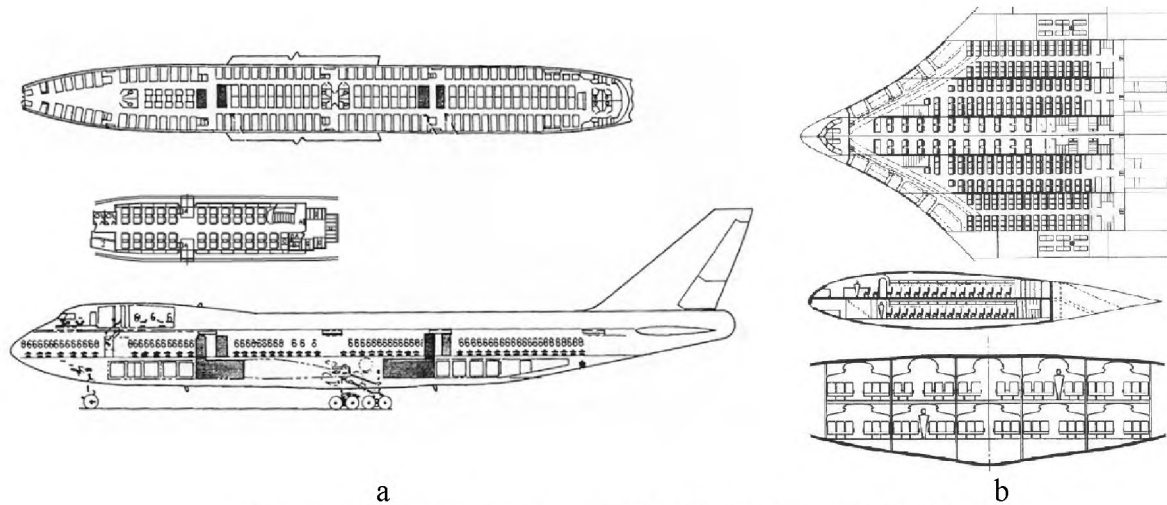


Figure 5: Seatmaps for: a – typical wide-body aircraft B747,
b – possible future passenger aircraft BWB [1,2,4]

Example 3. Wing location in the vertical plane

When we look at aircraft, we seldom think about wing location. Passengers who have a window seat over the wing may think it's not such a good idea as the wing obstructs their view in flight. At this stage, a passenger might wonder about those cargo aircraft that they've seen and recall that many of them had their wings located at the top of the fuselage, rather than the bottom, and wonder why?

So, what factors influence wing location?

In Fig. 6a, the Antonov An-124 cargo plane (kneeling to load/unload) with its high wing.

In Fig. 6b, the Airbus A380 passenger plane with its low wing.

An-124 is a super-heavy cargo aircraft which can carry 150 t. The high-wing configuration on this aircraft has these advantages [1,2,5]:

1. Smaller interference drag between wing and fuselage. These are the biggest structural members of the aircraft, and reducing drag is essential.
2. Reducing drag also reduces fuel consumption.
3. Creates ease of operations during loading/unloading.
4. Servicing and maintenance is also made easier because maintenance vehicles and devices can move under the wing

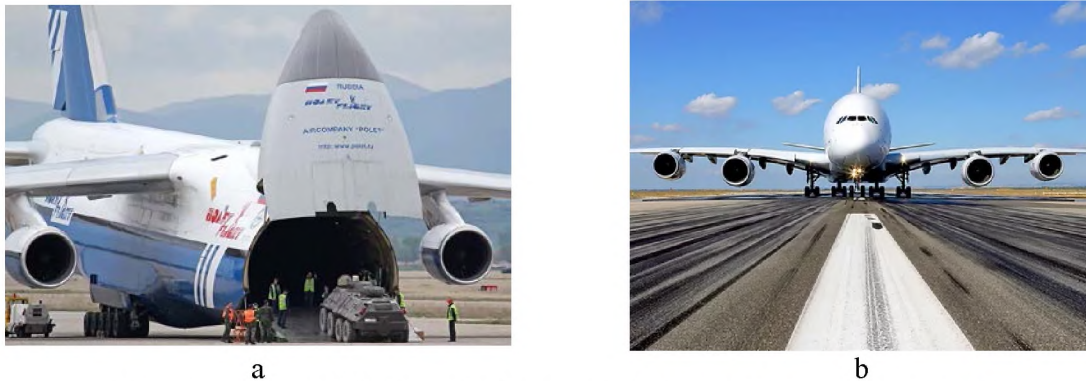


Figure 6: Largest World Aircrafts: a – An-124 super-heavy cargo aircraft, b – A380 super-passenger aircraft [1,2]

The Airbus A380 super-passenger aircraft, which can carry up to 800 passengers, has a low-wing configuration. Why?

One of the Airworthiness Standards Regulations FAR-25 [6] requires that an aircraft must be able to float for 60 minutes after a water landing (ditching), if its flight path is over a large body of water (e.g. sea or ocean). In this situation, a high-wing aircraft will have less stability and floatation on the water, and, being unable to sit flat on the surface, will be more likely to tip, allowing water to ingress the cabin and sink more quickly. By comparison, a low-wing aircraft will have more surface area on the water to provide much greater floatation. So, from this perspective, and despite theoretically higher fuel consumption, long-range over-water passenger flights should be serviced by low-wing aircraft.

Example 4. Continuity of an airframe structure– lifecycle and variations

The first aircrafts 100 years ago were very simple. Modern aircraft consists of a lot of systems and subsystems. Aviation design companies employ many people, often hundreds of employees. The gestation period and lifecycle of an aircraft can be quite long. For example, the world's largest passenger aircraft, the Airbus A380, according to an Airbus company designer, was first mooted in 1988 [6]. Officially the project started in 1994, its first flight was in April 2005, so even ignoring that the idea was floated well before 1994, the project time from beginning to the first flight was over 10 years, entering service with Singapore Airlines two and a half years later in October 2007.

Is it possible (or desirable) to reduce the design time of new aircraft, and if so, how?

The time-honored way is continuity and modification of existing airframes and structures. Some examples:

In 1949, the USSR design company Tupolev started a new bomber project, the Tupolev Tu-16 (Fig. 7a). In 1952 the company started a new passenger airplane project powered by turbojet engines, the Tupolev Tu-104 (Fig 7b) [1,2].



Figure 7: a – Chinese version of Tu-16: Xian H-6, b – Tu-104 passenger aircraft

As a base, Tupolev used the Tu-16 airframe, redesigning the fuselage for passengers, and modifying specific subsystems. The Tu-104's gestation period was very short by industry standards, as its first flight took place in 1955.

Another example is the Boeing B737 [1,2]. The first iteration of the B737 was the B737-100 (Fig. 8a). This short- to medium-range, narrow-body, single-aisle twinjet aircraft, is based on the B707 and B727 models, the first B707 entering service in 1958. The B737 was approved for development in 1965, but was well behind its rivals, Douglas's DC-9, BAC's 1-11, and Fokker's F28 all already into flight certification. To expedite development, Boeing used 60% of the B727's structure and systems by using a slightly widened version of the fuselage cross-section to offer 6-across seating (compared to its competitors' 5), and using a thicker version of the span arrangement of the airfoil sections of the 707/727 wing, the B737 took its first flight in 1967 and entered service in 1968 (Fig. 8).



Figure 8: a – B-737-100, b – B-737-900

Developing the aircraft through 7 variants in the Original and Classic models, the 737 has now developed into a family of ten passenger models with capacities from 85 to 215 passengers, with the B737 Next Generation (-700, -800, and -900ER) and the re-engined and redesigned B737 MAX variants currently being built. Each time Boeing developed a new variant, it changed some of the systems and structures, to the point now where the current models are different from the original. This system has enabled Boeing to create new airplanes for different applications

and performance while keeping development timeframes shorter and using far less of the company's financial resources than they would if developing a new aircraft from scratch.

The Ukraine-based company Antonov has used its resources in the same way. For example [1,2], it was able to complete the An-132 (Fig. 9a) cargo airplane project in 2 years by using the military AN-32 as a base An-32 (Fig. 9b).



Figure 9: a – An-132 cargo airplane, b – An-32 military cargo airplane

One of the most rational processes for modifying existing designs is by deep analysis of operational experience. After this analysis, the designers can include new solutions and, equally importantly, exclude others which have proven not to provide the desired result or shown less than optimal efficiency.

The Russian helicopter manufacturer Mil is renowned for its military rotary wing aircraft and produces the very successful Mi-24 military helicopter (Fig. 10a). It has enjoyed a long and successful operational life. However, the company created a new helicopter, the Mi-35 (Fig. 10b) [1,2].

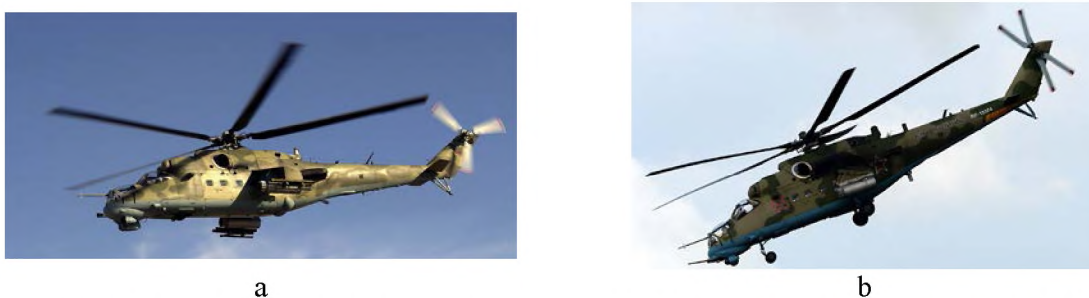


Figure 10: a – Mi-24 landing gear retracted, b – Mi-35 non-retractable landing gear [1,2]

In Fig. 10 you can compare both helicopters. The Mi-35 has a new gun, plus some changes in equipment and, most importantly for this example, changes in landing gear. The Mi-24 landing gear is retractable, while the Mi-35 features non-retractable gear. Using NASA research [1,8] for aircraft, Mil designers found that at speeds less than 330km/h, external shapes actually play a smaller role in creating drag than previously thought. The main idea of retractable landing gear is to reduce drag, but with maximum straight and level flight speeds of 335 km/h

and 300 km/h for the Mi-24 and Mi-35 respectively, and with cruise speeds less than these, to have retractable landing gear gives very little benefit in the quest to reduce drag. When considering the disadvantages of designing and installing a retractable gear system, for example: additional weight; greater complexity for servicing maintenance and repair; foreign object damage to the gear mechanisms during take-off, landing and taxiing; the Mil company designers found that all of these conditions create potential for failure or malfunction. After this analysis, they came to the obvious conclusion that there was little to be lost but significant savings to be gained and so replaced the retractable gear with a fixed structure.

CONCLUSIONS

We could continue to explore similar examples almost indefinitely, all of which would be useful, in varying degrees, to those who aspire to learn the art and science of design, and to make both simple and complex systems as safe and effective as possible. Communicating with students who have graduated from university more than 30 years ago, most are convinced that many such examples still remain in their memories and are a good guide for the future in the design.

REFERENCES

- [1] Wikipedia, the free encyclopedia. [Electronic resource].
https://en.wikipedia.org/wiki/Main_Page
- [2] Уголок неба. Большая Авиационная энциклопедия [Electronic resource].
www.airwar.ru/index.html
- [3] Holaero. [Electronic resource]. <http://www.holaero.com/>.
- [4] BWB (Blended Wing Body) [Electronic resource].
<http://www.testpilots.ru/tp/usa/boeing/bwb/>
- [5] Torenbeek E. Synthesis of Subsonic Airplane Design. [Text]. Kluwer Academic Publishers. 1982. 598 p.
- [6] Federal Aviation Regulations [Text]. Part 25. Airworthiness Standards: Transport Category. FAA. 2011.
- [7] Megastructures: Airbus A380. [Media source]. National Geographic. Movie. 2004-2011.
- [8] NACA Program. [Electronic resource]. www.nasa.gov.

Authors



Clifton Read



Dmytro V. Tiniakov

THE TRANSPORT SYSTEM FOR THE INITIAL DEVELOPMENT OF THE MOON

Liu Jun, Zhang Cong

Supervisor **Anatolii Kretov**

Nanjing University of Aeronautics and Astronautics,

College of Aerospace Engineering

29 Yudao St. Nanjing 210016, P.R.China

e-mail: liujunwm@foxmail.com, unwto@126.com, kretov-ac@nuaa.edu.cn

†

Key words: Rocker System, Transportation, Conceptual Design, Mass Estimate

Abstract. *This article gives an idea to form a new moon landing program by combining the American program Apollo-Saturn V and Russian rocket-carrier Energia which is used to launch the command module (CM), lunar module (LM) and service module (SM) to the moon.*

1. INTRODUCTION

Nowadays, with the progress of space technology and deep space exploration, the desire of man to explore the moon and the universe is even more pressing. First of all, exploring the moon will help mankind to know more about the moon, and to have a good development and utilization of the lunar resources; secondly, it has developed other new technologies, such as *information, materials, energy and micro electro mechanics*, which are of great significance to the development of social economy and the sustainable development of human society. At the same time, it is an important symbol of the country comprehensive strength.

The idea (Fig.1) is to form a new transport system to the moon by combining the American *Appollo* plan, *Saturn V* and Russian *Energia*. The spacecraft is based on the rocket, "Energia", using the rocket to move the useful load, which includes lunar booster(LB), command module (CM), lunar module (LM) and service module(SM) into the low earth orbit (LEO).

For our project, the main parameters are in the Table 1.

Table 1: Main parameters of suggested program

Parts	Mass of First Launch	Mass of Second Launch
Lunar booster	70tons	70tons
Lunar module	20tons	0
Command module	0	5.6
Service module	20tons	20tons
Cargo	0	14.4tons
Total	110tons	110tons

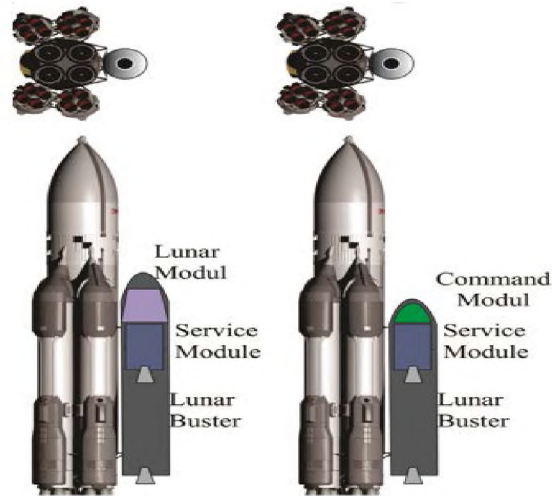


Figure1: Conceptual design of the new transport system

2. MAIN PART

2.1 Flight Mission

The transport system needs two starts. First, the lunar module and service module will be taken into the low earth orbit by the rockets. After that, the lunar booster will accelerate and send the two parts into the low moon orbit. In the second starts, the rockets are working to launch the command module which has three astronauts and service module. It is the situation as we can see in the Fig.2.

In the first expedition (Fig.2), when the C-S Module and L-S Module are both in the low moon orbit, they need to dock together. And then, the LM will re-dock with the CM to carry two astronauts in the CM. After some preparations, the reusable LM is going to land on the moon to open the new base of exploring the moon. And further the SM sends the CM with one astronaut to the Earth. The reusable LM is being designed on 10-20 launches from moon.

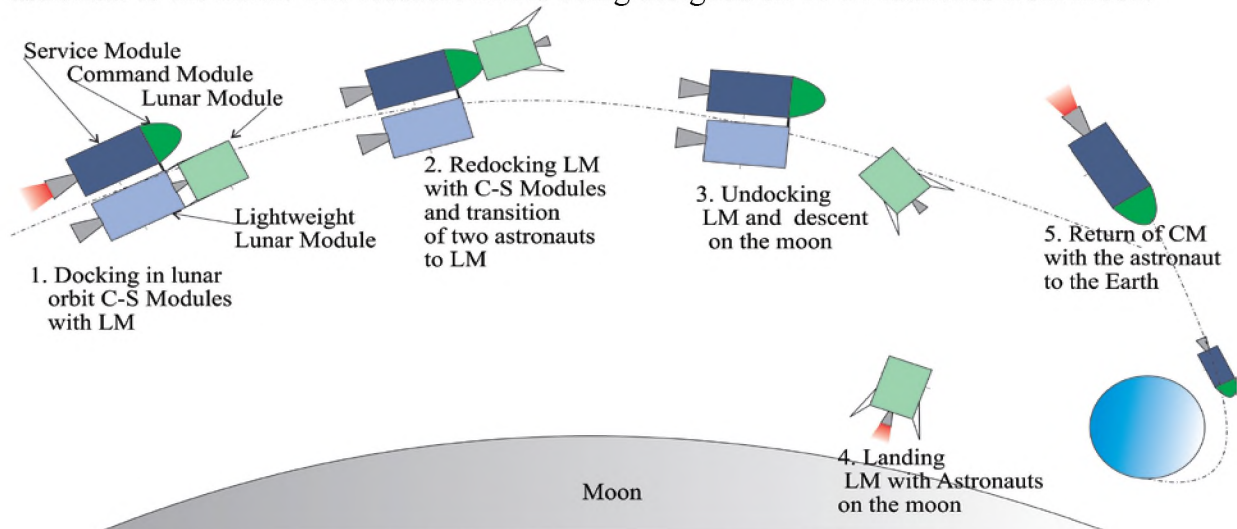


Fig.2 The first expedition included the two launches

In the subsequent expeditions (Fig.3), we can take more cargos because of no lunar module. The LM after launch from moon surface is docking with cargo module if it is unmanned expedition. In manned expedition the LM first is docking with CM where there are astronauts and the crews are changing. Then the LM is re-docking with the cargo module and taking them to descend on the moon. The C-S module will go back to the earth, taking the astronauts.

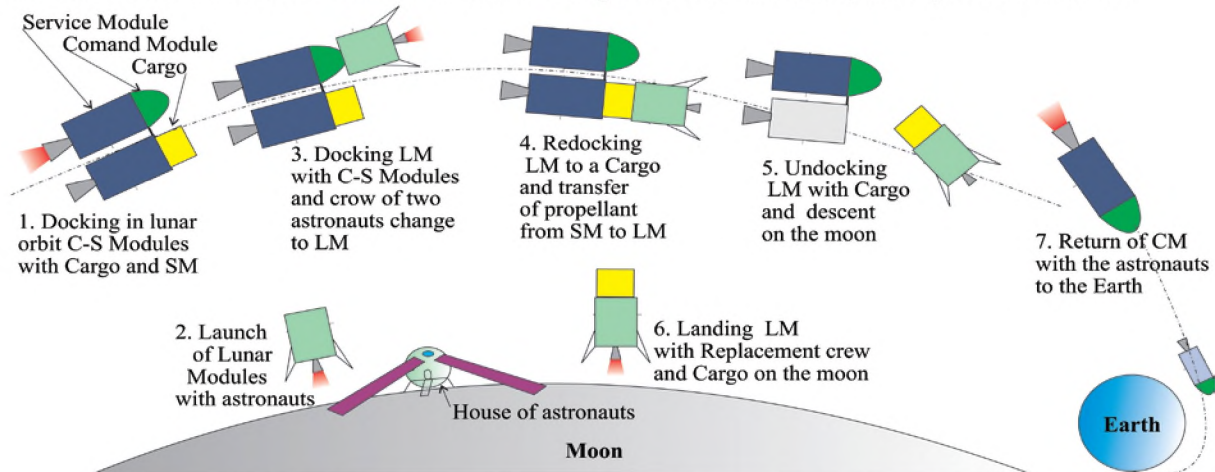


Fig.3 The second and subsequent expeditions included the two launches

2.2 Rocket Energia

Energia rocket was a Soviet rocket that was designed by NPO Energia to serve as a heavy-lift expendable launch system as well as a booster for the Buran spacecraft. Control system main developer enterprise was the NPO "Electropribor". The Energia used four strap-on boosters each powered by a four-chamber RD-170 engine burning kerosene/LOX, and a central core stage with 4 one-chamber RD-0120 (11D122) engines fueled by liquid hydrogen/LOX.



a



b

Figure 4: Rocket-carrier Energia:

a – with module Polus (15.06.1987); *b* – with aerospace craft Buran (15.11.1988)

The launch system had two functionally different operational variants: Energia-Polus (Fig.4, *a*), the initial test configuration, in which the Polyus system was used as a final stage to put the payload into orbit, and Energia-Buran (Fig.4, *b*), in which the Buran spacecraft was the

payload and the source of the orbit insertion impulse. But in our project, we have new payload for it.

2.3 Lunar Booster

Firstly, it is necessary for our lunar booster to be used twice during a lunar mission: first to take the lunar module and service module into the low moon orbit, and then to send the command module and service module into it. Secondly, we choose our engine for our booster. Consider our payload is lower than Saturn V (Fig.5).

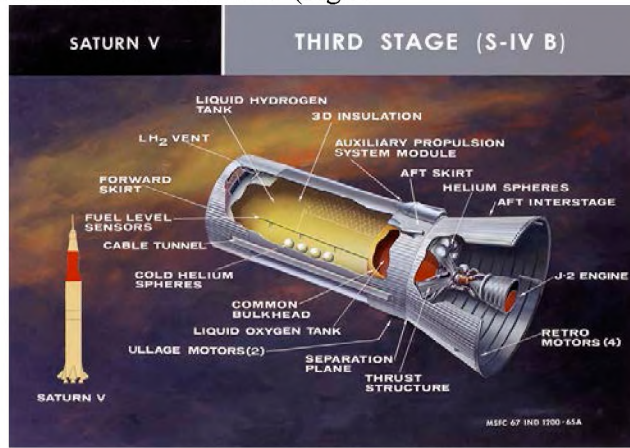


Figure 5: The third stage of Saturn V

The booster in our transport system is different from that of Saturn V. Also, the mass of our payload is about 110 tons so that it defined the mass of lunar booster should be less than 70 tons. First and foremost, we should calculate how many fuel we need to take the spacecraft to the velocity of 11.2 km/s.

The relationship between of the fuel mass (m_{fuel}) and of the booster initial mass (m_0) is:

$$\mu_f = \frac{m_{fuel}}{m_0} = 1 - \frac{1}{e^{\frac{\Delta v}{v_e}}} \quad (1)$$

where Δv is the change of the lunar booster velocity; v_e is the specific impulse measured in m/s.

In our project, we should make the spacecraft leave the earth orbit and go to the moon, so Δv is about 4000 m/s.

Then,

$$m_{fuel} = 110 \times \left(1 - \frac{1}{e^{\frac{4000}{450 \times 9.8}}} \right) \approx 64t$$

By the contrast between Saturn V and our lunar booster, we can calculate the volume of hydrogen and oxygen tank we need. The main parameters of our lunar booster are given in the following table

Table 2: The propellants parameters of lunar booster

Parts	Full fuel in S-IVB	Our project
The mass of LH2	18t	9.85t
The volume of LH2	253m ³	138m ³
The mass of LOX	87.2t	54.15t
The volume of LOX	73.3m ³	45.52m ³
The mass of fuel	105.2t	64t

2.4 Lunar Module

The lunar module carries two astronauts from lunar orbit to the surface of the moon; serves as living quarters and a base of operations on the moon, and returns the two men to the CSM in lunar orbit. For our project, we are going to design a lunar module which is different from this one. For the ascent stage and descent stage, the whole module is integral so that we could recycle the whole module for next research and flight mission. Certainly, it will be lighter than Apollo's, since we will take the integral tanks, and we only need one engine. It could save more time for our study and more funds.

According to the formula (1) in ascent stage, we take the Δv as about 2102 m/s, and v_e is about 3000 m/s, m_{dry} is about 4160 kg.

$$\mu_{f \text{ ascent}} = 1 - \frac{1}{e^{\frac{\Delta v}{v_e}}} = 0.5038$$

$$\mu_f * m_0 (\text{ascent}) = \mu_f * (m_{\text{ascent fuel}} + m_{\text{dry}}) = m_{\text{ascent fuel}}$$

$$m_{\text{ascent fuel}} \approx 5016 \text{ kg}$$

In descent stage, Δv is about 2373 m/s, v_e is about 3000 m/s, m_{dry} is about 4160 kg.

$$\mu_{f \text{ descent}} = 1 - \frac{1}{e^{\frac{\Delta v}{v_e}}} = 0.546$$

$$\mu_f * m_0 = \mu_f * (m_{\text{descent fuel}} + m_{\text{ascent fuel}} + m_{\text{dry}}) = m_{\text{descent fuel}}$$

Then,

$$m_{\text{descent fuel}} \approx 11065 \text{ kg}$$

$$m_0 = m_{\text{eng}} + m_{\text{crew}} + m_{\text{propellant}} + m_{\text{str}} + m_{\text{ce}}$$

$$= m_{\text{descent fuel}} + m_{\text{ascent fuel}} + m_{\text{dry}} \approx 20240 \text{ kg}$$

2.5 Service Module

The main spacecraft propulsion system and supplies (oxygen, water, and propellant) are contained in service module. The main subsystems of service module are electrical power system, environmental control system, reaction control system, service propulsion system and telecommunications system. Our transport system is going to use solar cells instead of fuel cells. So we won't need tanks to take the oxygen and hydrogen for fuel cells, which are much dangerous. Also, the integral tanks could reduce the mass for our service module. It's quite

different from Apollo. So we had our own initial design on the base of Apollo's service module (Fig.6).

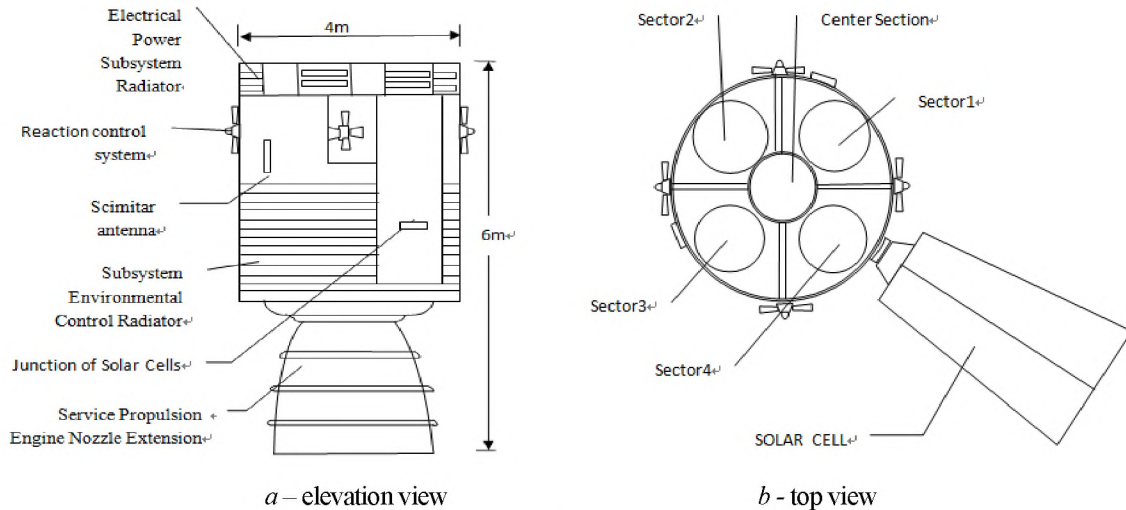


Figure 6: The draft of service module

The exterior of the service module are space radiators for the environmental control and electrical power subsystems, reaction control subsystem engines, three antennas, umbilical connections, and several lights.

As for the interior, Sector 1 is not currently planned to install any equipment. And the space is going to be utilized if there is any additional equipment needs to be added to the spacecraft for the lunar mission or the scientific experiments. Ballast may be stowed to keep the service module's center of gravity if no equipment is added. Sector 2 contains part of a space radiator and a reaction control subsystem engine quad on its exterior panel, and the integrated oxidizer tank, its plumbing, and the reaction control engine tanks and plumbing within the sector. Sector 3 contains part of an environmental control radiator and a reaction control engine quad on the exterior panel, and the integrated fuel tank within the sector. The integrated fuel tank occupies almost all of the space with the sector. Sector 4 contains control system, which is the crucial part of the whole module. It includes the whole electrical and electronic equipment within this part, which could decide the time to propel and control the solar cells. The center section or tunnel contains two helium tanks and the service propulsion engine. The energy is supplied by the solar cells. It uses the new energy to replace the fuel cells, which is more environmental.

2.6 Command Module

For our transport system, we are going to take the same command module as Apollo (Fig.7). The CM contains three compartments: forward, crew, and aft. The forward compartment is the relatively small area at the apex of the module, the crew compartment occupies most of the center section of the structure, and the aft compartment is another relatively small area around the periphery of the module near the base.

The command module (Fig.7) is the only part of the spacecraft recovered at the end of the mission. Another main design of our transport system is the parachute system of the command module. It is an important part to ensure the safe of the crew in return.

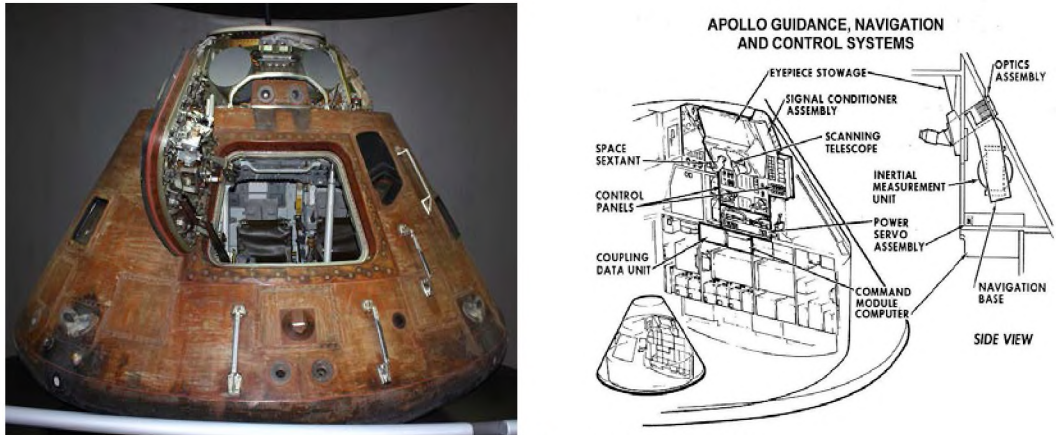


Figure 7: Command module of Apollo

3. FURTHER DEVELOPMENT

The project is just an idea to form a transport system for lunar program. All the thoughts and calculation may need more time to examine. But we would like the situation in the Fig.8 will take place in reality. Maybe we will build a moon-village someday like that someday.

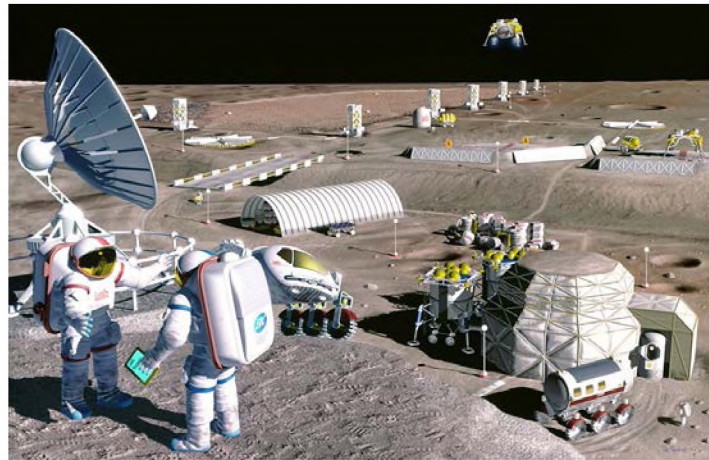


Figure 8: A Moon's village in the near future

4. CONCLUSIONS

From this project, we have talked all the parts of the transport system for the lunar program. We have our own conceptual design, descriptions and estimates. Much of experience is from the Energia-Buran system and Apollo program, but we also have our own ideals about the transport system. They have formed some contrasts that may help us to think more about the new program.

REFERENCES

- [1] Gubanov B.I. "Triumph and the tragedy of "Energia". Reflections of the Chief Designer. "N.Novgorod: Publishing house of the Nizhny Novgorod Institute of Economic Development", 1998. (In Russian)
- [2] Bart Hendrickx, Bert Vis. Energiya-Buran. The Soviet Space Shuttle. ISBN 978-0-387-60848-9. 2007. 523 p.
- [3] Saturn S-IVB, Apollo Saturn, Archived from the original on 19August 2012.
- [4] Gary J. Harloff, "Hypersonic Aerospace Sizing Analysis for the Preliminary Design of Aerospace vehicle", [R], NASA-24105, November 1988.
- [5] Lie Lu, "Weight Estimation of aerospace Craft", [D], Nanjing University of Astronautics and Aeronautics, March 2016. (In Chinese)
- [6] The Apollo Program Summary Report, JSC-09423.
- [7] Apollo NewsReference, Grumman AerospaceCorporation, 1969.

Authors



Liu Jun



Zhang Cong

ANALYSIS OF ADAPTIVE LANDING GEAR USED FOR NEAR SPACE LANDER

Mingyang Huang^{*}, Xiaohui Wei[†], Hong Nie

^{*}Nanjing, Nanjing University Aeronautics and Astronautics
YudaoStreet, 29, Nanjing, Jiangsu, China, 210016
e-mail:huangmingyang@nuaa.edu.cn

[†]Nanjing, Nanjing University Aeronautics and Astronautics
YudaoStreet, 29, Nanjing, Jiangsu, China, 210016
e-mail:wei_xiaohui@nuaa.edu.cn

Key words: Mission adaptive, Landing gear, Overall design, Scaled test, Dynamic simulation

Abstract. *The ability to perform vertical takeoff and landing (VTOL) reliably and safely is great concern for a near space travel lander carrying passengers. Oblique and uneven terrains can severely limit the degree of landing safety, so mission adaptive landing gear is designed and analyzed for its function of automatic adjustment before touchdown. The legs are composed of shock absorbers and actuating cylinders and they can change angles of the main struts relative to the capsule under control, ensuring all feet touch the irregular surface together. Compared with a conventional landing gear, scaled test and dynamic simulation in three typical conditions verify that the new design can reduce the rotation angle and the translational motion of the capsule to less than 3 degrees and 1 meter, respectively. For shock absorbers, the overall design reduces peak load of the lander by more than 24%, enhances efficiency of shock absorbers to more than 85% and optimizes stroke lengths of shock absorbers. The manned capsule's maximum overload is reduced to less than 5 in all cases. Landing performance shows that mission adaptive landing gear is robust to uncertain conditions of the touchdown surface.*

1. INTRODUCTION

Near space generally refers to 20km to 100km airspace from the ground, which is a new airspace that does not belong to the traditional category of the aerospace nor the space of aviation[1,2]. Near space travel vehicle lift by a helium balloon is rapidly developing[3], because it can arrive in vision in areas such as the stratosphere unreachable by some fixed-wing aircraft. For safe landing and takeoff of the vehicle carrying passengers, design and analysis of the lander are great concern.

Since it was first developed, the landing gear of VTOL aircraft has proven to be an invaluable tool for landing in remote areas so that its application becomes more and more extensive [4]. There are some successful examples, for instance, the helicopter landing gear [5], VTOL rocket landing gear [6] and lunar lander [7] etc. The lander containing payload is in danger of bouncing and tipping over while landing on an oblique terrain, so a landing gear with a function of automatic adjustment adaptive to different landing surface is necessary.

To achieve slope landing requirements, several adjusting approaches were developed. Georgia Institute of Technology has designed a legged robotic gear system for rotorcraft [8-10]. If a leg touches the ground, the corresponding joint stiffness zero-load point will be reset to the current joint deflection and the joint damping will be reset to nominal values. When all feet are on the ground, all joint damping constants will be reset to nominal values and the stiffness zero-load point will remain at its previous value. The development of the articulated landing gear may enhance the usability of this kind of VTOL aircraft, but it cannot adjust before touchdown.

Mission adaptive landing gear is built and a dynamic simulation model is present here. The new design employs infrared distance sensors located on skid plates to properly sense the vertical height of each foot before they touch the ground. On the basis of the measured datum, actuating cylinders on each leg work and adjust the angles of main struts, ensuring that four skid plates touch the oblique terrain at the same time and the payload maintains horizontal during the whole process of slope landing. In addition, the mathematical model and the virtual prototype for the new design have established the vision in the dynamic simulation software ADAMS. The dynamic analysis is performed to properly show the optimized results including peak overload, landing attitude and buffering property while using vision adaptive landing gear.

2. ANALYSIS

2.1. Virtual Prototype Design.

The lander simulated is chosen to be a reusable space travel capsule with 140oz er adaptive landing gear replacing the conventional landing gear. The modeled capsule has a mass of 2250kg and is lift by a helium balloon during touchdown. The lift 140oz e continues to be 2/3 of the gravity during the whole landing process. The lander can only perform vertical takeoff and landing, because it lacks airplane wheels that can handle horizontal motion. The vehicle lands down on the soil terrain which can provide soil spring 140oz e and attenuate the stroke. A detailed schematic is shown in Figure 1.

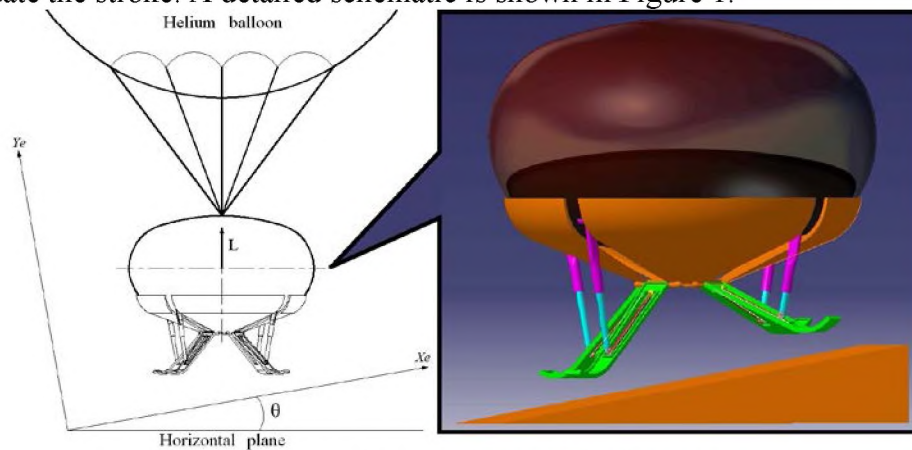


Figure1: Virtual prototype of the lander

It is necessary to guarantee the security and stability of the lander which drops at a vertical speed of 5m/s. To tackle incline terrains of various sizes, 140oz er adaptive landing gear composed of an infrared distance sensor, a skid plate, an actuating cylinder, a shock absorber and a main strut per 140oz er designed. A 'four legs – 140oz ero140140r beam' is adopted as the landing gear configuration. The detailed schematic is shown in Figure 2.

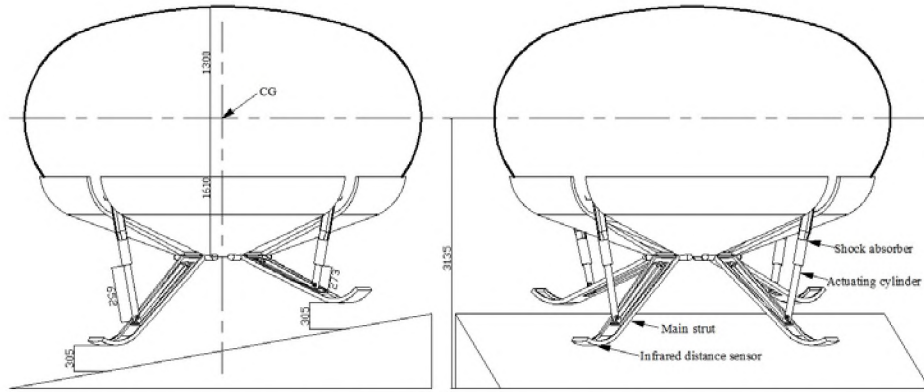


Figure 2: Mission adaptive landing gear configuration (dimensions in millimeters)

2.2. Mathematical Model.

Virtual prototyping technology is used for simulating the drop process of the lander. Landing modes including 1-2-1 and 2-2 mode [11] which are investigated in this thesis. A lander's two-dimensional dynamic model (using 1-2-1 mode) is shown in Figure 3.

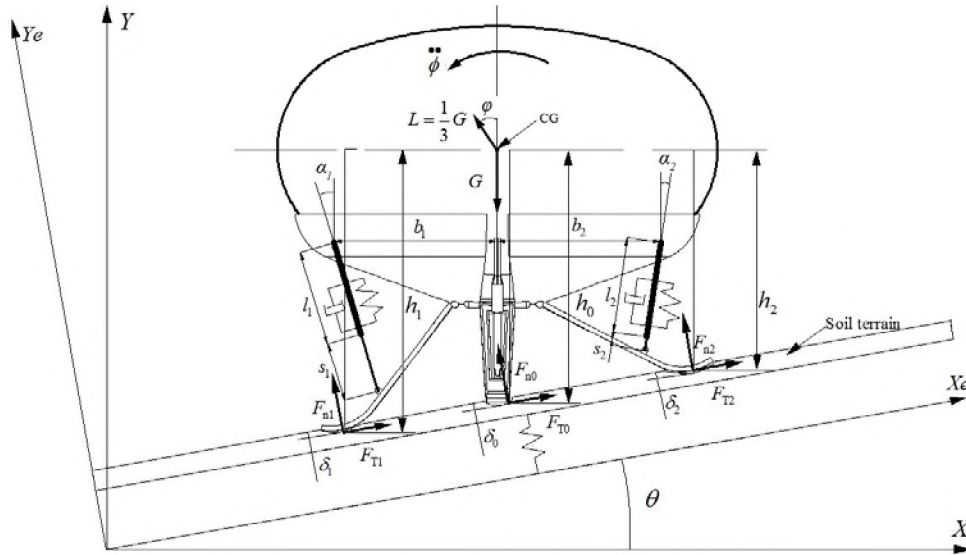


Figure 3: Two-dimensional lander configuration

Dynamic differential equations in inertial coordinate system O-XY are developed and denoted as:

$$m\ddot{Y} = 2F_{n0}\cos\theta + 2F_{T0}\sin\theta + F_{n1}\cos\alpha_1 + F_{T1}\sin\alpha_1 + F_{n2}\cos\alpha_2 + F_{T2}\sin\alpha_2 + L\cos\phi - G \quad (1)$$

$$m\ddot{X} = -2F_{n0}\sin\theta + 2F_{T0}\cos\theta - F_{n1}\sin\alpha_1 + F_{T1}\cos\alpha_1 - F_{n2}\sin\alpha_2 + F_{T2}\cos\alpha_2 - L\sin\phi \quad (2)$$

$$I\ddot{\phi} = -2F_{n0}\sin\theta \cdot h_0 + 2F_{T0}\cos\theta \cdot h_0 - F_{n1}\sin\alpha_1 \cdot h_1 + F_{T1}\cos\alpha_1 \cdot h_1 + F_{n2}\sin\alpha_2 \cdot h_2 + F_{T2}\cos\alpha_2 \cdot h_2 \quad (3)$$

Where \ddot{X} , \ddot{Y} and $\ddot{\phi}$ are the acceleration value of elastic support mass along O-X direction, the acceleration value of O-Y direction and the angular acceleration under inertial coordinate system, respectively; ϕ is the vehicle's altitude angle; θ is the angle between the landing surface and the horizontal; G is the weight of the lander; L is the lift 141oz e of the helium balloon; l , s and h are the length of the shock absorber, the length of the actuating cylinder and the vertical distance from the skid plate to the center of gravity (CG),

respectively; F_{n0} , F_{n1} and F_{n2} are the forces normal to the surface, positive direction is along the positive direction of Ye-axis, respectively; F_{T0} , F_{T1} and F_{T2} are the forces normal to the surface, positive direction is along the positive direction of Xe-axis, respectively; δ_0 , δ_1 and δ_2 are the deformations of the soil under different skid plates, respectively.

The actuating cylinder is composed of a motor and a screw mandrel. The analysis of the auto locking function of screw thread joint is 142oz ero142 the in equation [12]:

$$\psi < \arctan(f) \quad (4)$$

Where ψ , f and $\arctan(f)$ are the thread angle, the static friction coefficient and the static friction angle of the screw thread joint of the actuating cylinder, respectively. Parameters of the actuating cylinder are shown in Figure 4.

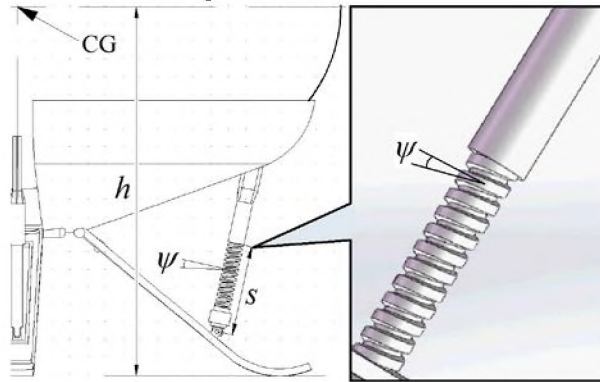


Figure 4: Parameters of the actuating cylinder

2.3. Landing Simulation.

The dynamic model of the lander is established and implemented with ADAMS. Landing simulation is performed for comparison between 142oz er adaptive landing gear and a traditional landing gear with the same configuration and structure parameters. All components of the traditional landing gear are assembled together and the actuating cylinders are all rigidly fixed so that they cannot relatively move.

The lander impacts the soil terrain at a vertical speed of 5 m/s and shock absorbers take actions in order to approximate a soft landing. In all cases studied in this paper, the four feet of 142 oz er adaptive landing gear touch down together. While landing on an inclinesurface(the first and second condition), four feet of rigidly fixed landing gear touch down with 1-2-1 and 2-2 mode, respectively. It indicates that landing performance using 2-2 mode is better, so the angle of the oblique terrain is 15 degrees in second condition. While landing on a horizontal terrain with a pit (the third condition), four feet of rigidly fixed landing gear touch the ground with 3-1 mode because the foot above the pit touches down at last.

Through analyzing the difference of 142oz er adaptive landing gear and rigidly fixed landing gear, the capsule's overloads as a function of time are compared and shown in Figure 5.

Simulation results show that mission adaptive landing gear adopted reduces the 142oz ero overload during the process of slope landing. According to Figure 12, 142oz ero overload of the capsule using 142oz er adaptive landing 142oz ero 15 degrees slope is less 142oz that of the capsule implementing rigidly fixed landing 142oz ero 10 degrees slope. The curve of 142oz er adaptive landing gear only have two obvious 142oz ero values which represent the 142oz ero of the first touchdown and maximum compression of the shock

absorbers, respectively. The curve of rigidly fixed landing gear has three obvious 143oz ero values because four skid plates touch down at different time.

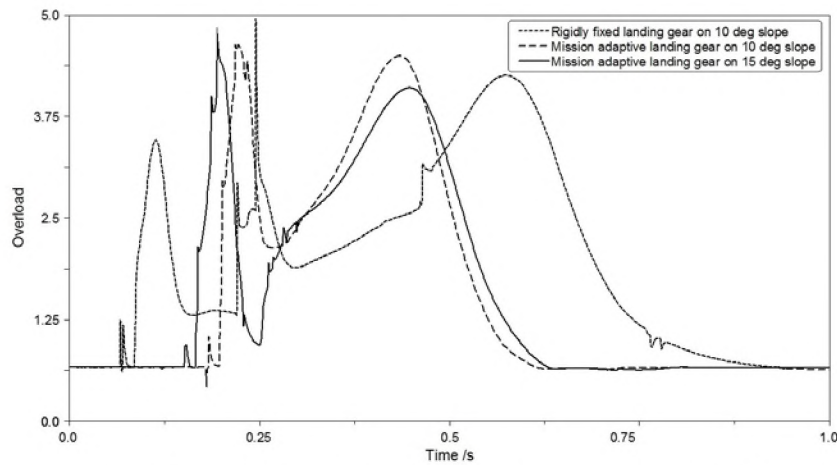


Figure 5: Comparison of capsule's overload as a function of time

2.4. Comparison.

With rigidly fixed landing gear, the lander eventually settles on the incline or uneven surface but undergoes significant translational motion along the ground due to the 143oz ero 143 tilting away after touchdown. When using 143 oz er adaptive landing gear, displacements of the lander are all less 143oz 1 meter and rotation angles of the 143oz ero143 are all less 143oz 3 degrees. The new design reduces 143oz ero overload of the capsule in slope landing and ensures the value of 143oz ero overload less 143oz 5 in three conditions.

As the oleo-pneumatic shock absorber provides air spring 143oz e, one of the skid plates may bounce off slightly. Simulation shows the overload and angular acceleration of the cabin has almost no change, so that the use of oleo-pneumatic shock absorbers is reliable. Comparison between shock absorbers of 143oz er adaptive landing gear and rigidly fixed landing gear in three landing conditions are presented in Figure 6-8, respectively.

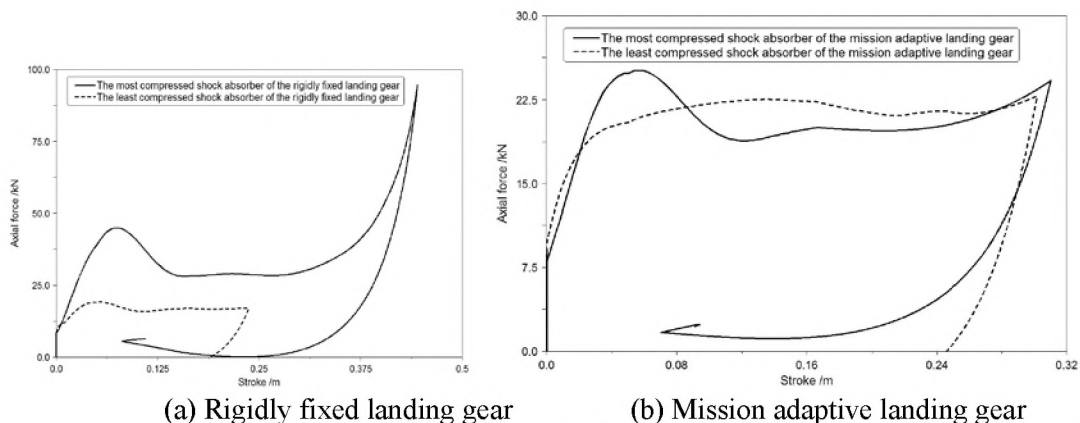
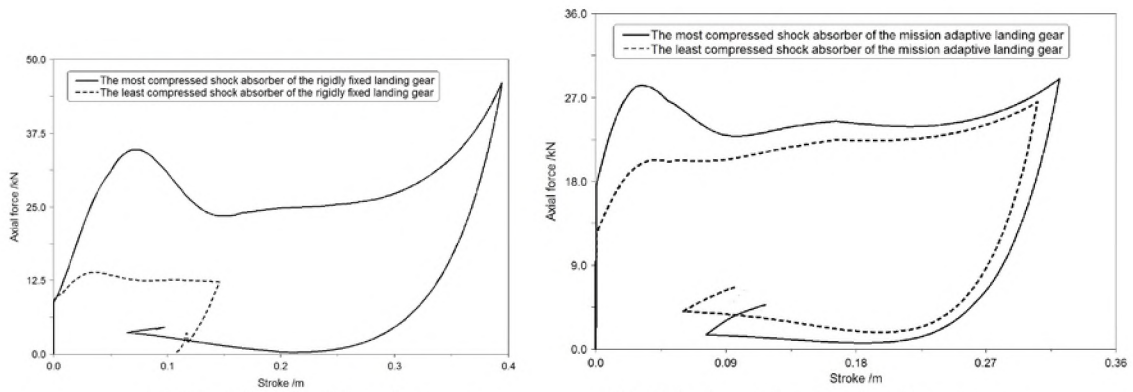
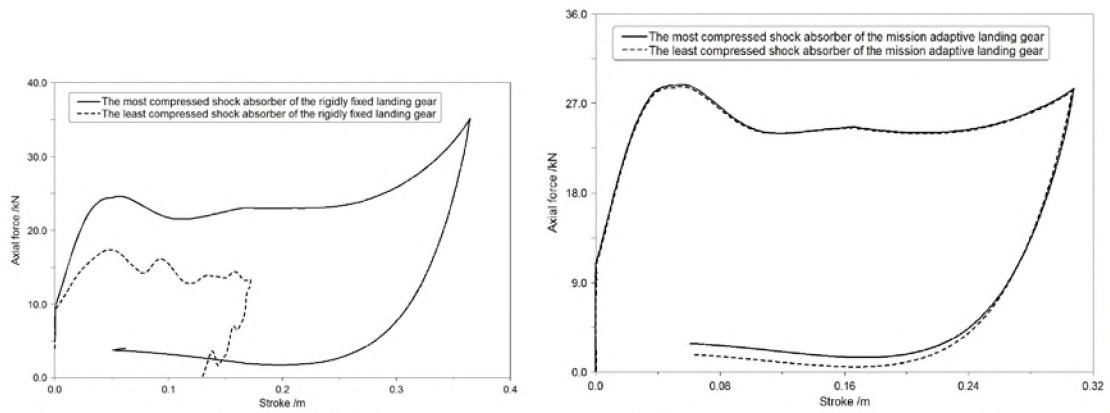


Figure 6: The axial 143oz e-stroke curve of shock absorbers in first landing condition



(a) Rigidly fixed landing gear (b) Mission adaptive landing gear
Figure 7: The axial 144oz e-stroke curve of shock absorbers in second landing condition



(a) Rigidly fixed landing gear (b) Mission adaptive landing gear
Figure 8: The axial 144oz e-stroke curve of shock absorbers in third landing condition

Based on the comparison among the axial 144oz e-stroke curves, it can be shown that the most compressed shock absorber of rigidly fixed landing gear obviously has a longer stroke length and a lower efficiency which is less than 60% in all conditions. As the adaptive landing gear is adopted, efficiencies of the most and least compressed shock absorbers all increase to more than 85% during the landing process, and deviations of gear stroke lengths in different shock absorbers are all less than 0.03 m. Simulation results show that the peak loads of the most compressed shock absorber are reduced by more than 24% while using the adaptive landing gear in place of the conventional landing gear. Landing performance illustrates that the new design is adaptive and robust to uncertain conditions. In some cases, the axial force decreases quickly after the peak during the backward stroke because the ground friction forces avoid the skid plates to move back to the initial position as the actuating cylinders reset.

3. CONCLUSIONS

Mission adaptive landing gear is designed for VTOL aircraft such as near space travel lander. It uses infrared distance sensors to measure the vertical distances from the ground directly beneath the skid plates. Based on the datum processed in the controller, actuating cylinder stake actions and adjust the angles of main struts, ensuring four skid plates touch the incline terrain at the same time. At last the shock absorbers work and absorb the kinetic and potential energy. The buffering process happens after the process of adjustment and the axial forces of the actuating cylinder are in the same direction with the shock absorber, so that the structure has rational mechanical behavior.

Landing simulation and scaled test show the new design enhances the capability of landing on oblique or uneven surface. Landing performance of mission adaptive landing gear adopted is studied and compared with rigidly fixed landing gear. As a result, maximum overload of the capsule carrying passengers can be reduced effectively and efficiencies of shock absorbers increase with the decrease of the most compressed shock absorbers' stroke length.

REFERENCES

- [1] Lesley A. Weitz. "A New Spacing Algorithm to Support Near-Term Interval Management Operations", 14th AIAA Aviation Technology, Integration, and Operations Conference, AIAA Aviation, (AIAA 2014-3149).
- [2] Cao Xiu-yun. Overview of the Development of the United States Near Space Vehicle Technology[J]. Military Technology, 2007(03):54-58.
- [3] Matthew R. Longo, Stella F. Lourenco. On the nature of near space: Effects of tool use and the transition to far space[J]. Neuropsychologia, 2005, 44:6.
- [4] Prasun N. Desai, Jill L. Prince, Eric M. Queen, Mark M. Schoenenberger, Juan R. Cruz, and Myron R. Grover. "Entry, Descent, and Landing Performance of the Mars Phoenix Lander", Journal of Spacecraft and Rockets, Vol. 48, No. 5 (2011), pp. 798-808.
- [5] Tri D. Ngo and Cornel Sultan. "Nonlinear Helicopter and Ship Models for Predictive Control of Ship Landing Operations", AIAA Guidance, Navigation, and Control Conference, AIAA SciTech, (AIAA 2014-1298).
- [6] Andrew A. Gonzales, Carol R. Stoker. An Efficient Approach for Mars Sample Return Using Emerging Commercial Capabilities[J]. Acta Astronautica, 2016, .
- [7] Carpenter J D, Fisackerly R, Rosa D D, et al. Scientific Preparations for Lunar Exploration with the European Lunar Lander[J]. Planetary & Space Science, 2012, 74(1):208-223.
- [8] Dooroo Kim and Mark Costello. "Virtual Model Control of Rotorcraft with Articulated Landing Gear for Shipboard Landing", AIAA Guidance, Navigation, and Control Conference, AIAA SciTech, (AIAA 2016-1863).
- [9] Vasudevan Manivannan, Jared P. Langley, Mark Costello, and Massimo Ruzzene. "Rotorcraft Slope Landings with Articulated Landing Gear", AIAA Atmospheric Flight Mechanics (AFM) Conference, Guidance, Navigation, and Control and Co-located Conferences, (AIAA 2013-5160).
- [10] Kiefer JJ, Ward MM, Costello MM. Rotorcraft Hard Landing Mitigation Using Robotic Landing Gear. ASME. J. Dyn. Sys., Meas., Control. 2016;138(3):.
- [11] Chen J, Nie H. Overloading of Landing Based on the Deformation of the Lunar Lander[J]. Chinese Journal of Aeronautics, 2008, 21(1):43-47.

Mingyang Huang, Xiaohui Wei, Hong Nie

[12] Jan Christoph Katthagen, Michael Schwarze, Mara Warnhoff, Christine Voigt, Christof Hirschler, Helmut Lill. Influence of plate material and screw design on stiffness and ultimate load of locked plating in osteoporotic proximal humeral fractures[J]. Injury, 2016.

Authors



Mingyang Huang



Xiaohui Wei



Hong Nie

BASIC UAV DEVELOPMENT IN UNDERGRADUATE LEVEL

Allan A. Dias

Nanjing University of Astronautics and Aeronautics, College of Aerospace Engineering,
[email: allan.adias@nuaa.edu.cn](mailto:allan.adias@nuaa.edu.cn)

Key words: UAV, Unmanned Aerial Vehicle, Drone, DIY, Undergraduate, Project

Abstract. *Starting from my second semester studying Aircraft Design & Engineering in NUAA (Spring 2016), I engaged in a project which had the objective of exploring multirotor aircraft dynamics and from there develop one, designing its structural features, circuitry, controllers and navigation systems. After a short while, I ended taking the project almost exclusively my myself, and have been developing it parallelly to my academic activities since then. By the end of the spring semester of 2017, NUAA's College of International Education started building interest in the activity. The following is a report of this UAV design, methodology and development history as of October 2017.*

1. Multirotor Dynamics

When the project started, it was designed to be carried out by the majority of the members of the Science & Innovation Club. At that time, none of the participating members had had any formal education in any aspect concerning aircraft dynamics, controls, or aerodynamic forces. In the beginning a research experiment was carried out to understand the means of motion of a multirotor aircraft, its principles of balance and the control surfaces used to perform each specific maneuver. It was this research that clarified the less intuitive aspects of a multirotor movement. Such clarifications follow:

- The number of blades in the rotors always sums to an even number, of which half rotate clockwise (CW) and the rest rotates counter-clockwise (CCW). Such dynamics serve to balance the angular momentum generated by the rotation of the blades, without which the aircraft would yaw uncontrollably. Moreover, for reasons of balancing during yaw, CW rotating and CCW rotating blades should be positioned alternately in the arms of the aircraft for drones with even number of arms, and one above the other in drones with odd number of arms (Figure 1);
- The pitch and roll of the aircraft are actuated by the lift generated by the rotor blades. They are both controlled by reducing the rotation speed in the direction of desired movement. The rotation speed of the rotors opposite to the desired direction can be increased to maintain altitude (Figure 2);
- The yaw motion of the aircraft, unlike the pitch and roll, is not actuated by lift, but by controlling the net angular momentum exerted on the aircraft by the rotor blades. That is, to achieve positive yaw, the speed of the rotors rotating CCW is increased, while the speed of the rotors rotating CW is decreased; the opposite results in negative yaw (Figure 3);

- For a multirotor aircraft with number of arms different from 4, paths in angles of 0, 90, 180 and 270 ('straight' paths) can be achieved simply by regulating the speed of all the rotors so that the resultant force exerted by them fits those angles;

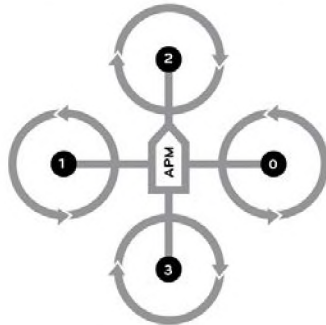


Figure 1

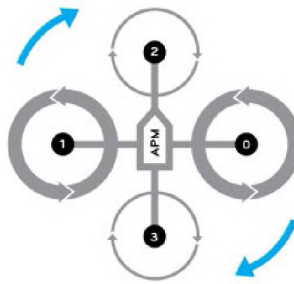


Figure 2

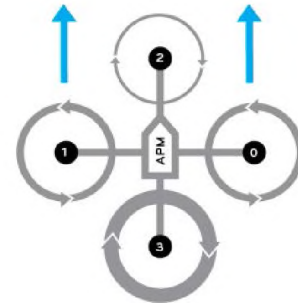


Figure 3

2. Structure Design

After the initial research was conducted, the Science & Innovation Club requested the next step to be the design of the structure. By that time, the group, which had already been reduced to around 5 students, agreed that the UAV would be used to take pictures once completed. It was also learned that the number of rotors is usually proportional to the UAV's general stability, so it was decided that the design would have 6 rotors. The structure also was required to be as cheap as possible, as well as easy to manufacture by the students at the time.

2.1. Overall Structure

After sketches, I accomplished the final design in Autodesk ©Inventor, for it was a software I already had some familiarity with, and which possesses considerable compatibility. The final design measures 1020 mm from the tip of one arm to the same point in the arm opposite to it, and is 170 mm tall with its landing gear open and without any electronic components. It is symmetrical every 60 degrees in its yaw axis, and most of the components are planar or of rectangular profile, to facilitate manufacturability and availability of adequately shaped components. As none of the members had knowledge in aerodynamics, and all of us discarded the importance of aerodynamic influences due to the low speeds at which the UAV would operate, the structure is devoid of any aerodynamic design, apart from the readily purchased rotor blades. An isometric view of this structure follows in Figure 4:

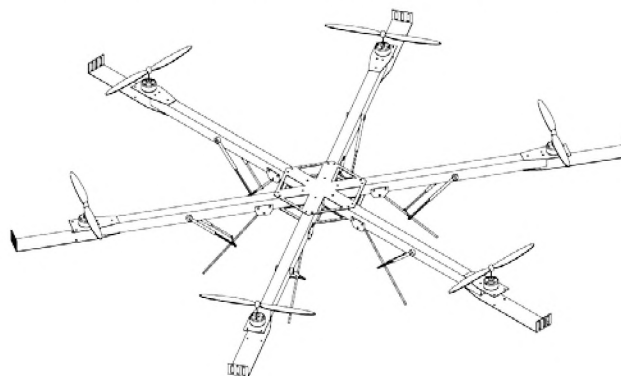


Figure 4

2.2. Materials

The structure was assigned with components made of aluminum and ABS plastic. Both materials were chosen by their low weight, low cost, considerable resistance and workability, and availability. Aluminum, as heavier and more expensive than ABS plastic, was set only for the arms and for the centerpiece that would hold all together. ABS plastic would comprise the more complex shapes, such as the supports for the motors and electrical components.

2.3. Arms

The arms consist of square 20X20 mm aluminum profiles with a 0.8 mm wall, which measure 540mm in length. The profiles have several holes drilled in specific places along its span, with the objective of attaching several other components to the limbs. The tip of the profile holds two 1mm thick ABS plastic trapezoidal shapes that hold the motor in place. The motor stands at the top plate, and it is screwed using hexagonal brass supports in both plates. The bottom plate also extends for 100 mm more than the top, and has an upward pointing edge at its tip, forming an L shape. The tip was done in such a way to hold an ultrasound proximity sensor to detect obstacles before they hit the propellers. Both top and bottom supports were cut by hand from an ABS plastic plate, and holes made by hot iron.

2.2. Centerpiece

The centerpiece is formed by two aluminum hexagonal plates, with the objective of holding the limb aluminum profiles in place. The aluminum used in both is 2.5mm thick, thicker than the all the other parts, since it should hold the bending exerted by all the limbs, and providing a stable support for the later-to-be-installed electrical components. the top centerpiece has a solid center, whereas the bottom one has a big circular hole cut in the center, exposing the free space in the center that is not occupied by the limbs. The centerpieces were commissioned from Taobao, and laser cut according to a CAD file prepared through the Inventor model.

The above structure parts are the parts of the original project idealized up to October 2017. The landing gear part was ignored until that date, and is planned to be absent until flight tests are complete. All structural parts are assembled together using M3 bolts, nuts and washers.

3. Circuitry and Electronics

By the time the structure was complete, the project had been abandoned by all the members, and its development has since been done almost exclusively by me. Since the starting phase of the project, after brief research, the Arduino platform was chosen as a definite best for acting as the on-board computer of the UAV. Some advantages of using the Arduino platform include:

- Accessibility & Affordability: The Arduino itself is an open-source board design, which means small electronics manufacturers have access to the design, allowing for an extremely affordable microprocessor;
- Online Support: The Arduino is the choice of the great majority of the online DIY community, which means previously made projects using the platform offer their documentation online for further use;
- Ease of use: By the time the circuitry part of the project was being carried, I took a course on C Programming in NUAA, which is exactly the same programming language used for programming the Arduino platform;
- Extensive Sensor Support: Not only the Arduino support a vast array of different sensor kinds, it also does not demand any specific requirements from these, such as brands or

industry standard, meaning it will not reject or be incompatible with different kinds of the same sensor;

With all these considerations in mind, the on-board computer chosen to operate the UAV was an Arduino Mega 2560, because of its considerable number of ports, which can support any number of sensors I would require to equip the UAV. For its motion control, the UAV is equipped with 6 XA2212 1400KV brushless motors, each one controlled by a 30A ESC, connected to the Arduino board. As of the date of the report, all the motors were installed with their respective rotors in place, but only 2 are connected to the ESCs and operational. This was carried for reasons of testing the control in one single axis first, before testing all the motors on. The power is supplied either by a AC/DC transformer or by a 4200mAh Li-Po battery. For all the testing, the power was supplied using the transformer. For the sensors, up to the date of the report, the UAV counts with a 10 DOF GY-80 Inertial Measurement Unit for measuring its acceleration and angle (the same unit also enables measuring magnetic field, temperature and pressure, if required in the future), and 6 ultrasound sensors for detecting the proximity to an obstacle. The rest of the electronic equipment is limited to a power distribution board for supplying the ESCs and the wiring.

4. Controller

Once the wiring was complete, the work on the most extensive and easily the most important part of the project was started to be carried: designing a controller algorithm.

4.1. Basic Notions

The Arduino board operates mainly by uploaded, pre-compiled C code written in its own IDE, but it is also supported (though not to the same extend) by MATLAB. Since MATLAB is well known for its versatility, extensive visualization capabilities and ease of use, I decided to start the code development in MATLAB. By the time, I've had almost no contact with MATLAB, so I relied heavily on the MATLAB built in library and its examples to design a basic controller. Reading the C library codes of the sensors and converting it to MATLAB, and analyzing the register map and operation guide of the sensors, I've been able to interface the IMU and the ESCs to MATLAB. The following sections of MATLAB code show the interfacing done with the Arduino and the Inertial Measurement sensors:

```
a = arduino('COM3', 'Mega2560');
accel= i2cdev(a, '0x53');
gyro= i2cdev(a, '0x69');
magn = i2cdev(a, '0x1E');

writeRegister(gyro, hex2dec('20'), bin2dec('00001111'));
writeRegister(gyro, hex2dec('23'), bin2dec('10000000'));

writeRegister(accel, hex2dec('21'), bin2dec('0'));      %Disables Tap
writeRegister(accel, hex2dec('2C'), bin2dec('00001001')); %25 Hz sampling
writeRegister(accel, hex2dec('2D'), bin2dec('00001000')); %Measure Mode
writeRegister(accel, hex2dec('31'), bin2dec('00'));      %2g range

writeRegister(magn, 2, bin2dec('0'));
writeRegister(magn, 1, 224);
```

In the above section of the code, the Arduino function creates the board object, and i2cdev starts the interface between the sensors (I2C Devices) and MATLAB. The first section of the writeRegister functions tunes the registers of the Gyroscope, the second section tunes the Accelerometer and the last, the Magnetometer. The binary values in the arguments are taken from the register manual included with the sensor. Since up to date only the Accelerometer is used in the controller, its register tuning is accompanied by comments showing the meaning of each parameter. To test the response of the Accelerometer in real time, the animatedLine object of MATLAB was used to create a plot resembling a heartbeat monitor. The code which performs this plotting follows:

```
h = animatedline;
axis([0,10,-200,200]);

while 1
time = tic;

while toc(time) < 9.8
accelRead(1) = readRegister(accel, 52);
accelRead(2) = readRegister(accel, 53);
xA = bitor(bitshift(int16(accelRead(2)), 8, 'int16'), int16(accelRead(1)), 'int16') + 13;

if abs(xA) < 200
    last = xA;
end

if abs(xA) > 200
    xA = last;
end

addpoints(h, toc(time), double(xA));
drawnow;
end

clearpoints(h);
end
```

The actual reading of values from the sensor only happens in the readRegister function, and the operation assigning xA is what transforms the raw sensor data (binary) into a human-legible value. The if statement following it performs a simple filtration of data in case it experiences bumps or certain sudden raises in value which are not actually affecting the structure. addpoints and drawnow creates the animated line plot. The inner loop runs for little less than 10 seconds, after which the figure grid is cleared, and the outer loop runs indefinitely.

With this program, data acquired from the accelerometer can be read and visualized in real time. Without the animation, a 5 second sample of data gathered by the sensor, with the drone supported, rotors off and performing hand-driven oscillatory motion is shown in Figure 5:

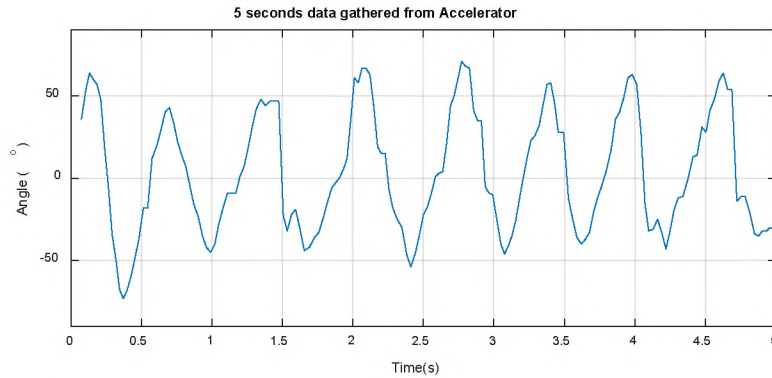


Figure 5

4.2. Preliminary Controller

For controlling the angle change of the UAV, a better understanding of its flight behaviour was needed. At this point, I was certain I wanted to design a controller to actuate on the drone through pre-loaded instructions, instead as through remote-controller-input commands. This means the UAV would actually be autonomous. For such, the controlled variable of the controller would be decided to be the angle, whereas if I controlled it by remote the most suitable controlled variable would be angular velocity. With the angle measurement being the controlled variable, I could feed instructions to change the angle of the UAV so that the thrust from its propellers would provide thrust in the direction opposite of its path, and its total distance could be integrated from its acceleration in that given direction. The algorithm I considered to be the trivial way to control a value with feedback looked something like:

$$\theta_f = \theta + \Delta\theta$$

In which θ_f stands for final angle, θ for the current angle and $\Delta\theta$ the difference of the desired final angle from the measured angle. At the time, in my understanding, for the angle to change, the rotation speed of one of the motors would be decreased, while the one opposite to it would be increased. The controller, in this way, could be represented by:

$$T_1 = T_0 \pm K \times \Delta\theta$$

$$T_2 = T_0 \mp K \times \Delta\theta$$

In which T_1 and T_2 represent the value passed to rotors 1 and 2 respectively, T_0 represents the value passed to the rotors if no movement is desired (or Equilibrium Value, if preferred), $\Delta\theta$ is the difference between the desired angle and the present angle, and K is some constant to determine how much the $\Delta\theta$ value will affect the result. For the ESCs, the units which control the power supplied to the motors, and therefore, the power delivered by the rotors, the value of T_1 and T_2 varies from 0 to 180 when written in C and from 0 to 1 in MATLAB. In MATLAB, after numerous tests, a stable value of T_0 was found to be 0.36. Thus, a piece of the code performing the basic controller function is shown below:

```
pos1 = 0.36;
pos2 = 0.36;
writePosition(prop1, pos1);
writePosition(prop2, pos2);
```

```

while 1

    accelRead(1) = readRegister(accel, 52);
    accelRead(2) = readRegister(accel, 53);
    mesAccel = double(bitor((bitshift(int16(accelRead(2)), 8, 'int16')), int16(accelRead(1)), 'int16'));

    if abs(mesAccel) < 80
        mesLast = mesAccel;
    end

    if abs(mesAccel) > 80
        mesAccel = mesLast;
    end

    errAccel = (mesAccel - ref) / 8000;
    pos1 = 0.36 + Kp * errAccel;
    pos2 = 0.36 - Kp * errAccel;

    writePosition(prop1, pos1);
    writePosition(prop2, pos2);

end

```

The values 0.36 written to propellers 1 and 2 sets them in the stable equilibrium position, equivalent to the drone hovering in place without moving. First the computer reads the values gathered by the Accelerometer, then after a filtering to detect bumps, it compares it with a reference value. In this piece of code, **ref** is highlighted to indicate it is acquired through means not shown. In a remote-controlled drone, this would be the value passed by the remote-controller. In case of my drone, this value would be pre-set to the drone, maybe through a list of previously calculated angle changes or displacement coordinates. This is yet to be addressed in the future, after the controller is properly designed. After reducing the values measured to a range the controller can be properly managed (dividing it by 8000), the proportional gain is applied and the new positions are written to the propellers.

It is important to emphasize that though not shown here, the value of K_p is constant and predefined.

4.3. PID

After doing some research and reading source codes of previously done Arduino UAV projects found online, I came to know of a ‘step further’ in the controller used, not only in all these projects, but in many engineering applications. This concept, called PID (Proportional Integral and Derivative) controls three different aspects of the controlled variable, in this case the movement of the UAV. In general, such controller can be expressed as:

$$R(t) = K_p e(t) + K_i \int_0^t e(\tau) d\tau + K_d \frac{de(t)}{dt}$$

In which R is the resultant correction, e is the error between the measured value and the desired value, both functions of time, K_p is called the proportional gain, K_i the integral gain and K_d the derivative gain.

In the first place, I learned the controller I had so far was a controller of P type, or proportional type. This controller addresses the difference between the actual measured value and

the desired value. After the result is passed to the actuation unit, the error is measured and calculated again, in a repeating cycle. This is where the name proportional comes from, since the correction value passed to the actuation is always proportional to the error, and it is regulated by the K_p term of the equation.

As for the ID part, the integral error is the error that builds over time, in case the proportional correction is not enough to counterbalance a disturbance, such as a constant wind blow for example; and the derivative error is the rate at which the error is changing. Addressing the derivative gain can make the controller more responsive to abrupt changes.

Since the code, both in C and MATLAB happens in discrete loops, in contrast to a continuous mathematical function domain, the integral error is the sum of the error in each iteration, regulated by the K_i gain, and the derivative error is the difference between the current error and the past iteration's error, regulated by the K_d gain. In MATLAB, the code for the first PID controller I came up with follows:

```
pos1 = 0.36;
pos2 = 0.36;
writePosition(prop1, pos1);
writePosition(prop2, pos2);

while 1

    accelRead(1) = readRegister(accel, 52);
    accelRead(2) = readRegister(accel, 53);
    mesAccel = double(bitor((bitshift(int16(accelRead(2)), 8, 'int16')), int16(accelRead(1)), 'int16'));

    if abs(mesAccel) < 80
        mesLast = mesAccel;
    end

    if abs(mesAccel) > 80
        mesAccel = mesLast;
    end

    errAccel = (mesAccel - ref) / 8000;
    errIAccel = errIAccel + errAccel;
    pos1 = 0.36 + Kp * errAccel + Kd * (errAccel - errAccel_last) - Ki * errIAccel;
    pos2 = 0.36 - Kp * errAccel - Kd * (errAccel - errAccel_last) + Ki * errIAccel;

    writePosition(prop1, pos1);
    writePosition(prop2, pos2);

    errAccel_last = errAccel;

end

writePosition(prop1, 0.3);
writePosition(prop2, 0.3);
```

Just as with the previous code, this section works by gathering the value of the angle at each loop, comparing it with a pre-set angle value, and passing the arguments to the actuation units. At this point though, the differential and integral errors are present with the calculation after the proportional error. The proportional gain acts on the difference between `errAccel` and

errAccel_last(which is measured at the end of the loop), whereas the integral gain acts on errIAccel (which is the sum of all previous error values, equal to 0 in the beginning of the first loop).

Just as with the previous P type controller, the values of the gains, Kp, Ki and Kd, are declared before the loop and are kept constant while the drone is at work. It is also important to mention that though in a Control Systems Engineering perspective the values of Kp, Ki and Kd would be determined analytically with the help of a mathematical model of the plant and MATLAB, in this case they had to be determined closely by trial and failure, precisely because of the lack of a mathematical model. At the time, I had little to none knowledge of a Control Systems Engineering way of approaching the design of a controller, less even the knowledge of concepts of dynamic systems representation, differential equations and transfer function analysis, concepts core to the design of a controller, and at the present state of the project, using such methods for this particular system (which was designed without taking them into consideration) would be as time and effort consuming as keep on testing for the gains by trial and error.

5. Vibration

The sensor value gathering, together with the controller code designed, in theory should have made the UAV controllable. In practice, however, once the code was set to run in the UAV, it rendered this completely unresponsive. Not only once it was on the UAV was on it became completely unstable, its movements also suggested nothing like the behaviour expected from the code. After adjusting the parameters numerous times, all of them were unsuccessful and apparently had no effect, the only possible explanation was that the values gathered by the sensors had to have some error. Since the Arduino does not support running two codes at the same time, the code for gathering a 5 second sample of the Accelerometer readings was run with the drone idle. Running the code 3 times provided the following, shown in figure 6:

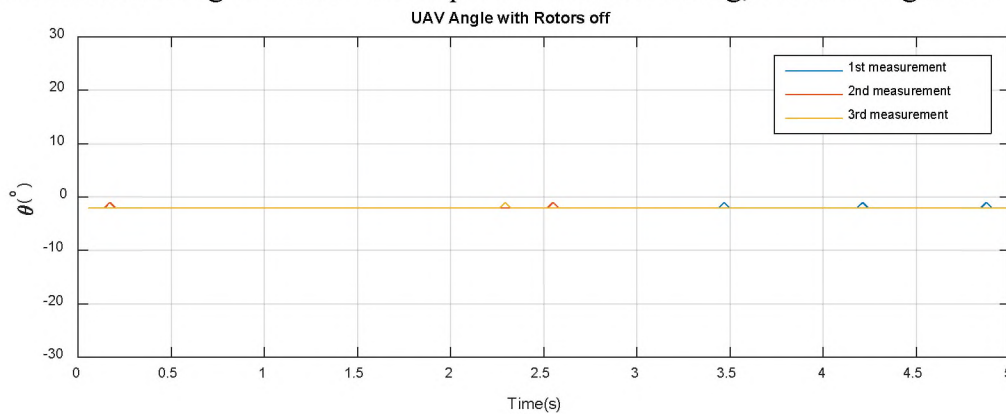


Figure 6

Such behaviour suggests that the readings from the sensor are also accurate, since they seemed to describe the state of the drone's movement with complete accuracy. After reading the Accelerometer manual of use, adjusting parameters against sudden bumps or presses, only to yield the same results, I changed the code to gather the 5 second sample with the rotors on, also in the equilibrium position. To my surprise, the results gathered are as follows, shown in figure 7:

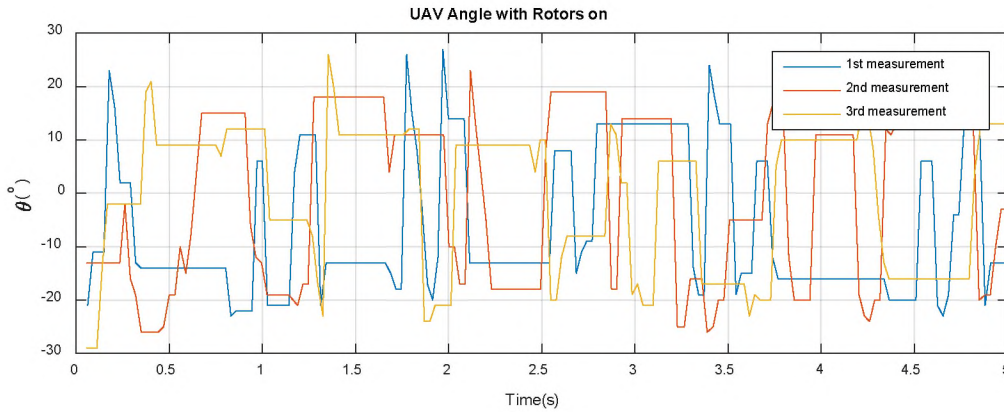


Figure 7

It was surprising to me that turning on the rotors would make such an enormous difference, as well as clearly rendering the gathered data useless. By looking at the plot of the 3 measurements, one cannot tell for sure what the position of the drone is, much less say it is idle. Yet the only different thing was the motion of the rotors. I immediately came to realize the problem had to be the vibration of the sensor.

In fact, with the thought of vibration in mind, one could see the UAV was actually very poorly prepared to deal with this kind of problem at that stage, especially because the sensor was directly attached to the main frame through a metal bar, with no damping mechanisms to avoid vibrations to be passed to the sensor. Searching for online solutions to the same problem in previous UAV projects, I found this problem could be easily solved with a vibration dampening support. This would be a plate held away from the frame through the use of gel, foam or vibration absorbing material. After some considerations, the design I came up with for such was as follows in figure 8:

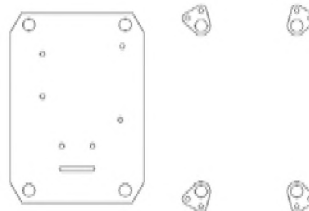


Figure 8

The top four attachments connect to the hexagonal centerpiece by the M3 holes, whereas the previously mentioned vibration dampening material connects to the top through the larger hole. The board holds holes for attaching the Arduino and the IMU, instead of only the IMU, since vibrations from the Arduino could be transferred to the sensor if it wasn't protected against vibrations as well.

The structure was originally planned to be laser cut from an ABS plate, but since the machine in NUAA's Engineering Training Center was off service it had to be cut by hand. This did not affect the overall functioning of the structure much. After being cut and properly installed, a single test proved it to be effective, reducing the vibrations to the point where the difference caused by the vibrations did not result in visible actuation differences in the rotors.

6. C code

Since visualizations from MATLAB had proven the vibration dampening to have been effective, but the MATLAB code has no way of running in the Arduino without a computer, that is, in standalone, the code had to be translated to C and implemented directly in the Arduino IDE. The code, in its entirety, is not yet complete, but works similar to the MATLAB equivalent,

actuating one axis. The function responsible for the controller ended up looking like the following:

```
void pidController()
{
  Wire.beginTransmission(0x53);
  Wire.write(0x32);
  Wire.endTransmission();

  Wire.beginTransmission(0x53);
  Wire.requestFrom(0x53, 6, true);

  inti = 0;
  while((Wire.available()) && (i<= 6))
  {
    accelRead[i] = Wire.read();
    i++;
  }

  Wire.endTransmission();

  mesAccel_x = (((int16_t)accelRead[1]) << 8) | accelRead[0];
  mesAccel_y = (((int16_t)accelRead[3]) << 8) | accelRead[2];
  mesAccel_z = (((int16_t)accelRead[5]) << 8) | accelRead[4];

  //CONTROLS ONLY Y

  if (abs(mesAccel_y) < 80)
    mesLast_y = mesAccel_y;
  else if (abs(mesAccel_y)>80))
    mesAccel_y = mesLast_y;

  errAccel_y = (mesAccel_y - ref_y) / 2000;
  errIAccel_y += errAccel_y;

  pos1 = 180 * (0.36 - Kp_y * errAccel_y + Kd_y * (errAccel_y - errAccel_y_last) - Ki_y * errIAccel_y);
  pos2 = 180 * (0.36 + Kp_y * errAccel_y - Kd_y * (errAccel_y - errAccel_y_last) + Ki_y * errIAccel_y);

  prop1.write(pos1);
  prop2.write(pos2);

  Serial.println(prop1.read());
  Serial.println(prop2.read());

  errAccel_y_last = errAccel_y;
}
```

In C, to run standalone, the calculation of the PID controller works much faster than in MATLAB. This is because not only C code is very fast, but the Arduino, when running in standalone the program uploaded to its memory, dedicates its computing power entirely to run

this single program. Up to this point, the optimal values for Kp_y , Kd_y and Ki_y are yet to be determined (as are the other control gain constants).

7. Final Considerations & Conclusions

As of October 2017, the development of the drone, nicknamed “Roxelle,” has been limited to the presentation in this report. The project has drawn a lot of attention from NUAA’s College of International Education for its potential as a self-study mechanism for the student or students engaging in its development, and I see it being developed further in the future.

When I started the project, I had no knowledge of how an engineer should approach designing such a system, but also no technical knowledge to approach this development in an analytical manner. Developing Roxelle to the stage it is today helped me get familiar with those skills, and develop my skills in 3D CAD, MATLAB, control systems, C programming, laser cutting and soldering, besides the idea of how an engineering project should be conducted. I’m going to plan on starting a new project soon, to develop parallel to this one, in which I will take a more careful approach in the aspects I failed to appreciate in this project, and apply the knowledge I’ve been able to obtain from university studies in these 2 years.

As for Roxelle, I will develop it more as time goes by, focusing in building a robust controller before anything else, so it can be stable and perform the pre-programmed actions accurately; when such system is implemented, I will develop its navigation system, so that it can run a set of instructions determined by its user. I look forward to interfacing such system with a mobile application, but that is too far ahead of the present state of development. What lies ahead is no doubt an incredible amount of unexplored knowledge, which should bring about the previously mentioned potential a project like this has to teach extracurricular skills to the student dedicated to developing it.

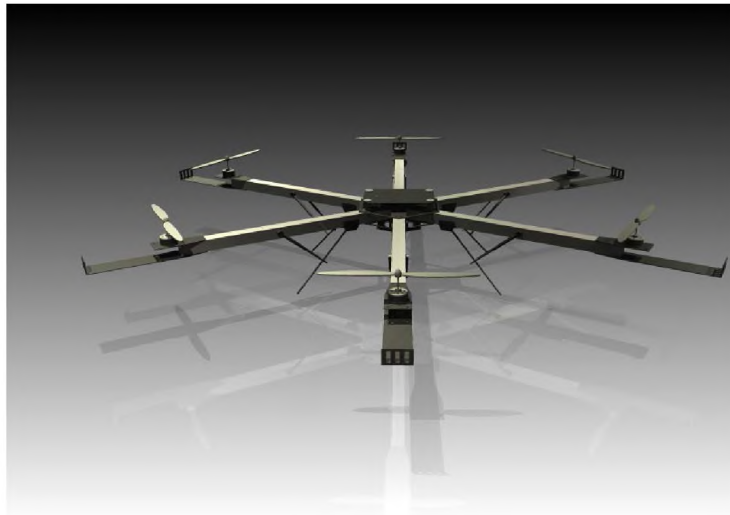
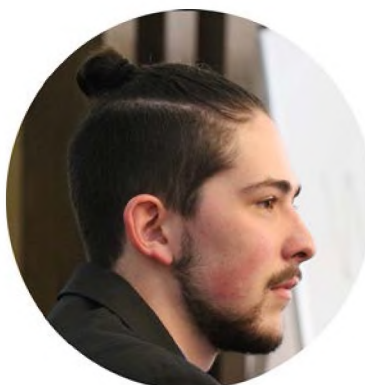


Figure 8

REFERENCES

- [1] Liang, Oscar. Build a Quadcopter - Beginners Tutorial 1. Oscar Liang. [Online] June 2017. <https://oscarliang.com/build-a-quadcopter-beginners-tutorial-1/>.
- [2] STMicroelectronics.L3G4200D: MEMS motion sensor: ultra-stable three-axis digital output gyroscope. s.l. : STMicroelectronics, 2010.
- [3] Analog Devices, Inc.ADXL345: Digital Accelerometer: Data Sheet. s.l. : Analog Devices, 2016.
- [4] Brokking, J. Project YMFC-AL - The Arduino auto-level quadcopter. Brokking. [Online] 30 October 2016. http://www.brokking.net/ymfc-al_main.html.

Author



Allan A. Dias

FOCUS ON INTERDISCIPLINARY EDUCATION IN AIRWORTHINESS SKILLS CULTIVATION

Piao Li¹, Oleksiy Chernykh² and Weixing Yao³

¹ Nanjing University of Aeronautics and Astronautics
College of Aerospace Engineering
29 Yudao Street
Nanjing, 210016, Jiangsu, China
e-mail: lipiao@nuaa.edu.cn

² Nanjing University of Aeronautics and Astronautics
College of Civil Aviation
29 Jiangjun Avenue
Nanjing, 211106, Jiangsu, China
e-mail: alex@nuaa.edu.cn

³ Nanjing University of Aeronautics and Astronautics
College of Aerospace Engineering
29 Yudao Street
Nanjing, 210016, Jiangsu, China
e-mail: wxyao@nuaa.edu.cn

Key words: interdisciplinary education, Aircraft Airworthiness Technology, aircraft design.

Abstract. *This paper provides an approach to interdisciplinary education, especially introduces the interdisciplinary airworthiness cultivation in the Nanjing University of Aeronautics and Astronautics (NUAA) for students of the Aircraft Airworthiness Technology major. Both objective and personal viewpoints have been illuminated. Conclusions have been made that interdisciplinary education develops students' interdisciplinary thinking, which is essential for solving complex problems.*

1 INTRODUCTION

Nowadays, more and more scientific or academic issues have become more complex, calling for interdisciplinary cognition and cross-field solution^[1]. A professor on biodiversity conservation or agricultural cultivation should acquaint himself with both data science and center-field knowledge. A translator who focuses on a specific field like economics or politics has to combine language skills with serving industries. As for the aviation field, an airworthiness engineer deals with not only aviation regulations, but also technical verifications working with structure itself. Interdisciplinarity has been inevitable and significant.

According to Jacobs and Frickel, two experts on education, interdisciplinarity is defined as “communication and collaboration across academic disciplines”^[2]. Elinor Ostrom, the first female Nobel Laureate in Economic Sciences, developed her productive study on deforestation by conducting long-term interdisciplinary research in which her group analyzed the institutional factors affecting deforestation using multiple research methods including satellite image data, social-ecological measurements on the ground, and experimental laboratories. In her words, “Narrow disciplinary boundaries limit our science’s progress”^[2].

2 THE INTERDISCIPLINARY AIRWORTHINESS EDUCATION IN NUA

Up to date, most of present college and university graduate education is still on the stage of specialized education of single discipline. The Nanjing University of Aeronautics and Astronautics (NUAA) has developed airworthiness direction into a new major several years ago. Students of the Aircraft Airworthiness Technology major have been attempted to feature an interdisciplinary educational background.

In the first three years, students focus on their specialties, including aircraft design, electrical engineering, mechanical engineering, and so on. The three years' study for specialty is extremely necessary, since it lays the vital foundation of students' knowledge system. They have got systematic curriculum for engineering, including mathematics, mechanics, electronic technology, materials and processing, physics, computer science, and aerodynamics. For the fourth year, they enter studies of airworthiness.

Based on the previously accumulated knowledge, they can go further into airworthiness field with a good understanding of correlative technological issues. When relating to structural and electronic reliability in airworthiness, they can connect mechanics and electronics (they have learnt before) with reliability technology. When coming to civil aviation regulations, they are clear about the aircraft structure, aerodynamic characteristics and corresponding techniques to satisfy various requirements. Airworthiness is a complicated discipline which can never support itself without professional knowledge^[3]. From this aspect, interdisciplinary education enriches and systematizes students' intellect and enables their professional abilities.

3 INTERDISCIPLINARY THINKING CASE – LIGHT AIRPLANE DESIGN

A significant achievement of interdisciplinary cultivation is interdisciplinary thinking. Focusing on a certain field can lead to deep researching outcomes, whereas width of perspective can be limited, at the same time. Most of technical problems require the ability to change disciplinary perspectives, to switch between depth and breadth, and to transfer new knowledge structures to other appropriate contexts. Jacobs and Frickel wrote in their articles that interdisciplinarity is expected to integrate knowledge and solve problems that individual disciplines cannot solve alone^[2].

A graduation project accomplished by a student of the Aircraft Airworthiness Technology major in NUAA can be taken as an example to identify and support the significance of interdisciplinary thinking. Based on four-year learning of aircraft design and airworthiness, the composite wing of a domestic light general aircraft named “NH40” (Figure 1) was designed. China Civil Aviation Regulations was taken as the designing criteria^[4].



Figure 1: NH40 light general aircraft

Firstly, according to accumulated experience of predecessors and airworthiness regulations, the configuration of the wing was determined^[5-7]. The wing was divided into three segments: an outer segment, an inner segment, and an intermediate segment. The outer segment is of the shape of trapezoidal wing, and the inner segment and the middle segment are straight wings. There was a certain wing dihedral angle and torsion angle adopted. At the root and tip of the inner wing, the airfoil adopted was NACA 64414 and the dihedral angle and torsion angle were 2° and 1.3° , respectively. The relative thickness of the airfoil was 0.14. For the outer segment, NACA 64414 was applied for wing root, and NACA 64412 for wing tip. The dihedral angle was 2° , the torsion angle was -0.677° , and the relative thickness of the airfoil was from 0.14 to 0.12 (Figure 2).

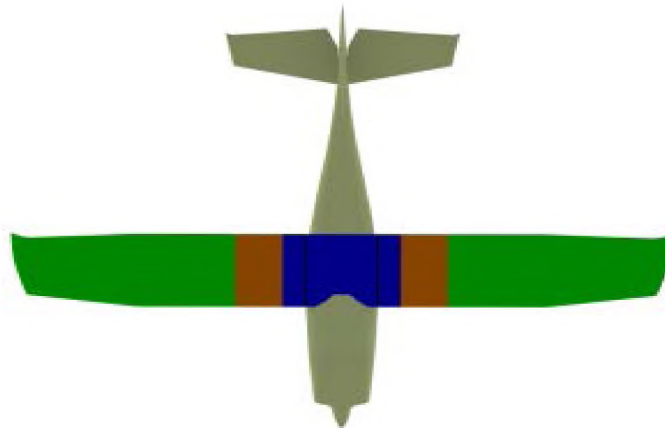


Figure 2: The composite wing configuration

Secondly, the internal supporting structural elements of the wing were allocated. Three reinforcing ribs, which support much of loads, were placed in the wing tip, root, and middle parts. Three common ribs were allocated between the reinforcing ribs for maintaining

the airfoil shape and bearing a small part of shear. In order to facilitate industrial processing, the cross-sectional shape of the truss was designed to be Z-shaped (Figure 3).

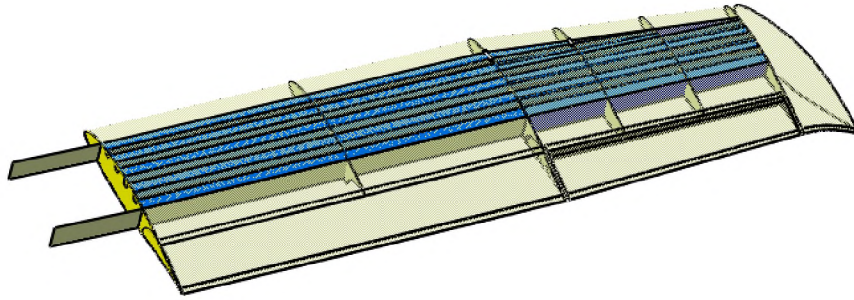


Figure 3: The internal arrangement of the composite wing

Thirdly, according to limited design airspeed, the coefficient of maneuvering load and gust load factor in regulations^[4], the flight envelop was estimated (Figure 4). Then the normal distribution of the load along the wing span was obtained.

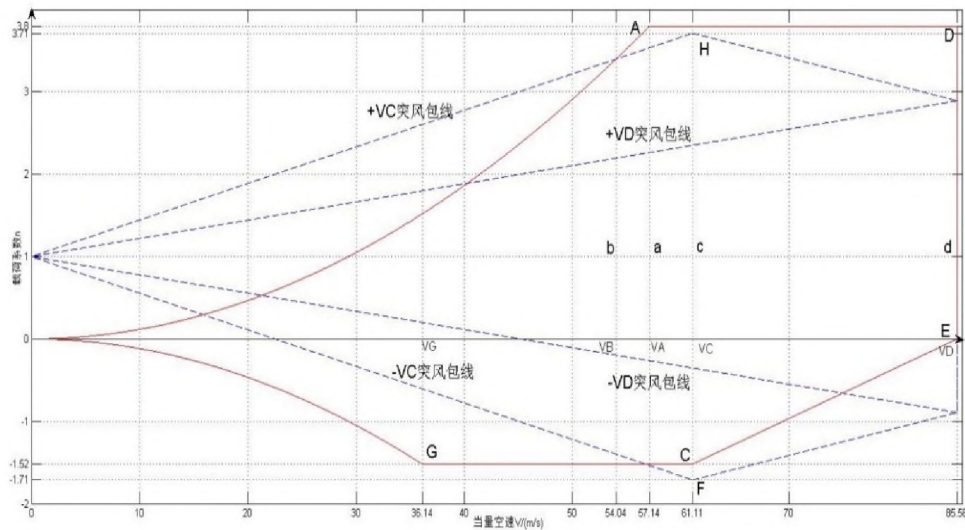


Figure 4: Flight envelope

In order to meet strength requirements, the finite element analysis was applied to do prior verification^[8-10] (Figure 5). After several modifications, a satisfactory design, which can meet the requirement of safety factor of 1.5, was developed^[11].

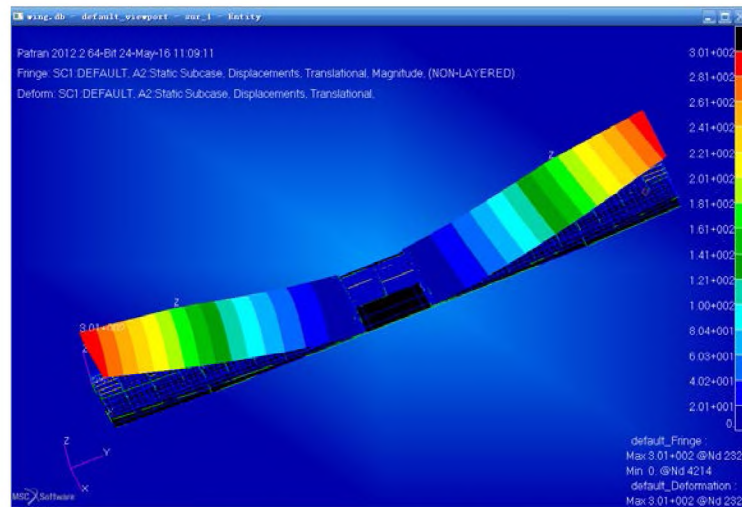


Figure 5: Finite element analysis of the composite wing

4 CONCLUSIONS

Interdisciplinary education develops students' interdisciplinary thinking, which is essential for solving complex issues such as a real aircraft designing work. In a personal point of view, interdisciplinary education can be treated as an outcome-based educational approach. Standing on a broader stage of knowledge, students can get through ambiguous cognition and step towards directly their goals. They are not limited within a narrow field; they can grasp the point and make directive efforts. Interdisciplinary thinking leads to comprehensive designing plan and global cognition.

REFERENCES

- [1] Yonjoo Cho. Identifying Interdisciplinary Research Collaboration in Instructional Technology. *TechTrends*, 2017, 61:46–52.
- [2] Elisabeth J. H. Spelt, Harm J. A. Teaching and Learning in Interdisciplinary Higher Education: A Systematic Review. *Educ Psychol Rev*, 2009, 21:365-378.
- [3] Jianzhong Yang. *Interpretation of Airworthiness Requirements for Transport Aircraft*. Beijing: Aviation Industry Press, 2013. (in Chinese)
- [4] China Civil Aviation Regulations. *CCAR 23. Airworthiness Requirements for Normal, Utility, Special and Commuter Aircrafts*. Beijing: Civil Aviation Administration of China, 2014. (in Chinese)
- [5] Zhijin Wang, Weixing Yao. *Aircraft Structural Design*. Beijing: National Defense Industry Press, 2004, 47-149. (in Chinese)

- [6] Xiasheng Sun. *Guide for Civil Aircraft Design and Verification of Structural Strength and Stiffness*. Beijing: Aviation Industry Press, 2012. (in Chinese)
- [7] Chunyun Niu. *Practical Aircraft Structural Engineering Design*. Beijing: Aviation Industry Press, 2008, 620-662. (in Chinese)
- [8] Kai Long, Changzhi Jia, Baofeng Li. *From Entry to Mastery: Patran2010 and Nastran2010 Finite Element Analysis*. Version 2. Beijing: Machinery Industry Press, 2011. (in Chinese)
- [9] Guofeng An, Shengli Lv, Qinglan Zhao. *Structural Finite Element Analysis of All-Composite Wing of Unmanned Aerial Vehicle. Strength and Environment*. 2009, 36(6), 40-43. (in Chinese)
- [10] Suraparb Keawsawasvong, Boonchai Ukritchon. Finite Element Limit Analysis of Pullout Capacity of Planar Caissons in Clay. *Computers and Geotechnics*, 2016, 75.
- [11] V. S. Sipetov. Accurate Analysis of the Behavior of Laminated Composite Structures on the Thermal and Static Effects. *Mechanics of Composite Materials*, 1989, 25(1).

Reporter



Piao Li

Co-authors



Oleksiy Chernykh



Weixing Yao

JOINT AIRWORTHINESS EDUCATION FOR HEAT TRANSFER CHARACTERISTIC RESEARCHES ON AERO-ENGINE INLET STRUT WITH FILM-SLOT CAP

Lu Yi^{1*}, Oleksiy Chernykh² and Ke Peng^{1**}

¹ Beihang University (Beijing University of Aeronautics and Astronautics)
School of Transportation Science and Engineering
37 Xueyuan Road
Beijing, 100191, China
e-mail: kepenggroup@163.com

² Nanjing University of Aeronautics and Astronautics
College of Civil Aviation
29 Jiangjun Avenue
Nanjing, 211106, Jiangsu, China
e-mail: alex@nuaa.edu.cn

Key words: airworthiness education, aero-engine inlet strut; film heating; film-slot cap; blowing ratio.

Abstract. *The paper displays results achieved under student research work highlighting joint educational cooperation of two Aerospace-related universities in China at the “university-university” level. This educational model has been found to be a beneficial strategy resulting in larger opportunities for students’ education involving twice more guidance and resources within the same timeframe. In particular, the student’s research on heat transfer aspects for aero-engine inlet strut with a film-slot cap has been started by a student of the Aircraft Airworthiness Technology major in Nanjing University of Aeronautics and Astronautics and enlarged within additional guidance for further study in Beijing University of Aeronautics and Astronautics, as follows. The anti-icing structure with film slots in the leading edge has advantages in improving internal jet impingement heat transfer and external film heating efficiency, and helping to blow the droplet away to decrease local collection efficiency. In order to further improve the efficiency of the film heating and avoid the flow choking, a unilateral-opened cap was designed for the aero-engine inlet strut with film-slot of 5° angle. Firstly, the basic flow field calculation of the complex structure was carried out by using six different turbulence models and wall conditions. By comparing with the experimental data, the standard k-ε model with enhanced wall condition was confirmed with the best compliance. Then the best cap opening angle and the effect of blowing ratio on the heating efficiency of the film were studied under the condition of coupled and uncoupled heat transfer. It was found that the cap enhanced the adhesion of the heat jet outflow and improved the heating efficiency of the outer surface. And 30° was the best cap opening angle when the heat flow rate was 0.0586kg/s, which made the heating efficiency the highest. In addition, as the blowing ratio increased, the vortex near the jet outlet led to the local heating efficiency decreasing, but the heating influence range along the flow was wider.*

* The Presenting Author: Lu Yi, Graduate Student, lu_yi@buaa.edu.cn.

** The Corresponding Author: Ke Peng, Associate Professor, p.ke@buaa.edu.cn.

1 INTRODUCTION

The educational process always benefits a lot from interaction and cooperation of relevant research teams. Teaming may happen at the level of “*student-student*” interaction within the same laboratory, “*laboratory-laboratory*” interaction within the same department or college. But when it goes beyond boundaries of the same college, when it reaches the level of “*college-college*” or even “*university-university*” interactions, a studied research task also expands in its feasibility to much higher levels due to more resources being involved. The described work strategy has long been maintained between the two Aerospace-related top universities of China: Beijing University of Aeronautics and Astronautics (BUAA) and Nanjing University of Aeronautics and Astronautics (NUAA). In particular, students of the Aircraft Airworthiness Technology major in NUAA who are intending to go for their Master’s degree study to BUAA already start their further study research directions while yet studying in NUAA for their Bachelor’s degree. Such student researches are usually guided by two supervisors from both mentioned universities gaining access to twice larger knowledge database and laboratory resources at the same time. During work, students really appreciate understanding of teachers of the former university who have been helping them to get better ready for entering another university in the nearest future.

Such a research work has been done by an undergraduate student on heat transfer aspects for aero-engine inlet strut with a film-slot cap. The project was started in NUAA, and teachers inspired quite a lot in relative airworthiness background and English writing. BUAA professors and seniors also gave much technical guidance when facing software problems. It has been beneficial for the student to have both strong educational resources. And the results of such a student joint research work are presented in this paper covering aspects from aircraft flight safety to design for aircraft airworthiness.

Flight safety of aircraft operating under natural icing conditions is one of the major concerns of certification authorities and aircraft manufacturers. Ice accretion on the aero-engine inlet strut will affect the intake flow and thus degrade engine performance. Furthermore, it will also lead to some more serious mechanical damage because of the shed ice sucked into the engine.

To make the aero-engine more safe, Civil Aviation Administration of China (CAAC) issued strict regulations in CCAR33.68 [1], which require that engine, with all icing protection systems operating, must

“(a) Operate throughout its flight power range (including idling) without the accumulation of ice on the engine components that adversely affects engine operation or that causes a serious loss of power or thrust in continuous maximum and intermittent maximum icing conditions as defined in Appendix C of Part 25 of this chapter; and

(b) Idle for 30 minutes on the ground, with the available air bleed for icing protection at its critical condition, without adverse effect, in an atmosphere that is at a temperature between -9°C and -1°C and has a liquid water content not less than 0.3 grams per cubic meter in the form of drops having a mean effective diameter not less than 20 microns, followed by a momentary operation at takeoff power or thrust. During the 30 minutes of idle operation the engine may be run up periodically to a moderate power or thrust setting in a manner acceptable to the Administrator.”

As always, a hot air anti-icing system is the main anti-icing method of engine, which makes use of the hot gas from the low or high pressure compressor to heat the targeted region [2-3]. Nowadays, the impacting heat transfer of typical heat anti-icing system with metallic material has been adequately studied. Hot air bled from the compressor impacts the front inside wall to get it heated, then, the heat transfers to the outside surface through heat conduction. This method, the so-called "Surface Type Heat Transfer", separates the hot air and outside surface and has been widely applied to some airfoil anti-icing systems [4], aero-engine inlet strut anti-icing systems [5] and double skin corrugated chord direction anti-icers [6].

In order to make better use of the exhaust heat of hot air that has already impacted the front inside wall, a new design that adds some film holes or slots to the anti-icing chamber has been announced. The target of this design is still to enhance the impacting heat transfer effect and has been successfully applied to the Russian aero-engine AL31-F. For more research work, Li Yundan et al. [7] used a numerical model to study the effect of impacting distance, hole diameter, hole spacing and Reynolds number (Re) on the heat transfer of impacting structure for the heat anti-icing system. Ma Hui et al. [8] developed a new hot-air anti-icing structure of an engine inlet vane with micro channels and narrow gaps. And then they moved forward the position of the jet hole and moved backward the exhaust hole to get a better heat transfer.

Nevertheless, as low thermal conductivity composites tend to be more and more popular in the field of aircraft material, it poses a challenge for the heating effect of the aforementioned "Surface Type Heat Transfer" method that is suitable for the anti-icing system with metallic materials. Therefore, a new kind of structure with film holes or slots purposely in the leading edge has become to be studied and valued [9-10]. In this structure, both the internal impacting heat transfer and external hot film heat transfer play an important role. Exhaust air out of the leading edge holes or slots can not only enhance the internal impacting effect, but also heat the external surface and weaken the external heat convection as it jets out and flows close to the outside wall. Furthermore, the hot jet is able to affect the trajectory of oncoming water droplets, reducing the surface water collection efficiency. Hence, many researchers like Yang Huiyun [9] and Zhang Yun [10] have done work to study the heat transfer characteristics and water droplet impingement characteristics referring to some relevant research work (like impingement heat transfer [11-13], and cold film heat transfer [14-18]) in the mature film cooling field.

In order to further improve film heated efficiency and prevent the clogging of film slots, we firstly designed a kind of film cap based on the structure in reference [10]. Then, the best cap opening angle and the effect of blowing ratio on the heating efficiency was studied in detail. Lastly, some aerodynamic forces and drags were also taken into consideration.

2 STRUCTURE DESIGN AND SOLVER SETTINGS

2.1 Film-Slot Cap Design

It has been proved that the film slots of the aero-engine inlet strut have a significant effect on the flow field and temperature field of the structural surface, and among the four different film slots angle (5°, 30°, 90°, 150°) discussed, the angle 5° shows the superiority [10].

However, it still has some shortcomings. On the one hand, the 5° film slots will make the internal hot jet and external cold mainstream blend too quickly at the intersection, leading to energy waste. On the other hand, the film slots are more likely to be blocked with such a small angle. Therefore, a unilateral-opened cap as shown in Fig. 1~3 was designed for the film slot.

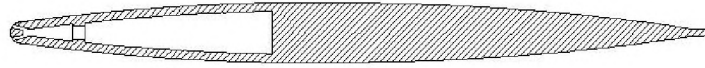


Figure 1: Profile of Aero-engine Inlet Strut with Film-Slot Cap.

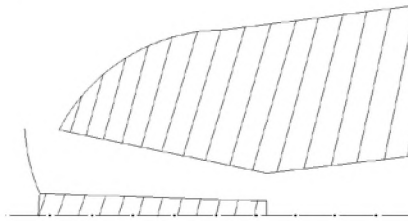


Figure 2: Partial Enlarged Profile of the Front Edge of Fig.1.

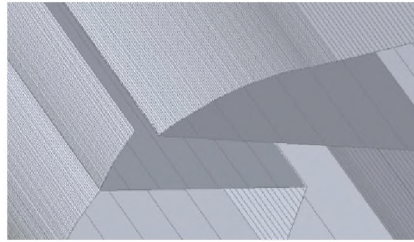


Figure 3: The 3D rendering of Fig. 2.

2.2 Algorithm and Verification

Because the structure is similar to the confined channel with one-line heated jets [19], our algorithm and verification work just depends on the experiment data in reference [19]. The computational domain of the model was given in Fig. 4 (Unit: mm), where the mainstream started horizontally at 400mm from the hot jet inlet, and the outlet was set 1200 mm behind the mainstream inlet.

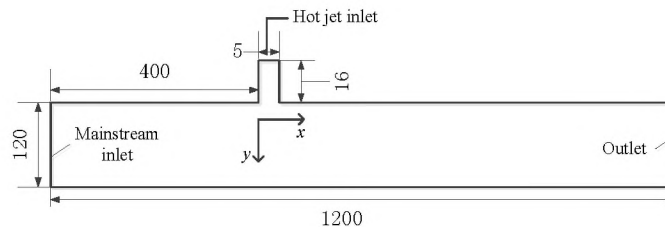


Figure 4: Model of Confined Channel with One-Line Heated Jets.

The structured meshes were constructed for above computational domain. Local grids were refined near the wall, and the final mesh has 190,000 nodes after grid independency check, as demonstrated in Fig. 5.

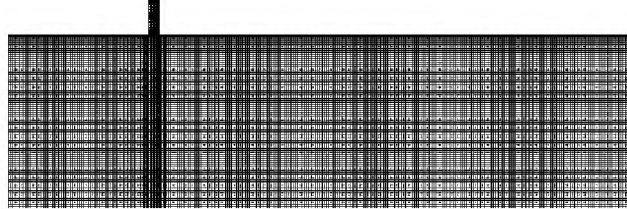


Figure 5: Partial Computational Mesh for the Model.

Different turbulent models (standard $k-\varepsilon$ model, RNG $k-\varepsilon$ model, Reynold Stress model and SST $k-\omega$ model) and different near-wall treatments (standard wall functions and enhanced wall treatment) in Ansys Fluent were combined for the later simulation to make it clear which was the most suitable one.

The governing equations for air flow, including the mass conservation equation, the momentum conservation equation and the energy conservation equation, were given below,

$$\frac{\partial \rho_a}{\partial t} + \nabla \cdot (\rho_a \mathbf{u}_a) = 0 \quad (1)$$

$$\frac{\partial}{\partial t}(\rho_a \mathbf{u}_a) + \nabla \cdot (\rho_a \mathbf{u}_a \mathbf{u}_a) = -\nabla p + \mu_a \nabla^2 \cdot \mathbf{u}_a \quad (2)$$

$$\frac{\partial}{\partial t}(\rho_a E) + \nabla \cdot [\mathbf{u}_a (\rho_a E + p)] = \nabla \cdot (k_{\text{eff}} \nabla T + \mathbf{u}_a \cdot \mu_a \nabla \mathbf{u}_a) \quad (3)$$

Where $\rho_a, \mu_a, \mathbf{u}_a$ are the density, the molecular viscosity, and the velocity of air respectively E, p, k_{eff}, T are the internal energy, the pressure, the effective conductivity and the temperature respectively.

The air was considered compressible as the ideal gas, and its viscosity was calculated according to Sutherland equation. And some boundary conditions were summarized in Table 1.

Boundary	Condition	Velocity(m/s)	Temperature (K)	Pressure (Pa)
Mainstream inlet	Velocity inlet	3	300	101325
Hot jet inlet	Velocity inlet	16.78	373	101325
Outlet	Pressure outlet	—	300	101325

Table 1: Boundary Conditions

The mainstream and hot jet conditions were set based on the experiment case in reference [19], among which the momentum flux ratio J was set to 25.2. The momentum flux ratio was defined as

$$J = \frac{\rho_j V_j^2}{\rho_\infty V_\infty^2} \quad (4)$$

Where ρ_j , ρ_∞ are the densities of hot jet and mainstream, V_j , V_∞ are the velocities of hot jet and mainstream.

Fig.6 showed the typical mean vertical velocity profile at $X/D = 2$ plane with different turbulent models and near-wall treatments, where D is jet nozzle width. The label H of Y/H at y coordinate axis is the duct height. And the dimensionless velocity \tilde{U} at x coordinate axis was defined as:

$$\tilde{U} = \frac{\bar{U} - U_\infty}{U_{\max} - U_\infty} \quad (5)$$

Where \bar{U} is the mean velocity in the x direction, U_∞ is the mainstream velocity and U_{\max} is the maximum mean velocity at the vertical profile in the x direction.

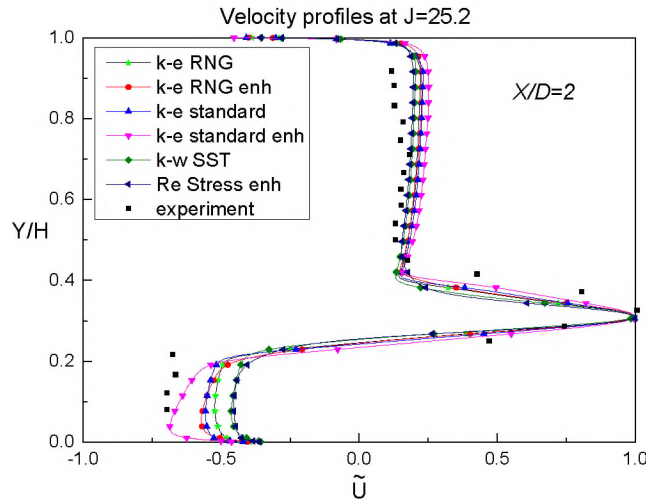


Figure 6: Velocity Profile at the $X/D = 2$ Plane.

It could be seen from the Fig.6 that the flow velocity calculated by each turbulence model was in good agreement with the experimental data in the mixing zone away from the jet exit. However, the standard $k-\varepsilon$ turbulence model with the enhanced wall treatment could better simulate the details of the flow at the heat jet exit with the lowest error. Hence, it was chosen as the most suitable algorithm to simulate the internal and external flow field of aero-engine inlet strut with film-slot cap.

3 RESEARCHES ON THE FILM-SLOT CAP

3.1 Determination of the best cap opening angle

Numerical simulations were conducted for the aero-engine inlet strut with no film-slot cap and film-slot cap of 10° , 20° , 30° , 40° , 50° respectively. The solid material was set for the wall and it was set to be titanium alloy material with thermal conductivity $7.44 \text{ W/(m}\cdot\text{K)}$. The flow field and the temperature field coupled the solid thermal conduction. Standard $k-\varepsilon$ turbulence model with the enhanced wall treatment was chosen based on researches above. The calculation was performed with a 2nd-order upwind format to discrete the advection and the pressure terms. Some more detailed boundary conditions were listed in Tab.2. And the mainstream condition was set based on aero-engine actual working condition. The hot air flow rate was calculated based on the blowing ratio M , as defined in Eq. (6)

$$M = \rho_h u_h / \rho_g u_g \quad (6)$$

Where ρ_h, u_h are the density and the velocity of the hot air. And ρ_g, u_g are the density and the velocity of mainstream.

Boundary	Condition	Velocity	Temperature (K)	Pressure (Pa)
Mainstream inlet	Pressure far field	0.314Ma	253	101325
Hot jet inlet	Mass flow inlet	Based on blowing ratio	413	202000
Outlet	Pressure outlet	—	253	101325

Table 2: Boundary Conditions

According to the above boundary conditions, a set of numerical simulations were carried out under the conditions of the blowing ratio $M=0.5$ and the hot jet mass flow $Flux = 0.0586 \text{ kg/s}$. Fig.7 showed the distribution of film heating efficiency η along the part of external wall that was behind the film slot. The labels S and D at x coordinate axis are the curve length from the film slot and the film slot width. And the film heating efficiency η was defined to measure heating efficiency as in Eq. (7),

$$\eta = \frac{T_w - T_g}{T_h - T_g} \quad (7)$$

Where T_w , T_g , and T_h are the adiabatic wall temperature, the mainstream temperature and the hot air temperature respectively.

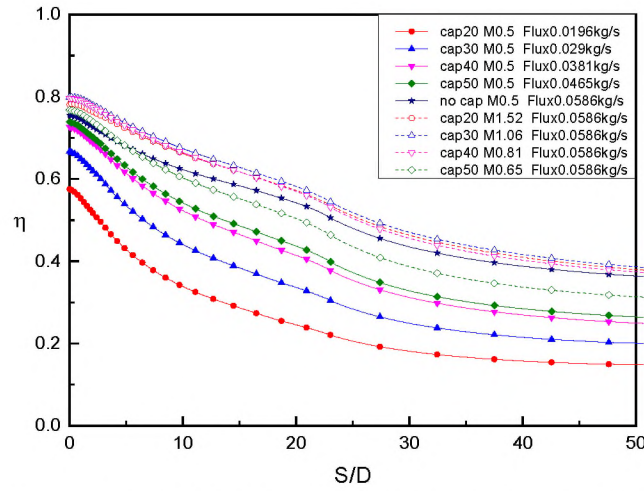


Figure 7: Comparison of Film Heating Efficiency along the External Wall.

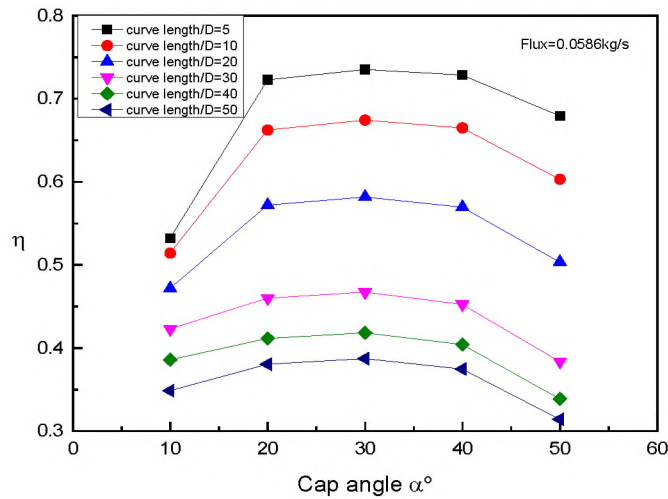


Figure 8: Film Heating Efficiency at different position with different angle as Flux = 0.0586kg/s.

It could be seen from the Fig.7 that the film heating efficiency decreased downstream exponentially along the flow direction, showing a very good consistency in the trend under different conditions. When the blowing ratio was 0.5, the heating efficiency curve moved up as the cap opening angle increased, which indicated a better anti-icing effect. This was because when the cap had a broader opening but at a constant blowing ratio, the mass flow of the hot jet would definitely increase. So would the kinetic energy and internal energy. Then after the blending consumption at hot jet exit, there were still much hot air left to heat the external wall, leading to the high film heating efficiency.

However, when the hot jet mass flow was maintained at 0.0586 kg/s, the heating efficiency curve just went up then went down as the cap opening angle increased, which showed a two-sided effect. The reason lay in the blowing ratio changes. Since the hot jet mass flow was a constant,

the blowing ratio would decrease as the cap opening angle enlarged. When the blowing ratio was too high and the cap opening angle was small, there would be a large vortex near the hot jet exit, which could lift the hot flow away from the external surface to make the heat dissipate quickly. And as the blowing ratio became too small and the opening angle was big, the hot jet would be short of momentum and was easy to blend with the cold mainstream at the exit, which was also bad for the heating efficiency. Therefore, it could be seen from Fig.7 that 30° was the best cap opening angle when the heat flow rate was 0.0586 kg/s.

In order to make it more intuitional, Fig. 8 gave the other version of the film heating efficiency curve, which would draw the same conclusion as above.

3.2 Effect of Blowing Ratio on the Film Heating Efficiency

Another set of numerical simulations were conducted for the aero-engine inlet strut with such 30° film-slot cap to find out the blowing ratio effect. In order to eliminate the interference of the solid heat conduction, uncoupled simulations were carried out only towards the fluid field. Seven different blowing ratios ($M = 0.17, 0.34, 0.5, 0.7, 0.89, 1.06, 1.47$) were selected as typical conditions by changing the hot jet mass flow rate. The results of film heating efficiency curve were showed in Fig. 9.

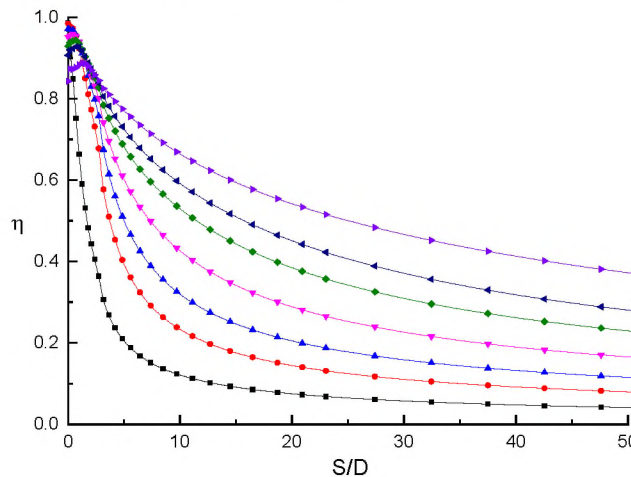


Figure 9: Comparison of Film Heating Efficiency along the External Wall at Different Blowing Ratios.

It could be found that the heating efficiency got higher with the increase of blowing ratio in the posterior region of the external surface. However, near the hot jet exit ($S/D < 1.5$), the law was totally different. Heating efficiency was the highest when blowing ratio reached 0.34, then it reduced as the blowing ratio kept increasing. That was because the vortex near the jet exit got larger as blowing ratio increased, then it lifted the local hot air up to make the wall cooled down. While in the posterior region, the hot air would reattach to the wall. The larger blowing ratio that had higher momentum then would help to make the hot air cover a larger range, which is good for the heating.

Furthermore, the reason why film heating efficiency inside the red circle part in Fig.9 was lower than the surrounding was due to our uncoupled simulation. In that case, the hot jet in the deicing cavity was adiabatic, and the total temperature was a constant. When the hot jet got to the exit, the speed would accelerate quickly since the film-slot cap narrowed the cross-section. Then the static temperature of the flow would decrease to make the film heating efficiency lower.

4 CONCLUSIONS

This paper has presented some numerical simulations on heat transfer problems. A unilateral-opened cap was designed for the aero-engine inlet strut with film-slot of 5° angle. And the best cap opening angle and the effect of blowing ratio on the heating efficiency of the film were studied under the condition of coupled and uncoupled heat transfer. The main conclusions were as followed:

1) The standard $k-\varepsilon$ turbulence model with the enhanced wall treatment could better simulate the details of the flow under the conditions in this paper.

2) The film-slot cap could better improve the film heating efficiency. When the blowing ratio was 0.5, the heating efficiency increased as the cap opening angle increased. However, when the hot jet mass flow was maintained at 0.0586 kg/s, the heating efficiency just went up then went down as the cap opening angle increased, which showed a two-sided effect. And 30° tended to be the best cap opening angle in that case.

3) For the structure with film-slot cap opening angle of 30° , the vortex near the jet exit got larger as blowing ratio increased, which made the heating efficiency lower in the very anterior region and higher in the posterior region of the external surface.

Last but not least, the presented work has been a result of joint cooperation of the two universities as it has been done within graduation study in Nanjing University of Aeronautics and Astronautics and continued within a postgraduate study in Beijing University of Aeronautics and Astronautics. The work accomplished required involvement of books and papers of the two university libraries. Visits to the Air and Space Museums in both universities offered observing anti-icing systems of real aero-engine structures, such as AL-31F engine in particular. The work process has gained much from interaction with teachers and students of the two schools when dealing with difficulties. The current educational model has been regarded quite successful and it can be extended to many schools in order to strengthen cooperation chains not just in practical research activities but also in education of students that will obviously result in more and more students benefiting from it.

REFERENCES

- [1] CCAR 33.68. Induction System Icing. *China Civil Aviation Regulations Part 33 (R2)*.2004.
- [2] Bragg M B, Broeren A P, Blumenthal L A. Iced-airfoil aerodynamics. *Progress in Aerospace Sciences*, 2005, 41(5):323-362.

- [3] FAR33. Aircraft Engines. *Federal Aviation Regulations*. FAA. 2015.
- [4] Guo Tao, Lin Li, Zhu Chengxiang. Simulation calculation of hot air anti-icing system based on internal-external conjugate heat transfer. *Journal of Aerospace Power*, 2016, (11): 2621-2627. (in Chinese)
- [5] Yang Jun, Zhang Jingzhou, Guo Wen, et al. Experiment of anti-icing and icing on inlet strut of aero-engine. *Journal of Aerospace Power*, 2014, 02: 277-283. (in Chinese)
- [6] Chang Shinan, Han Fenghua. Performance Analysis on Hot-Air Anti-Icer of Airplane Engine Inlet. *Journal of Beijing University of Aeronautics and Astronautics*, 1999, 02. (in Chinese)
- [7] Li Yundan, Lu Haiying, Zhu Huiren. Study of Impacting Heat Transfer Characteristic for Aero-engine Heat Anti-icing Structure. *Aeroengine*, 2011, 37(5): 16-20. (in Chinese)
- [8] Ma Hui, Chen Weijian, Meng Fanxin, et al. Improvement of Hot-Air Anti-icing Structure of Engine Inlet Vane. *Journal of Nanjing University of Aeronautics & Astronautics*, 2013, 01: 70-74. (in Chinese)
- [9] Ke Peng, Yang Huiyun, Wang Junkai, et al. Investigation of heating characteristics of aero-engine nose cone with film-heating anti-icing system. *Journal of Aerospace Power*, 2016 (in Chinese)
- [10] Ke Peng, Zhang Yun, Yu Guangfeng, et al. Influence of exterior hot-film on droplet impingement characteristics over aero-engine inlet strut. *Journal of Aerospace Power*, 2017, (03): 621-629. (in Chinese)
- [11] Zhou Leisheng, Zhu Huiren, Xu Duchun, et al. Numerical simulation on internal heat transfer of an contraction channel with jets impingement. *Machinery Design & Manufacture*, 2011 (6): 230-232. (in Chinese)
- [12] Fenot M., Dorignaca E., Vulliermea J. J. An experimental study on hot round jets impinging a concave surface. *International Journal of Heat and Fluid Flow*, 2008, 29(4): 945-956.
- [13] Joshua Gottlieb, Roger L. Davis, John P. Clark. Simula-tion Strategy for Film-Cooled Multistage Turbine Design and Analysis. *Journal of Propulsion and Power*, 2013, Vol.29: 1495-1498, 10.2514/ 1.B34656.
- [14] Dai Ping, Lin Feng. Numerical simulation of film cooling in leading edge of turbine blade. *Journal of Aerospace Power*, 2009(3):519-525. (in Chinese)
- [15] Rozati A., Tafti D. K. Large eddy simulation of leading edge film cooling---Part I: Heat transfer and effect of blowing ratio. *Journal of Turbomachinery*, 2008, 130(4):41015-41017.

- [16] Sanga Lee, Kwanjung Yee, Dong-Ho Rhee. Optimization of the Array of Film-Cooling Holes on a High-Pressure Turbine Nozzle. *Journal of Propulsion and Power*, 2017, Vol.33: 234-247, 10.2514/1.B35968.
- [17] C. El Ayoubi, W. S. Ghaly, I. G. Hassan. Aerothermal Optimization and Experimental Verification for Discrete Turbine Airfoil Film Cooling. *Journal of Propulsion and Power*, 2015, Vol.31: 543-558, 10.2514/1.B35235.
- [18] Zhihong Gao, Diganta Narzary, Shantanu Mhetras, Je-Chin Han. Full-Coverage Film Cooling for a Turbine Blade with Axial-Shaped Holes. *Journal of Thermophysics and Heat Transfer*, 2008, Vol.22: 50-61, 10.2514/1.31206.
- [19] Chen K. S., Hwang J. Y. Experimental study on the mixing of one- and dual-line heated jets with a cold crossflow in a confined channel. *AIAA Journal*, 2012, 29(3).

Reporter



Lu Yi

Co-authors



Oleksiy Chernykh



Ke Peng

TO THE 60TH ANNIVERSARY OF THE LAUNCH OF THE FIRST SATELLITES: HISTORICAL AND TECHNICAL ANALYSIS

ZhiJin Wang, Anatolii Kretov

Nanjing University of Astronautics and Aeronautics, College of Aerospace Engineering,
29 Yudao St., Nanjing 210016, P.R.China

e-mail: zhijin@nuaa.edu.cn; kretov-ac@nuaa.edu.cn

Key words: Satellite,

Abstract. *October 4, 1957 the first satellite was launched from the planet Earth. A month later, a second satellite was launched, a dog was on its board. These launches were preceded by many works and researches and events which had to be accomplished that centuries-old dream of man of flights to space could be become a reality. Let us dwell only on some historical and technical facts that played an important role in the creation of a carrier rocket, which can be considered the most important element in the initial stage of space exploration.*

1. INTRODUCTION

Questions of history are important in the learning process, as they help to better understand the context of any topic, including those related to aircraft design. Designing is not accidentally considered the most difficult discipline, and the inclusion of historical events and facts contributes to the growth of interest in the student audience. They make this course more understandable and memorable.

When we talk about aerospace engineering, we involuntarily recall the great dates associated with this field of human activity. One of these dates falls on 1957.

We would like to start our little review of vast story about first launches satellites with the famous fantastic novel of the great French writer Jules Verne (1828-1905). His "From Earth to the Moon", which he wrote in 1865 was the first vessel project for space missions. We will not dwell on the obvious impossibility of man flying on such a spacecraft on the mistakes of the author, and the lack of attention to the problem of the high heat of his aircraft. However, it is obvious that the aluminum construction of a shell of its inhabited aero-spaceship with thickness of 0.3 meters could not sustain the escape velocity of its motion in the atmosphere and also all living things that are inside this flight vehicle (FV) also could not withstand the enormous overload.

Authoritative experts in the field of rocket technology Obert and Valle involved in future in the creation of the ballistic missile V-2, decided to test the characteristics of the "cannon" Jules Verne (Fig.1) in 1925. In their estimation, the projectile had to be made of high-quality steel, for example tungsten, and be a solid. In this case, the caliber of the projectile was determined at 1200 mm, and its length was 6 calibers. The barrel of the cannon had to have a length up to 900 m and to dig into the mountain not at the 28th parallel, but near the equator. At the same time, the muzzle of the barrel should had been at least at an altitude of 4900 m above sea level not lower than 4900 m. (In the novel, the trunk was cut at an altitude of 600 m above sea level.) In addition, scientists suggested that before the shot the air from the trunk was deflated, and the muzzle hole

covered with a sufficiently strong metal membrane. When a shot is fired, the projectile would squeeze out the remaining air and tear off the membrane when the missile reaches the muzzle.

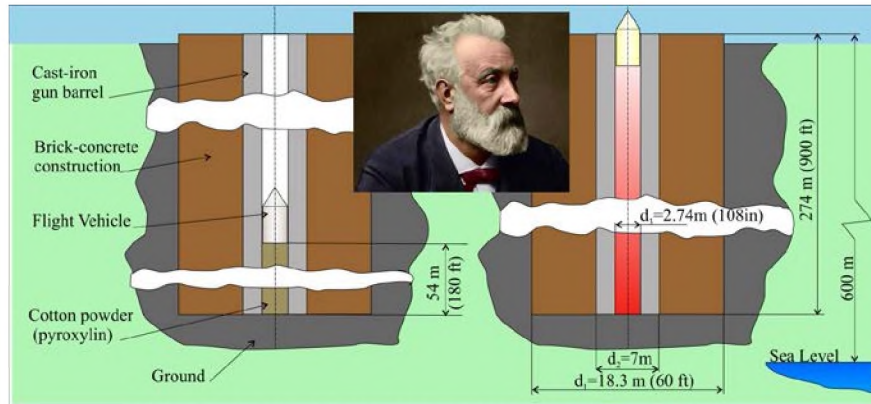


Figure 1: The first project of space FV by J.Vern:
a – the state of Columbiad before launch; b – the launch

Nevertheless, this novel had given a great food for thought and it pushed many creative people to work in this direction including the founder of theoretical astronautics, Konstantin Tsiolkovsky (1857-1935), to the idea of creating space FV based on the principle of jet propulsion. Along with the French Robert Esnault-Pelterie (1881-1957), the German-Romanian Hermann Oberth (1884-1989) and the American Robert H. Goddard (1882-1945) K.Tsiolkovsky is considered as one of the founding fathers of modern rocketry and astronautics.

2. MAIN PART

K.Tsiolkovsky dealt with various issues, including philosophy, aerodynamics, all-metal airships, heat engines, applied mechanics, watering deserts and cooling human dwellings in them, using tidal and wave energy, astronomy, geophysics, biology and other problems. Since 1896, he systematically studied the theory of motion of rocket apparatus (Fig.2). Thoughts on the use of the rocket principle in the cosmos were expressed by him as early as 1883, and the rigorous theory of rocket propulsion was developed in 1896. K.Tsiolkovsky derived the formula, which he called the "formula of aviation" (now it is called Tsiolkovsky's formula) connecting a change in the rocket's speed (δv) without taking into account aerodynamic and gravitational losses with exhaust velocity of the engine (w) and initial (m_0) and final (m_E) mass of the rocket

$$\delta v = w \times \ln(m_0/m_E) \quad (1)$$

His most important and famous work was published in 1903. Tsiolkovsky calculated that the horizontal speed required for a minimal orbit around the Earth 8.000 m/s could be achieved by means of a multistage rocket fueled by liquid oxygen and liquid hydrogen. The formula for finished ideal speed $v_{E.Id}$ of a multistage rocket with n stages follows from Eq.1 (ideal speed means without taking into account aerodynamic and gravitational losses)

$$v_{E.Id} = \sum_{s=1}^n (w_s \ln(m_{0s}/m_{E.s})) \quad (2)$$

where s is the stage number.

For the first time from Eq.2 was proved that a rocket could perform space flight. In the article [1] and its subsequent K.Tsiolkovsky developed some ideas of missiles and considered the use of liquid rocket engines.

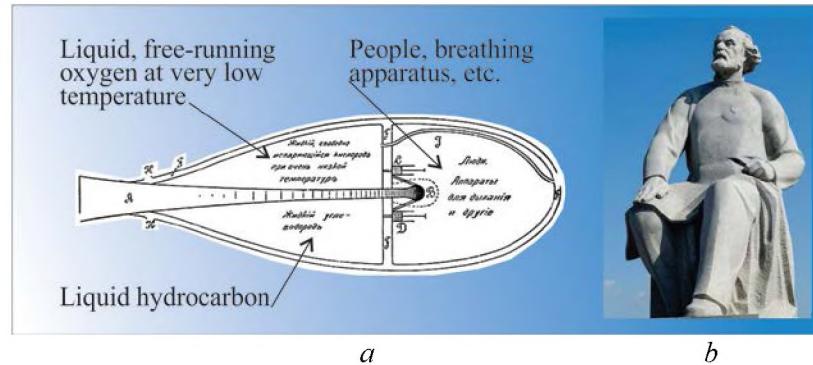


Figure 2: Konstantin Tsiolkosky: *a* – scheme of interplanetary rocket;
b – the monument to great scientist in Moscow

The use of the reactive principle of motion was hampered by the complexity of its practical implementation. An American engineer, professor, physicist, and inventor Robert Goddard (Fig.3) was the first man who could build and launch the world's first liquid-fueled rocket (March 16, 1926). Between 1926 and 1941 he and his team launched 34 rockets. If his first rocket rose 12.3 m (41 feet) in 2.5 seconds and his record rockets achieved altitudes as high as 2.6 km.

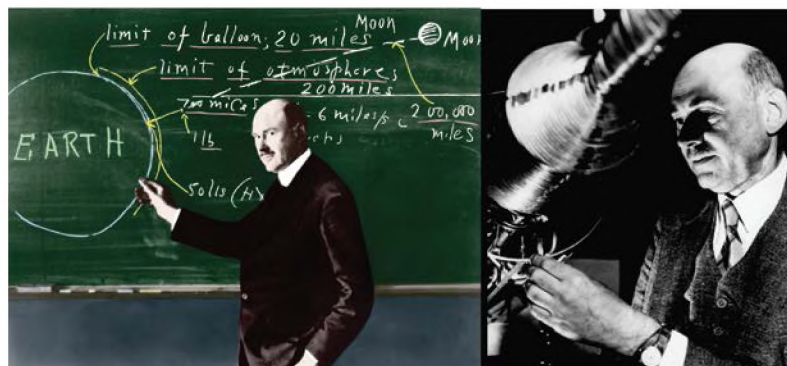


Figure 3: Professor and inventor Robert Goddard

In 1931 in the USSR in Moscow and Leningrad were organized groups for the study of the jet movement (GIRD), uniting on a voluntary basis rocket enthusiasts.

In 1934 propagandistic and educational functions were assigned to the newly organized Reactive Group of the Central Council of Osoaviakhim (GIRD – Fig.4), which successfully continued to work until the end of the 1930s and created a number of original small experimental rockets.

The successes of the GIRD contributed to a more serious attitude towards them by the leadership of the country and the army. This led to the creation in 1933 of the Reactive Scientific Research Institute.

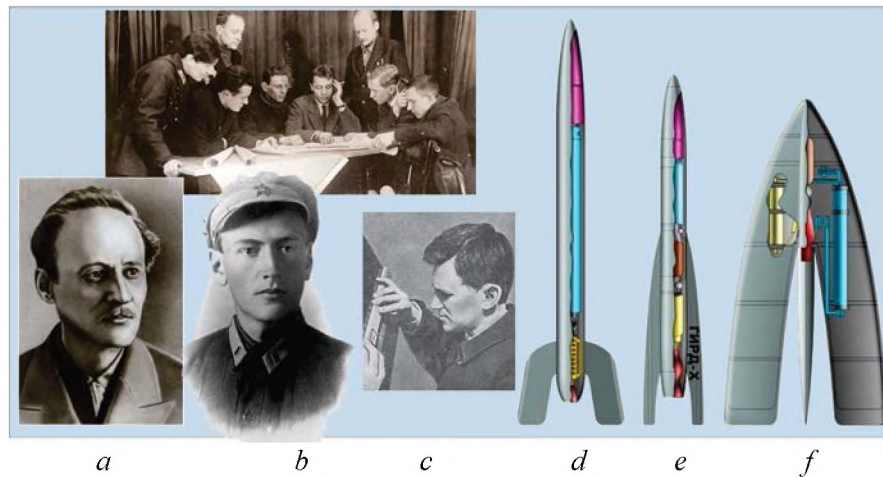


Figure 4: GIRD: *a* – Fridrich Zander; *b* – Mikhail Tikhonravov; *c* – Sergey Korolev; *d-f* – rockets of GIRD; *d* – the rocket GIRD-09 of the M. Tikhonravov's design; *e* – rocket GIRD-X by the F. Zander's

In World War I, the Germans had developed long-range artillery and bombarded Paris from the German lines; because of this, the Treaty of Versailles forbade future German development of heavy artillery. The treaty, however, said nothing about rockets. During World War II, German rocketeers developed "V" weapons. The "V" was short for "Vergeltungswaffen", roughly translated "vengeance weapons".

In 1931, the German military established a rocket research facility at Kummersdorf Weapons Range, near Berlin. The first civilian employee at this facility was Young designer Wernher von Braun (1912-1977). In 1937 the German rocket facility was moved to Peenemunde on the Baltic Coast. Starting with about 80 researchers in 1936, the facility comprised nearly 5000 personnel by late 1942.

Created rockets A1-A3 showed the problems, of which the mains were:

- ensuring stability and controllability of the missile
- creation of high thrust engine
- fuel supply and engine control.

The Peenemünde was the Army Research Center founded in 1937 as military proving ground under the German Army Weapons Office (the Baltic island of Usedom.) At the center, missiles were designed, production halls and test benches were available, an installation for launching ballistic missiles and a catapult for launching V-1 aircraft. In Peenemünde worked about 15 thousand people. V-1, A-4 (V-2), A-3, A-5 rockets were tested here, development of two-stage A-6 A-10 rockets was launched, and Vasserfal anti-aircraft missiles were tested and "Typhoon".

By the end of the war, Germany managed to create fundamentally new type of weapon – ballistic missile A-4 (V-2) with a range up to 300 km (Fig.5). This rocket with a starting mass of about 13 tons was able to transfer about 1 ton of explosives at a distance of 270 km in 5 minutes. The engine of V-2 worked on liquid oxygen and 75-percent ethyl alcohol and it developed the thrust of 250 kN (25 tons). The maximum rocket velocity was: at the time of engine shutdown 1500 m/s, and at the time of contact with the ground – about 800 m/s.

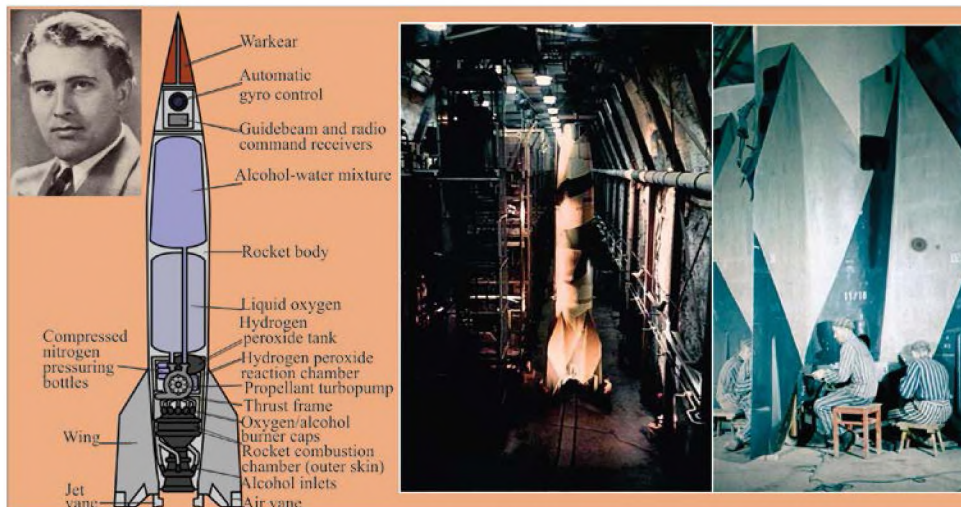


Figure 5: Wernher von Braun and scheme of the first ballistic missile A-4 (V-2) and assembly of missiles at the underground military factory of the concentration camp Dora

And although the rocket had an imperfect design and low accuracy of flight, it was obvious that it could become the basis for creating a terrible weapon in the case of developing a nuclear charge.

In the first half of 1944 there were series of vertical launches with increased up to 67 seconds time of engine work with the purpose of debugging. Lifting height had been 188 km. So this FV became the first artificial object which reached the outer space of Earth.

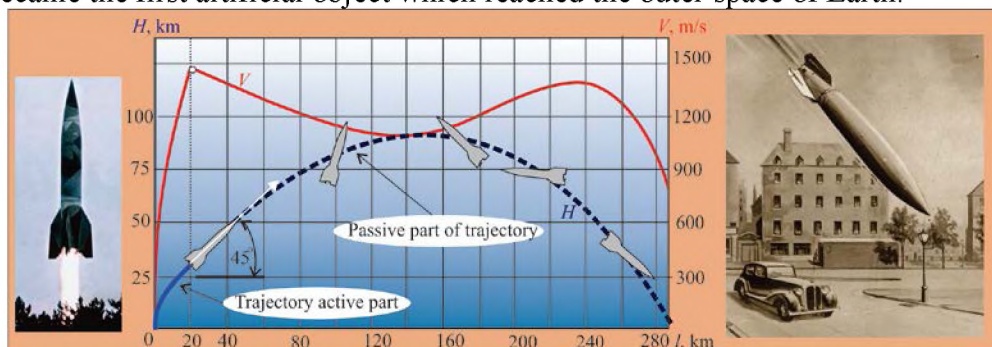


Figure 6: The vertical launch of ballistic missile A-4 (V-2) and its flight trajectory and fragment of picture of Roland Davies "V-2 landing in a London street"

Without a doubt, the main ideas used in the A-4 (V-2) rocket became the basis for the creation of future missiles intended for space flight. But we must not forget about how many victims this missile was cost:

- about 2,700 people were killed in the combat use of V-2;
- about 20,000 people died of hunger and overwork in a concentration camp, which was built especially for an underground plant;
- some thousands of people were shot at the factory before the arrival of US troops.

On May 3, 1945, Wernher von Braun surrendered to the advancing American army, along with documentation and about 120 main specialists of his scientists signed contracts to work with the US Army. About 100 rockets were departure to USA. Following the war, von Braun worked for the United States Army on an intermediate-range ballistic missile program before his group

was assimilated into NASA. At the first time he and his team used captured V-2s to teach American scientists and engineers about rocketry.

In Western countries and mainly in the United States, a broad program of research in the field of rocket science was launched. Abroad, they were absolutely sure that the Soviet people, bleeding from the war, would not be able to solve the problem of creating powerful guided missiles for a long time.

The fate of the first Soviet missile creators was difficult, in particular, in 1938, Valentin Glushko (1908-1989), Sergei Korolev (1906-1966), were arrested. In 1940, V. Glushko was transferred to the Kazan Aviation Engine Plant No. 16, where was organized a special design bureau, consisting of prisoners (OKB-16). V. Glushko continued to develop auxiliary airplane liquid rocket engines with pumping fuel. In 1942 Sergei Korolyov got into this bureau.

In 1944, they were released, and in 1945, on their initiative, the first in the world department of rocket engines was created at the Kazan Aviation Institute.

Under NASA, Wernher von Braun served as director of the newly formed Marshall Space Flight Center and as the chief architect of the Saturn V launch vehicle, the superbooster that propelled the Apollo spacecraft to the Moon. But he was not destined to become the protagonist in launching the first satellite. The Soviet Union made a powerful breakthrough in this most important historical event, under the leadership of Chief Designer Sergei Korolev, the world's first carrier rocket was built, capable of reaching the first space speed.

In the beginning of 1945 information in the USSR about the ballistic missile V-2 was very minor: A study of the materials found at the missile test site in Poland in the Debica district, intelligence data, the meager reports of the Allies-the English, the testimony and the stories of a few information-capturing outline in general terms for the scope of the work in Germany for a new type of weaponry guided long-range missiles.

Very important information was received on February 8, 1945 when, from the airfield of the secret base Peenemünde, the prisoner-of-war, fighter pilot Mikhail Devyataev (1917-2002) and his nine associates managed to hijack a German Heinkel-111 aircraft. The aircraft was equipped with the latest V-1 missile control system. For a long time the details of this escape remained unknown. Before his death, Mikhail Devyataev in one of the interviews said that his introduction to one of the most secret bases of the Wehrmacht was carried out not without the aid of military intelligence. In 1957, he was awarded the highest award - the golden star of the Hero of the Soviet Union.

At the end of the Second World War a group of Soviet specialists in the field of rocketry was urgently sent to the Peenemünde base to study the documentation, the rocket itself and the technology of its manufacture. The result of this work was the upgraded copy of the R-1 created under the leadership of SP Korolev on the basis of the A-4 (V-2) rocket, which successfully launched in 1948 and flew about 300 km. And soon a version of the R-1 missile designed specifically for launching along a vertical trajectory and having received the designation B-1A was developed at the OKB Korolyov. The launch mass of the rocket is about 14 tons. The lift height is up to 100 km. The RD-100 LPRE was installed on the rocket, which was developed by Valentin Glushko. The high-altitude rocket V-1B was distinguished by the detachable head part. They contained containers with geophysical institute equipment for sampling air at high altitude.



Figure 7: Map of the secret base of Peenemünde, the starting position of the missiles, the Heinkel-111 aircraft, Mikhail Devyataev and the monument dedicated to ten prisoners who escaped from hell

S.Korolev was confident that, based on materials exported from Germany, he could create his own, "improved" model of the German V-2 rocket. But Stalin forbade any changes or improvements: "First you will reproduce the rocket, and then you will do yours." Only at the beginning of 1949 Korolev will receive directly from the lips of Stalin the permission to "do his own".

The arms race that broke out during the Cold War between the United States and the Soviet Union facilitated the development of a carrier rocket capable of achieving the first space velocity.

In 1950, a special KB-1 under the direction of S.Korolev was organized as part of the NII-88. In the same year, a ballistic single-stage R-2 missile with an aiming range of 600 km was created. In 1951, it was adopted.

In 1953 the first launches of the R-5 missile with a flight range of 1200 km were made, and its modification was considered as the carrier of the atomic charge. The idea of an unmanned satellite began to acquire real outlines, when the range of combat rockets began to sharply increase.

At the second International Congress on Astronautics, hold in London in September 1951, most reports were devoted to manned space stations. An exception was the report of members of the British Interplanetary Society headed by K. Getland was entitled "Minimum dimensions of rockets for artificial satellites."

The report analyzed three three-stage missiles conventionally called "Scheme A", "Scheme B" and "Scheme C". In the last two "Schemes" the third stage was supposed to carry a useful load of 100 kg, in "Scheme A" no payload was provided. The launching weight of the missiles was as follows: in Scheme A - 16 800 kg, in Scheme B - 62400 kg and in Scheme C - 90900 kg. In the fourth system ("Diagram D"), which was presented as "very far from practical implementation", the starting weight was the same as that of the rocket in "Scheme C", but the payload of the last stage had a weight of 220 kg. In 1952 - 1953, the number of published articles on unmanned satellites continuously increased.

Authors of the published publications have suggested that in two or three years the first satellite can be launched. Von Braun said that this could be done in a shorter time if using the

Redstone rocket as the first stage and several bundles of Loki rockets as the next steps. The main advantage of this proposal was that it could use existing missiles.

Redstone was the first large American ballistic missile which was a direct descendant of the German A-4 (V-2) rocket. The design used an upgraded engine from Rocketdyne that allowed the missile to carry the warhead which weighed 3,100 kg with its reentry vehicle to a range of about 282 km. It was created under the leadership of Wernher von Braun. The first Redstone lifted off at Cape Canaveral on August 1953. Loki, officially designated 76mm HEAA Rocket T220, was an American unguided anti-aircraft rocket based on the German Taifun. During the preliminary consideration of the project implementation options, it was decided to bring the Orbiter satellite into orbit around the Earth, starting from the point on the equator so that the plane of the orbit coincided with the plane of the Earth's equator. The launch was tentatively scheduled for the summer of 1957.

On July 28, 1955, the White House made an official announcement that the US was going to launch an artificial Earth satellite.

His message is that the "package" from developed missiles R-3 with a range on thousands kilometers is able to reach any range of flight, and even to put into orbit artificial satellites of the Earth, caused a storm of negative and even stinging responses and speeches. But loaded with the creation of long-range missiles, the chief designer S. Korolev seriously "fell ill" of this idea, eventually infecting its entire design bureau.

In May 1954, the USSR Government decreed the development of a two-stage ballistic missile R-7 (8K71). In July 1954, a preliminary design for the R-7 missile system was ready. The first flight sample of the R-7 missile was sent to the test site in late 1956.

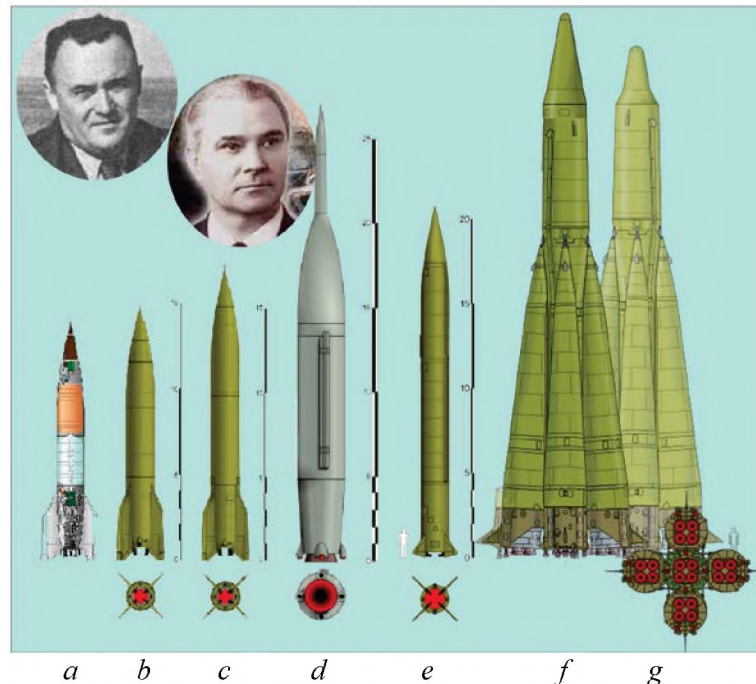


Figure 8: Sergey Korolev, Valentin Glushko and the origin of the rocket for the first satellite. Rockets:
a – A-4 (V-2) (1942); *b* – R-1 – (8A-11, 1948); *c* – R-2 (8Zh-38, 1948); *d* – R-3 (8A-67, 1949);
e – R-5M (8K-51, 1956); *f* – R-7 (8K-71, 1957); *g* – R-7A (Sputnik, 1957);

At the same time in Kazakhstan construction of the future Baikonur cosmodrome begins in the area of the station Tyura-Tam. In early 1957, the R-7 missile was ready for testing. In April 1957, the launch complex was also prepared. The first three launches showed the presence

of serious shortcomings in the design of the R-7. When analyzing telemetry data, it was found that at some point during the emptying of fuel tanks, pressure fluctuations occurred in the flowlines, which led to increased dynamic loads and, ultimately, to structural failure (American designers also encountered this problem).

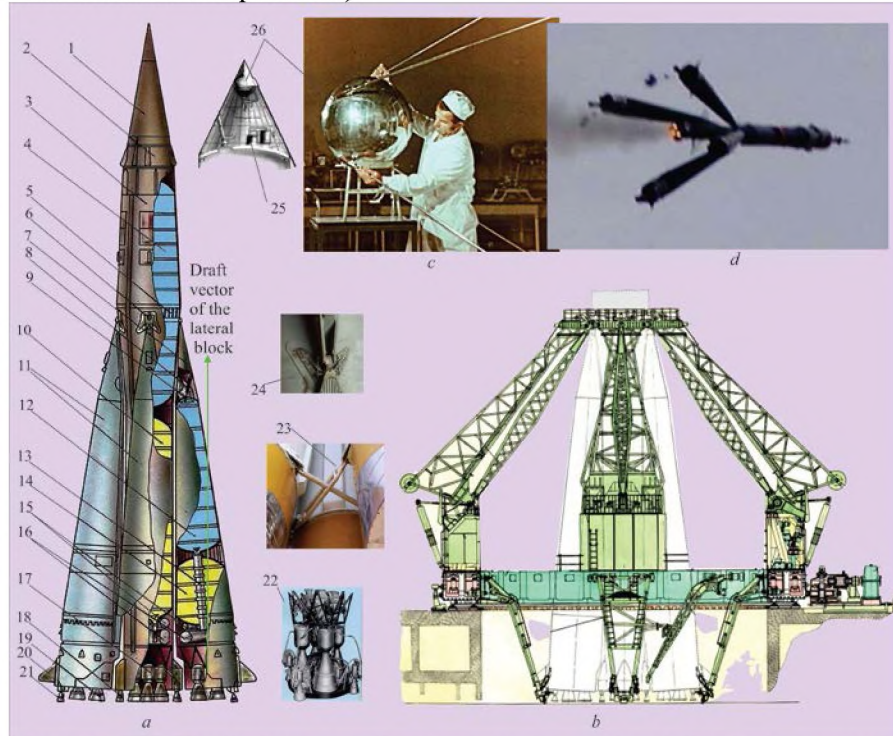


Figure 9: Rocket R-7: a – missile layout and main parts: 1 – warhead; 2 – instrumentation section; 3 – core stage (central block); 4 – core stage oxidizer tank; 5 – reinforcement band; 6 – core stage ball pivot; 7 – strapon heating cone; 8 – stage separation nozzle; 9 – cover; 10 – core stage fuel tank; 11 – strapon; 12 – strapon oxidizer tank; 13 – oxidizer feed pipeline duct; 14 – strapon fuel tank; 15 – toroidal liquid nitrogen tanks of core stage and strapon; 16 – toroidal hydrogen peroxide tanks of core stage and strapon; 17 – core stage sustainer; 18 – core stage control motor; 19 – strapon sustainer; 20 – aerodynamic vane; 21 – strapon control motor; 22 – engine of core stage; 23 – lower load-carrying connections of the side blocks; 24 – fixing unit for the side block with a pocket under the bracket of the starting structure; 25 – head compartment; 26 – the first satellite; b – launch facility; c – the first satellite assembly; d – turn of side blocks after breaking of load-carrying connections

But, the fourth launch, which took place on August 21, 1957 as a whole was partially successful - the missile reached the target area, although for 15-20 seconds before the fall the headpiece was destroyed. In the Fifth launch on September 7, 1957, the test of the R-7 military missile was completely successful.

Launch vehicle "Sputnik" was an R-7 with which the head part was removed, all the flight control system equipment together with the compartment in which it was located. The compartment was replaced by a light conical transition compartment, which housed the minimum necessary for flight support control system equipment.

The historical event - the opening of the space age was held on October 4, 1957. Three hundred years after Newton estimated the magnitude of the first cosmic speed, a 267-tonne R-7A rocket was able to reach this speed and put into orbit a satellite with a mass of 83.6 kg, which was only 0.03% of the launch mass of the rocket. The satellite was a sphere with a diameter of

0.58 m. The perigee of its orbit was 228 km, the apogee - 947 km. The first satellite lasted exactly three months and made 1.440 orbits around the Earth during this time.

3. CONCLUSIONS

Often we have the question – how, just 12 years after the most terrible war, which claimed tens of millions lives, the Soviet Union was able to launch an artificial satellite first? We think the answer lies in fulfilling ten conditions.

1. State will, which provided priority to the space program and the concentration of all necessary resources.
2. Presence of the authoritative and strong-willed leader of the space program.
3. Competition of social systems.
4. Patriotic spirit of society.
5. Fundamental education.
6. Effective science.
7. High-tech production
8. Balanced interaction of education, science and production.
9. High discipline and responsibility of performers.
10. High personal qualities of all participants.

The reasons given for the success of launching the first satellites and the subsequent great results in World astronautics (launch of the Man on April 12, 1961, the lunar program “Apollo” on 1969, work on the reusable missile systems) conform to made conclusions about the importance of the conditions considered.

But this may raise the question of the International Space Station. As in this case paragraph 3 “Competition of social systems” works. Fortunately, this paragraph has been successfully replaced by a more peaceful option the international collaboration.

REFERENCES

- [1] K.Tsiolkovsky. Exploration of Outer Space by Means of Rocket Devices 1903 (Циолковский К.Э. Исследование мировых пространств реактивными приборами.1903. In Russian).

Authors



ZhiJin Wang



Anatolii Kretov

Generation of the Drag Map and Derivative Plots for Commercial Aircraft

Anthony P. Hays

Aircraft Design and Consulting

San Clemente, California

Email: ahays@alum.mit.edu Web: www.adac.aero

Key words

Aircraft design, transonic aerodynamics, transonic drag rise, drag map

Abstract:

The drag map provides important information about the transonic aerodynamic characteristics of an aircraft design. In an aircraft design course, students should be aware of the significance of the drag map and its derivative plots. This paper describes how a drag map and its derivatives can be constructed that are representative of a given configuration.

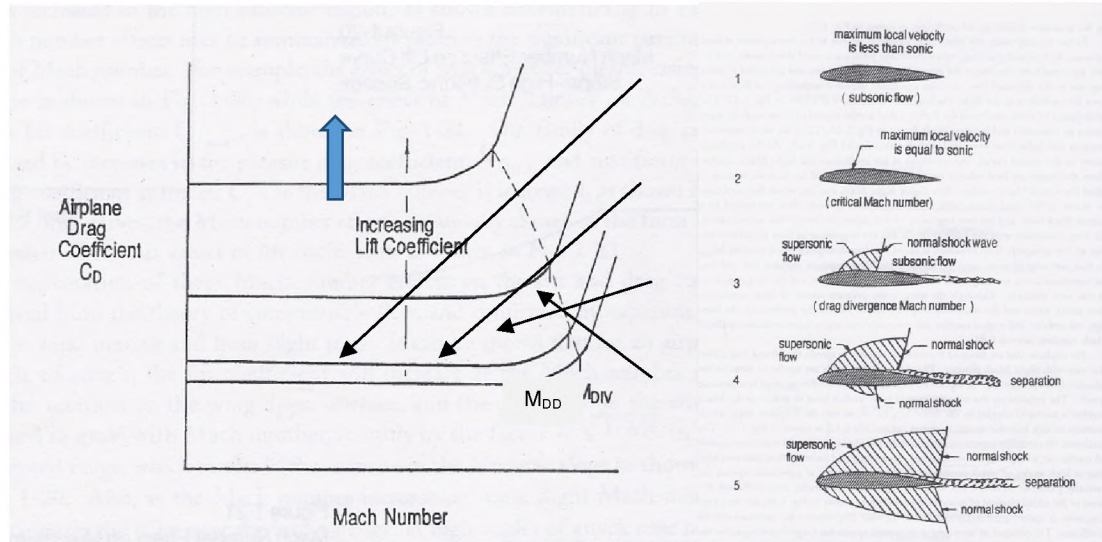
1. INTRODUCTION

The drag map (plot of airplane drag coefficient (C_D) as a function of Mach number for different values of lift coefficient (C_L)) is the most useful way of comparing the relative aerodynamic efficiencies of different configurations in the high-subsonic flight regime. Important plots are derived from the drag map, such as lift/drag ratio (L/D) and ML/D as a function of lift coefficient for different Mach numbers. Drag maps are shown extensively in publications describing the aerodynamics of subsonic transport aircraft, but are omitted from the leading textbooks on aircraft design. Students should be aware of the importance of the drag map and its derivative plots. At the conceptual design level, the exact shapes of the drag map curves cannot be determined without detailed definition of the complete airplane configuration and especially the wing sections. A drag map for detailed aircraft performance would require data from wind tunnel analysis and/or CFD. This paper therefore describes a procedure for generating a representative drag map and its derivatives. This procedure uses Excel, but other software (such as MATLAB) may be equally (or maybe more) appropriate.

2. BACKGROUND

Two of the most popular textbooks related to aircraft conceptual design are those authored by Raymer (Ref. 1) and Nicolai and Carichner (Ref. 2). Examples of drag maps do not occur in either of these books, nor in almost all other textbooks on aircraft design, except for Schaufele (Ref. 3), from which much of the methodology in this paper is taken. In encompassing the conceptual design of a wide variety of aircraft, the Raymer and Nicolai/Carichner books have not examined the aerodynamics of commercial jet aircraft operating in the high-subsonic Mach regime to any significant level of detail. This is in part because both of these books cover the design of both commercial and military aircraft. Except for airlifters (and to a lesser extent maritime patrol

aircraft), military aircraft do not spend much of the mission in the high-subsonic Mach regime. The measure of aerodynamic efficiency of an aircraft may be defined in the Breguet range equation as ML/D . To maximize range for a given structural weight fraction, the effect of speed on engine specific fuel consumption must also be included. An enormous amount of time and effort is expended in increasing ML/D by an amount as small as 0.01. Billions of dollars in aircraft sales (as exemplified by the ongoing battle between the Boeing 737 and A320) can depend on which airplane has the higher value.



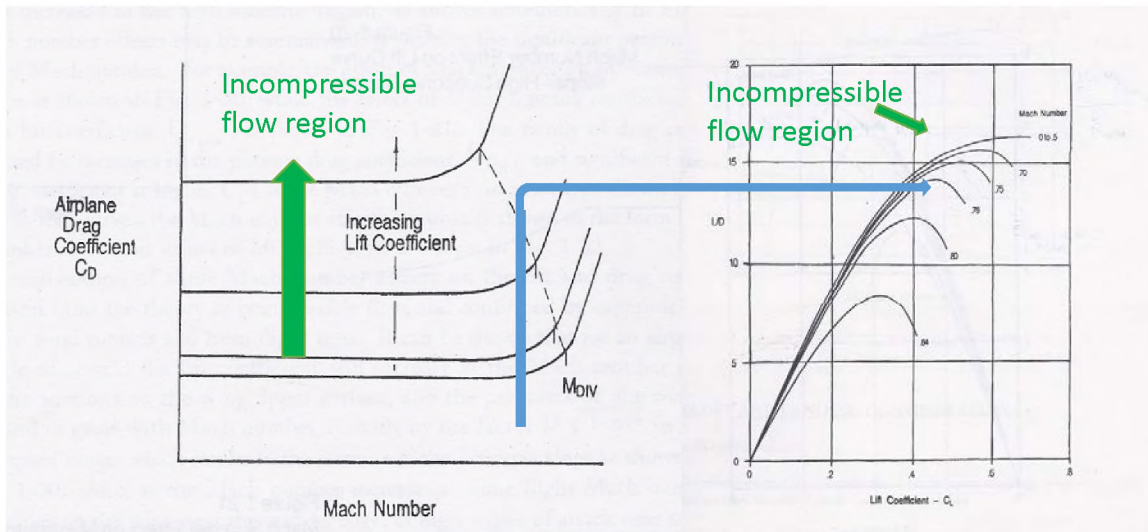
Source: Schaufele

Figure 1: Typical Drag Map

A useful way to define the transonic characteristics of an aircraft is by means of the drag map (Fig. 1), which shows the airfoil or airplane drag coefficient and in particular the drag rise (increase in compressibility drag, C_{DC}) with increasing Mach number for different lift coefficients, in the region of the drag divergence Mach number, M_{DD} (or M_{DIV} in Schaufele terminology). For a given wing thickness/chord ratio (t/c) and sweep (Λ) the aerodynamicists in the design team try to increase the Mach number at which drag rise occurs. From a knowledge of the drag map, three derivative plots can be generated: the drag polars as a function of Mach number, a plot of L/D as a function of C_L for different values of Mach number (a simple cross-plot of drag map data, as illustrated in Fig. 2), and a similar plot of ML/D as a function of C_L , so that the maximum value of ML/D can be determined. In addition, the sensitivity of the design parameters to these plots can be investigated.

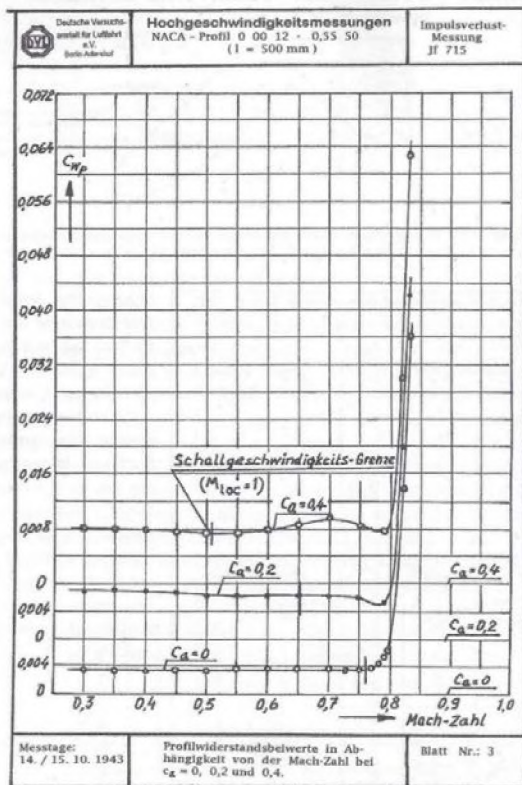
Presentation of data in this format appeared early in the investigation of airfoils in compressible flow, as illustrated in Fig. 3, dated 15 October 1943. This, and other drag maps (Fig. 4) appear in Obert (Ref. 4) in at least thirty instances, indicating the importance of this data format. This figure also illustrates that the shape of the drag rise curve can take many forms.

The drag map can be particularly useful in comparing the high-speed aerodynamic efficiency of similar aircraft, as illustrated in Fig. 4. Unfortunately, the lack of industry consensus on definitions adds to the difficulty of comparing values.



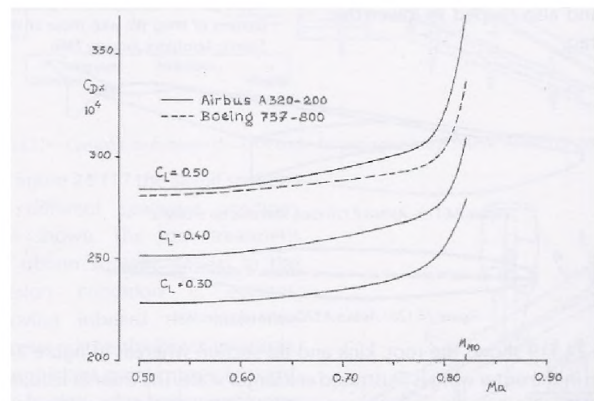
Source: Schaufele

Figure 2: Derivative Plot of L/D vs. C_L for Different Mach Values



Source: Obert

Figure 3: Drag Map for NACA 0012 Airfoil



Source: Obert

Figure 4: Drag Rise Comparison Between B.737 and A320

In this paper, the notation of Raymer (Ref. 1) is used. M_{crit} is the Mach number at which compressibility drag first appears (Fig. 1). $M_{DDBoeing}$ is the Mach number at which compressibility drag reaches 20 counts ($\Delta C_{DC} = 0.0020$). $M_{DDDouglas}$ is the Mach number where the gradient of the C_{DC} vs. Mach curve has a gradient of 0.10. The shape of the A320 drag rise is fairly typical for commercial transports with supercritical wing sections, although there are differences between aircraft types. Examples of differences between these values are shown in Table 1, taken from Fig. 4 at $C_L = 0.5$. The values in the last two columns are somewhat different from those in Raymer Section 12.5.10, suggestive of the variation of these values. The reality is that the differences in values can vary widely, depending on the configuration design. The Douglas definition has gained greater acceptance, and if a value is stated without its definition, it can generally be assumed to be based on the Douglas definition (i.e. M_{DD} occurs at $dC_{DC}/dM = 0.10$), and for the rest of this paper, that will be the case.

Table 1: Examples of Differences in Drag Divergence Mach Number values

Aircraft	$M_{DDDouglas}$	$M_{DDBoeing}$	M_{crit}	$M_{DDDouglas} - M_{DDBoeing}$	$M_{DDBoeing} - M_{crit}$
A320-200	0.80	0.78	0.575	0.020	0.205
B.737-800	0.805	0.80	0.50	0.005	0.30

3. DRAG MAP GENERATION

To generate a drag map using a spreadsheet, the relationship between C_{Dc} and $(M - M_{DD})$ must be expressed algebraically. Figures 3 and 4, and Ref. 6, Fig. 12.14, show that this relationship is a weak function of C_L and wing design. In particular, it is a function of wing sweep, with a slightly larger knee radius for higher wing sweep. The simplifying assumption must be made that it is independent of C_L and wing design. An empirical equation which was derived by adjustment of the constants in the equation, and which may be used to plot a drag map is given by Eq. 1. This is broadly similar to the shape suggested by Schaufele, but adjusted to meet the Douglas definition of M_{DD} , ($dC_{DC}/dM = 0.10$) which the Schaufele curve does not, and with a knee radius more appropriate for modern airfoil sections.

$$C_{Dc} = 0.04 \left(\frac{(M - M_{DD}) + 0.308}{0.36} \right)^{2.2} + 0.017((M - M_{DD}) + 0.308)^{2.5} \quad (1)$$

Small changes in the shape of the drag rise can have a significant effect on the Mach number for maximum ML/D on a plot of ML/D as a function of C_L and M . This function is not valid when $(M - M_{DD}) < -0.3$, so the value of C_{Dc} must be set to zero for that condition in a spreadsheet using an Excel conditional function:

IF (condition, value_if_true, value_if_false)

It will also only be valid for Mach numbers up to about $M_{DD} + 0.04$.

Equation (1) is plotted in Fig. 5 and compared with the drag rise curve due to Schaufele (Ref. 3) and Lock (Ref. 5). The Power function and Schaufele curves are reasonable fits to the drag rise of commercial aircraft. Note that the value of M_{DD} on Schaufele's curve does not quite meet either the Boeing or Douglas definitions of M_{DD} . Schaufele's curve only exists in a tabular format, so the

equation above is preferred for generating a drag map. Equation 1 is a better fit to drag rise curves for a configuration with a supercritical wing than Lock's 4th Power function, used in Ref. 5 to generate a drag map. Lock's function matches the drag rise for a wing with a NACA 0012 airfoil and 35° sweep at low values of C_L (0 to 0.2), but is not a good match at higher lift coefficients. In addition, it does not exhibit drag creep (Fig.4) which is evident for many configurations, and underestimated by Schaufele. Both the Power Function and Lock's 4th Power meet the Douglas definition of M_{DD} . A discussion of different procedures for determining C_{DC} as a function of $(M-M_{DD})$ may be found in Sforza (Ref. 7), but none of these procedures generate curves that are representative of supercritical wing configurations.

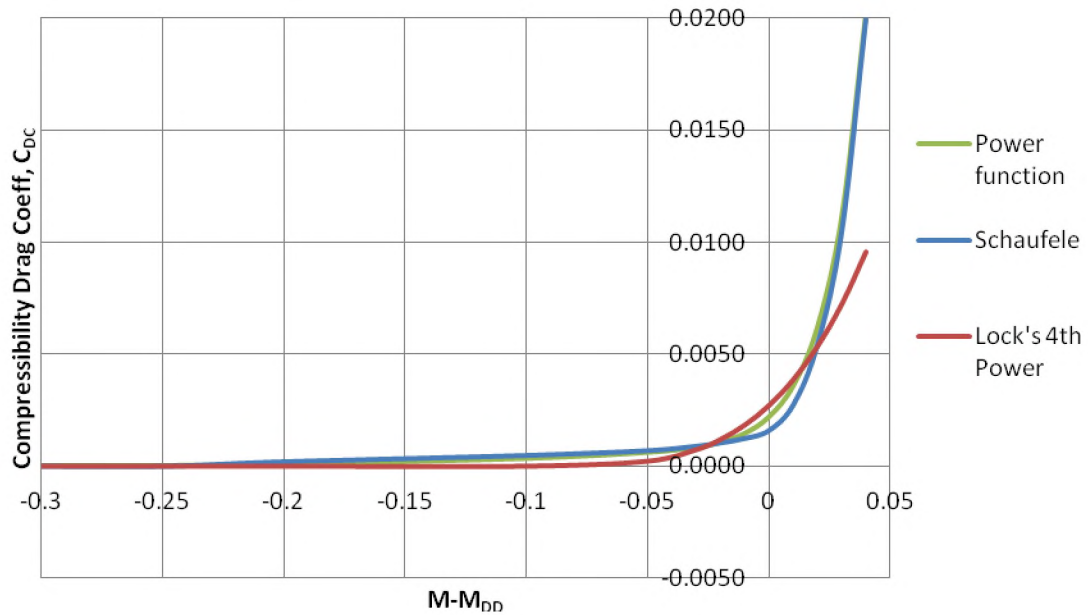


Figure 5: Drag rise comparison, C_{DC} vs. $(M-M_{DD})$

In Ref. 1, Section 12.5.10, Raymer describes a method for determining the value of M_{DD} (Boeing definition) for a given wing design. This includes adjustments to M_{DD} for different values of C_L and t/c (Raymer Fig. 12.30). Provided that the shape of the drag rise is known (or assumed), it is therefore possible to generate a drag map based on the methods in this section. However, Raymer's method is not readily amenable to the use of MATLAB or a spreadsheet, so its use is not recommended.

An alternative is to use Schaufele Fig. 4-8, which shows M_{DD} (or M_{DIV} in Schaufele) as function of C_L , A , and $(t/c)_{av}$. In these charts M_{DD} is a linear function of C_L , so it is relatively easy to establish the relationship. The definition of M_{DIV} is unstated for these charts, but Schaufele Fig. 12-10 shows a value of M_{DIV} for which the drag rise is 16 counts. From this figure, $M_{DD_{Douglas}} - M_{DIV} = 0.015$, so when using this method, this value should be added to the values in Schaufele Fig. 4-8 to obtain Douglas values.

Another alternative (and preferred) approach is to use the Korn equation (Ref. 5) to determine M_{DD} . This approach will therefore be used in this paper.

$$M_{DD} = \frac{\kappa_a}{\cos \Lambda_{c/2}} - \frac{\frac{t}{c}}{\cos^2 \Lambda_{c/2}} - \quad (2)$$

where

M_{DD} = wing drag divergence Mach number (Douglas definition)

κ_A = airfoil technology factor

C_L = wing section lift coefficient

$\Lambda_{c/2}$ = wing sweep at mid-chord

For a wing with different airfoil sections at different spanwise locations, Ref. 5 suggests that this equation should be applied to each wing spanwise section with the same airfoil section, and values of M_{DD} for all spanwise sections should be averaged. During conceptual design, this level of detail may well not be known, so taking the average values of t/c and $\Lambda_{c/2}$ for the whole wing is an approximation to the more exact method, and can be used for this analysis. The mid-chord is selected for defining wing sweep because the upper surface shock is approximately at that location. This method is preferred because it contains a technology factor (κ_A) so that the equation can be applied to non-supercritical and supercritical wing sections. The effect of increasing κ_A can also be evaluated. Reference 5 suggests a value of $\kappa_A = 0.87$ for a NASA 6-series section, and 0.95 for a supercritical wing. This value will increase as supercritical wing sections are further developed. This equation correlates reasonably well in the operational area of interest ($C_L = 0.5$ to 0.6 and $\Lambda_{c/2} = 25^\circ$ to 35°) with Schaufele, Fig.4-8.

Sweep at any fraction of the chord may be calculated using the equation

$$\tan \Lambda_x = \tan \Lambda_{LE} - \frac{4x(1 - \lambda)}{A(1 + \lambda)} \quad (3)$$

where

Λ_x = wing sweep at fraction x of chord

Λ_{LE} = wing sweep at leading edge

x = fraction of wing chord

A = wing aspect ratio

λ = wing taper ratio

The incompressible drag polar is calculated conventionally using the equation

$$C_{D_{incomp}} = C_{D_0} + \frac{(C_L)^2}{\pi AR e} \quad (4)$$

where

$C_{D_{incomp}}$ = incompressible drag coefficient

C_{D_0} = incompressible zero lift drag coefficient

AR = aspect ratio

e = Oswald efficiency factor based on symmetric polar

Values of C_{D_0} and e can be calculated using standard textbook methods. The total drag coefficient is therefore the sum of $C_{D_{incomp}}$ and C_{D_C} . From a knowledge of the aircraft incompressible drag polar, plus the drag rise assumptions described above, it is possible to generate a drag map.

4. GENERATION OF DERIVATIVE PLOTS

This plot enables other plots to be generated; in particular:

- the compressible flow drag polar (Fig. 7)
- a plot of L/D as a function of C_L and Mach number (Fig. 8)
- a plot of ML/D as a function of C_L and Mach number (Fig. 9).

This last set is critically important in telling the designer the maximum value of ML/D that can be obtained, and the associated Mach number. Each of these plots was generated using Excel, but other software, such as MATLAB, could equally well have been used.

For these plots a value of $\kappa_A = 0.925$ was used. Selecting an appropriate value for κ_A is difficult for supercritical wings, because airfoil technology is constantly improving. Reference 3 (published in 2010) suggests a value of 0.95 for supercritical wings. A rough rule of thumb is to assume that the value of κ_A increases by 0.005 every decade.

This procedure does not include compressibility effects on fuselage and empennage drag. Raymer (Ref.1, Fig. 12.31) shows fuselage M_{DD} in terms of the fuselage length and diameter, and for a typical wide-body airliner, the fuselage M_{DD} is above that of the wing, even at low C_L . However, comparison with aircraft drag polar shows an underestimation of drag creep prior to divergence, a feature of many modern wing designs. Drag creep may also be due to the need to modify wing root sections to minimize wing/fuselage interference effects. Obert (Ref. 4) has extensive examples and discussion on this subject.

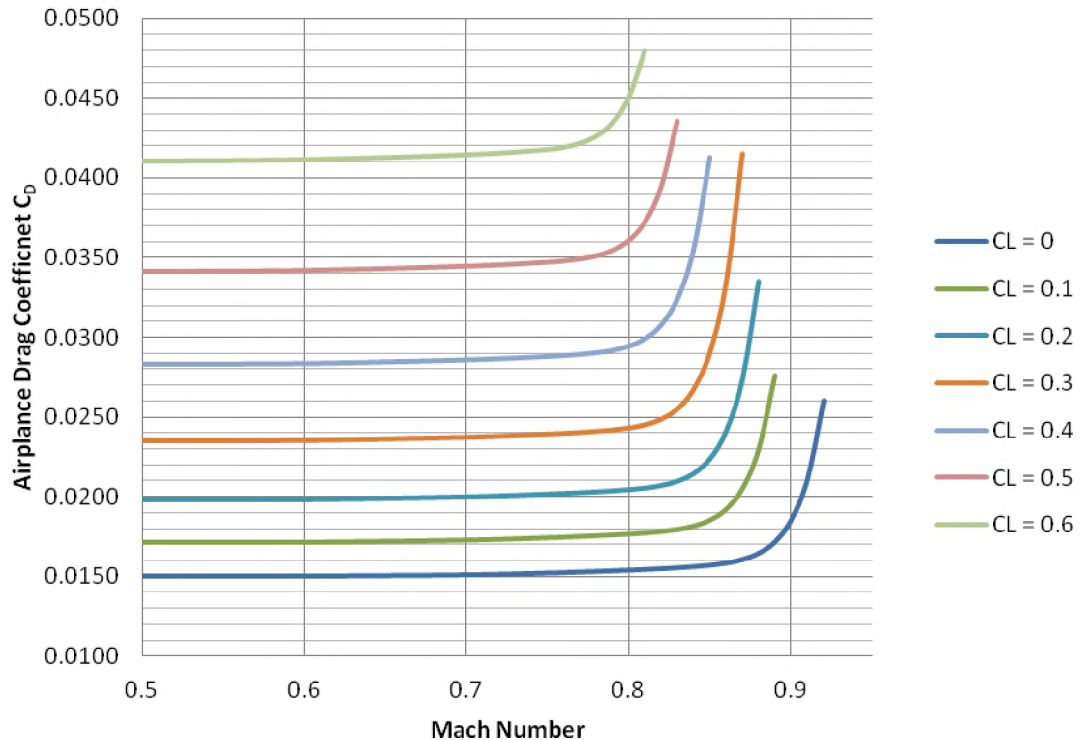


Figure 6: Excel-generated drag map for typical airliner

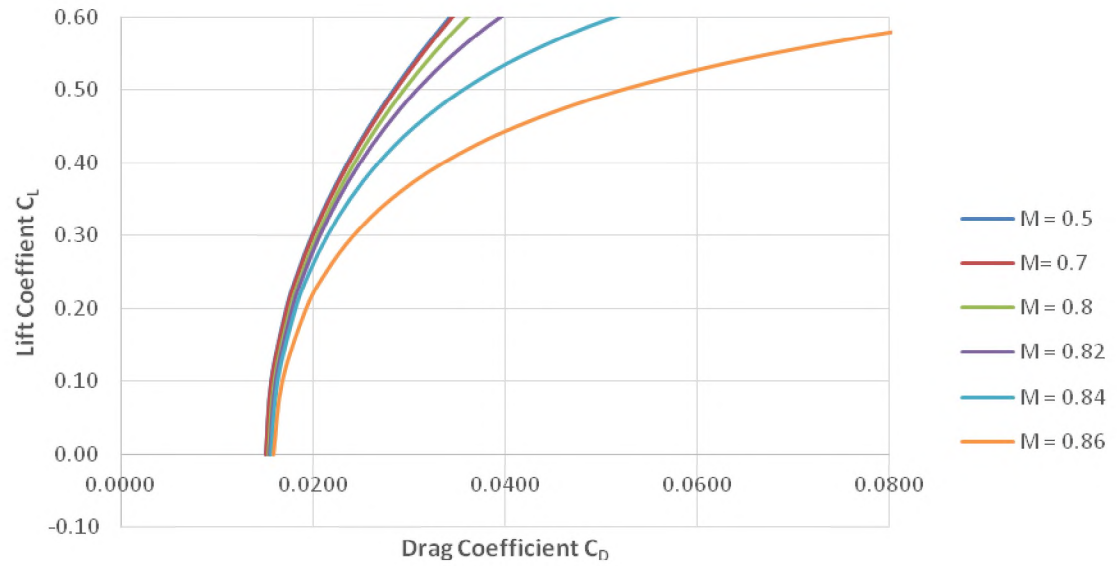


Figure 7: Excel-generated drag polars for a typical airliner

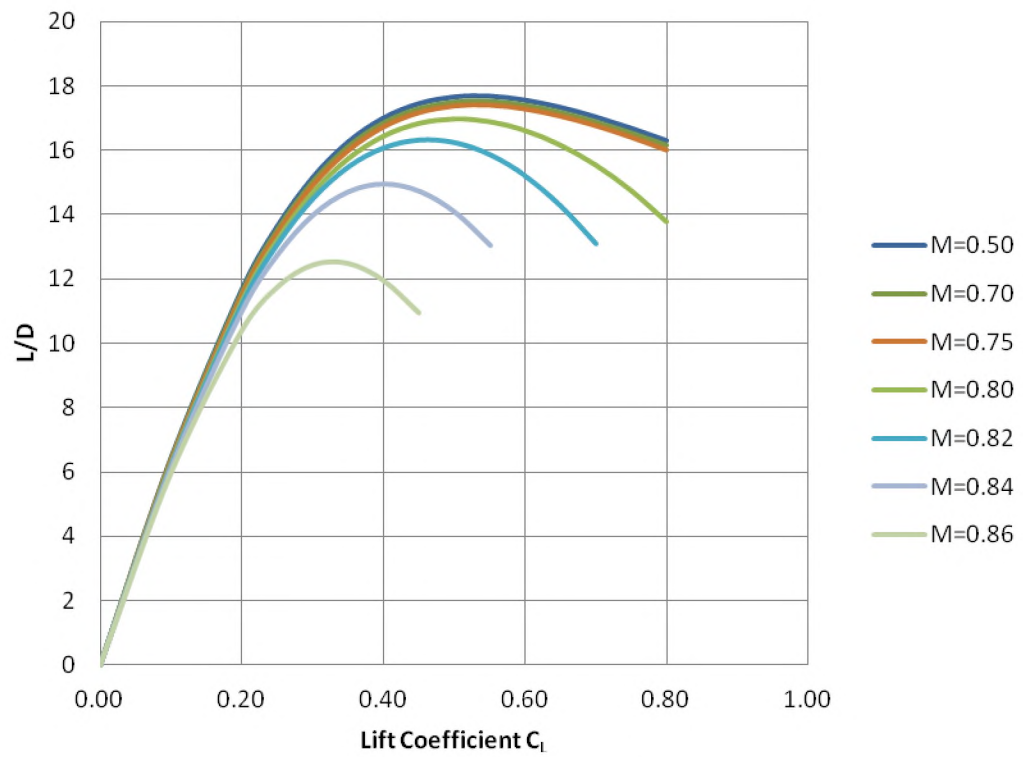


Figure 8: Excel-generated plot of L/D vs. C_L for typical airliner

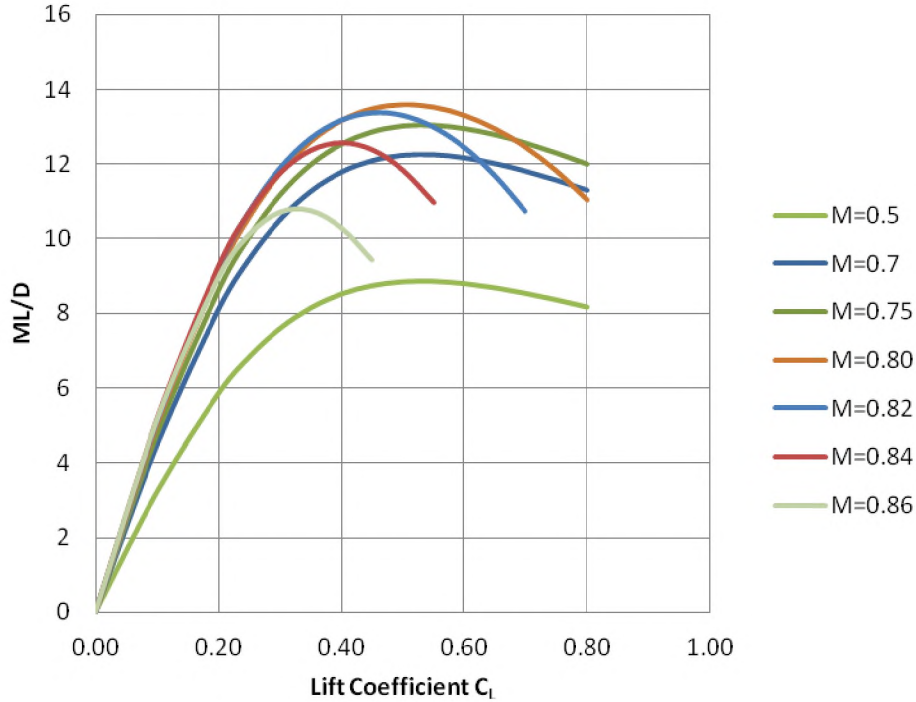


Figure 9: Excel-generated plot of ML/D vs. C_L for typical airliner

A spreadsheet is available online at www.adac.aero that was used to generate some of the figures in this paper:

Drag Map+Polars+LoD vs C_L +MLoD vs C_L using Korn rev 8.0.xlsx.

This spreadsheet produced Figures 5 through 9. It can easily be modified for changes in airplane geometry, value of technology factor, or shape of drag rise.

5. CONCLUSIONS

The generation of a drag map is a critical part of defining aerodynamic characteristics of a configuration that operates in the high subsonic region. It is important for students to understand the significance of the experimentally-generated drag map (from wind tunnel or CFD data), and also to know how a representative drag map and derivative plots can be generated at the conceptual design level. In particular, the plot of ML/D as a function of C_L and M suggests the optimum cruise values for these variables. This process appears only in Schaufele's textbook (Ref. 6), from which these procedures were drawn. The major deviation from Schaufele's method is that whereas he used a fixed relationship between C_L , Λ , t/c and M_{DD} , this method uses the Korn equation, which includes a technology factor, κ_a , to reflect the level of technology in the airfoil section. Both design and technology variables can be perturbed and the effect of these changes evaluated.

REFERENCES

- [1] Raymer, D.P., *Aircraft Design: A Conceptual Approach*, 5th Edition AIAA, 2012
- [2] Nicolai, L.M, and Carichner, G.E., *Fundamentals of Aircraft and Airship Design, Volume 1 – Aircraft Design*, AIAA, 2010
- [3] Schaufele, R.D, *Elements of Aircraft Preliminary Design*, Aries Publications, 2007
- [4] Obert, E., *Aerodynamic Design of Transport Aircraft*, IOS Press, 2009
- [5] Gur, O., Mason, W.H., and Schetz, J.A., *Full-Configuration Drag Estimation*, Journal of Aircraft, Vol 47 No 4, July-August 2010
- [6] Shevell, R.S., *Fundamentals of Flight*, Prentice Hall, 1989
- [7] Sforza, P.M, *Commercial Airplane Design Principles*, Elsevier, 2014

Author



Anthony P. Hays

THE AIRCRAFT NOISE SOURCES AND ANALYSIS OF WAYS FOR NOISE LIMITATION

Dmytro V. Tiniakov¹, Yuliya V. Babenko

1 – Nanjing, Nanjing University Aeronautics and Astronautics

Jiangjun Road, 29, Nanjing, Jiangsu, China, 211106

2 – Kharkov, National Aerospace University “KhAI”

Chkalova str, 17, Kharkiv, Ukraine, 61070

e-mail: Tiniakov_Dm@mail.ru, web page: <https://www.facebook.com/tinyakov.d>

Key words: aircraft, noise, aerodynamic drag.

Abstract. *The objective of this paper is to analyze the existing methods of the aircraft noise measurement and propose methods for noise level decreasing by taking into account the criterion of reducing drag, also to implementation of this method in the learning process. These methods provides in modern time to create aircraft structure with the noise level, which confirms with actual ICAO requirements for noise. But, every time these requirements to stay stronger and stronger, as result designers must find new solutions for noise decreasing. These are solutions will base on innovation methods. For creation of these methods require deep investigation in the direction of high structural efficiency from the point of these tasks. Also we know, that the main sources of noise are engines, but in the same time the airframe creates considerable part of noise level too. Hence, analysis of existing methods and research for new methods of airframe noise is important and actual task. The including results of this research to real learning process also important.*

INTRODUCTION

The development of aviation at now time has a high level. It includes not only flight or economical performers of aircraft, but also and their ecological characteristics. That is provided by the level of designer culture, manufacturing and operational conditions. However, requirements to the environment influence every time become stronger. ICAO created forecast to 2020 year about environment requirements to aircraft (Fig. 1) [1,2,3,14,15]. As shown, the noise level must be decrease before 2020 year at 10% compared with 2006. Also, the forecast about noise was create by ACARE (fig. 2) [1,2,3,14,15]. It is shown that noise from aircraft must be decrease before 2050 year at twice time compare with 2000 year. It is very strong task and without clear and understanding solution, it may be impossible.

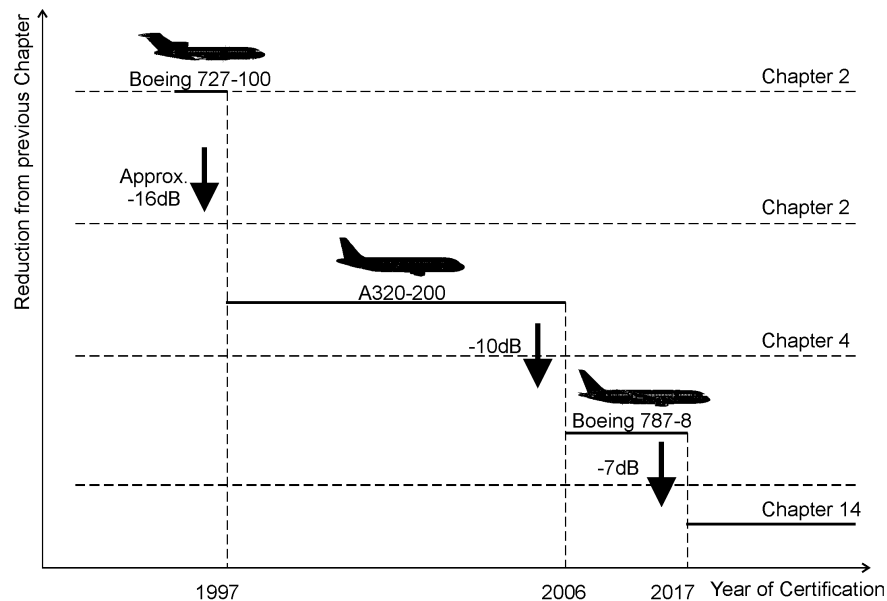


Figure 1: Steps of noise decreasing per years

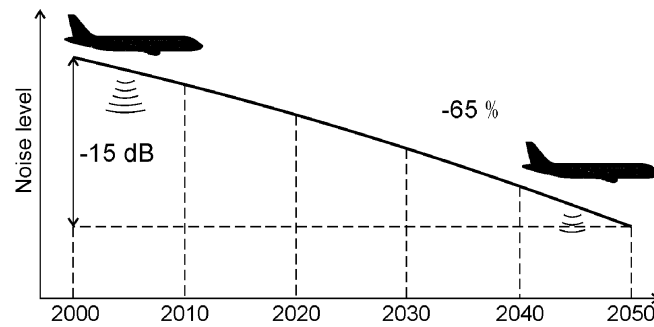


Figure 2: Analysis results of forecast for noise decreasing by ACARE
(Source: Flightpath 2050 research)

So, the task for noise decreasing is important and for society it is realistically needed.

Before research starting, it is needed understand nature, sources of aircraft noise, also analyses of modern methods of noise decreasing and measurement.

At the first, we need to determine the kinds of noise by the operation areas. It will be by two types:

- 1) External noise – noise at the environment, outside aircraft body.
- 2) Internal noise – noise inside aircraft – cockpit, passenger or cargo compartments.

If it relates about external noise, it is clear that the noise creates problems only at relative small area near the airport, where it flies at low altitude, because at cruise altitude distance from it and living area very high. So, for analysis interesting only next stages of a flight: take-off, climbing, landing approach, landing and taxing. The internal noise presents full time of flight.

As example, the diagram of a landing approach is shown on Fig. 3 [1,3,4].

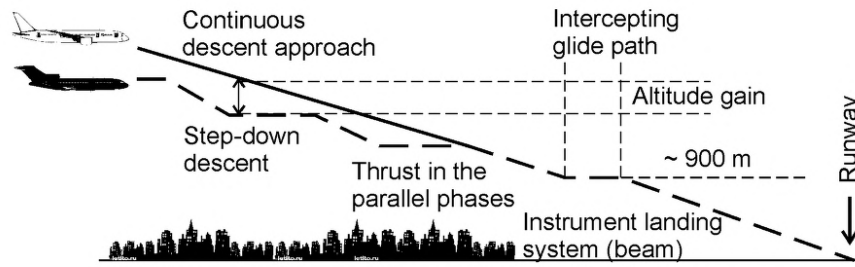


Figure 3: Diagrama of aircraft landing approach.

About the nature of the aviation noise. The aircraft consist of two main subsystems: airframe and powerplant system [2,5,6,7,8]. The main source of the aircraft noise, of course, is the powerplant system (engines). It may be 100% at the taxing stage. But, at the stages take-off and etc. the airframe creates the air drag, and as result airflow around aircraft together with aircraft parts, which are deflect from the base position, make high noise too, it may be equal 40% from total value.

It is understanding, that needed decrease both types of noise: from engines and airframe. In analysis of my paper, I will look to the airframe noise prediction.

Airframe noise is created from own body of aircraft and from members, which are deflected at the time takeoff or landing. The noise depends on surface area (it is slightly increase at these stages, from the point to improving flight performants) and also, it depends on the deflection members.

We cannot decrease seriously surface area – it depends on different reason kinds. Some of them – wing area is determinates by lift force, area of fuselage surface is determined by diameter of fuselage and its length, which, in turn, depends on aircraft purposes etc.

What kind of deflection member we know? There are flaps, ailerons, slats, rudders, elevators, landing gears etc. (Fig. 4) [8].

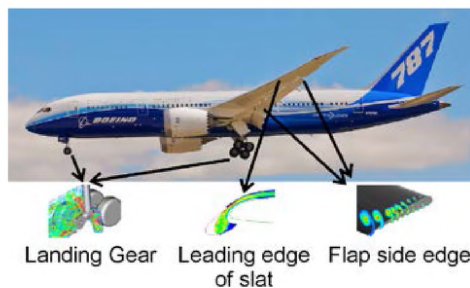


Figure 4: Main noise sources of Airframe

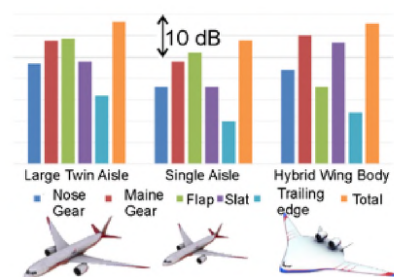


Figure 5: Airframe noise depends from aircraft dimensions

As it shown at Fig. 5 [8], the airframe noise depends on overall dimensions of aircraft. So, what rational way to analysis and founding optimal solution for airframe noise decreasing?

It will be by the next way (see fig. 6) [8,9,10].

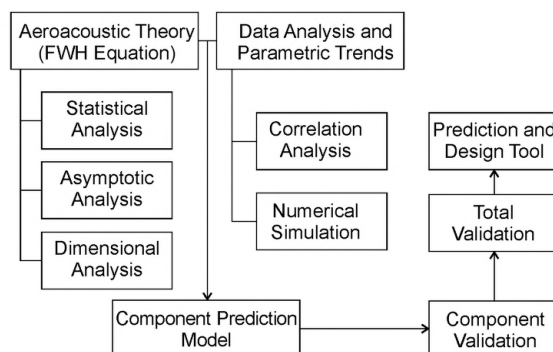


Figure 6: Approach to design tools of airframe prediction.

As shown at Fig. 6 for rational way of noise limitation it is needed to form base of design solutions, which can provide require effect. And after that, we can start to analysis every of this solution. At time of the analysis it is possible to find new ways, which can help to solve this task.

So, what kind of design solution is it possible to use? These are:

- design solutions;
- manufacturing solutions;
- operational-logistic solutions.

Design solutions depend on type of noise (internal or external). The pat of design solutions may be same for both types:

1. Improoving sound proof properties of structural materials – it is good way for internal noise and partly for external (for engines cover) [5,8,11].
2. Optimization for geometrical parameters of airframe structural members – it is good for both noise types [8,9,13].
3. Optimization of deflection motion parameters (angel, speed of deflaction etc.) for airframe structural members (like aileron, flaps, landing gear etc.) – it is good for both noise types [8,11,13].

At Fig. 7 and it is present results of Yueping Guo from NEAT Consulting for flap geometrical parameters [8].

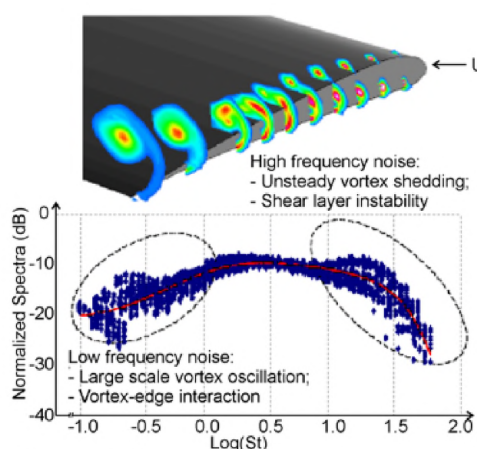


Figure 7: Flap side edge noise sources.

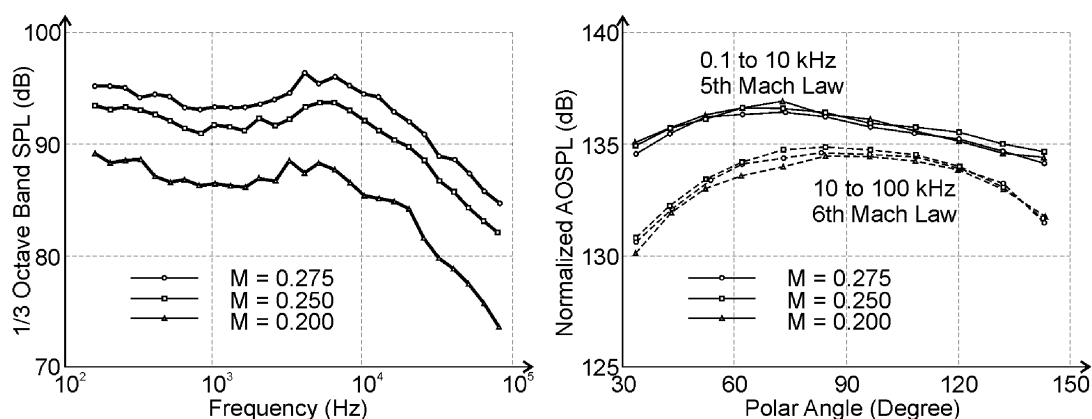


Figure 8: Flap Side edge noise characteristics

Frequency Domain	Source Mechanism	Spectrum	Mach Scaling	Peak Directivity
Low	Vortex-edge Interaction	Gradual Variation	5 th Power	Overhead
High	Shear Layer Instability	Fast Falloff	6 th Power	Forward Quadrant

4.7 % DC-10 Model; Slat angle = 20 degrees; Flap angle = 50 degrees;
Frequency in small scale

Important role for the analysis plays the noise measurement. In ICAO documents Annex 16 Volume 1 Chapter 2 presents information for this purpose. For example conditions for lateral noise measurement point are present on Fig. 9 [3,6].

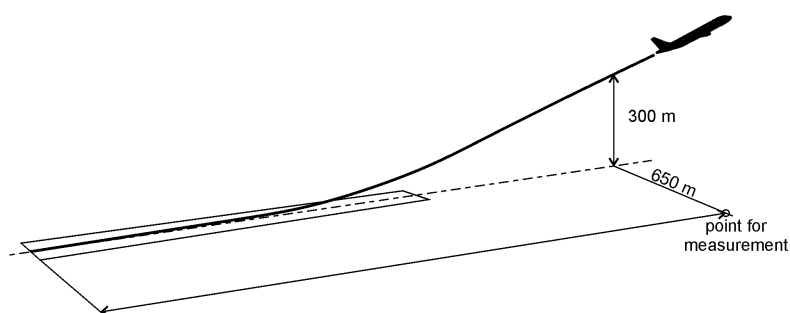


Figure 9: Lateral noise measurement point

The last point in the research of this paper about using the material for absorbing aircraft noise is in learning process. This area very wide and includes a lot of theoretical questions from difernet aviation subareas. Some of them: structural features of airframe, it includes as classical questions, but also new approaches for structure creation are present in it [9]; aerodynamics – also there are classical tasks and new approaches for noise decreasing [9], etc.

So, the noise decreasing task is very important not only for aviation specialists, but for society too, and solving of this task is the problem of the nearest future.

CONCLUSIONS

From the present roundup, it is possible to create next conclusions:

1. Aircraft traffic will growth and, by forecast analysis, by 2050 it will increase at twice time.
2. ICAO has made tougher requirements for noise limitation. And by 2050 it will decrease by 65 %.
3. Noise decreasing is actual problem, which requires new approaches for its solving.
4. Design approach is perspective way for noise deceasing, because airframe creates considerable part of the noise at takeoff and landing stages of the flights.
5. Deep analysis of modern structural features provides rational ways for noise decreasing by improving airframe structural members.

REFERENCES

- [1] Aircraft noise report 2015. Luftfahrt bewegt. BDL – Bundesverband der Deutschen Luftverkehrswirtschaft e. V. 2015. 24 p.
- [2] P. Malbequi, Y. Rozenberg, J. Bulte. Aircraft Noise Prediction in The IESTA Program. ONERA, BP-72, 29 avenue de la Division Leclerc, 92322 Châtillon Cedex, France.
- [3] Getting to grips with aircraft noise. Flight Operations Support & Line Assistance. Airbus. December 2003, 85 p.
- [4] Russell H. Thomas, Yueping Guo, Jeffrey J. Berton, Hamilton Fernandez. Aircraft Noise Reduction Technology Roadmap Toward Achieving the NASA 2035 Noise Goal. American Institute of Aeronautics and Astronautics, 2017, p. 25.
- [5] D. Casalino, F. D'ozzib, R. Sannino, A. Paonessa. Aircraft noise reduction technologies: A bibliographic review. Aerospace Science and Technology 12 (2008), pp. 1–17.
- [6] Aircraft Noise Analysis. Appendix A. Joint Primary Aircraft Training System. USA USAF, 1998, p. 19.
- [7] Miguel Marquez-Molina, Luis Pastor Sanchez-Fernandez, Sergio Suarez-Guerra, Luis Alejandro Sanchez-Perez. Aircraft take-off noises classification based on human auditory's matched features extraction. Applied Acoustics. 84 (2014) 83–90 pp.
- [8] Yueping Guo. Airframe Noise Modeling and Prediction. NEAT Consulting. Seal Beach, CA 90740. USA. September, 2016
- [9] D. V. Tiniakov. The improvement of the Aircraft Lift Surfaces Integrated Design Taking into Account the Inductive Drag. Asian Workshop on Aircraft Design Education. AWADE 2016. Nanjing University of Aeronautics and Astronautics (NUAA), 08-11 October 2016. <http://aircraftdesign.nuaa.edu.cn/AWADE2016>. pp. 135-141.
- [10] Thomas L. Connor. Aircraft Noise Control and the Role of Federal Research. NASA's Environmental Compatibility Research, Workshop II, May 19-21, 1998, Cleveland, OH
- [11] S. Redonnet. Aircraft Noise Prediction via Aeroacoustic Hybrid Methods – Development and Application of Onera Tools over the Last Decade: Some Examples. Aerospace Lab. Issue 7 - June 2014 - Aircraft Noise Prediction via Aeroacoustic Hybrid Methods.

- [12] Antonio Filippone. Aircraft noise prediction. Progress in Aerospace Sciences 68 (2014) 27–63 pp.
- [13] Serhat Hosder, Joseph A. Schetz, Bernard Grossman, William H. Mason. Airframe Noise Modeling Appropriate For Multidisciplinary Design And Optimization. 42nd AIAA Aerospace Sciences Meeting and Exhibit. 5-8 January 2004, Reno, Nevada. p. 12.
- [14] Aircraft and Airliner Noise - Facts and Pictures. <http://aviationExplorer.com/>
- [15] Aircraft & Airport Noise Monitoring. <http://www.cirrusresearch.co.uk/>

Reporter



Dmytro V. Tiniakov

Dieter Scholz (Ed.)

Book of Abstracts

13th European Workshop on Aircraft Design Education (EWADE 2017)

in co-operation with the
2nd Asian Workshop on Aircraft Design Education
(AWADE 2017)

co-located with the
6th CEAS Air & Space Conference
(CEAS 2017)

Date: 19 October 2017
Venue: Palace of the Parliament, 2-4 Izvor St., Sector 5,
050563, Bucharest, Romania
Room: Nicolae Iorga Hall No. 2

EWADE is part of the
CEAS Technical Committee Aircraft Design (TCAD)
<http://AircraftDesign.org>

The Council of European Aerospace Societies (CEAS) is an association with the aim to develop a framework within which the major Aerospace Societies in Europe can work together.
<http://CEAS.org>

EWADE and EWADE 2017 online: <http://EWADE.AircraftDesign.org>
<http://EWADE2017.AircraftDesign.org>
<http://ProceedingsEWADE2017.AircraftDesign.org>

© 2017 by the respective author(s)



Creative Commons copyright license for the public
Attribution 4.0 International (CC BY 4.0)
<https://creativecommons.org/licenses/by/4.0>

The abstracts are sorted in this Book of Abstracts according to the chronological order of the related presentations in the workshop program.

Content

Dieter Scholz

Welcome to EWADE 2017209

Octavian Pleter, Sterian Dănăilă

Education in Aerospace Engineering at the University "Politehnica" of Bucharest209

Petter Krus

Aircraft Systems Engineering and Concept Evaluation210

Fabrizio Nicolosi

Innovative Tools for Aircraft Preliminary Design – Development, Applications and Education 211

Dieter Scholz

Specific Fuel Consumption of Jet Engines – Implications in Aircraft Design and Performance Calculations211

Jizhou Lai

Welcome to Asian AWADE and European EWADE..... 212

Pinqi Xia

Aerospace Engineering Education at Nanjing University of Aeronautics and Astronautics213

Zhijin Wang, Anatoly Kretov

The 60th Anniversary of the Launch of the First Satellites – Historical and Technical Analysis 213

Anthony Hays

Generation of the Drag Map and Derivative Plots for Commercial Aircraft.....214

Dmitry Tinyakov, Yuliya Babenko

Aircraft Noise Sources and Analysis of Possibilities for Noise Reduction.....214

Oleksiy Chernykh

Airworthiness Knowledge Comes into Focus of Chinese Aviation Education 215

Emmanuel Bénard, Peter Schmollgruber

Review of Aircraft Design activities at ISAE-SUPAERO / ONERA 216

Lorenzo Trainelli, Carlo Riboldi

Award-Winning Innovative Aircraft Design Projects at Politecnico di Milano ...12

Diane Chelangat Uyoga

Aerospace Education in Kenya – The Case of Moi University..... 217

Tomasz Goetzendorf-Grabowski

**Results of READ/SCAD 2016 – Proposal of a Joint READ/EWADE/SCAD Workshop
2018217**

Abstracts

EWADE Session 1, AWADE Session 4

Dieter Scholz

Hamburg University of Applied Sciences (HAW Hamburg), DE Aircraft Design and Systems Group (AERO)

Welcome to EWADE 2017

The "Welcome to EWADE 2017" gives an introduction to the program including the video conferencing with AWADE in Nanjing, China. The history of EWADE is briefly explained for those new to the workshop. The first workshop was held in 1994 on invitation only. EWADE has links to several other workshops and organizations: READ, CEAS, SCAD and AWADE (in order of the length of the established contact). EWADE is an important activity in the CEAS Technical Committee Aircraft Design (TCAD) together with SCAD. Both share the URL www.AircraftDesign.org. Available presentations from EWADE reach back to the year 2000. In some cases full papers were written after the presentation. Also these are published on the web page. EWADE has always discussed possibilities for journal publications in aircraft design. Several cooperations exist.

Keywords:

EWADE 2017 programme, history, cooperations, web pages, publications

Octavian Pleter, Sterian Dănăilă

University Politehnica of Bucharest (UPB), RO Faculty of Aerospace Engineering

Education in Aerospace Engineering at the University "Politehnica" of Bucharest

Romanian has contributed to pioneering aviation. The University "Politehnica" of Bucharest (UPB) stands in this tradition. Higher education in aviation started in 1928, when Prof. Elie Carafoli opened the first conference on Aeronautics at the Polytechnic school in Bucharest. He also built the first wind tunnel in South-Eastern Europe (1931), still in operation. Today, graduates from the Faculty of Aerospace Engineering can be found in all sectors of aviation and space in many countries of the world. Alumni of the faculty have contributed to major aerospace programs. UPB is active in aerospace research and teaching and offers Bachelor and Master

degrees as well as doctoral studies. Fields of study are: Aerospace Constructions, Propulsion Systems, Equipment and Aviation Instruments, Engineering and Management in Aeronautics, Air Navigation, and Aeronautical Design. 180 to 200 students commence their studies in the faculty each year. The faculty has more than 1000 students, more than 40 professors and lecturers, several laboratories. An international network with partner universities results in many opportunities for incoming and outgoing students.

Keywords:

aerospace, education, research, industry, alumni, history

Petter Krus

Linköping University (LiU), SE

Division of Fluid and Mechatronic System (Flumes)

Aircraft Systems Engineering and Concept Evaluation

Methods and tools are presented that facilitate the evaluation of aircraft system concepts in various ways. One such tool is HOPSAN-NG. It allows a wide range of simulations from the aircraft hydraulic system, via aircraft dynamics up to the simulation of a whole aircraft mission based on pre-defined way points. This allows an evaluation of the aircraft including its fuel consumption due to aircraft systems and the evaluation of many more details of the aircraft's behavior.

Keywords:

aircraft systems, systems engineering, simulation, evaluation

Fabrizio Nicolosi

University of Naples "Federico II" (UNINA), IT

Design of Aircraft and Flight Technologies Research Group (DAF)

Innovative Tools for Aircraft Preliminary Design – Development, Applications and Education

The Design of Aircraft and Flight Technologies Research Group (DAF) at University of Naples is involved in research activities addressing the development and application of new and innovative tools and frameworks for aircraft preliminary design. To build such new tools for aircraft design we believe that the following activities should be carried out: (a) derive new semi-empirical formulations (even through the construction of surrogate methods) which can be more accurate in the prediction of aircraft characteristics (especially for non-conventional configurations);

(b) integrate medium to high fidelity tools into the analyses; (c) design with a multi-disciplinary approach (i.e. including systems and direct operating costs); (d) include innovative propulsive systems; (e) deal with innovative configurations; (f) include new and efficient optimization algorithms; (g) use advanced software engineering to enhance tool capabilities, speed and usability (for example user-friendly graphic interface or interoperability with other software). Recent research activities of the DAF group have been focused on the development and application of a new framework. Examples and applications in relevant European research projects can be presented. The development of these tools play also a relevant role in educational activities at the University of Naples as far aircraft design is concerned.

Keywords:

aircraft design tool, aircraft design framework, aircraft MDO, innovative configuration

Dieter Scholz

Hamburg University of Applied Sciences (HAW Hamburg), DE Aircraft

Design and Systems Group (AERO)

Specific Fuel Consumption of Jet Engines – Implications in Aircraft Design and Performance Calculations

Basic considerations about an overall efficiency of an aircraft lead to the conclusion that a power-specific fuel consumption (PSFC) has to be constant, whereas a thrust-specific fuel consumption (TSFC) has to be proportional to speed. This however, leads to a contradiction, because the fuel consumption at zero speed cannot be zero. Furthermore, specific fuel consumption is a function of thrust (or drag) which varies

with speed. This links SFC not only to engine characteristics, but to the whole aircraft and its flight condition. We understand that (in contrast to tradition) the Breguet range equation for jets could be written with a (constant) power-specific fuel consumption (PSFC). Optimizing for maximum range now leads to a different optimum speed compared to a derivation based on a constant thrust-specific fuel consumption (TSFC). We also understand why flying low and slow (for reduced fuel consumption) does not work as well as expected – even for a newly designed aircraft for which the wing area is not yet fixed.

Keywords:

specific fuel consumption, SFC, Breguet, range, fuel, saving, flight, low, slow

EWADE Session 2, AWADE Session 5

Jizhou Lai

Nanjing University of Aeronautics and Astronautics (NUAA), CN
International Affairs Office

Welcome to Asian AWADE and European EWADE

The presentation looks at the international dimension of aerospace at Nanjing University of Aeronautics and Astronautics. Many international contacts exist. The Asian Workshop on Aircraft Design Education (AWADE) started with its first workshop in 2016. It was inspired by Prof. Anatoly KretoV who joint NUAA from Kazan State Technical University, Russia. Prof. KretoV had participated in EWADEs already since 2007 and was able to bring the special spirit of this workshop to Asia. CEAS 2017 is now the first opportunity for EWADE and AWADE to hold a joint meeting.

Keywords:

NUAA, international relations, EWADE, AWADE, AWADE 2016

Pinqi Xia

Nanjing University of Aeronautics and Astronautics (NUAA), CN
College of Aerospace Engineering (CAE)

Aerospace Engineering Education at Nanjing University of Aeronautics and Astronautics

The presentation considers the system of education and preparation of students at Nanjing University of Aeronautics and Astronautics at the Aerospace Engineering College.

Keywords:

aerospace industry, education, directions, preparing of specialists

Zhijin Wang, Anatolii Kreto

Nanjing University of Aeronautics and Astronautics (NUAA), CN
College of Aerospace Engineering (CAE)

**To the 60th Anniversary of the Launch of the First Satellites –
Historical and Technical Analysis**

Students' interest can be increased by studying the history of technology developments. The presentation describes the history of creating and the launches of the first satellites Sputnik1 and Sputnik2 in 1957. The historical background is given followed by a brief analysis and conclusions.

Keywords:

teaching, aerospace, history, technology development, satellite, Sputnik

Anthony Hays

Aircraft Design and Consulting (ADAC), US California
State University, Long Beach (CSULB), US

Generation of the Drag Map and Derivative Plots for Commercial Aircraft

The drag map provides important information about the transonic aerodynamic characteristics of an aircraft design. In an aircraft design course, students should be aware of the significance of the drag map and its derivative plots. The presentation describes how a drag map and its derivatives can be constructed that are representative of a given aircraft configuration.

Keywords:

aircraft design, transonic aerodynamics, transonic drag rise, drag map

Dmitry Tinyakov¹, Yuliya Babenko²

¹ Nanjing University of Aeronautics and Astronautics (NUAA), CN

² National Aerospace University – Kharkiv Aviation Institute (KhAI), UA

Aircraft Noise Sources and Analysis of Possibilities for Noise Reduction

This presentation analyzes the existing methods of aircraft noise measurements and proposes methods to decrease noise levels by taking into account drag reduction criteria. The implementation of this method in the learning process is discussed.

Keywords:

aircraft, noise, aerodynamic drag

Oleksiy Chernykh

Nanjing University of Aeronautics and Astronautics (NUAA), CN Civil
Aviation Engineering Department (CAED)

Airworthiness Knowledge Comes into Focus of Chinese Aviation Education

Air Transportation is the safest mode of transportation, because it has long been under comprehensive aircraft airworthiness management. The airworthiness chain consists of three main components (a machine, environment, and a man) which all ensure highest levels of safety through well coordinated work. The last (but not the least) component of the airworthiness chain is a human, professional specialist. Once China has started to develop its own aircraft, the need for well educated airworthiness professionals has strongly increased. The College of Civil Aviation of Nanjing University of Aeronautics and Astronautics offers airworthiness knowledge, which has been delivered by a number of professional teachers: local professors, who continuously advance their knowledge working abroad, and foreign professors invited from overseas universities to strengthen airworthiness education in China. Strong emphasis in teaching has been put on professional English, which opens better opportunities for graduates at Chinese and foreign aviation enterprises, because aircraft airworthiness is a worldwide issue.

Keywords:

airworthiness management, airworthiness education, Chinese aviation education, air transportation, aviation safety

EWADE Session 3, AWADE Session 6

Emmanuel Bénard¹, Peter Schmollgruber²¹ Institut Supérieur de l'Aéronautique et de l'Espace (ISAE), FR² Office National d'Etudes et de Recherches Aérospatiales (ONERA), FR**Review of Aircraft Design activities at ISAE-SUPAERO / ONERA**

During last years, ISAE-SUPAERO and ONERA reinforced their collaboration in aircraft design. The objective of this presentation is to illustrate the various studies that have been performed. First, the common Sizing Tool FAST (Fixed-wing Aircraft Sizing Tool) that has been developed during last years through projects will be presented. In a second part, aircraft design activities related to distributed propulsion using FAST and other disciplinary codes are detailed. These studies concern regional aircraft as well a small-medium range missions. Always regarding innovative concepts, ISAE-SUPAERO launched many disciplinary studies related the the Blended Wing Body Concept: high fidelity structural analyses, aerodynamics, and control. Later on, it is planned to integrate these refined capabilities in the overall aircraft design tool. These recent activities are summarized to provide an clear overall status for this concept. To conclude the presentation, information about the Scaled Demonstrator used to support student projects will be given. ISAE- SUPAERO's activities in aircraft design are made under the Chair CEDAR sponsored by Airbus.

Keywords:

sizing tool, OAD, FAST, distributed propulsion, BWB, scaled demonstrator

Lorenzo Trainelli, Carlo Riboldi

Politecnico di Milano (POLIMI), IT

Department of Aerospace Science and Technology

Award-Winning Innovative Aircraft Design Projects at Politecnico di Milano

The presentation addresses the Aircraft Design graduate course at Politecnico di Milano and a series of projects developed in recent years that have been submitted to various international design competitions, achieving a remarkable success rate.

Keywords:

innovative aircraft design, aircraft design education, electric aircraft, hybrid-electric aviation, morphing tilt rotor, student competition

Diane Chelangat Uyoga

Moi University, KE

School of Aerospace Sciences

Aerospace Education in Kenya – The Case of Moi University

Learning is the heart of existence and education is the main driver of economic activities in the world. Education cuts across continents, generations and races where it is believed that having a formal education is a gateway to better living. Moi University (Kenya), has taken on a challenge to demystify a myth of “how a small stone when thrown up comes down and a plane that is big do not fall off from the skies”. Aircraft design has not been explored in the African context and aerospace education has captured limited attention, more so in a higher education context. Moi University, a state owned institution situated in the Eastern part of the continent attempts to address the technical and softer issues that are tailored to equip learners with knowledge on aerospace and its dynamics.

Keywords:

education, aircraft design, aerospace

Tomasz Goetzendorf-Grabowski

Warsaw University of Technology (WUT), PL Aircraft

Design Department

**Results of READ/SCAD 2016 – Proposal of a Joint
READ/EWADE/SCAD Workshop 2018**

The results from READ/SCAD 2016 are published online at READ and SCAD web pages and in the journal "Aircraft Engineering and Aerospace Technology".

<http://PapersSCAD2016.AircraftDesign.org>,

<http://www.emeraldgrouppublishing.com/aeat.htm>,

http://read.meil.pw.edu.pl/wp-content/uploads/Program/READ_SCAD_2016.html.

Keywords:

education, research, aircraft design, workshop, publication, journal

CONCLUSION

According to the results of the work of the 2nd workshop and held discussions for further successful development of the AWADE event, the following suggestions are considered:

1. The AWADE Workshop will be held at NUAA in even-numbered years, which can be staggered with the EWADE Workshop that is held in odd-numbered years.
2. It is necessary to increase the number of participants from the aviation-related universities of China. To promote this with the aim of informational interaction, it is important to involve all teachers of College of Aerospace Engineering.
3. The positive experience of participation in the workshop via video-conferencing is to be continued at the next workshops with the aim of attracting maximum number of participants.
4. The Organizing Committee has to provide great opportunities for student participation and dedicate an individual session to this.
5. To provide the organization of thematic sessions of the AWADE Workshops.
6. Strengthen further communication with EWADE Workshop and also with READ, SKAD events.
7. To consider academic citation indexing for the AWADE paper collection.
8. To consider recommending the best papers of the AWADE presentations for publishing in famous indexed journals.
9. To consider the opportunity to combine two events in frame of AWADE: conducting of seminar with international student Olympiad on aircraft design, thus, to attract aviation companies.
10. At the administrative level of the University to consider establishing strong relations of AWADE with Chinese Society of Aeronautics and Astronautics.
11. To promote AWADE-2018 more widely in international sources from January 2018 for inviting greater number of foreign participants.
12. To improve network equipment and quality of connection for futures video-conferencing.

ASIAN WORKSHOP ON AIRCRAFT DESIGN EDUCATION



PHOTO GALLERY OF THE SECOND AWADE SEMINAR

NANJING

OCTOBER 17-20

2017



ASIAN WORKSHOP ON AIRCRAFT DESIGN EDUCATION 2017



ASIAN WORKSHOP ON AIRCRAFT DESIGN EDUCATION 2017 SESSION 1



Dean of the College
of Aerospace Engineering,
NUAA, Prof. Pinqi Xia
welcomes the participants
in his opening speech
of the 2nd AWADE Seminar



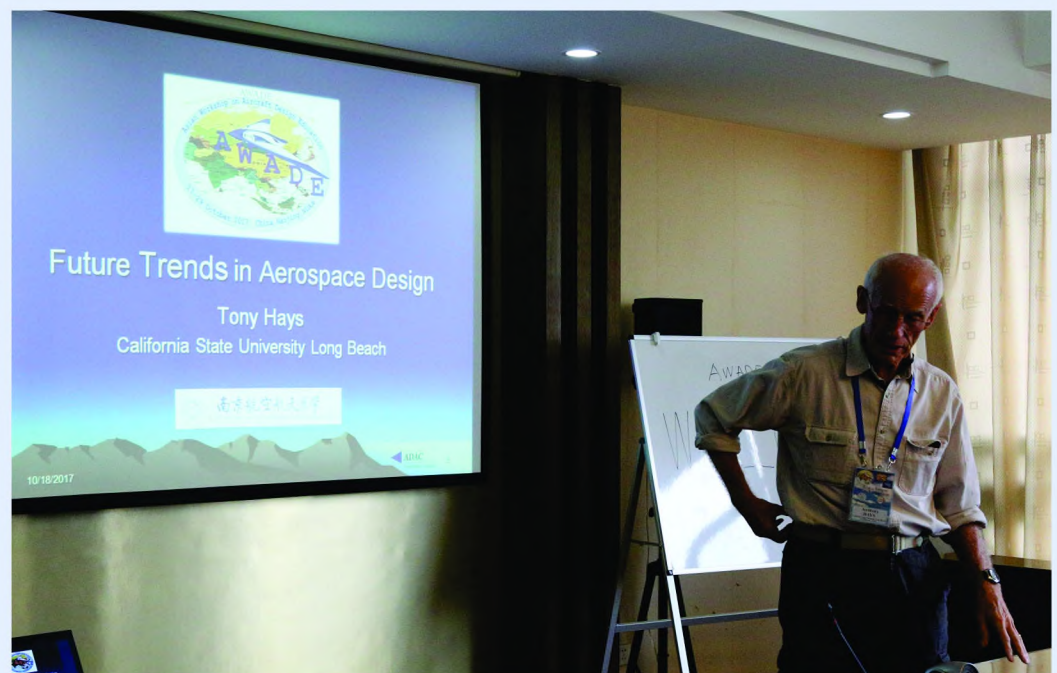
ASIAN WORKSHOP ON AIRCRAFT DESIGN EDUCATION 2017

SESSION 1



Prof. Anatolii Kretov spoke about the history of appearance of the European and Asian Workshops on Aircraft Design Education

The experienced designer
Anthony P. Hays
from California State
University Long Beach,
California (USA),
talked about the future
trends in aircraft design



Nature as the Best Creative Designer was sounded by Prof. Stanislav Gorb from Kiel University (Germany) and Prof. A. Kretov

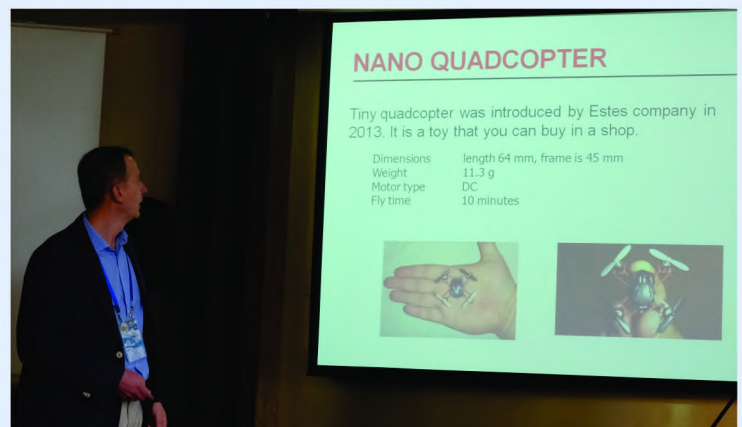
ASIAN WORKSHOP ON AIRCRAFT DESIGN EDUCATION 2017

SESSION 1



The critical question in the aircraft design is the material selection. The report of an experienced material scientist from Antonov Company (Kyiv, Ukraine) Oleksandr Moliar and his colleagues from the College of Material Science and Technology, NUAA

Economic Efficiency of Aircraft with Air Cushion Chassis Landing Gear - the report of Victor Morozov from Novgorod State Technical University named after R.E. Alekseev (Nizhny Novgorod, Russia), and Zhang Cong, master student from College of Aerospace Engineering



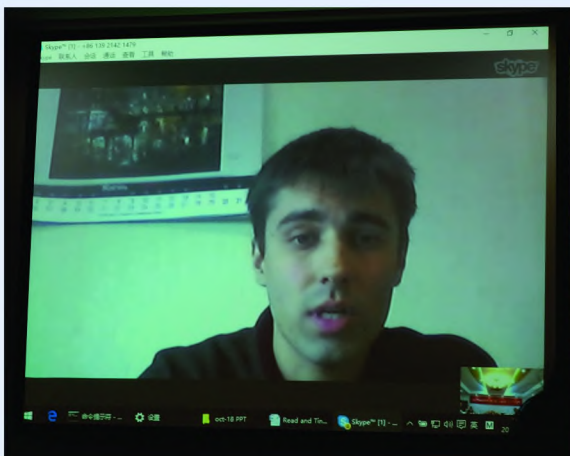
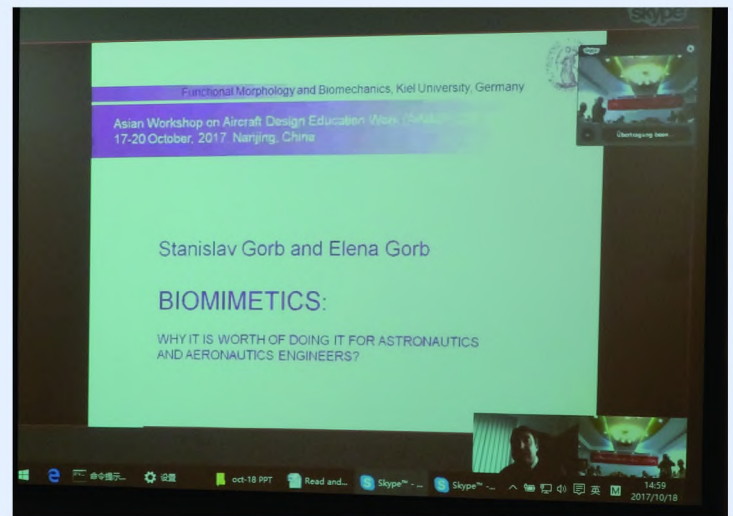
The report of the group of Lithuanian developers of mini engines “Piezoelectric Motors for Micro-Helicopters”. Professors Dalius Mazeika, Piotr Vasiljev, Sergejus Borodinas(Vilnius, Lithuania)

ASIAN WORKSHOP ON AIRCRAFT DESIGN EDUCATION 2017 SESSION 2



The report by video conference from Kazan National Research Technical University named after A. N. Tupolev – KAI (Russia) “Design and Manufacturing of Polymer Composite Tail Rotor Hub”

The report by video conference format from Department of Functional Morphology and Biomechanics, Zoological Institute of the Kiel University (Germany) "Biomimetics: Why It Is Worth of Doing It for Astronautics and Aeronautics Engineers" by Prof. Stanislav Gorb and Elena Gorb



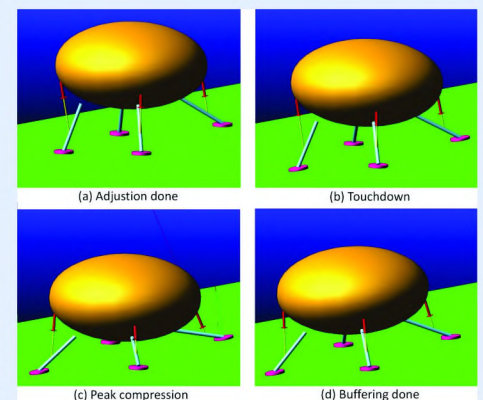
The video report from National Aerospace University KhAI, Kharkiv (Ukraine) and its discussing

ASIAN WORKSHOP ON AIRCRAFT DESIGN EDUCATION 2017 SESSION 3

Works involving students



Masters students showed their conceptual project using design experience of the Energia-Buran system and Apollo program for the creation of lunar transport system



Great interest was aroused by the work
"Analysis of Adaptive Landing Gear Used for Near Space Lander"
which was made by Mingyang Huang
under the leadership of



Prof. Xiaohui Wei



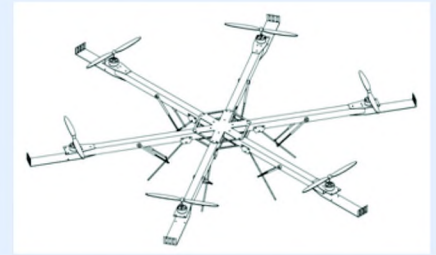
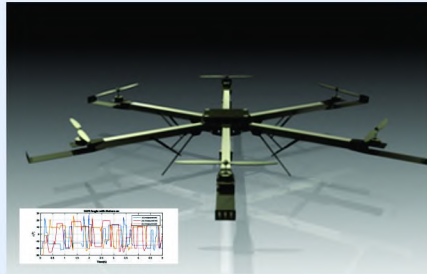
and Prof. Hong Nie



ASIAN WORKSHOP ON AIRCRAFT DESIGN EDUCATION 2017

SESSION 3

Works involving students



BASIC UAV DEVELOPMENT IN UNDERGRADUATE LEVEL

Allan A. Dias



ASIAN WORKSHOP ON AIRCRAFT DESIGN EDUCATION 2017

SESSION 4

Video bridge Bucharest EWADE Session 1 —→ Nanjing AWADE Session 4



ASIAN WORKSHOP ON AIRCRAFT DESIGN EDUCATION 2017

SESSION 5

Video bridge Nanjing AWADE Session 5 —> Bucharest EWADE Session 2



Welcome Speech on
AWADE 2017 With joint participation of **EWADE 2017**
by
Professor Lai Jizhou
Executive Director of International Cooperation Office
October 19th
Nanjing University of Aeronautics and Astronautics

I appreciate all the participants, especially those from the other side of the video, for joining us and sharing your valuable experience and inspirations.

I believe that your academic exchanges and discussions about the achievements will further promote the development of the field of aircraft design.

I am sure this workshop will create a new era for strengthening the academic collaboration between China, Asian countries and European countries, and also between you all and NUAU.

1



The 2nd Asian Workshop on Aircraft Design Education

3. Suggestion for AWADE

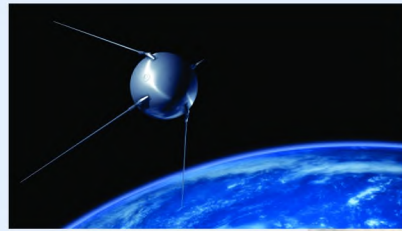
Suggestion for AWADE holding year

	2015	2016	2017	2018	2019	2020	2021	2022
EWADE	12 th		13 th		14 th		15 th		
AWADE		1 st	2 nd	3 rd		4 th		5 th	

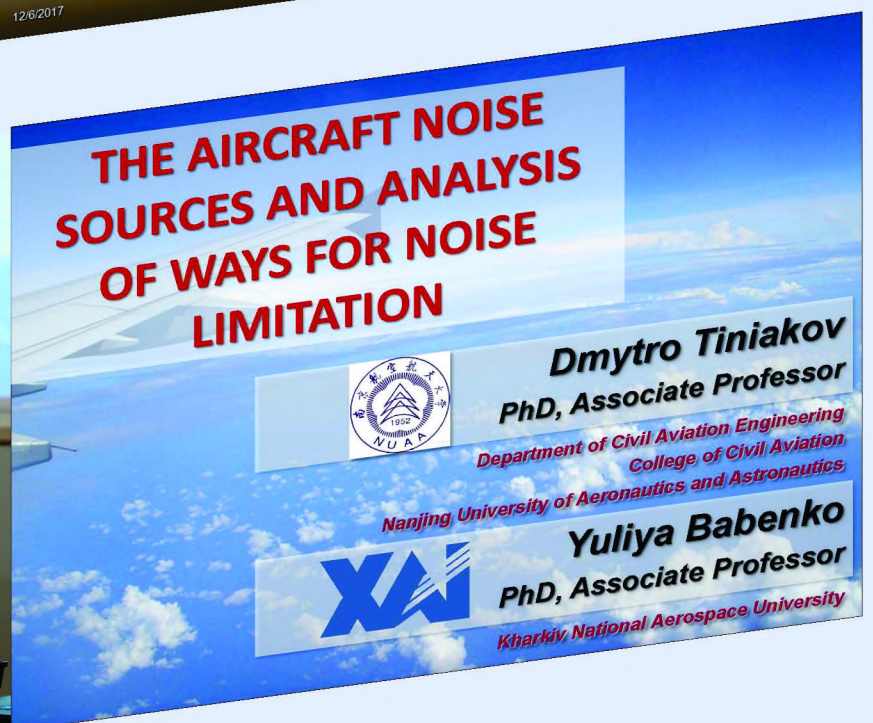
↑ ↑ ↑

ASIAN WORKSHOP ON AIRCRAFT DESIGN EDUCATION 2017 SESSION 5

Video bridge Nanjing AWADE Session 5 —> Bucharest EWADE Session 2

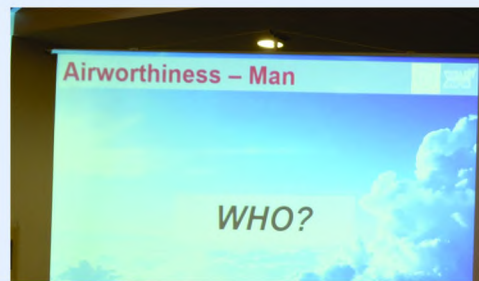


The 60th Anniversary of the
Launch of the First Satellites –
Historical and Technical Analysis
Zhijin Wang and Anatoly Kretov



ASIAN WORKSHOP ON AIRCRAFT DESIGN EDUCATION 2017 SESSION 6

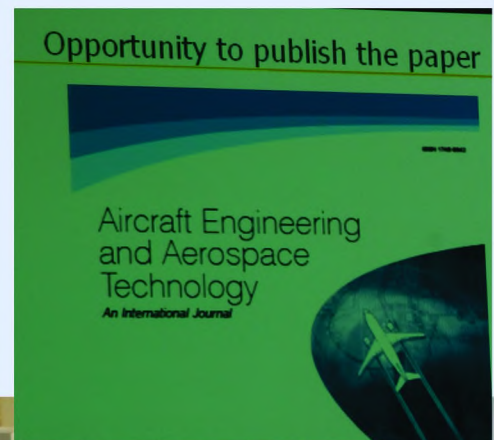
Video bridge Bucharest EWADE Session 3 → Nanjing AWADE Session 6



Ass.Prof. Oleksiy Chernykh. NUA.
**AIRWORTHINESS KNOWLEDGE COMES
INTO FOCUS OF CHINESE AVIATION
EDUCATION**



**Discussion – Next EWADE and Cooperation
with AWADE, READ, SCAD and CEAS 2019**



ASIAN WORKSHOP ON AIRCRAFT DESIGN EDUCATION 2017

FINAL REMARKS



LETTER OF APPRECIATION

DEAR MR. DIETER SCHOLZ AND EWADE COLLEAGUES

THE AWADE ORGANIZING COMMITTEE EXPRESSES YOU THE GREAT GRATITUDE FOR THE POSSIBILITY OF WORKING TOGETHER AND FOR THE EXCELLENT ORGANIZATION OF OUR COMMON SESSIONS.

YOU HAVE DONE HARD WORK AND WE TAKEN ANOTHER STEP TOWARDS CREATING OUR NEW DIRECTION, WHICH WE CALL AWADE.

WE STARTED TO MASTER NEW TECHNOLOGIES THAT WILL GIVE US THE ADDITIONAL CAPABILITIES AND SOLVE THE MAIN TASK OF AWADE - TO ADVANCE THE LEVEL OF KNOWLEDGE OF OUR STUDENTS IN ONE OF THE MOST COMPLEX AEROSPACE ENGINEERING INDUSTRIES - AIRCRAFT DESIGN.

ALSO, WE THANK ALL YOUR COLLEAGUES AND ASSISTANTS WHO TOOK PART IN THIS HUGE WORK.

WE LOOK FORWARD TO NEW STEPS IN THIS DIRECTION AND WE WILL DEFINITELY DO THEM.

AWADE ORGANIZING COMMITTEE





Asian European Workshop on Aircraft Design Education



Nanjing, China

Bucharest, Rumanian

17-20 October 2017